Modelling the Effects of Land Use and Land Cover Change on Hydrologic Regime of Ramganga River Basin

the Thesis Submitted

by

S. S. Tripathi

(ID No: 11PHSWSC103)

for

the Award of the Degree of Doctor of Philosophy

in

Agricultural Engineering

(Soil and Water Conservation Engineering)

Department of Soil Water Land Engineering and Management

VAUGUE INSTITUTE OF AGRICULTURAL ENGINEERING AND TECHNOLOGY

SAM HIGGINBOTTOM UNIVERSITY

OF AGRICULTURE, TECHNOLOGY AND SCIENCES

ALLAHABAD - 211007 (U.P.) INDIA.

2017

SELF - ATTESTATION

This is to certify that I have personally worked on the research work entitled, "Modelling the effects of Land Use and Land Cover change on Hydrologic Regime of Ramganga River Basin". The data stated in the thesis have been generated during the investigation and are genuine. Data / information obtained from other agencies have been duly acknowledged. None of the findings / information pertaining to the work has been concealed. The results embodied in this thesis have not been submitted to any other university or institute for the award of any degree or diploma.

Sant Sharan Tripathi

Date : ……..

Place: Allahabad

CERTIFICATE OF ORIGINAL WORK

This is to certify that **Mr. Sant Sharan Tripathi** (ID.11PHSWSC103) conducted the studies reported in the present thesis during 2011-2016 under my guidance and supervision. The results reported by him are genuine and the candidate himself has written the script of this thesis.

The thesis entitled, **"Modelling the effect of Land Use and Land Cover change on Hydrologic Regime of Ramganga River Basin"** is therefore being forwarded for fulfilment of the requirements for the award of the Degree of Doctor of Philosophy in Soil and Water Conservation Engineering (Agricultural Engineering) under Faculty of Engineering and Technology, SAM HIGGINBOTTOM UNIVERSITY OF AGRICULTURE, TECHNOLOGY AND SCIENCES, ALLAHABAD.

Prof. (Dr.) R. K. Isaac

Advisor

ACKNOWLEDGEMENT

All praise to the almighty whose blessing is the success behind this study. Though this study is the result of patient work and persistent effort on my part, it could have hardly been possible without a few who have ungrudgingly and painstakingly spared both time and energy for it.

I wish to express my indebtedness, profound and heartfelt thanks to Prof. (Dr.) R.K. Isaac, Professor, Department of Soil, Water, Land Engineering and Management, Vaugh Institute of Agricultural Engineering and Technology for his inspiring and creative suggestions, constructive criticisms and prolific encouragement offered during the course of research and preparation of the manuscript.

I would express my special thanks and respect to Prof. (Dr.) D.M. Denis, Dean, Vaugh Institute of Agricultural Engineering and Technology for his noble guidance and valuable suggestions during the study.

I express my sincere thanks to the members of my advisory committee, Prof. (Dr.) Ajit Paul, and Dr. Arpan Sherring, (Associate Professor), for their cooperation, suggestions and help during the study.

I express my sincere thanks to Dr. Narendra Swarup, Dr. Alex Thomas, (late) Dr. Md. Salim, and also to all my teachers and well wishers for their unconditional encouragements and support.

I would like to express my sincere thanks to Dr. Ajey Kumar Pathak, Principal Scientist NBFGR, Lucknow, Er. P. R. Chaurasiya, Chief Engineer Minor Irrigation, Lucknow, Mr. Sahni, Senior Hydrogeologist, Bareilly, Er. S. G. Sahu, and Officer in charge, Nazarat, Collectorate Bareilly for their help and guidance to get necessary computer lab facilities, Hydrogeological data, Mateorological data etc. Needed in research and analysis work for my thesis.

I would also like to express my sincere thanks to my employer, the Director, ICAR-IVRI, Izatnagar for being kind enough to permit me for pursuing my Ph.D. work.

Last but not the least my earnest thanks would also go to my beloved wife Seemaa, daughter Nikita and son Nirmit for their whole-hearted and unconditional support in this endeavour.

Allahabad **(Sant Sharan Tripathi)**

TABLE OF CONTENT

LIST OF TABLES

LIST OF FIGURES

LIST OF ABBREVIATIONS

ACF	:	Autocorrelation Function
AIC	:	Akaike Information Criterion.
ANN	:	Artificial Neural Network
AR	:	Autoregressive.
BGL	:	Below Ground Level
cm	:	centi meter
CN	:	Curve Number
DDM	:	Data Driven Modeling
et al.	:	et alibi and others.
ET	:	Evapotranspiration
etc.	:	etcetera.
Fig.	:	Figure.
GIS	:	Geographic Information System
GLCF	:	Global Land Cover Facility
GWL	:	Ground Water Level
ISE	:	Integral Square Error.
km^2	:	square kilo meter.
LU/LC	:	Land Use/Land Cover
m	:	meter.
m^3	:	cubic meter.
MAE	:	Mean Absolute Error.
MFE	:	Mean Forecast Error.
mm	:	millimeter.
MRE	:	Mean Relative Error.
MSE	:	Mean Square Error.

NN	:	Neural Network
NRSA	:	National Remote Sensing Agency
PACF	:	Partial Autocorrelation Function
pp	:	plural of pages.
RMSE	:	Root Mean Square Error.
RS	:	Remote Sensing
SCS	:	Soil Conservation Service
SOC	:	Soil Organic Carbon
SOM	:	Soil Organic Matter
SSE	:	Sum of Squares error
Train	:	Training
USGS	:	United States Geographic Survey

LIST OF SYMBOLS

° C	:	degree centigrade
′		minute .
L	:	Maximum number of lags.
□	:	sigma.
$□^2$	:	chi-square.
K	:	Lag of K time.
□	:	Autoregressive parameters.
%	:	Percent.

ABSTRACT

The land use land cover (LULC) change refers to the man made modifications affected upon the earth surface. In order to understand the effect of the land use/cover change on the hydrologic regime of the Ramganga River basin at district Bareilly, Uttar Pradesh, India, a 31 years period from 1979 to 2009 was selected for which historical data was available. The present study area is confined to latitude 28°01′ to $28^0$54′ North and longitude 78°58′ to 79^o47′ East, covering an area of 4120 km^2. The Satellite images of the study area for three epochs (year 1979, 1990 and 2009) were acquired, analysed and classified under Settlements, Croplands, Forest/Plantations, Water Bodies, and Waste Land classes. The result indicated increasing trend of crop land (from 60.6% to 83.6%) and built up area (from 4.1% to 6.1%) and decreasing trend of vegetation and Plantation land (from 28.3% to 6%). We also calculated the Curve Number (CN) for study area under three AMC conditions. The values of CN-I, CN–II, and CN-III in the year 1979 were found to be 56.59, 75.63 and 87.71 respectively. Similarly, for the year 1990 and 2009, these values were calculated as 57.96, 76.65, 88.30 and 60.38, 78.40, 89.30 respectively. The runoff study at different land use systems of the Study area shows that the highest runoff occurs in the August month in the region followed by July and September due to monsoon season and also due to saturated soil moisture regime after onset of monsoon. The study shows the variation in runoff is highly but not only dependent on rainfall occurrence and their temporal variation throughout the months but also depends upon temporal LULC dynamics. As is evident from the fact that, despite receiving lesser monsoon rainfall (865.2 mm) in 2009 produced alarmingly higher runoff (221.9 mm) in comparison to 123.74 mm of runoff generated with higher monsoon rainfall received (950.52 mm) in 1990. Similarly the recharge pattern over the study area has been also found to be in reducing trend. The percentage recharge had an increasing trend during 1979-1990 but was found to be declining during 1990-2009. Also quantum of recharge was higher till 1999 than quantum of runoff, but the trend reversed and runoff volume surpassed the recharge volume from 1999 and beyond. This study has modelled the relationship between rainfall and runoff/Recharge under changing LULC dynamics by developing Neural Network model using LULC, Rainfall, and observed runoff data as input and predicted Recharge and Runoff as output. As part of the ANN model development, the data sets of 31years (1979-2009), were considered. The 70% of data was used as the training data while the remaining 30% was used as the testing and validation data. The observed data of Recharge (water table) has been used for cross validation. The simulated results of recharge reveal that with increase in settlement, and crop land at the cost of forest land, the recharge rate has decreased causing lowering of water table. Results of this study revealed that the developed ANN-based models were able to map relationship between input and output data sets used.

Keywords: Land use Land cover (LULC), CN, Runoff, Recharge, RS&GIS, ANN, Modelling, and Simulation.

CHAPTER - I

INTRODUCTION

The land use land cover change refers to the man made modifications afflicted upon the earth surface like riparian forest is converted to range lands or agricultural fields; agricultural fields are converted to build up area for residential or industrial purpose. Though such alteration on the land surface was being done regularly by the humans for their food and other essential needs for centuries, but it has been very intense during the recent past. It has been observed that the rate of conversion was significant but slow during 1700-1850. However after 1850, the pace of conversion quickened and particularly from 1990 onwards the expansion of croplands was very rapid in many parts of the world. By the final quarter of the twentieth century, the transformation of the Earth's land had become staggering in scale (Ramankutty and Foley 1999; and Tian et. al. 2014). Land surface with various land use and land covers provides the catchment area for all our surface water and ground water resources. Land use and land cover influences catchment hydrological responses (The hydrologic regime) by partitioning rainfall between return flow to the atmosphere as evaporation and transpiration ("green water") and flow to aquifers and rivers ("blue water") (Hope et al. 2003). The hydrological process that converts net precipitation to surface runoff and ground water recharge depends upon the soil type, topography, LULC type, and rainfall characteristics (Kumar C.P. 1993). Water is constantly circulated between earth and atmosphere. This global circulation is accomplished by the heat of the sun and the pull of gravity. During precipitation, some of the moisture is evaporated back into the atmosphere before reaching the ground. Some precipitation is intercepted by plants, a part of it infiltrates the ground, and the remainder flows off the land into lakes, rivers or oceans. Some may be directly evaporated if adequate transfer from the soil to the surface is maintained. This occurs where a high groundwater table (free water surface) is within the limits of capillary transport to the ground surface. Water that is infiltrated replenishes soil moisture deficiencies and enters storage provided in groundwater reservoirs, which in turn maintains dry weather stream flow. Water that is stored in depressions eventually evaporates or infiltrates into the ground. Surface runoff reaches minor channels (gullies, rivulets and the like), flows to major streams and rivers and finally reaches the ocean. Along the course of a stream, evaporation and infiltration can also occur

(Viessman et al., 1989).The spatial variation in topography, geology, and land uses cause significant local variations in water quality and quantity. Various studies (Sikka et.al.1998; Ramesh 2001; Idrisi et. al. 2000; Garg et. al. 2012; Mutie et. al. 2006; Kumar B.M. 2005; Panahi et.al.2010; Ashagrie et.al.2006; Mohan and Shrestha 2000) indicate that conversion of natural forest to other land uses like agriculture and plantation have lead to soil compaction, reduced infiltration, lesser ground water recharge and discharge, and excessive runoff. The above said changes will impact the functional characteristics such as catchment yields, infiltration rate, nutrient transfer, dissolved organic carbon etc. in the catchment scale causing reduction of perennial streams to seasonal one and disappearance of water bodies (Ahmad et al 2008). It has been observed that the hydrological characteristics are inextricably entwined and complexly related with the type of LULC present in the catchment. This requires understanding of hydrological components and their relation to LULC dynamics. Researchers have used various techniques to establish relationship between land use land cover types and hydrological responses (Panahi et al 2010). A clear cut understanding about the factors causing land use land cover changes is very essential to improve the hydrologic regime in a basin. The hydrologic responses can be estimated by determining land use changes using temporal remote sensing data and traditional approaches. The traditional approaches account spatial variability by dividing a basin into smaller geographical units and aggregating the results to obtain a simulation for the basin as a whole.

Remote sensing and GIS techniques are used to determine some of the model parameters like basin geometry, drainage network, land use land cover, soil moisture, topography, soil maps, rainfall distribution etc. Both monitoring and modelling approaches are used for conjunctive investigation of surface water and groundwater. The monitoring approach is expensive and time demanding yet measuring actual changes in stream and groundwater levels over time may lead to more direct estimates of the impact of land development on both surface and subsurface flows. Models are used in land change science to help improve our understanding of the dynamics of land-use, to make predictions and/or evaluate scenarios for use in assessment activities (Brown et al., 2004). Since 1972, the LANDSAT satellites have provided repetitive, synoptic, global coverage of high-resolution multispectral imagery. Their long history and reliability have made them a popular source for documenting

changes in land cover and use over time (Turner et al., 2003) and their evolution is further marked by the launch of LANDSAT 7 by the US government in 1999. Multispectral Scanner (MSS) data from the U.S. Geological Survey's (USGS) EROS Data Centre (EDC) has provided a historical record of the Earth's land surface from the early 1970s to the early 1990s. According to the Modified UNESCO Classifications scheme, there are only about 157 different land cover types and no study site will have all of those different land cover types (GLOBE toolkit, 2003). Hence, it will be necessary to group pixels together into a smaller number of closely related "classes", based on spectral similarity. This is done in a process known as "Classification". Similar to gray scale, bright regions of colour composite images have high reflectance, and dark areas have low reflectance. However, interpretation may get difficult when we combine different bands of data to produce what is known as false-colour composites (Engineering manual, 2003). But this can be addressed by using field knowledge of the areas and historical information. There are numerous approaches to characterizing land cover change. Each one of it has a set of strengths and weaknesses and as a result no single approach is optimal for all types of landscapes and land cover features (EPA, 1999). There are two major approaches of classification of remotely sensed images for various applications. In a supervised classification, the software is "trained" to recognize that certain types of pixels represent specific land cover types. Knowledge of the area and information collected during field work are important inputs, which are used by the software to classify the pixels into similar groups based on sample signatures specified. In an unsupervised classification, or "clustering", the desired number of groups, or "clusters", will be inputs to the software (GLOBE toolkit, 2003). The software then groups the pixels according to similar spectral characteristics in order of decreasing brightness. These groupings are not made on the basis of land cover, but on the similarity in spectral characteristics of the pixels. It is also common to come across a third approach known to be hybrid classification that combines both supervised and unsupervised classification techniques.

GIS is a valuable tool for use in parameterization of large scale physically based distributed models. A number of models like SWAT, SWRRB, FESHM, MIKESHE, MODFLOW, etc. and MATLAB, SPSS, SCS Curve Number and Water Budget Equation are commonly used in the study. Through the modelling approach, interaction between surface water and groundwater is investigated by; (1) developing

an integrated surface-groundwater model (Bouraoui et al., 1997; Jayatilaka et al., 1998; Yu 1998); (2) linking an existing groundwater model with a surface model (Ramireddygari et al., 2000; Ross et al., 2005); or (3) using packages of existing groundwater models (Pucci and Pope, 1995). Modular Three-Dimensional Ground-Water Flow Model (MODFLOW) is the most widely used and supported groundwater model (Anderson and Woessner, 1992). MODFLOW has been used to simulate the effects of pumping or land development on groundwater discharge rates to streams. A study by Morgan and Jones (1995) showed that decreased recharge in urbanizing areas had a direct effect on groundwater discharge rates to streams and springs. The effect of past and future human-caused changes to the groundwater system was estimated by Morgan and McFarland (1994) using MODFLOW. The results indicated that combination of reduced recharge and increased groundwater draft reduced discharge to rivers and streams. In addition, linkage between MODFLOW and existing surface models such as Hydrological Simulation Program, FORTRAN (HSPF) and Soil and Water Assessment Tool (SWAT) has also been developed to consider surface water and groundwater interactions because MODFLOW does not have a surface modelling component (Ross et al., 2005; Sophocleous et al., 1999).

During the last decade empirical modelling has received an important boost due to advancements in the field of machine learning. It can be said that now it has become a well-developed tool and thus deserves a special name, “data-driven modelling” (Solomatine et al 2008). Data-driven modelling (DDM) is based on the analysis of all the data characterizing the system under study. A model can then be defined on the basis of connections between the system state variables (input, internal and output variables) with only a limited number of assumptions about the "physical" behaviour of the system. The methods used nowadays can go much further than the ones used in conventional empirical modelling: they allow for solving numerical prediction problems, reconstructing highly non-linear functions, performing classification, grouping of data and building rule-based systems (Remesan and Mathew 2016). Data-driven modelling has been developed with the contributions from artificial intelligence, data mining, knowledge discovery in databases, computational intelligence, machine learning, intelligent data analysis, soft computing, pattern recognition, etc. Data Driven Models rely solely on previous hydrological and meteorological data without directly taking into account the underlying physical

process (Pandey and Srinivas 2015). We see data-driven modelling as a modelling approach which focuses on using the machine learning methods in building models of physical processes. These models can complement or replace the "knowledge-driven" models describing behaviour of physical systems. Examples of the most popular methods used in data-driven modelling of hydrological systems are: statistical methods, artificial neural networks and fuzzy rule-based systems.

It is hoped that this study will provide information for decision makers and development practitioners about the magnitude and dimensions of long term land use and land cover changes, their impacts and mitigating strategies in the study areas and the surroundings. The Bareilly district falls under the Rāmgangā Basin. The land use / Land cover pattern of this area has also undergone significant alteration and thus have problems of depletion in groundwater reserves, reduction in groundwater recharge, and increased soil erosion. The structural changes in basin ecosystem are making greater impacts on perennial streams, Ponds and the water bodies. The continuous, non-judicious use of fertilizers and land management practices are leading to water logging and poor soil health. Due to increase in human population and also due to socio-economic compulsions the resulting changes in land use dynamics are making adverse impact on hydrology of the area. It has now become necessary to understand the various factors governing hydrological variables in the study area for formulating effective environmental policies, development activities and management strategies. Also, based upon the information generated, issues that need immediate attention could be identified and prioritized. To achieve this goal the research work has been planned with the following objectives:

Objective:

1. To characterize and quantify land use and land cover changes in a watershed area of Rāmgangā river Basin.
2. To estimate the hydrological parameters like runoff and ground water recharge on different land use and land covers.
3. To develop suitable model for assessment and prediction of impacts of land use and land cover changes on runoff and ground water recharge.
4. To test and validate the developed model.

CHAPTER - II

CHAPTER - II

REVIEW OF LITERATURE

The purpose of this chapter is to review and summarize available literature related to the work on effects of land use land cover change on hydrologic regime that has been carried out by different researchers and organizations in India and abroad. These studies have revealed the nature and extent of progress made and also difficulties encountered. An attempt has been made to present the observations of various researchers in brief as per the following:

2.1 Land Use and land cover dynamics:

India has experienced significant loss of grass lands/shrub lands and forests in favour of expansion in crop lands and built up area during 1880-2010. A total of 26 million hectare forest (from 89 million ha in 1880 to 63 million ha in 2010) and 20 million hectare of grass lands/ shrub lands (from 45 million ha in 1880 to 25 million ha in 2010) has decreased in India. In contrast the total crop land area has increased by 48 million ha (from 92 million ha in 1880 to 140 million ha in 2010). The built up area has increased fivefold from 0.46 million ha to 2.04 million ha during 1880-2010. (Tian et al 2014). India's land resources consists of 329 million ha geographical area (only 2% of the world) and has only 4% of the world's fresh water resources to cater its population's need accounting for 16% of the world population. It receives a total of about 4000 BCM precipitation annually. Out of this about 1123 BCM is utilizable with 690 BCM as surface water and 433 BCM as ground water (Singh, 2013). With rapidly growing population and their improving living standards, the LULC changes are bound to be faster and would cause increased pressure on our already scarce water and other natural resources. The per capita availability of water resources is reducing by every passing day (Mishra et. al. 2014). Land use and land cover dynamics comprises of the processes such as accelerating the significant changes influenced by human actions with consequences involving changes that impact humans. These dynamics cause the availability of various biophysical resources including soil, vegetation, water, animal feed. The Land-use and land-cover changes are one of the

main human induced activities altering the groundwater system. Nevertheless, the impact of future land-use changes on the groundwater system has not been investigated extensively. Throughout the entire history of mankind, intense utilization of land resources by human has resulted in significant changes of the land-use and land-cover Calder (1993). Riebsame *et al.* (1994), Meyer and Turner (1994) have reported that a close relationship has been noticed in land use and land cover as these are complimentary to each other. It has been found that land use affects land cover and changes in land cover affect land use. Sahin and Hall (1996); DeFries and Eshleman, (2004) reported that the changes in land cover and land use alter both runoff behavior and the balance that exists between evaporation, groundwater recharge and stream discharge in specific areas and in entire watersheds, with considerable consequence for all water users. Elke *et al*. (2004) have revealed that the land-use and land-cover changes affect ecological landscape functions and processes. Results showed that, between 1945 and 1998, land-cover changes correlated with the physical attributes of the underlying landscape. Gregersen *et al.* (2004) found a major change in land use pattern and high groundwater abstraction leading to drinking water crisis especially during the premonsoon period. Mustard and Fisher (2004) have highlighted the complex relationship between land use change and hydrology, with linkages existing at a wide variety of spatial and temporal scales; however, land use change unquestionably has a strong influence on global water yield. Land cover and land use directly impact the amount of evaporation, groundwater infiltration and overland runoff that occurs during and after precipitation events. Farley *et al.* (2005) reported that the amount and type of vegetative land cover is one determinant of the water yield of a drainage basin. Forests produce higher rates of evapotranspiration and interception (the storage of water on leaf surface) than do grass or shrublands, all of which influence the amount of water that is available for direct drainage into streams or for aquifer recharge. Scanlon *et al.* (2005) hypothesized the conversion of natural rangeland ecosystems to agricultural ecosystems impacts the subsurface portion of the hydrologic cycle by changing groundwater recharge and flushing salts to underlying aquifers. Replacement of rangeland with agriculture changed flow directions from upward (discharge) to downward (recharge). Wang Genuxu *et al.* (2005) reported that land use and land cover changes have a great impact on the regional hydrological process. Boulain *et al*. (2006) reported that rain deficits have coincided with increased water runoff, meaning less water availability for the vegetation. Conversely,

changes in vegetative cover have had strong repercussions on the hydrologic cycle. Scanlon *et al.* (2006) reported that LU/LC changes such as deforestation increased recharge. Changes from natural grassland and shrub lands to dry land (rain-fed) agriculture altered systems from discharge (evapotranspiration, ET) to recharge. The impact of LU change was much greater than climate variability in Niger (Africa), where replacement of savanna by crop lands increased groundwater recharge even during severe droughts. Sensitivity of recharge to LU/LC changes suggests that recharge may be controlled through management of LU. Joshi (2006) revealed that soil under different land use system viz; bare land and open forest are highly susceptible to surface runoff, soil and nutrient loss. He found that vegetative barriers and grass lands are important conservative measure necessary to minimize losses. Dams *et al.* (2007) stated that Land-use change and climate change, along with groundwater pumping are frequently indicated to be the main human-induced factors influencing the groundwater system. They found that there would be adverse impact due land-use changes in the near future, (from 2000 until 2020), on the groundwater quantity and the general hydrologic balance of a sub-catchments of the Kline Nete, Belgium. Sikazwe (2008) reported that the impact of land use change on groundwater quantity in Shentou spring basin is a general decrease in spring discharge. This decrease is a consequence of reduced precipitation recharge due to continuous variations in the spatial patterns of land use and land cover in the basin such as cultivation and construction in the area. Temporal scale is another important aspect of land use impacts, as it determines the perception of the impact as well as the economic cost associated with it. Two aspects are important with regard to temporal scale of land use impacts. First, the time it takes for a land use to have an impact on downstream uses, and, second, in the case of negative impacts, the time it takes for remedial measures to take effect, if the impact is reversible. The temporal scales of land use impacts vary widely. Depending on the impact, they may range from less than one year, as in the case of bacterial contamination, to hundreds of years, as in the case of salinity. Similarly, time scales of recovery from adverse impacts are very diverse, depending on the impact. However, in most cases, the time it takes to restore an aquatic system after an adverse impact is much longer than the time it takes for an impact to appear (Peters and Meybeck, 2000, Hu et.al 2009).

2.2 Remote sensing and Geographical information system:

Remote sensing (R.S.) has played a major role in watershed research and hydrological sciences (Engman, 1995). Land cover informations derived from remote sensing are being used in a variety of hydrological modelling studies (Sekhar and Rao, 2002). The addition of geographical information system (G.I.S.) technology has further enhanced these capabilities and added confidence in the accuracy of modelled watershed conditions (Bhuyan et al, 2003). Several studies have utilised R.S. and G.I.S. with hydrological modelling for accessing the impacts of LULC change to the hydrological response of water shed. Olorunfenic (1983) has the view that satellite remote sensing technique developed, have proved to be of immense value for preparing accurate land use land cover maps. Petchprayoon et al (2010) conducted the study on hydrological impacts of land use/land cover change in a large river basin in central–northern Thailand. From the results of the study, it was concluded that the Satellite remote sensing is useful in classifying and studying LULC and detection of change in the Yom watershed. The area was subjected to urbanisation and this was mainly at the expense of agricultural area. Higher resolution satellite imagery was found helpful in identifying subclasses on LULC, especially in urban areas. A slight increase occurred concurrently in the long term discharge with changes in LULC, especially an increase in urban areas and a decrease in forested areas. The relatively small increase in the coverage of urban areas may have had a disproportionally large impact on discharged behaviour (mean and extreme flow) due to the location of these LULC changes adjacent to the banks of the Yom River. Vijaindra et al (2009) evaluated the efficacy of GIS application in evaluating LULC change and its impact on Hydrologic regime in Langat River Basin, Malaysia. He employed an integrated methodology for searching and forecasting a catchment's area hydrologic response with the use of HEC HMS model and satellite remote sensing techniques. The preliminary results denoted the crucial role of urban sprawl phenomenon in the increase of runoff rate within the spatial limits of a catchment area and highlighted the importance of searching land use regime with the use of satellite remote sensing imageries. It was proved that the incorporation of multi-temporal remote sensing data in hydrological models can effectively support decision making in the areas of risk and vulnerability assessment, sustainable development and general management before and after flood events. In addition, the implementation of CA–Markov

provided indication of the potential impact of land use change on flood vulnerability in the near future. Idrissi et al. studied the impact of long-term land use change on the hydrological regime of Dyle catchment(Belgium) using a distributed hydrological model coupling with the GIS for the land use dynamics. They found that the change in hydrological behavior in terms of the historical land use change is attenuated by the presence of compensating effects within the changing land use patterns. However, if the sector development plan (SDP) is executed, urbanization will increase by up to 21% of the total area, and thereby the flooding risk, even if rainfall events with a small return period occur. Idrissi et al. studied the impact of long-term land use change on the hydrological regime of Dyle catchment (Belgium) using a distributed hydrological model coupling with the GIS for the land use dynamics. They found that the change in hydrological behaviour in terms of the historical land use change is attenuated by the presence of compensating effects within the changing land use patterns. However, if the sector development plan (SDP) is executed, urbanization will increase by up to 21% of the total area, and thereby the flooding risk, even if rainfall events with a small return period occur. Daniel et al. (2002) have used five methods for detecting and classifications cross tabulation cross correlation analysis for comparing the land use system land cover change. They reported no single approach being totally reliable in solving land use change detection work. An analysis of land use and land cover changes using land use map and MSS LANDSAT data revealed that land use land cover could be evaluated by using Remote Sensing for calculating index of changes. Dimyati (1995), investigated the advantage of remote sensing techniques in relationship to field survey in providing a regional description of vegetative cover. The results were used to produce future vegetation cover maps that provided valuable information on spatial and temporal distributions of vegetation.

2.3 Impact of land use / land covers change on surface runoff, peak flow:

The impact of LULC change on runoff depends upon ET characteristics of cover present, water infiltration and water holding capacity of soil and ability of plant cover to intercept moisture. Surface runoff may increase due to change in land use if the infiltration capacity of soil is reduced. Sub surface flow/ Base flow may increase after trees are cut down (Bruijnzeel 1990; and Alansi 2009). Relative increase in storm flow after tree removal is smallest for large events and largest for small events.

Because, as the amount of precipitation increases the influence on storm flow due to soil and plant cover diminishes (Bruijnzeel, 1990; Brooks et al 1989; and Panahi et. al; 2010). The change in land cover from lower ET to higher ET will lead to decrease in annual stream flow. Conversely a change from higher ET plants to lower ET plants will increase the mean surface runoff. Reduction in forest cover increases water yield (Bosch and Hewlet, 1982; and Calder 1992.). Similarly, because of urbanization, the built up area increases resulting decreased infiltration and ground water recharge. Also demand for various industrial and domestic needs increases resulting over exploitation of water resources particularly ground water. The study has confirmed about drying up of interfluves in Budaun city and depletion and degradation of ground water in Aligarh district in Uttar Pradesh. (Ahmed et. al.2003). Urbanization also increases peak runoff and causes flooding. The ground water recharge also decreases (Singh, 2013). Garg et el (2012) studied the impact of LULC change on hydrological regime of Asan River watershed situated near the capital city of Uttarakhand i.e. Dehradoon. As the capital and plane region of hilly state Uttarakhand, the Dehradun city is favorable spot for industrialization. Even, Government of Uttarakhand has taken steps to develop industry in Dehradun city for economic growth of the state. Thus, huge industries are established and number of industries are being constructed in this area. It was noted that wherever, built-up area increases runoff potential increases. Such change in hydrology may lead to urban flooding in years to come in the region. Moreover, the industrialization in the region has been taken place along tributaries of river Asan, which may lead to pollution and deteriorate the quality of water. In larger basins the impact on peak flow are often offset due to time lag between different tributaries and rain fall variations in the watersheds. This de-synergic effect often leads to lesser peak discharge in the whole water shed though total storm flow will be higher due to land use changes in individual sub-watersheds. (Bruijnzeel 1990; Brooks et al 1991; Garg et al 2012; Mutie et al 2008, and Swingly et al 2012. Alansi (2009) studied the effect of development and land use change on rainfall-runoff and runoff-sediment relationship under humid tropical condition at Bernam watershed, Malaysia. In the studied area and for the studied period 1989-1998, the land use pattern has undergone significant change. The Oil Palm and Urban area increased while the same proportion of rubbr area reduced. The change of land use altered the rainfall-runoff and runoff-sediment relationship. More soil and water

loss occurred in 1990 due to increase in deforestation and urbanization. He used double mass curve analysis technique.

2.4 Impact of land use / land cover change on base flow/dry season flow:

The effect of LULC change on dry season flow depends on several competing processes, most notably the change in ET and infiltration capacity. In tropical areas afforestation may lead to decreased dry season flow due to increased ET (Thanapakpawin et al 2006, Kiersch, 2000). The study conducted at Chi river basin, Thailand has reported a decrease in dry season flow by 1.70% when 10% of forest area is converted to farm land. Similarly an increase in dry season flow of 2.20% was observed when 12% of farm land is converted to forest land (Homdee et. al. 2011). Most experimental evidences in rainfall dominated regimes suggest that forest removal or establishment of lower ET plants in place of higher ET plants increases dry season flow (Brooks et al. 1991). In contrast dry season flows from deforested land may be comparatively lesser if the infiltration capacity is reduced, e.g. through use of heavy machinery (Bruijnzeel, 1990). The study carried out in Minab catchment, Iran, has established that reduction of area under forest cover and rangelands from 45% to 8% of the total catchment area undergone between 1976-2002 caused a decrease in base flow due to reduced infiltration (Barkhordari, 2003). Also Idrissi et al. 2000; studied the impact of long-term land use change on the hydrological regime of Dyle catchment Belgium, using a distributed hydrological model coupling with the GIS for the land use dynamics. He observed that the change in hydrological behaviour, in terms of the historical land use change is attenuated by the presence of compensating effects within the changing land use patterns. However, if the proposed sector development plan (SDP) is executed, in which the urbanized area will increase by up to 21% of the total area, and thereby the flooding risk, even if rainfall events with a small return period occurs.

2.5 Impact of land Use / land Cover change on Ground water recharge:

The ground water recharge may be increased or decreased as a result of changing land use practices. The major contributing factors are ET of vegetation cover present and infiltration capacity of the soil. The water table may rise as a result of decreased ET e.g. after logging or conversion of forest to grassland for grazing. Recharge may also

increase due to an increased infiltration rate e.g. through afforestation of degraded areas. In contrast the water table may fall as a result of decreased infiltration rate e.g. through non-conservation farming practices and compaction (Tejwani,1993). Also heavy grazing may lead to reduced infiltration and ground water recharge (Chomitz and Kumari, 1996). If the infiltration capacity is substantially reduced, it can lead to water shortage in the dry seasons even in regions where precipitation is usually in abundant, like in case of Cherapunji region, India, (FAO,1999). The effects of farming system type on in situ ground water recharge and quality was conducted in the hilly area of North east India where it was found that the ground water recharge in case of newly developed live stock based farming system is highest (99.40%), where as it was 82.30% in Bun method and 77.40% in shifting cultivation (Sharma, 2001), estimated the ground water recharge pattern under different land covers and landscapes present at a study site in parts of western ghat, Karnataka, India has observed higher groundwater recharge in the forest and afforested land than degraded land (Purandara et. al. 2010). Cho.et al 2008, also observed in his study carried out in Virginia watershed, USA that increase in urbanization had adversely affected the ground water recharge rates and stream flows. Mc. et al (2007), conducted the study on impacts of vegetation cover change on regional climate in Australia. The results indicated that replacing the native woody vegetation with crops and grazing in southwest Western Australia and Eastern Australia has resulted in significant changes in regional climate, with a shift to warmer and drier conditions, especially in southeast Australia, the nation's major agricultural region. The simulated changes in Australia's regional climate suggest that LCC (Land Cover Change) is likely a contributing factor to the observed trends in surface temperature and rainfall at the regional scale. The outcomes raise important questions about the impact of LCC of Australia's regional climate, and highlight a strong feedback effect between LCC and the severity of recent droughts impacting on Australia's already stressed natural resources and agriculture.

2.6 Impact of land Use / land Cover change on water quality:

Surface water bodies are the potential recipients of contamination contained in surface runoff from their catchment. The chemical composition of surface water and its properties in a particular region is governed by natural process such as precipitation

rate, weathering process, soil erosion and anthropogenic processes like urban, industrial, and agricultural activities. Zamani, et al 2013; studied the impact of LULC changes on surface water quality in the Ziarat catchment, Golestan province, Iran. He reported that during last 45 years during 1967-2012, the area of forest decreased by 981.7 ha while areas under crop land-Range land increased by 657.18 ha and residential area increased by 84.28 ha leading to an increase in fertilizer and pesticide use, tilling practices on steep slopes, construction of access roads. This has caused dissolution of minerals like calcite showing increasing trend in EC values in in river discharge, reflecting a direct result of increased agricultural land use and built up in the river catchment. Ramesh (2001), conducted the study to know the effects of land use change on ground water quality in a coastal habitat of south India. Groundwater samples were collected from 22 locations for a one year period to evaluate the spatial and temporal variability in water quality. Concentrations of total dissolved solids (TDS) and some elements, including CI and Na, exceed the maximum permissible limits at some locations due to seawater intrusion. The concentration range of N 0 3 and NO_2 was 5-48 mg/1 and 0.23-2.13 mg/1, respectively. The elevated concentration of NO_3 in drinking water, are attributed to non-point sources, such as seepage from agricultural areas and effluent discharge from shrimp farms. Weatherhead and Howden (2009) studied the relationship between land use and surface water resources in the UK. He observed that while there is no absolute shortage of water resources across the UK as a whole, spatial and temporal variations already result in water stress across much of the south and east of England during dry summers. In the future, water stress is expected to become more widespread in response to population growth, increasing environmental protection and climate change. Surface water quality is reported to be improving at present, though there are doubts as to the adequacy of the monitoring coverage. To conserve usable water resources, land uses which increase evapotranspiration or rapid runoff should be discouraged, particularly in the south and east, and there need to be continuing efforts to maintain good chemical water quality in rivers and groundwater. Water resource constraints will limit opportunities to use irrigation as a counter to climate change, and will influence where irrigated production can be located. Sharma (2001) studied the effects of farming system type on in situ groundwater recharge and quality in northeast India. He found that Groundwater recharge was highest in newly developed land-use systems consisting of livestock-based, forestry, agripastoral, and agri-horti-silvi-pastoral; recharge as a

percentage of annual precipitation was 99.4%, 95.3%, 98.8% and 97.2%, respectively. In contrast only 82.3% and 77.4% of the annual precipitation was recharged in the traditional systems, the bun method and shifting cultivation, respectively. Groundwater quality exceeded permissible limits for pH, and nitrate, iron and aluminium concentration in some farming systems. The new systems retained more water in situ resulting in low movement of water and nutrients out of the system. The quality of the groundwater was affected by the land use, deforestation, and nutrient and pesticide application.

2.7 Hydrological Modelling:

Bouraoui et al. (1997) studied the influence of Surface cover and soil type upon groundwater recharge and groundwater quality in agricultural watersheds. In this study, ANSWERS, a distributed parameters surface nonpoint source model has been modified to include the simulation of water transport in the vadose and saturated zones. This model has taken into account the spatial and temporal variability of crop cover and management practices, and the spatial variability of soil type and rainfall distribution. It is physically based and uses parameters that can be easily determined from readily available soil and plant information. It has been validated at multiple scales: local scale, field scale and watershed scale. At the local and field scale, it predicts accurately drainage below the root zone and evapotranspiration on different type of soil cover. At the watershed scale, it reproduces well the piezometric levels and trends of groundwater level variation. Clark. (1973), found that with artificial neural network hydrological modelling solutions are best described under the lumped deterministic black box models. In this model river basin study is treated as a single unit and simulations are only the gross response of the system. French et al. (1992), used a neutral network to forecast rainfall intensity fields in space and time. On the other hand, Raman and Sunil Kumar (1995) used an ANN to synthesize reservoir in flow series for two sites in the Bharathapuha basin in South India. Hall and Minns (1993), also supported the idea advanced earlier for applying neural networks for small urban catchment area. However, his work was limited to small area as more emphasis was given for artificial neutral networks which of developed could serve for the real hydrological data. The problem needs to be addressed to rainfall-runoff modelling for effectiveness of modelling of the data documented. Hwang et al (2014),

This study applied three statistical downscaling methods: (1) bias correction and spatial disaggregation at daily time scale (BCSD daily); (2) a modified version of BCSD which reverses the order of spatial disaggregation and bias correction (SDBC), and (3) the bias correction and stochastic analog method (BCSA) to downscale general circulation model daily precipitation outputs to the sub-basin scale for west-central Florida. Each downscaled climate input dataset was then used in an integrated hydrologic model to examine differences in ability to simulate retrospective stream flow characteristics. Results showed the BCSD daily method consistently underestimated mean stream flow because the highly spatially correlated small precipitation events produced by this method resulted in overestimation of evapotranspiration. Highly spatially correlated large precipitation events produced by the SDBC method resulted in overestimation of the standard deviation of wet season daily stream flow and the magnitude/frequency of high stream flow events. BCSA showed better performance than the other methods in reproducing spatiotemporal statistics of daily precipitation and stream flow. This study demonstrated differences in statistical downscaling techniques propagate into significant differences in streamflow predictions, and underscores the need to carefully select a downscaling method that reproduces precipitation characteristics important for the hydrologic system under consideration. Jayatilaka et al. (1998), carried out study on a small catchment of a nine hectare experimental irrigation site in a shallow water table area in the Tragowel Plains, Australia, with the aim of quantifying the processes affecting surface drainage and groundwater levels. The irrigation site was intensively monitored to provide the required input and calibration data for modelling the physical processes. Simulation of flow processes, including infiltration, capillary rise, evapotranspiration, overland flow, groundwater ex-filtration and groundwater flow into the drain, was performed using the physically-based, distributed model MIKE-SHE. The model was calibrated against the observed piezometric levels, drain flow and soil moisture data collected over a 19-month period that represented different field conditions under seasonal changes. Model simulations were generally consistent with the observed data. However, the results highlighted inadequacies of the model, particularly in representing variations in rapid flow through macro pores that occur due to the cracking and swelling properties of the soil. Despite this deficiency, the modelling study allowed quantification of the effective flow processes and provided an insight into their implications in determining the quality (i.e. salinity) and quantity

of drain flow and groundwater levels. Loaiza et al assessed the effect of soil use changes on soil moisture regimes in mountain regions in spain. Two models were applied to the estimated water moisture regimes. The results of Jarauta simulation model (JSM) were found more precise than the results obtained from Newhall simulation model (NSM). Pucci and Pope. (1995), studied the effects on water resources in the Coastal Plain of New Jersey due to development activities undertaken through simulation modelling. The stream flow in the study area is primarily controlled by ground-water discharge. Ground-water flow in a 400 square mile area of the Potomac-Raritan-Magothy aquifer system (PRMA) in the northern Coastal Plain of New Jersey was simulated to examine development effects on water resources. Simulations showed that historical development caused significant capture of regional ground-water discharge to streams and wetlands. The aquifer outcrops are the principal areas of recharge and discharge for the regional flow system and have many traversing streams and surface-water bodies. A quasi-three-dimensional numerical model that incorporated ground-water/surface-water interactions and boundary flows from a larger regional model was used to represent the PRMA. To evaluate the influence of ground-water development on interactions in different areas, hydrogeologically similar and contiguous model stream cells were aggregated as 'stream zones'. Significant differences in simulated ground-water and surface-water interactions between the predevelopment and developed system, include; (1) redistribution of recharge and discharge areas; (2) reduced ground-water discharge to streams. In predevelopment, the primary discharge for the Upper and Middle aquifers are to low-lying streams and wetlands; in the developed system, the primary discharge is to ground-water withdrawals. Development reduces simulated ground-water discharge to streams in the Upper Aquifer from 61.4 to 10% of the Upper Aquifer hydrologic budget (28.9%, if impounded stream flow is included). Ground-water discharge to streams in the Middle Aquifer decreases from 80.0 to 22% of the Middle Aquifer hydrologic budget. The utility of assessing ground-water/surface-water interaction in a regional hydrogeologic system by simulation responses to development is demonstrated and which can compensate for lack of long-term stream-gauging data in determining management decisions. Querner (1999), studied the effect of human intervention in the Water Regime over the last 50 years in the Netherlands. The physically based ground water and surface water model SIMGRO was used. Changes in natural recharge of ground water and water tables were used as

indicators for the hydrological degradation. The results show that the natural recharge increases when water table is deep. Variations in meteorological conditions have pronounced effect on the natural recharge and the effect is greater than the changes caused. Ramireddygari et al (2000), reported the results of a comprehensive modelling study of surface and groundwater systems, including stream-aquifer interactions, for the Wet Walnut Creek Watershed in west-central Kansas. The main objective of this study was to assess the impacts of watershed structures and irrigation water use on stream flow and groundwater levels, which in turn affect availability of water for the Cheyenne Bottoms Wildlife Refuge Management area. The surface-water flow model, POTYLDR, and the groundwater flow model, MODFLOW, were combined into an integrated, watershed-scale, as a continuous simulation model. Major revisions and enhancements were made to the POTYLDR and MODFLOW models for simulating the detailed hydrologic budget for the Wet Walnut Creek Watershed. The simulated stream flows showed that watershed structures decrease both stream flows and groundwater levels in the watershed. The amount of water used for irrigation has a substantial effect on the total simulated stream flow and groundwater levels, indicating that irrigation is a major budget item for managing water resources in the watershed. Soliman. (2013), constructed a numerical groundwater model to evaluate the effect of switching to rotational groundwater withdrawal on mitigating excessive drawdown. In this regard, a MODFLOW package Visual MODFLOW 4.2 was utilized to simulate the proposed rotational withdrawal policy. The model was calibrated for steady state flow conditions and acceptable accuracy was achieved. The calibrated model was run under the rotational withdrawal policy for 3 years to predict the rate of change in groundwater drawdown. The obtained results were analyzed. Consequently, conclusions were deduced that the rotational withdrawal is a good policy to be adapted and the groundwater levels indicated a sustainable recovery throughout the prediction run period. Yu. (1998), in his study conducted at upper west branch of the Susquehanna River basin Pensylvania, to assess the response of subgrid hydrologic processes to atmospheric conditions using subgrid approach at a basin level via HMS. He found that HMS can account for the complexities of surface and subsurface hydrologic processes and can be driven by conventional weather and climate data, as well as output from three-dimensional meteorological and climatological models. It utilizes remotely sensed and digital data as a basis for quantifying the spatial variability in key parameters. The

model was applied using observed and MM5-simulated precipitation from a mid-latitude cyclone passing over the upper west branch of the Susquehanna River basin Pensylvania. The results suggest that the subgrid-scale spatial and temporal variability in some variables (eg. Soil moisture and precipitation) play an important role in simulating hydrologic response in large river basins.

CHAPTER – III

HYDROLOGICAL MODELS: THEORETICAL CONSIDERATIONS

3.1 Conceptual Description:

The concept of watershed modelling is embedded in the interrelationships of soil, water, climate and land use/ cover and represented through mathematical equations. The behaviour of each process is controlled by its own characteristics as well as by its interaction with other processes active in the catchment. The predominant hydrologic processes include rainfall, snowmelt, interception, evapotranspiration, infiltration, surface runoff, percolation and subsurface flow. The researchers have been actively involved in formulating various mathematical models to represent the various processes prevalent in the catchment. There is plethora of mathematical models available in literature. These models vary from empirical models for the evaluation of flood events to simple ones containing a certain degree of physicality, to stochastic models of various kinds and finally to the more recent distributed models. A brief summary of few prevalent models is presented below:

3.1.1 Lumped hydrologic models

The representation of hydrologic processes in lumped hydrologic models is usually very simplified; however they can often lead to satisfactory results, especially if the interest is in the discharge prediction only. None of such models is capable for representing all hydrologic processes required by the project. However, they can effectively solve partial project's tasks such as modeling the potential climate change impact on river basin, water balance or seasonal snow accumulation and melt. The following sections describe these models in more detail.

IHACRES

The IHACRES (Identification of unit Hydrographs and Component flows from Rainfalls, Evaporation and Stream flow data) model is the result of collaboration between the Centre for Ecology and Hydrology (CEM) Wallingford, UK and the Australian National University (ANU), Canberra (Jakeman et al. 1990). IHACRES employs a transfer function/unit hydrograph (UH) approach to the lumped hydrologic modeling. The allows the simulation of stream flow either continuously or for

individual events from basins of various sizes using any data time step equal or greater than 1 min. The model has minimum input data requirements (rainfall, stream flow (for calibration), air temperature or evapotranspiration (optional) and basin size). Geographic descriptive data (topography, vegetation, soils) are not required.

SRM

The SRM (Snowmelt-Runoff Model) model was originally developed by Martinec (1975) at the Swiss Snow and Avalanche Research Laboratory, US Department of Agriculture, Agricultural Research Service (USDA-ARS). The model is designed to simulate and forecast daily stream flow in mountainous basins where snowmelt is a major runoff component; SRM is a simple degree-day model that requires input in the form of basin or zonal snow cover extent, temperature, precipitation, and the area-elevation curve of the basin. Additional parameters such as forested area, soil conditions, antecedent precipitation, and runoff can be also provided. Snowmelt in each zone is predicted from air temperature, any rainfall is added on, and the total new water is routed through a single store (USDA-ARS, 1998). The model also includes loss coefficients (at half-monthly intervals) applied to be snowmelt and rainfall terms. There is no provision for sub-basins or land cover types.

WATBAL

WATBAL is an integrated water balance model developed for climate change impact assessment of river basin runoff. The model evolved from a DOS based version known as CLIRUN (Kaczmarek, 1993) to the present MS Excel add-in form (Yates and Strzepek, 1994). There are two main components within the model; first is the water balance component that uses continuous functions to describe water movement into an out of a conceptualized basin. The second component is the calculation of potential evapotranspiration using the Priestly-Taylor radiation approach. The soil moisture balance is calculated using a differential equation and storage is lumped as a single bucket. Snowmelt component is used for computing an adjusted effective precipitation. The model can be applied using daily or larger time steps and for any basin size. The input data includes precipitation, runoff and potential evapotranspiration (which can be also calculated internally, using temperature, mean monthly relative humidity and sunshine duration data). Model outputs include PET,

evapotranspiration, albedo, effective precipitation, surface and subsurface runoff. Some parameters of the model can be optimized.

3.1.2 Semi-distributed hydrologic models:

Several semi-distributed hydrologic models summarized in the following sections can be successfully used for simulating all hydrologic processes required by the project. The main advantage of semi-distributed models is that their structure is more physically-based than the structure of lumped models, and that they are less demanding on input data than fully distributed models.

HBV-96

The HBV-model (Hydrologiska Byrans Vattenbalansavdelning) is a general-purpose hydrologic model developed at the Swedish Meteorological and Hydrological Institute (SMHI). The HBV mode is a standard forecasting tool in nearly 200 basins throughout Scandinavia, and has been applied in more than 40 countries worldwide. The model is designed to run on a daily time step (shorter time steps are available as an option) and to simulate river runoff in river basins of various sizes. The basin can be disaggregated into sub-basins, elevation zones, and land-cover types. Input data include precipitation, air temperature (if snow is present), monthly estimates of evapotranspiration and melt in HBV is based on a simple accounting (degree-day) algorithm (SMHI, 2003). The existence and amount of snowfall is predicted using meteorological input data extrapolated to the mean elevation of each sub-area of the basin. A simple model based on bucket theory is used to represent soil moisture dynamics (Lindstrom et al, 1997). There is a provision for channel routing of runoff from tributary basins, using a modified Muskingum method. Outflow from lakes is usually specified by a stage-discharge rating curve but can be given by a lookup table to allow for power station operating rules. The HBV model can be linked with real time weather information and river monitoring systems.

HEC-HMS

The US Army Corps of Engineers (US-ACE) Hydrologic Engineering Center HEC-HMS (Hydrologic Modeling System) model is designed to simulate to simulate events continuously over long periods of time, using grid-cell depiction of the watershed (US-ACE, 2002). HEC-HMS is comprised of a graphical user interface, integrated

hydrologic analysis components, data storage and management capabilities, and graphics and reporting facilities (US-ACE, 2001). Infiltration losses can be simulated for event modelling by SCS curve, gridded SCS curve number, and Green & Ampt methods. The five-layer soil moisture accounting model can be used for continuous modelling of complex infiltration and evapo-transpiration environments (US-ACE, 2000). Excess precipitation can be transformed into surface runoff by unit hydrograph methods (Clark, 1945 and Snyder 1938), and SCS technique. A variety of hydrologic routing methods are included for simulating flow in open channels. Most parameters for methods included in sub-basin and reach elements can be estimated automatically using the optimization manager, Version 3.0. A new, substantial version written in Java will include additional reservoir capabilities for modelling interior flood zones, energy budget snow accumulation and melt, frequency curve generation, reservoir outlet structures, dam break, animated graphs of gridded precipitation and runoff results.

HSPF

The US Environmental Protection Agency (US-EPA) HSPF (Hydrologic Simulation Program-FORTRAN) program has its origin in the Standard Watershed Model developed by Crawford and Linsley (1966). Hydrocomp, Inc. Developed in its present form is a comprehensive, conceptual, continuous watershed simulation model designed to simulate all water quantity and quality processes that occur in a watershed, including sediment transport and movement of contaminants (Bicknell et al., 1997). It can reproduce spatial variability by dividing the basin in hydrologically homogeneous land segments and simulating runoff for each land segment independently. A segment of land can be modelled as previous or impervious. In pervious land segments HSPF models the movement of water along three paths: overland flow, interflow and groundwater flow. Snow accumulation and melt, evaporation, precipitation and other fluxes are also represented. Routing is done using a modified version of the kinematic wave equation. HSPF includes an internal database management system for input and output.

PRMS

The US Geological Survey (UsGS) PRMS (Precipitation-Runoff Modeling System) model is a modular-design, deterministic modeling system developed to evaluate the

impacts of various combinations of precipitation, climate, and land use on stream flow, sediment yields, and general basin hydrology (Leavesley et al., 1983). In PRMS a watershed can be divided into subunits based on basin characteristics (slope, aspect, elevation, vegetation type, soil type, land use, and precipitation distribution). Two levels of partitioning are available. The first divides the basin into homogeneous response units (HRU) based on the basin characteristics. The sum of the responses of all HRU's, weighted on a unit-area basis, produces the daily system response and stream flow for a basin. A second level of partitioning is available for storm hydrograph simulation. The watershed is conceptualized as a series of interconnected flow planes and channel segments. Surface runoff is routed over the flow planes into the channel segments; channel flow is routed through the watershed channel system. Output options include observed (if available) and predicted mean daily discharges, annual and monthly summaries of precipitation, interception, potential and actual evapo-transpiration, and inflows and outflows of the ground water and subsurface reservoirs. Parameter-optimization and sensitivity analysis capabilities are provided to fit selected model parameters and evaluate their individual and joint effects on model output.

SSARR

The SSARR (Stream flow Synthesis and Reservoir Regulation) model was developed by USGS North Pacific Division (USGS-NPD) to provide hydrologic simulations for the planning, design, and operation of water control works (USGS-NPD, 1991). The model consists of two modules, the snow computation module and the runoff analysis module. The runoff analysis module uses a single soil-moisture reservoir, which determines the percentage of available rainfall or snowmelt. For the snow computation module, SSARR computes snowmelt based on a temperature index approach or by a generalized snowmelt equation. The watershed can be divided into bands of equal elevation, on which snow accumulation and ablation, as well as soil moisture, are accounted for independently. The model time routine is flexible so that the time step may be set consistent with the data definition and project purpose. The hydraulic response of reservoirs, channel reaches, and backwater systems may be simulated individually or as components of a complex river system for study or real time operation. SSARR simulates all hydrologic processes required by the project. The original program runs of DOS and its input-output structure is very complex.

SAR Consultants have developed a GUI for the SSARR module and the product is sold under the name SSARRPC.

SWAT

The USDA-ARS SWAT (Soil and Water Assessment Tool) program was developed to predict the impact of land management practices on water, sediment and agricultural chemical yields in large complex watersheds with varying soils, land use and management conditions over long periods of time (Neitsch et al., 2005b). The latest version SWAT2000 has a comprehensive structure that models basically all hydrologic processes in the watershed. Basins can be subdivided into sub-basins to account for differences in soils, land use, crops, topography, weather, etc., Snow model allows the sub-basin to be split into a set of elevation bands. Snow cover and snow melt are simulated separately for each elevation band. The model offers three options for estimating potential evapotranspiration: Hargreaves, Priestley-Taylor, and Penman-Monteith. Surface runoff volume is computed using a modification of the SCS curve number method or the Green & Ampt infiltration method. Flow is routed through the channel using a variable storage coefficient method or the Muskingum routing method. The model also includes controlled reservoir operation, groundwater flow model and a weather generator daily values (precipitation, air temperature, solar radiation, wind speed and relative humidity) from average monthly values. A new Arc View interface, AVSWAT2000 (Di Luzio et al., 2002) provides a user-friendly GUI.

SWMM

The US-EPA Storm Water Management Model (SWMM) is a comprehensive dynamic hydrologic simulation model for analysis of quantity and quality problems associated with urban runoff (CHI, 2003). Both single-vent and continuous simulation can be performed on urban basins. Modellercan simulate all aspects of the urban hydrologic and quality cycles, including rainfall, snowmelt, surface and subsurface runoff, flow routing through drainage network, storage and treatment. Flow routing can be performed in the runoff, transport and extran blocks, in increasing order of sophistication. Extran block solves complete dynamic flow routing equations for accurate simulation of backwater, looped connections, surcharging, and pressure flow. The hydrologic simulation in the Runoff block uses the Horton or Green & Ampt equations where the data requirements include area, imperviousness, slope,

roughness, width (a shape factor), depression storage, and infiltration values for either the Horton or Green & Ampt equations for up to 100 sub-basins. The program is driven by precipitation for up to ten gauges (distributed spatially), and evaporation. Basic SWMM output consists of hydrographs and pollutographs at any desired location in the drainage system. The model performs best in urbanized areas with impervious drainage. The model lacks GUI, but various vendors have developed user-friendly GUIs.

TOPMODEL

TOPMODEL is a hydrologic model that bases its distributed predictions on an analysis of basin topography. The development of TOPMODEL was initiated by Michael Kirkby at the School of Geography, University of Leeds. The model was further developed by Keith Beven at the Lancaster University. Since 1947 there have been many variants of TOPMODEL but never a "definitive" version (Beven et al., 1995). The version described in report was developed at the Lancaster University, runs on DOS, and its source codes (in FORTAN) are in public domain. The model allows basins to be divided into a set of sub-basins. Evaporation is estimated by using the Penman-Monteith method. Surface runoff is computed based on variable saturated areas. The subsurface flow is calculated using an exponential function of water content in the saturated zone. Channel routing and infiltration excess are calculated using the Beven and Kirkby method. The spatial component requires a high quality DEM without sinks. There is an extensive coverage of TOPMODEL in the scientific literature.

3.1.3 Distributed hydrologic models

Distributed hydrologic models can provide the highest accuracy in the modeling of precipitation-runoff processes. Parameters of these models are fully spatially-varied at a given resolution and therefore require considerably more input data (often unavailable) than semi-distributed models. Most of the selected models described in the following sections can be used to address all project requirements.

CASC2D

CASC2D was originally developed at the US Army Research Office (ARO) funded Centre for Excellence in Geosciences at Colorado State University (Julien et al.,

1995). CASC2D is a fully-unsteady, physically-based, distributed-parameter, raster (square-grid), two dimensional, infiltration-excess (Hortonian) hydrologic model (Ogden, 1998). Major components of the model include: continuous soil-moisture accounting, rainfall interception, infiltration, surface and channel runoff routing, soil erosion and sediment transport. CASC2D can be used to simulate single events, or long periods of record at the users' discretion. A high-quality input data set is required for good model performance, and the quantity of input required is large. Continuous simulations require hourly input values of relevant meteorological and radiation variables, as well as Penman-Montieth evapotranspiration inputs (spatially-varied input maps of surface shortwave radiation albedo, vegetation height, canopy-average stomatal resistance, soil wilting point water content, and canopy shortwave radiation transmission coefficient). Also required are representative hourly estimates of air temperature, relative humidity, wind speed, and cloud cover. At present, there are two optional infiltration methods used in CASC2D (Ogden, 1998). The first is the traditional Green & Ampt approach. The use of this method requires input maps of soil porosity, saturated hydraulic conductivity, wetting-front suction head, and initial volumetric water content. The second method is an addition to the Green and Ampt approach that allows redistribution of soil water during inter-storm periods. Soil water redistribution requires two additional inputs, pore distribution index, and the soil water content at residual saturation. CASC2D can produce output maps of most hydrologic variables at user-specified intervals, including time-series maps of distributed soil surface moisture content surface water depth cumulative infiltrated depth channel flow depth channel and overland flow discharges overland flow erosion/deposition.

CEQUEAU

CEQUEAU is a distributed water balance model developed at the INRS-ETE (Institut National de la Recherche Scientifique, Eau, Terre et Environment). The model takes into account the spatial variability of basin physical characteristics by sub-dividing it into elementary representative areas, called "whole squares" (Morin, 2002). The characteristics required for each whole square are altitude and the percentage of forested area, lakes and marches. Whole squares are further sub-divided into "partial squares" according to sub-basin divides, which allows the formation and evolution of stream flow in time and for proper routing of runoff (St-Hilaire et al., 2000). Data

required for each partial square are direction of water flow and its percentage with respect to the sub-divided whole square. The hydrologic model performs two main functions. First the production functions, to quantify vertical movement of water. This function is modelled by a series of interconnected reservoirs representing different components of the hydrologic water balance (rainfall, snow accumulation and melt, evapo-transpiration, water in the unsaturated and saturated zones, and lakes and marshes). The production function calculates volumes of water in each whole square. Second, i.e. the transfer function then routes these volumes downstream from one square to the other. The water volume available in a partial square is obtained by multiplying the volume produced on a whole square by the percentage of area occupied by the partial square. This volume is added to volumes entering a given element from other partial square(s) located directly upstream. The routing process is repeated from one element to the next up to the exit of the watershed. The routing of each partial square is related to the hydraulic characteristics, and to the storage capacity of the drainage network. The adjustment of model parameters is done by trials and errors or by optimization. Temporal data required by CEQUEAU include maximum and minimum air temperatures, liquid and solid precipitation, and observed stream flow for the calibration period. The model provides outputs for daily rain, mean daily temperature, snow accumulation, mean daily snowmelt, daily evaporation, and modelled discharge. The CEQUEAU model allows real time stream flow forecasting for short and mid-term with or without updating. The model was applied in sixty watersheds in the province of Quebec ranging from 1 to 100,000 km^2. Some applications involved the determination of probable maximum floods (PMF). CEQUEAU model is presently used on a regular basis for real time forecasting by some institutions in the Province of Quebec (Morin, 2002).

GAWSER/GRIFFS

GAWSER (Guelph All Weather Sequential Event Runoff) model was developed to predict stream flow from rainfall and snowmelt precipitation events. The model was applied in the Grand River Watershed, where it gradually evolved into a real-time flood forecast model GRIFFS (Grand River Integrated Flood Forecasting System). The Grand River Conservation Authority (GRCA) uses GRIFFS to make flood forecasts and test reservoir operations during floods, to estimate design flows for floodplain mapping and to test the impact of land use changes on stream flow.

GRIFFS is capable of modelling single or multiple events and has provisions for recovery between events. The model includes temperature based snowmelt routines, distributed snow pack model, modified Green and Ampt infiltration model, Muskingum-Cunge channel routing, overland flow area per time curve routing and sub-surface flow routing (Boyd et al., 2000). The model provides comparison plots and statistics for observed and simulated flows at stream flow locations, detailed output of runoff calculations, a forecast summary which includes the forecast peak flow and time of peak flow at selected points of interest, reservoir storage forecast peak and time of peak, forecast peak inflows to reservoirs, automatic conversion of forecast flows to forecast levels for specified points of interest, summary table of when flooding is expected to start and stop at a given point of interest, summary table of parameter setting and full water balance. The model has shown excellent results on the Grand River Watershed. Future improvement to this model will focus on incorporation of real-time weather radar and numerical weather model precipitation information and integration with GIS (Boyd, et al., 2000).

HYDROTEL

The INRS-ETE's HYDROTEL is a spatially distributed hydrologic model with physical bases specifically developed to facilitate the use of remote sensing and geographical information system data (Fortin, 2000a). The program has a modular structure allowing easy addition or modification of algorithms. The complete drainage structure of a watershed is obtained with PHYSITEL, a module designed specifically to prepare the watershed database for HYDROTEL. The spatial variability is in HYDROTEL modeled using relatively homogeneous hydrologic units (RHHU). Daily snowmelt and accumulation are estimated by a modified degree-day method in which the energy budget at the snow-air interface is estimated by the degree-day approach but that within the pack by a more physical approach. Four equations are available to estimate potential evpotranspiration (Fortin et al., 2000a): Thornthwaite, Linacre, Penman-Monteith and Priestley-Taylor. The vertical water budget is simulated by the vertical algorithm of the CEQUEAU model or by a new algorithm more suited to remote sensing and GIS information (BV3C method). A kinematic wave approach is used to estimate downward flow from cell to cell, whereas river routing is simulated with the kinematic or diffusive wave equations. HYDROTEL has only few parameters that are influenced by the change in time step. This allows the

model to be first calibrated using daily data, and then the calibration obtained with daily data may be adjusted for simulations with shorter time steps. HYDROTEL has been applied in watersheds located in Quebec, Ontario and British-Colombia (Fortin et al., 2000b).

MIKE11/SHE

MIKE11 is a commercial engineering software package developed at the Danish Hydraulic Institute (DHI). The model is a dynamic, one-dimensional modeling tool based on an integrated modular structure with a variety of basic modules and add-on modules, each simulating certain phenomena in river systems. MIKE11 includes basic modules for rainfall-runoff, hydrodynamics, advection-dispersion, water quality and sediment transport. The rainfall-runoff module contains three different models that can be used to estimate runoff (DHI, 2000a): 1) the continuous simulation (NAM) module, a lumped, conceptual rainfall-runoff model that simulates overland flow, interflow and base flow; 2) the UHM module that simulates the runoff from single storm events by the use of unit hydrograph technique; 3) SMAP, a monthly soil moisture accounting model. A global optimization routine called the Shuffled Complex Evolution algorithm optimizes the model parameters. The Hydrodynamic module uses an implicit, finite difference computation method for modelling of unsteady flows in rivers and estuaries. Other extensions are the Dam break module, the Structure Operation module or the MIKE11 GIS, an Arc View-based application that provides both a spatial data and visual representation of MIKE11 various outputs MIKE112 can be coupled with MIKESHE, integrated, physically based, fully distributed, modular, dynamic modelling system, the DHI version of the original SHI (Systeme Hydrlogique European) program developed through a joint project of CEH Wallingford, Danish Hydraulics Institute and SOGREAH (France). The model is applicable on spatial scales ranging from single soil profiles (for infiltration studies) to regional watershed studies. MIKESHE includes all of the processes in the land phase of the hydrologic cycle: precipitation (rain or snow), evapo-transpiration, interception, overland sheet flow, channel flow, unsaturated sub-surface flow and saturated groundwater flow. Evapo-transpiration is calculated using the Kristensen and Jensen method. MIKESHE's overland-flow component includes a 2D finite difference diffusive wave approach using the same 2D mesh as the groundwater component. MIKESHE includes a traditional 2D or 3D finite-difference groundwater

model. There are three options in MIKESHE for calculating vertical flow in the unsaturated zone: the full Richards equation, a simplified gravity flow procedure vertical and a simple two-layer water balance method for shallow water tables (DHI, 2000b). MIKE11/SHE product is the most widely used hydraulic modelling system in the world and has been approved for use by regulatory authorities in many countries including USA, Australia and UK (DHI, 2003).

3.1.4 Data driven Modeling

In hydrology different types of models are used such as physical or scale models, mathematical models, lumped conceptual models, distributed physically based models, empirical models. During the last decade the area of empirical modeling received an important boost due to developments in the area of machine learning. It can be said that it now entered a new phase and deserves a special name – data-driven modeling.

Data-driven modeling (DDM) is based on the analysis of all the data characterizing the system under study. A model can then be defined on the basis of connections between the system state variables (input, internal and output variables) with only a limited number of assumptions about the "physical" behaviour of the system. The methods used nowadays can go much further than the ones used in conventional empirical modeling: they allow for solving numerical prediction problems, reconstructing highly non-linear functions, performing classification, grouping of data and building rule-based systems.

Data-driven modeling has been developed with the contributions from artificial intelligence, data mining, knowledge discovery in databases, computational intelligence, machine learning, intelligent data analysis, soft computing, pattern recognition, etc. There is a large overlap in the disciplines mentioned.

We see data-driven modeling as a modeling approach which focuses on using the machine learning methods in building models of physical processes. These models can complement or replace the “knowledge-driven” models describing behaviour of physical systems. Examples of the most popular methods used in data-driven modeling of hydrological systems are: statistical methods, artificial neural networks and fuzzy rule-based systems.

3.1.4.1 Data:

Data is usually split into three datasets. The first one is the training dataset. The training dataset is used to train the model (to determine the optimal parameter set). The testing dataset must not contain patterns from the training dataset. The predictive capability of the model is tested with the testing dataset during a procedure called validation (or testing). If the model's performance on the testing dataset is satisfactory then it can be put to operation. As measurements may often be noisy an attempt to maximize the fit to the training data may lead to the model capturing not only the process but also the noise - a phenomenon known as over fitting. An over fitted model may not perform well on a new dataset and the model is said to have a poor generalization capacity. In order to prevent this, third dataset is used, which is called the cross-validation dataset. The training (optimization of model parameters) is stopped when the error on the cross-validation dataset starts to increase. The cross-validation dataset must also not contain data points from the training and testing datasets.

A model is built using the training data and is tested with the testing data, while the cross-validation data is used to determine the extent of the training. It is therefore imperative that these three datasets should have identical statistical distributions to ensure that they come from the same population. If in a hydrological problem the training data belongs to a wet period and we test such trained model with data from a dry period then we are unable to reach a definite conclusion about the applicability of the model from this exercise.

3.1.4.2 Artificial Neural Network Model:

Artificial Neural Network (ANN) is a data driven modelling technique widely being used to model complex hydrological processes, such as rainfall, runoff, recharge, sediment generation etc and has been reported to be acknowledged as one of the promising tools in hydrology, particularly in problems for which the characterization processes is difficult to describe via physical or statistical based equations (Kumar et al., 2016). It is composed of a large number of interconnected processing elements (or nodes), arranged in an input layer, one or more hidden layers, an output layer and connection weights (Najjar and Ali, 1998a, b; Najjar and Zang, 2000). The input layer interacts with the external environment to receive the input vector; the hidden layer

transforms the information passed from the input layer by a non-linear function. Following that, the output layer produces the desired response of the network (Chang *et al*., 2001).

3.1.5 Simulation Modeling:

Simulation Modelling is the representation of the real systems either through physical reproductions at smaller scale, or via mathematical models that allow representing the dynamics of the system via simulation. It allows exploring system behaviour in an articulated way which is often either not possible, or too risky in the real world.

Monte Carlo simulation is a technique that uses a large number of random samples to find solutions to physical problems that cannot otherwise be easily solved. The first systematic development of Monte Carlo method derives its genesis from work on the atomic bomb during the Second World War (Hammersley and Handscomb (1964). In modelling hydrologic systems, there are two sources of random variation that may affect the estimated system outputs: (i) the natural temporal and spatial variability of climate and catchment factors being modelled, and (ii) the random variation resulting from unavoidable uncertainty in the definition of the model structure, the model inputs and in the estimated model parameters. Monte Carlo simulation has been widely used to determine the impacts of model and parameter uncertainty on simulation results; these are generally expressed in the form of confidence limits on hydrologic estimates. Most traditional rainfall-based flood estimation techniques are based on the design event approach, in which all parameter values and inputs other than rainfall are treated as fixed values. The application of these traditional methods generally involves the implicit assumption that the annual exceedance probability (AEP) of the flood is the same as its causative rainfall. To satisfy this probability-neutral assumption, it is necessary to select model inputs carefully to ensure that no probability bias is introduced in the transformation of rainfall to the flood characteristics of interest. Kuczera et al (2003), provide a number of examples that highlight the deficiencies of the design event approach. The design event approach also assumes that there is a critical rainfall duration that produces the design flood for a given catchment. In the most general Monte Carlo simulation approach for design surface runoff (Flood) estimation, rainfall events of different duration are sampled stochastically from their distribution. The simulated surface runoffs are then weighted

in accordance with the observed frequency of occurrence of rainfall events of different durations that produced them. This avoids any positive bias of estimated flood probabilities which may be associated with the application of the critical rainfall duration concept (Weinmann et al. 2002). The application of this generalised approach relies on the derivation of new design data for rainfall events that are consistent with a new probabilistic definition of storm 'cores' or complete storms (Hoang et al., 1999). Such new design rainfall data is currently not widely available, thus limiting the application of the generalised approach. Accordingly the description of the proposed generic Monte Carlo simulation approach for design flood estimation is still based on the concept of critical rainfall duration. Monte Carlo simulation is particularly suitable in cases where design flood characteristics need to be determined at multiple locations within a system. With Monte Carlo simulation, the sampling of input values over a wide range ensures that the changing influence of different factors is automatically allowed for when moving from sites of interest in the upper catchment to sites near the catchment outlet. There are, however, a number of problems in which the design objective is more easily accommodated by continuous simulation approaches. Predominately these involve systems which posses multiple flood controlling factors that are dependent on antecedent conditions and/or other correlated variables. Any application of Monte Carlo analysis requires the generation of random numbers. Random numbers are required as the first step in application of the inverse transformation approach, and in any scheme in which discrete inputs are sampled in random manner. Many algorithms have been developed for the generation of random numbers (or rather, pseudo-random numbers, as all algorithms exhibit non-randomness to varying levels of acceptability. Many software compilers provide random number generators as intrinsic functions, and a variety of source codes is available in the public domain (Press et al, 1993; Saucier, 2000; Griffiths et al, 1985). It is used to generate random numbers between 0 and 1 in the first step of the inverse transformation approach. The sum of many random processes generally conforms to the Normal distribution (regardless of the distribution of individual processes) whereas the product of many random processes conforms to the log- Normal distribution. Source code for estimation of the cumulative Normal distribution is freely available in spreadsheet software. It is worth noting that, while few hydrologic variables conform to the normal distribution, many data sets can be transformed into the Normal domain by the Box-Cox transformation (Box-Cox, 1964); with this

approach, a variate X can be transformed into the normal domain (Z) by the following equation:

$$Z = \frac{(x^2 - 1)}{\lambda}$$

where λ is a parameter determined by trial and error to ensure that the skewness of the transformed distribution is zero. A noteworthy special case of this transformation arises when λ is set to zero, then the transformation is equivalent to taking logarithms of the data. Fitting the parameter l is most easily achieved by optimisation or the use of "solver" routines that are commonly available in spreadsheet programs.

CHAPTER - IV

MATERIALS AND METHODS

4.1 Description of the study area:

4.1.1 Location and extent:

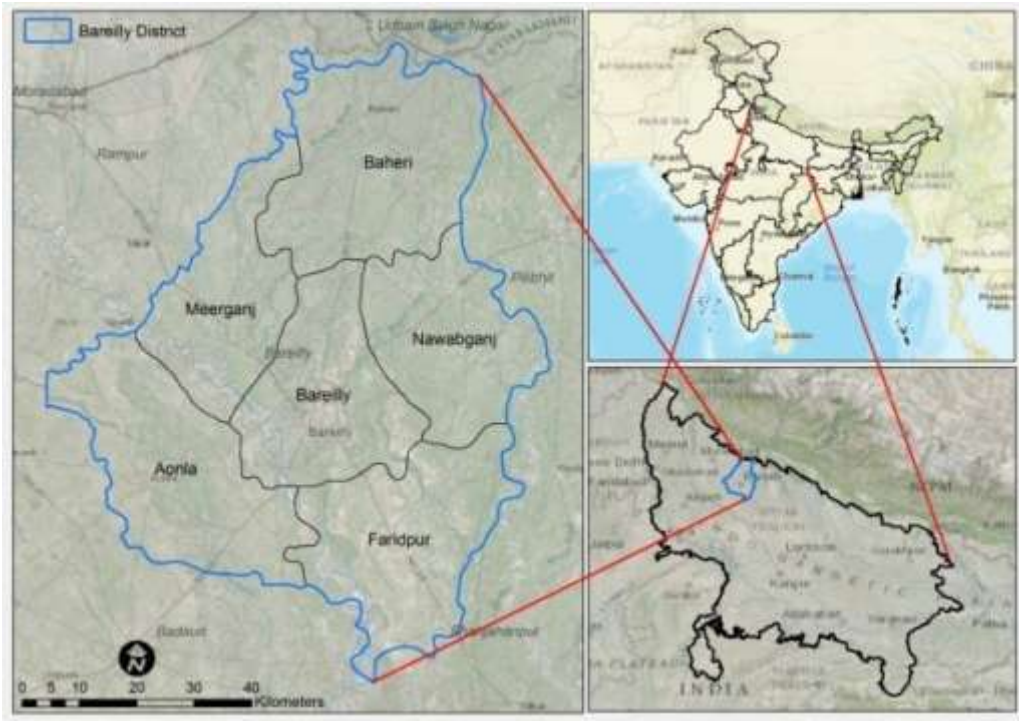

Figure 4.1 Map of the Study area (Bareilly District comprising of its six Tehsils)

The Study area, Bareilly district is located in north western segment of Uttar Pradesh between latitudes 28°01′ to 28^{0}54′ North and longitude 78°58′ to 79^{o}47′ East, and lies in northern India. It is a level terrain, watered by many streams, the general slope being towards the south. The soil is fertile and highly cultivated. The Ramganga River, which receives most of the hill torrents of the Kumaun Mountains through its tributaries, flows through this district. The Deoha is another drainage artery and receives many minor streams. For the administrative convenience the Bareilly district, has been divided into six Tehsils, which are (1) Bareilly Sadar, (2) Baheri, (3) Aonla, (4) Nawabganj, (5) Faridpur and (6) Mirganj. The rain gauge stations and groundwater well points are established in these tehsils. The geographical area is around 4,120 km^2. The main economic activity is agriculture having cropping intensity of about 167%. The main crops grown are: Wheat, Sugarcane, Rice, Mentha, oilseeds, vegetables etc.

(a) Rainfall: The summer monsoon is the major source of rainfall, which generally lasts from mid-June to mid-October. July and August being the wettest months, receiving about 490.5 mm and 543.4 mm rainfall respectively. The highest annual normal of rainfall has been recorded at Baheri (1734.2 mm) and lowest at Aonla (216.3 mm), the average of the district being 949.76 mm (Monsoon, 884.4 mm and non-Monsoon, 65.36 mm). It decreases from more than 1734 mm in the extreme northeast to less than 216 mm in the extreme south.

(b) Temperature: The maximum mean monthly atmospheric temperature of 40.5^{0}C has been recorded during the month of May and minimum (8.6^{0}C) in January.

(c) Humidity: During the peak monsoon period (i.e. August and September) and in mid winter season (during December) the relative humidity remains at its highest level ranging between 79% and 84%. It is lowest, around 38% during peak summer month of April and May.

(d) Wind: The wind speed is generally highest (7.3 Km/hr) during the month of June while it is lowest (2.2 Km/hr) during November, the average annual wind speed is 4.8 Km/hr.

4.1.2 Geomorphology & Soil Types

Bareilly district forms a part of Ramganga sub-basin in the central Indo-Gangetic plain. The Ramganga River divides the district into two unequal parts. Topographically, the area is almost an open plain with slight undulations which are more pronounced in the southern parts where the ground surface is being dissected by numerous river valleys. In the area lying north of Ramganga River, the general slope of land surface is from north to south, and in south of Ramganga River i.e. Aonla tehsil, it is from west to east. The highest elevation of land surface above mean sea level, as recorded on the extreme northern border of the district, is 202 meters and the lowest as recorded in the south eastern part of Fatehganj is 158 meters. A number of elevated structures i.e. mounds have been observed in Shergarh, Faridpur and Aonla area. The gradient of slope at land surface generally varies between 0.65-1.00 metres per km throughout the area. In general, the area shows the distinctive geomorphic units as inferred from I.R.S. Imagery, Survey of India toposheet and selective field checks as (a) Lower piedmont plain of Tarai, (b) Older alluvial plain or upland, (c) Younger alluvial plain or low land and (d) Meander flood plain.

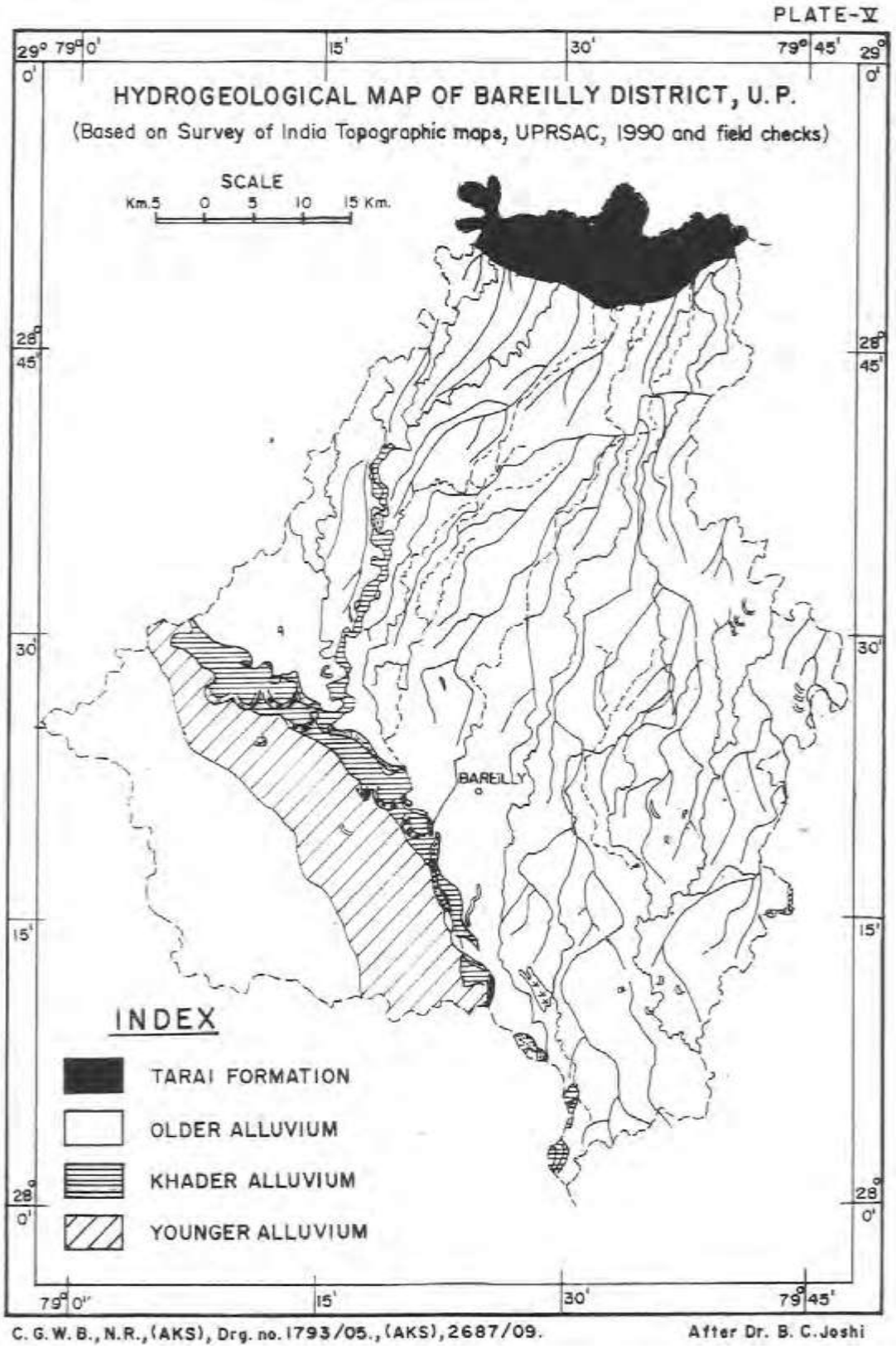

Figure 4.2 Hydro geological map of the study area

(Source: Central Groundwater Board: Bareilly)

Soils: As per the classification followed by the State soil survey organization, the soil of the district can be classified into three major groups, based on its texture and composition characteristics. Bareilly Type-1 (Tarai soils) Bareilly Type-2 (Khadar or low-land soils) Bareilly Type-3 (Upland or Bangar soils).

Bareilly Type-1 (Tarai soils): This type of soil is found in Tarai belt of Baheri tehsil and locally know as "Mar". The soil is characterised by fine texture, rich in organic matter, dark to grey in colour and rich in clay contents, especially in upper layers, the lower layers being lighter in texture, they are calcareous in nature,These soils possess the capacity of retaining moisture for longer period**.**

Bareilly Type-2 (Khadar or low-land soils): This type of soils is found in all tehsils in younger alluvial plain or low land along the river courses and are characterised by generally ash-grey to brownish-grey colour on the surface and their texture is silty loamy sand or sandy (the clay contents being low).

Bareilly Type-3 (Upland or Bangar soils): These soils occur in upland tract of older alluvial plain. The soil profile is generally mature, showing good development. It can be sub-grouped depending upon its topographic occurrence and textural nature into sandy soil, clayey soils and loamy soil.

4.1.3 Agro-climatic Zone Characteristics:

1. **Tarai agro-climatic zone:**

   Tarai Region of the district having heavy soils i.e. clay loam with high fertility, high rain fall and most suited for paddy, wheat and sugarcane cultivation, Oat of 15 development block of Bareilly district, Five blocks viz. Baheri, Damkhoda, Shergarh Nawabganj and Bhadpura falls in this Agro climatic zone.

2. **Mid-Western Plain agro-climatic zone:**

   Mid Western plain region of the district with loamy soils is having medium fertility, medium rainfall and suitable for all type of crops covers Meerganj, Fateganj West and Bhojipura blocks, Sandy soils with medium fertility and medium rain fall having proximity to the city and suitable for vegetable cultivation covers fertility and low rainfall but water logged with salinity problem most suited for paddy, oilseeds, pulses covers Faridpur, AlampurJaffrabad, Ramnagar, Majhgawan development blocks.

4.1.4 Water Bearing Aquifer Scenario:

The Gangetic alluvial plain occupies a structural trough in front of Himalayan ranges. It was interpreted to be like a great rift valley, filled with alluvium of enormous thickness varying from 4500 metres to as much as 25 Km (Oldham 1939). Bareilly district falls in one of such depression known as Ramganga depression. The area in Bareilly district occupies a small part of southern fringe of Tarai formation and flood plain deposits. These are underlain by quaternary sediments brought from Himalayas. The alluvial sediments mainly comprising clay, sand, gravel in varied proportion and grades are deposited is well stratified formation consisting of alternate bed of clay and granular material (sand fine to coarse) which is the main water bearings formation formed as aquifer. The district is underlain by a thick pile of alluvial sediments. The depth of basement in the area is not known so far as no borehole could reach up to the bedrock. The total annual replenish able groundwater resources are estimated to be about 103333.31 MCB. The Major water bearing formations are of medium to coarse sand. The storativity (S) of the aquifers is about $4.15x10^{-4}$. The Transmissivity of the aquifers ranges from 1555 to 2120 M^2/day.

4.2 Meteorological Data Collection:

Data regarding daily/monthly rainfall, Tehsil-wise pre and post groundwater level data (below ground surface) of last 16 years (1998- 2013), sources of irrigation, area irrigated by different irrigation sources was collected from the office of Senior Hydro-geologist at bareilly, Nazarat, collectorate Bareilly and India Meteorological Department (IMD).

4.3 Stochastic Process and Time Series:

A time series is a set of observations that are arranged chronologically. A mathematical expression which describes the probability structure of the time series is referred to as a stochastic process. When the joint distribution of any possible set of random variables from the process is time independent, then the process is said to possess strict stationarity. When only the statistical moments up to order f are time independent, the process is said to possess weak stationarity of order f. The term white noise refers to a sequence of uncorrelated random variables having a fixed distribution with mean zero. When the current value of a process only depends upon the previous value plus a random shock, the process is called a Markov process. The

general purpose of forecasting or prediction is to provide the best estimate of what will happen at specific points in time in the future. The objective of simulation is to use a fitted model to generate possible future values of a time series. Usually the observations are taken at regular intervals (days, months, years), but the sampling could be irregular. A time series analysis consists of two steps (i) building a model that represents a time series, and (ii) using the model to predict (forecast) future values. A simple but extremely useful stochastic model is the autoregressive (AR) model. In this model, the current value of the process Y_t is linearly related to previous values

If a time series has a regular pattern, then a value of the series should be a function of previous values. If Y is the target value that we are trying to model and predict, and Y_t is

$$\mathbf{Y_t = f\,(Y_{t-1}, Y_{t-2}, Y_{t-3}, \ldots, Y_{t-n}) + \delta_t} \qquad \ldots\ldots\ldots\ldots\ldots\ldots (4.1)$$

Where Y_{t-1} is the value of Y for the previous observation,
Y_{t-2} is the value two observations ago, etc., and
$\boldsymbol{\delta_t}$ represents noise that does not follow a predictable pattern (this is called a random shock).
Values of variables occurring prior to the current observation are called *lag values*. If a time series follows a repeating pattern, then the value of Y_t is usually highly correlated with $Y_{t\text{-}cycle}$ where *cycle* is the number of observations in the regular cycle. For example, monthly observations with an annual cycle often can be modeled by

$$\mathbf{Y_t = f\,(Y_{t-12})} \qquad \ldots\ldots\ldots\ldots\ldots\ldots\ldots.. (4.2)$$

The goal of building a time series model is the same as the goal for other types of predictive models which is to create a model such that the error between the predicted value of the target variable and the actual value is as small as possible. The primary difference between time series models and other types of models is that lag values of the target variable are used as predictor variables, whereas traditional models use other variables as predictors, and the concept of a lag value doesn't apply because the observations don't represent a chronological sequence.

4.3.1 Time Series Models:

A mathematical model representing stochastic process is called stochastic model or time series model. It has a certain mathematical form or structure and a set of parameters.

(i) A simple time series model can be represented by single probability distribution function **f (Y; ϕ)** with parameters **ϕ = (ϕ 1, ϕ 2, ...)** valid for all positions **t = 1,2,….N** and without any dependence between **Y_1, Y_2, ……Y_n**. If Y is normal with mean μ and variance σ^2 , the time series model can be written as

$$Y_t = \mu + \sigma \varepsilon_t, \qquad t=1,2, \ldots\ldots \qquad \ldots\ldots\ldots\ldots\ldots\ldots (4.3)$$

Where ε_t is normal with mean zero and variance one and are independent values. μ and σ are the parameters and do not vary with time and the model is stationary.

ii) A time series model with dependence structure can be formed as:

$$\varepsilon_t = \phi \varepsilon_{t-1} + \xi_t \qquad \ldots\ldots\ldots\ldots\ldots\ldots (4.4)$$

where,

ξ_t = An independent series with mean zero and variance $(1- \phi^2)$

ε_t = Dependent series

ϕ = Parameter of the model

In the Equation (4.4) ε_t is a dependent series because in a addition to being a function of ε_t, it is a function of same variable at time (t-1).

4.3.2 Time Series Modeling:

The techniques and procedure for finding a mathematical model that represents sample time series X_1, X_2,…….X_N of size N where N is years of annual value of the variable is called time series modelling.

The time series modelling is a process which can be simple or complex depending on the characteristics of the available sample series, on the type of model to use and on the selected technique of modelling.

Time series modelling can be organized in following stages (Salas and Smith, 1986):

1. Identification of model composition
2. Selection of model type
3. Identification of model form
4. Estimation of model parameters.
5. Diagnostic check of the model.

In hydrologic time series modelling it has to be decided whether the model will be univariate or multivariate model or a combination of a univariate and a disaggregation models. This decision is referred as the identification of model composition. Such identification generally depends on the characteristics of overall water resources system, the characteristics of time series and the models input. Salas and Smith, 1981 demonstrated physical consideration of these types of model. They used autoregressive and autoregressive moving average models to represent the annual Ground Water Level time series. Therefore, in this study AR model is used to represent time series for annual rainfall and pre and post monsoon groundwater level.

4.3.3 Autoregressive (AR) Model:

In the Autoregressive model, the current value of a variable is equated to the weighted sum of a pre assigned no. of part values and a variate that is completely random of previous value of process and shock. The p^{th} order autoregressive model AR (p), representing the variable Y_t is generally written as.

$$Y_t = \overline{Y} + \Phi_1 (Y_{t-1} - \overline{Y}) + \Phi_2 (Y_{t-2} - \overline{Y}) + ... + \Phi_p (Y_{t-p} - \overline{Y}) + \varepsilon_t \quad \text{.....} \quad (4.5)$$

$$Y_t = \overline{Y} + \sum_{j=1}^{p} \Phi_j (Y_{t-j} - \overline{Y}) + \varepsilon_t \quad \text{.....} \quad (4.6)$$

Where,

Y_t = The time dependent series (variable)

ε_t = The time independent series which is independent of Y_t and is Normally distributed with mean zero and variance σ^2

$\overline{Y}$ = Mean of annual rainfall and groundwater level data

$\Phi_1, \Phi 2 \ldots \Phi_p$ = Autoregressive parameter

4.3.4 Estimation of Autoregressive parameter (Φ) maximum likelihood estimate:

For estimation of the model parameter method of maximum likelihood was used (Box and Jenkins, 1970).

Consider the sum of cross-products,

$$z_i z_j + z_{i+1} z_{j+1} + \ldots\ldots\ldots + z_{N+1-J}\, z_{N+1-I}, \qquad \ldots\ldots\ldots\ldots\ldots (4.7)$$

and define

$$D_{ij} = D_{ji} = \frac{N}{(N + 2 - i - j)} \sum_{\ell=0}^{N+1-(i+j)} z_{i+\ell}\, z_{j+\ell} \qquad \ldots\ldots\ldots\ldots\ldots (4.8)$$

where,

D = difference operator

N = sample size

i,j = maximum possible order

The maximum likelihood estimates of the parameters $\Phi_1, \ldots\ldots\ldots, \Phi_p$ are found by solving the system of equations in particular,

$$D_{ij} = \Phi_1 D_{j2} + \Phi_2 D_{j3} + \ldots\ldots + \Phi_p D_{j,p+1},\ j=2, \ldots\ldots, p+1 \qquad \ldots\ldots\ldots\ldots (4.9)$$

for $\Phi_1, \ldots\ldots\ldots, \Phi_p$

$$AR(1): \Phi_1 = \frac{D_{1,2}}{D_{2,2}} \qquad \ldots\ldots\ldots\ldots\ldots (4.10)$$

$$AR(2): \Phi_1 = \frac{D_{1,2}D_{3,3} - D_{1,3}D_{2,3}}{D_{2,2}D_{3,3} - D_{2,3^2}} \qquad \ldots\ldots\ldots\ldots\ldots\ldots (4.11)$$

$$\Phi_2 = \frac{D_{1,3}D_{2,2} - D_{1,2}D_{2,3}}{D_{2,2}D_{3,3} - D_{2,3^2}} \qquad \ldots\ldots\ldots\ldots\ldots\ldots (4.12)$$

4.3.5 Autocorrelation function

The autocorrelation provides important information about the significance of the lag variables. An *autocorrelation* is the correlation between the target variable and lag values for the same variable. Correlation values range from -1 to +1. A value of +1 indicates that the two variables move together perfectly; a value of -1 indicates that they move in opposite directions. When building a time series model, it is important to include lag values that have large, positive autocorrelation values. Sometimes it is also useful to include those that have large negative autocorrelations. The autocorrelation shows the standard error which is followed by the t-statistics. It is also used to indicate positive or negative correlations right or left of the centerline. The dots shown in the chart mark are the point deviations from zero. If the autocorrelation bar is longer than the autocorrelation should be considered significant.

The autocorrelation function r_k of the variable Y_t of equation (4.6) is obtained by multiplying both sides of the equation (4.6) by Y_{t+k} and taking expectation term by term. The relationship proposed by Kottegoda and Horder (1980) for the computation of autocorrelation function of lag K was used which is expressed as:

$$r_k = \frac{\sum_{t=1}^{N-K}(Y_t - \overline{Y})(Y_{t+k} - \overline{Y})}{\sum_{t=1}^{N}(Y_t - \overline{Y})^2} \qquad \ldots\ldots\ldots\ldots\ldots\ldots (4.13)$$

Where,

r_k = Autocorrelation function of time series Y_t at lag k

Y_t = Ground Water Level series (historical data)

$\overline{Y}$ = Mean of time series Y_t

k = Lag of K time unit

N = Total number of discrete values of time series Y_t

The autocorrelation or serial correlation is a graphical relationship of autocorrelation function r_k with lag k. The autocorrelogram was used for identifying the order of the model for given time series as well as for comparing the sample correlogram with model correlogram. For an independent time series the population correlogram is equal to zero for $K \neq 1$. However, sample of independent time series due to sampling variability have r_k fluctuating around zero but they are not necessarily equal to zero. Therefore probability limits for the correlogram of an independent series is determined. The following equation was used to determine the 95 per cent probability levels (Anderson, 1942).

$$r_k\,(95\%) = \frac{-1 \pm 1.96\sqrt{N-K-1}}{N-K} \qquad \ldots\ldots\ldots\ldots\ldots\ldots (4.14)$$

where, N = Sample size.

4.3.6 Partial Autocorrelation function

The *partial autocorrelation* is the autocorrelation of time series observations separated by a lag of *k* time units with the effects of the intervening observations eliminated. Autocorrelation and partial autocorrelation tables are also provided for the residuals (errors) between the actual and predicted values of the time series. The first section compares the predicted values with the actual values for the rows use the train the model. If validation is enabled, a second table is generated showing how well the predicted validation rows match the actual rows.

4.3.7 Correlation between actual and predicted

This is the correlation coefficient between the actual values and the predicted values which measures whether the actual and predicted values move in the same direction. The possible range of values is -1 to +1. A positive correlation means that the actual and predicted values generally move in the same direction. A correlation of +1 means that the actual and predicted values are synchronized; this is the ideal case. A negative correlation means that the actual and predicted values move in opposite directions. A correlation near zero means that the predicted values are no better than random guesses.

The partial autocorrelation function or partial correlogram is used to represent the time dependence structure of a series. The partial autocorrelation PC_{kk} is the autocorrelation remaining in the series after fitting a model of order K-1 and removing the line independence. It is used to identify both the type and order of the model.

The following equation was used to calculate the partial autocorrelation function of lag K.

$$PC_{k,k} = \frac{r_k - \sum_{j=1}^{k-1} PC_{k-1,j} r_{k-j}}{1 - \sum_{j=1}^{k-1} PC_{k-1,j} r_j} \qquad \text{..... (4.15)}$$

where,

PC_{kk} = Partial autocorrelation function at lag K

r_k = Autocorrelation function at lag K

$PC_{k,j} = PC_{k-1,j} - PC_{k,k}, PC_{k-1,k-j}$ ..... (4.16)

j = 1, 2… K-1

The 95 percent probability limit for partial autocorrelation function was calculated using the following equation (Anderson 1942).

$$\mathbf{PC_{k,k}\ (95\%)} = \frac{1.96}{\sqrt{N}} \qquad \text{..... (4.17)}$$

The autocorrelation function and partial autocorrelation functions for the series Y_t was computed by the equation (4.1) and equation (4.4) respectively and were plotted against lag k with 95 percent probability limits. The general shape of correlogram was analysed to select tentative order of model.

4.3.8 Parameter estimation of AR (p) models

The average of sequence Y_t was computed by following equation:

$$\bar{Y} = \frac{1}{N}\sum_{t=1}^{N} Y_t \qquad \ldots\ldots\ldots\ldots\ldots\ldots (4.18)$$

The average σ^2_ε of Y_t was computed by the following equation:

$$\sigma^2_\varepsilon = \frac{1}{(N-1)}\sum_{t=1}^{N} (Y_t - \bar{Y})^2 \qquad \ldots\ldots\ldots\ldots\ldots\ldots (4.19)$$

After computation of $\bar{Y}$ and σ^2_ε, the remaining parameters Φ_1, Φ_2,…. Φ_p of the AR models were estimated by using the sequence:

$$Z_t = Y_t - \bar{Y}, \qquad \ldots\ldots\ldots\ldots\ldots\ldots (4.20)$$

$$t = 1,2,\ldots. N$$

The parameters Φ_1, Φ_2… Φ_p was estimated by solving the p system of following linear equations (Yule equation):

$$r_k = \Phi_1 r_{k-1} + \Phi_2 r_{k-2} + \ldots\ldots + \Phi_p r_{k-p} \qquad K>0 \qquad \ldots\ldots\ldots\ldots (4.21)$$

or

$$r_k = \sum_{j=1}^{p} \Phi_j r_{k-j} \qquad K>0 \qquad \ldots\ldots\ldots\ldots (4.22)$$

Where, r_1, r_2 were computed from equation (4.14).

4.3.9 Generation of predicted groundwater level using AR (P) model:

The fitted autoregressive AR (P) model was used for generation of predicted pre and post monsoon groundwater level at different observation wells at every tehsil in the study area district Bareilly. The predicted groundwater level was compared with the observed groundwater levels for different statistical characteristics and errors to evaluate its adoptability for prediction.

4.4 Statistical characteristics:

The following statistical parameters were calculated to evaluate the performance of the model for prediction of annual rainfall and pre and post monsoon groundwater level of study area district Bareilly.

4.4.1 Mean Forecast Error

Mean forecast error was calculated to evaluate the performance of auto regressive models fitted to time series of rainfall and Groundwater level The mean forecast error (MFE) was computed for the pre and post monsoon groundwater level by the following equation:

$$\text{MFE} = \frac{\sum_{i=1}^{n} \chi_c(t) - \sum_{i=1}^{n} \chi_0(t)}{\eta} \qquad \ldots\ldots\ldots\ldots\ldots\ldots (4.23)$$

Where,

$\chi_c(t)$ = Computed Ground water level value (Pre or post) Value

$\chi_0(t)$ = Observed Ground water level value (Pre or post) value

η = Number of observations

4.4.2 Mean Absolute Error

The performance of the model, were evaluated by mean absolute error was computed by following equation. (Raghuwanshi *et al.,* 2000)

$$\text{MAE} = \frac{\sum_{i=1}^{n} \left| \chi_c(t) - \chi_0(t) \right|}{\eta} \qquad \ldots\ldots\ldots\ldots\ldots\ldots (4.24)$$

4.4.3 Mean Relative Error

The mean relative error was computed by following equation: (Raghuwanshi *et al.*, 2000)

$$\text{MRE} = \frac{\sum_{i=1}^{n} \left| \chi_c(t) - \chi_0(t) \right|}{\frac{\chi_0(t)}{\eta}} \qquad \text{……. (4.25)}$$

4.4.4 Mean Square Error

The mean square error was computed by following equation (Raghuwanshi *et al.*, 2000)

$$\text{MSE} = \frac{\sum_{i=1}^{n} \left[\chi_c(t) - \chi_0(t) \right]^2}{\eta} \qquad \text{……..…….. (4.26)}$$

4.4.5 Root Mean Square Error

The root mean square error was computed by following equation: (Raghuwanshi *et al.*, 2000)

$$\text{RMSE} = \left[\frac{\sum_{i=1}^{n} \left[\chi_c(t) - \chi_0(t) \right]^2}{\eta} \right]^{1/2} \qquad \text{…… (4.27)}$$

4.4.6 Integral Square Error

The integral square error (ISE) is a measure of goodness of a fit of time series model. The integral square error is the relation of root mean square error to the mean observed data. It was estimated by following equation Singh *et al.*, (1991).

$$\text{ISE} = \frac{\sqrt{\sum_{i=1}^{n} \left[\chi_c(t) - \chi_0(t) \right]^2}}{\sum_{i=1}^{n} \chi_0(t)} \qquad \text{…….. (4.28)}$$

4.4.7 Standard deviation

The positive square root of the arithmetic mean of squares of the deviations of observations in a series about its arithmetic mean is called standard deviation.

4.4.8 Skewness

The Skewness characterizes the degree of asymmetry of a distribution around its mean. Positive skewness indicates a distribution with an asymmetric tail extending toward more positive values. Negative skewness indicates a distribution with an asymmetric tail extending toward more values.

4.4.9 Kurtosis

The Kurtosis characterizes the relative peakedness or flatness of a distribution. Positive kurtosis indicates a relatively peaked distribution. Negative kurtosis indicates a relatively flat distribution.

4.4.10 Goodness of fit of autoregressive (AR) models

The goodness of fit tests of AR models fitted to annual hydrologic series were accomplished by testing whether the residuals of a dependence model for correlation and whether the order of the fitted model is adequate compared with the order of the dependence model and whether the main statistical characteristics of historical series one preserved. The following tests were performed to test the goodness of fit of autoregressive (AR) models.

4.4.11 Box-Pierce Portmonteau lack of fit test

The Box-Pierce Portmonteau lack of fit test was used to check whether the residual of a dependence model for correlation. The test statistic was computed by using the following equation:

$$Q = N \sum_{k=1}^{L} r_k^{\,2} \qquad \text{……..} \qquad (4.29)$$

Where,

N = Number of observations

r_k = Serial correlation or autocorrelation of series Y_t

statistic Q follows χ^2 distribution with r = K-p degree of freedom. The estimated value of χ^2 was compared with tabulated values of χ^2.

4.4.12 Akaike Information Criterion

The Akaike Information Criterion (Akaike, 1974) was used for checking whether the order of the fitted model is adequate compared with the order of dependence model. Akaike Information Criterion for AR(p) models, was computed using the following equation.

$$AIC(P) = N\ 1n\left(\hat{\sigma}^2_{\varepsilon}\right) + 2(P) \qquad \ldots\ldots\ldots\ldots\ldots\ (4.30)$$

Where,

N = Number of observations

$\hat{\sigma}^2_{\varepsilon}$ = Residual variance

A comparison was made between the AIC (p) and the AIC (p-1) and AIC (p+1). If the AIC (p) is less than both AIC (p-1) and AIC (p+1), then the AR (p) model is best otherwise, the model which gives minimum AIC value was the one to be selected model.

4.4.13 Correlation between Observed and Predicted Values

The annual rainfall and pre and post monsoon groundwater levels were predicted by the best fitted models for all the locations within tehsils and compared with the observed values. Correlation coefficient between the observed and predicted values was estimated from the graphical comparison of the values to evaluate the performance of model.

4.5 R.S. & G.I.S. Data Acquired and Source:

For the study, satellite images of Bareilly district U.P; a part of Ramganga River Basin were acquired for three Epochs; 1979, 1990 and 2009 from Global Land Cover Facility (GLCF) an Earth Science Data Interface.

Table 4.1 R.S. & G.I.S. Data source:

Image ID	Status	WRS:P/R	Aquisition Date	Data set	Producer	AVR	Type	Location	Remarks
228-888	Online	1:156/040	26-10-1979	MSS	USGS	Ortho GLS 1975	Geo TIFF	India-Nepal	4 images
202-987	Online	2:145/040	15-11-1990	TM	USGS	Ortho GLS1990	Geo TIFF	India-Nepal	7 images
291-747	Online	2:145/040	18-10-2009	TM	USGS	Ortho	Geo TIFF	India-Nepal	7 images

4.5.1 Geo-referencing Properties of the Images:

The geo-referencing properties of both 1990 and 2009 are the same while image thinning was applied to the 1979 imagery which has a resolution of 80 m using a factor of two to modify its properties and resolution to conform to the other two images. Image thinning was carried out through contract in which an image is generalizes by reducing the number of rows and columns while simultaneously decreasing the cell resolution. Contraction may take place by pixel thinning or pixel aggregation with the contracting factors in X and Y being independently defined. With pixel thinning, every n^{th} pixel is kept while the remaining is thrown away.

4.5.2 Software Used

(a) Software such as (a) Gewulica 9.2, (b) Arc GIS 8.3, (c) Arc info, (4) Microsoft Excell and (5) Microsoft Word were used in the study:

(b) This was used for displaying and subsequent processing and enhancement of the image. It was also used for the carving out of the study area (District Bareilly) from the whole images.

(c) Arc GIS 8.3 and Arc info was also used to compliment the display and processing of the data.

(d) MS Excel and Word were used for graph and charts and manuscript writing.

4.5.3 Development of a Classification Scheme

Based on the prior knowledge of the study area and a brief reconnaissance survey with additional information from previous research in the study area, a classification scheme was developed for the study. The classification scheme developed gives classification where the land use land cover could be identified by a single digit.

Table 4.2 Land use land cover classification scheme

S.No.	Land use/land cover categories	Code
1.	**Crop land**	C
2.	**Waste land**	WL
3.	**Plantation/Vegetation/Forest**	F
4.	**Road, Built-up and Structures**	S
5.	**Water Bodies, water spills, Marsh-land**	WB

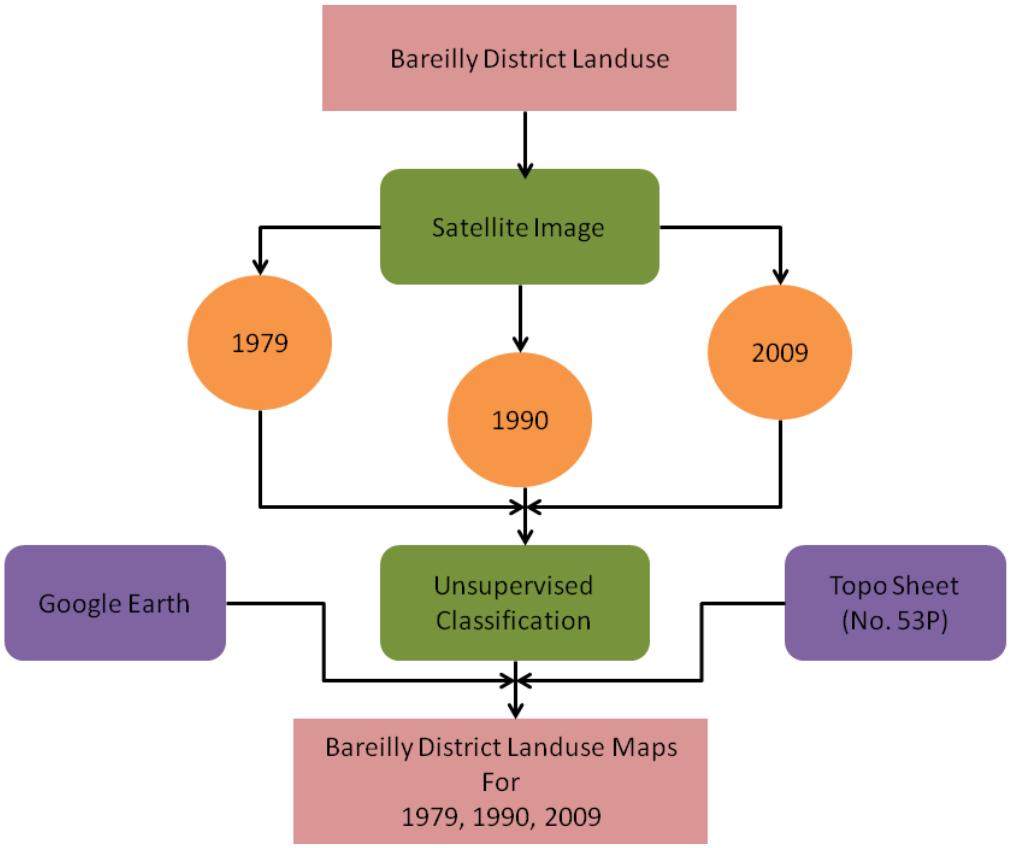

Figure 4.3

4.5.4 Limitation(s) in the Study

There was a major limitation in studying the images due to their resolution difference. LANDSAT image of 1979, acquired with the multi-spectral scanner (MSS) which has a spatial resolution of 80 meters, whilst the images of 1990 and 2009 were acquired with Thematic Mapper^{TM}, which has a spatial resolution of 30 meters. But this limitation was corrected through image thinning of the 1979 image.

4.5.5 Method of Data Analysis:

The three main steps of data analysis were adopted in this study.

(i) Image thinning
(ii) Maximum Likelihood classification
(iii) Calculation of the area in hectares of the resulting land use/land cover types for each study year and subsequently comparing the results.

The comparison of the land use land cover statistics assisted in identifying the percentage change, trend and rate of change between 1979 and 2009. In achieving this, the first task was to develop a table showing the area in hectares and the percentage change for each year (1979, 1990 and 2009) measured against each land use land cover type. Percentage change to determine the trend of change can then be calculated by dividing observed change by sum of changes multiplied by 100.

$$\text{(Trend) percentage change} = \frac{\text{Observed change}}{\text{Sum of change}} \times 100 \qquad \ldots\ldots\ldots (4.31)$$

In obtaining annual rate of change, the percentage change is divided by 100 and multiplied by the number of study year 1979 – 1990 (12yr) and 1990 - 2009 (20yr).

4.6 Estimation of ground water recharge:

(Source: Ministry of Water Resources, 1997)

Ground water recharge due to return flow from irrigation, seepage from canals, recharge from tanks and ponds and recharge form water conservation structures was estimated individually for both monsoon and non-monsoon seasons based on the recommended norms as given in Table 4.3.

Table 4.3 Estimation of Recharge from Other Sources

Parameters	Recharge Source	Range of Parameters
Canal Seepage Factor	Unlined canal	15 to 30 ha-m/day/million sq. m. Of wetted area
	Lined canals & canals in hard rock terrain	20% of above value for unlined canals
Return flow factor	Surface water irrigation	0.10 – 0.50 part
	Ground water irrigation	0.05 – 0.45 part
Seepage from Tanks and ponds	1.4 mm/day over the average water spread area	
Water conservation structures	50% of the gross storage. Out of this, 50% is during monsoon and remaining 50% during non-monsoon season	

Ground water recharge from rainfall was estimated for monsoon and non-monsoon seasons separately. Rainfall recharge during monsoon season was estimated using, Rainfall Infiltration Factor Method.

4.6.1 Water level Fluctuation (WLF) Method:

Under this method the change in storage will be computed by multiplying water level fluctuation between pre and post monsoon seasons with the area of assessment and specific yield.

Change is Storage = $\Delta S = h * Sy * A$ …….. (4.32)

Where,

h = rise in water level in the monsoon season, A = area for computation of recharge,

Sy = specific yield.

The specific yield values considered in the computations are to be taken preferably from field tests, in the absence of which, the recommended values of specific yield are to be considered. The range of specific yield recommended for different formations are given in the Table 4.4.

Table 4.4 Specific Yield for different Formations

Formation		Range of specific yield
Unconsolidated Formation	Alluvium	0.04 to 0.20
Semi-consolidated Formation	Sedimentary rocks	0.01 to 0.15
Consolidated Formation	Crystallines and other hard rocks	0.002 to 0.04

The change is storage is calculated from the above relation is the resultant of the recharge from rainfall and other sources during the monsoon period and the gross ground water draft during monsoon season. In order to segregate the rainfall recharge during monsoon season, the following equation is used

$Rrf = h \times Sy \times A + DG - Rc - Rsw - Rt - Rgw - Rwc$ …….. (4.33)

Where,

DG = Gross ground water draft for all uses during monsoon season

Rc = recharge due to seepage from canals during monsoon season

Rsw = recharge from surface water irrigation during monsoon season

Rt = recharge from storage tanks and ponds

Rgw = recharge from ground water irrigation during monsoon season

Rwc = recharge from water conservation structures during monsoon season

The rainfall recharge thus calculated is the normalized for the normal monsoon season rainfall.

4.6.2 Rainfall Infiltration Factor (RIF) Method:

The other method was for the estimation of rainfall recharge is using Rainfall infiltration factor. The recharge from rainfall was estimated as given below

$Rrf = f * A *$ normal monsoon rainfall …… (4.34)

Where ;

f = rainfall infiltration factor

A = area

The same Rainfall Infiltration Factor was used for computation of recharge due to rainfall during monsoon and non monsoon seasons.

The norms adopted for computation of recharge from rainfall is given in Table 4.5.

Table 4.5 Rainfall Infiltration Factor for difference formations

Formation		Range of specific yield
Unconsolidated Formation	Alluvium	0.08 to 0.25
Semi-consolidated Formation	Sedimentary rocks	0.03 to 0.14
Consolidated Formation	Crystallines and other hard rocks	0.01 to 0.12

The rainfall recharge computed by WLF method is to be compared with recharge computed by RIF method. In case the difference between the two sets of data are more than 20%, then rationalized RIF figure is to be considered, otherwise monsoon recharge using WLF method is to be considered. Whenever the percent difference is less than - 20%, 80 % of the recharge computed by RIF method is to be used and wherever, the percent difference is more than + 20 120 % of recharge computed by RIF method is to be taken.

5.6.3. Ground water Recharge during Monsoon Season:

The total recharge in monsoon season is the sum of the normalized rainfall recharge and the recharge from other sources as expressed in the following equation –

R(normal) = Rrf (normal)+ Rc + Rsw + Rt + Rgw + Rwc …..……... (4.35)

Where,

R (normal) = Total recharge during monsoon season

Rrf (normal) = Rainfall recharge during monsoon season for normal monsoon season rainfall

4.6.4. Ground water Recharge during non-Monsoon Season:

Similar expression as given in equation (4.35) above is used for recharge during non-monsoon season wherein all the recharge components including rainfall recharge and recharge from other sources during non-monsoon season are computed. Only difference is that rainfall recharge during non-monsoon is computed using RIF method only. If the rainfall during non-monsoon period is less than 10% of the annual rainfall, the recharge due to rainfall is taken as zero. The total recharge during non monsoon is the sum of recharge from rainfall and recharge from other sources.

4.6.5. Annual Replenishable Ground Water Resource:

The Annual Replenishable Ground Water Resource of the area is the sum of recharge during monsoon and non monsoon seasons. An allowance is kept for natural discharge during non monsoon season by deducting 5% of Annual Replenishable Ground Water Resource, wherever WLF method is employed to compute rainfall recharge during monsoon season and 10% if RIF method is used.

4.6.6. Net Annual Ground Water Availability:

The Net annual ground water availability is the available resource after deducting the natural discharges from the Annual Replenishable Ground Water Resource and is expressed as:

Net Annual Ground Water Availability = Annual Replenish able Ground Water Resource – Natural Discharge during non monsoon season …….. (4.36)

4.7. Ground Water System:

Aquifer is a geological formation, which receives water from different sources like rainfall, seepage from surface water bodies and percolation from irrigated land. The aquifer water is depleted through pumping from the aquifer and evapo-transpiration from ground water surface. To maintain the ground water resources indefinitely, a hydrologic equilibrium must exist between all waters entering and leaving the basin. If ground water is regarded as a renewable resource then only a certain quantity of water can be withdrawn annually from the ground water basin. The maximum amount of water which can be extracted from an underground reservoir depends on its safe yield. Any more withdrawal beyond the safe yield will lower down the water table which would increase cost of pumping as well as it would affect the surface supply of the bounding streams. It is, therefore, necessary to limit the exploitation of ground water to the safe yield of the aquifer.

For assessment of dynamics of ground water Fluctuation in Bareilly District the following balance equation is used:

Recharge – Discharge = ± Storage (i.e. hydraulic head) …….. (4.37)

4.8 Aquifer Parameters

In the absence of adequate pumping test data, the aquifer parameters (viz., specific yield and hydraulic conductivity etc.) have been determined indirectly using the information from well litho logical data. The average representative values of hydraulic conductivity and specific yield used for different types of formation materials were adopted from Todd (1980).

4.8.1 Hydraulic Conductivity

On the basis of the classification of various formation material depths wise, the representative value of hydraulic conductivity was assigned to each class of material as suggested by Todd (1980). The weighted average of all the layers was calculated to determine the equivalent hydraulic conductivity for the stratified material at a particular bore-hole site.

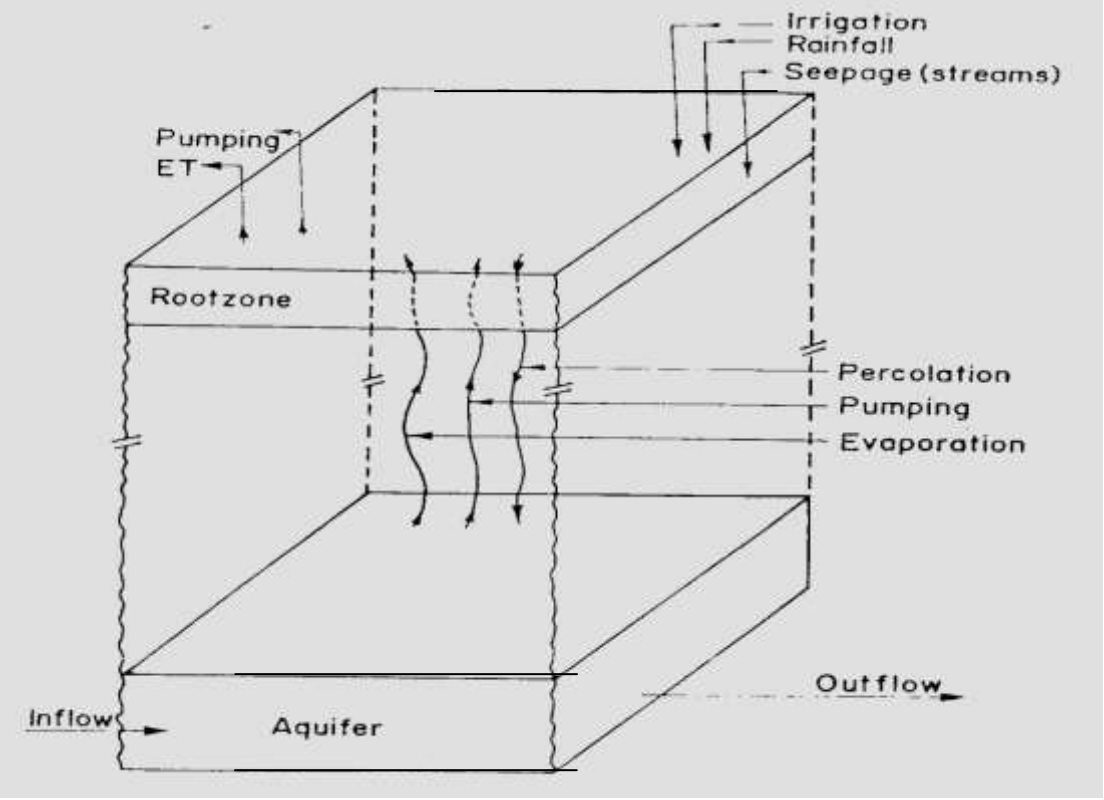

4.8.2 Specific Yield:

The specific yield of a soil mass is the quantity of water released from it by the force of gravity and is defined as the ratio of the volume of water drained to the total volume of the soil mass. The amount of water drained depends on particle size, shape and distribution of porous material. The temperature and mineral composition of the

water which affect the surface tension, viscosity and specific gravity of water, may also affect the volume of water drained.

4.8.3 Transmissivity:

The values of transmissivity are calculated making use of values of hydraulic conductivity and saturated thickness of the unconfined aquifer.

4.8.4 Modified Chaturvedi Formula:

Recharge(R) = $1.35(P-14)^{0.5}$

Where, R and P are in inches.

4.8.5 Kumar and Seethapati Formula:

Recharge(R) = $0.63\ (P - 15.28)^{0.76}$

Where, R and P are in inches.

4.9.1 Assessment of Net Regional Ground Water Recharge:

Net regional recharge (R_n) to ground water in any time period is estimated from

$$R_n = R_g \pm Q_g - Q_p \qquad \ldots\ldots\ldots\ldots \ldots (4.38)$$

Where,

R_g = Gross recharge to the ground water basin

Q_g = Ground water inflow/outflow to the neighbouring areas.

Q_p= Ground water extraction through wells.

The gross recharge (R_g) can be estimated by

$$R_g = R_p + R_{cm}\, R_{cnm} + R_{sim} + R_{sin\ m} + R_T \qquad \ldots\ldots\ldots\ldots (4.39)$$

Where,

R_p = Recharge due to rainfall.

R_{cm} = Recharge due to seepage from the canal system during monsoon.

R_{cnm} = Recharge due to seepage from canal system during non-monsoon period.

R_{sim} = Recharge due to seepage from area irrigated by surface water irrigation during monsoon.

R_{sinm} = Recharge due to percolation losses from the areas irrigated by surface irrigation in non-monsoon period.

R_T = Recharge from tanks.

The subsurface inflow or outflow across the aquifer boundaries cannot be estimated directly. It is therefore calculated as a residue from the annual water balance equation.

$$P + 1 = ET + E \pm Q_E + Q_P + Q_s + \nabla S_s \pm \nabla S_m \pm \nabla S_g \pm ET_f \quad .... \quad (4.40)$$

Where,

P = Rainfall over the region.

I = Sun of the water applied over the region by canal system and ground water.

ET = Evapotranspiration from the cropped area.

E = Soil evaporation from the uncultivated areas.

Q_s = Direct surface runoff from the area.

∇S_m = Change in soil moisture storage

∇S_s = Change in surface water storage.

∇S_g = Change in ground water storage

ET_f = Evaporation from the forested areas.

4.9.2 SCS Rainfall – Runoff Relation

The runoff curve number method for the estimation of direct runoff from storm rainfall is well established in hydrologic engineering. Its popularity is rooted in its convenience, its simplicity, and its responsiveness to four readily grasped catchment properties; soil type, land use/treatment, surface condition, and antecedent condition. The method was developed in 1954 by the USDA Soil Conservation Service (SCS, 1985).

In developing the SCS rainfall-runoff relationship, the total rainfall was separated into three components: direct runoff (Q) actual retention (F) and the initial abstraction (I_a). Conceptually, the following relationship between P, Q, I_a, and F was assumed:

$$\frac{F}{S} = \frac{Q}{P - Ia} \qquad \text{..... (4.41)}$$

in which S is the potential maximum retention. The actual retention is

$$F = (P - I_a) - Q \qquad \text{..... (4.42)}$$

Substituting equation (4.42) into equation (4.39) yields the following:

$$\frac{(P-I_a) - Q}{S} = \frac{Q}{P - I_a} \qquad \text{..... (4.43)}$$

Rearranging equation (4.43) to solve for Q yields

$$Q = \frac{(P-I_a)^2}{(P-I_a) + S} \qquad \text{..... (4.44)}$$

Equation (4.44) contains one known, P, and two unknowns, I_a and S. Before putting equation (4.44) in a form that can be used to solve for Q, it may be worthwhile examining the rationality of the underlying model of equation (4.41). The initial abstraction is the amount of rainfall at the beginning of a storm that is not available for runoff; therefore, $(P-I_a)$ is the rainfall that is available after the initial abstraction has been satisfied. Letting K_1 equal the ratio of Q to $(P-I_a)$, K_1 represents the proportion of water available that directly runs off. If S is the amount of storage (e.g., depression, interception, subsurface) available to hold rainfall, K_2 = F/S is the proportion of available storage that is filled with rainwater. Equation (4.41) indicates that $K_1 = K_2$; in other words, the proportion of available storage that is filled up equals the proportion of available water that appears as runoff. In equation (4.44), there are two unknowns to be estimated, S and I_a. The retention S should be function of the

following five factors: land use interception, infiltration, depression storage, and antecedent moisture. Empirical evidence resulted in the following equation:

$$I_a = 0.2S \qquad \text{……..…} (4.45)$$

If the five factors above affect S, they also affect I_a. Substituting equation (4.45) into equation (4.44) yields the following equation, which contains the single unknown, S:

$$Q = \frac{(P-0.2S)^2}{(P + 0.8S)} \qquad \text{……..……} (4.46)$$

Equation (4.39) represents the basic equation for computing the runoff depth, Q, for a given rainfall depth, P. It is worthwhile noting that while Q and P have units of depth (e.g., mm), Q and P reflect volumes and are often referred to as volumes because we usually assume that the same depths occurred over the entire watershed.

In order to use equation (4.46) to compute the runoff for a given P, it is necessary to provide a means for estimating the one unknown. S. For this purpose, the SCS runoff curve number (CN) was developed. A curve number is an index that represents the combination of a hydrologic soil group and a land use and treatment class. Empirical analyses suggested that the CN was a function of three factors: soil group, the cover complex, and antecedent moisture conditions.

SCS developed a soil classification system that consists of four groups, which are identified by the letters A, B, C, and D. The SCS cover complex classification consists of three factors: land use, treatment or practice, and hydrologic condition. There are approximately 21 different land uses that are identified in the tables for estimating runoff curve numbers. Agricultural land uses are often subdivided by treatment or practices, such as contoured or straight row; this separation reflects the different hydrologic runoff potential that is associated with variation in land treatment. The hydrologic condition reflects the level of land management; it is separated with three classes; poor, fair, and good. Not all of the land uses are separated by treatment or condition. Antecedent soil moisture is known to have a significant effect on both the volume and rate of runoff. Recognising that it is a significant factor, SCS developed three antecedent soil moisture conditions, which were labelled I, II and III.

As indicated previously, the CN was developed for use in equation (4.46). Thus, there was a need to relate S, which was unknown of equation (4.46), and the runoff CN. An empirical analysis led to the following relationship.

$$S = \frac{25400}{CN} - 254 \qquad \text{…….. (4.47)}$$

Equation (4.46) and (4.47) can be used to estimate Q when the values of P and CN are available. It is important to note the following constraint on equation (4.46):

$$P \geq 0.2S \qquad \text{…….. (4.48)}$$

When $P < 0.2S$, it is necessary to assume that $Q = 0$.

Table 4.6. Runoff curve number for various Land use land covers:

Curve Number			Cover description Hydrologic soil group			
Cover Type	Treatment	Hydrological Condition	A	B	C	D
Fallow	Bare soil	-	77	86	91	94
	Crop residue cover	Poor	76	85	90	93
		Good	74	83	88	90
Row crops (C_1)	Straight row (SR)	Poor	72	81	88	91
		Good	67	78	85	89
	SR + CR	Poor	71	80	87	90
		Good	64	75	82	85
	Contoured (C)	Poor	70	79	84	88
		Good	65	75	82	86
	C + CR	Poor	69	78	83	87
		Good	64	74	81	86
	Contoured & terraced (C & T)	Poor	66	74	80	82
		Good	62	71	78	81
	C & T + CR	Poor	65	78	79	81
		Good	61	76	77	80
Pasture, grassland, or range—continuous forage for grazing C_2		Poor	68	79	86	89
		Fair	49	69	79	84
		Good	39	61	61	80
Brush—brush-weed-grass mixture with brush the major element C_3		Poor	48	67	77	83
		Fair	35	56	70	77
		Good	30	48	65	73
Woods—grass combination (orchard or tree farm) F		Poor	57	73	82	86
		Fair	43	65	76	82
		Good	32	58	72	79
Residential districts by average lot size 1/8 acre or less (town houses) S			77	85	90	92
Newly graded areas (pervious areas only, no vegetation) S			77	86	91	94

4.10 Application of neural network

Neural networks are composed of simple elements operating in parallel. These elements are inspired by biological nervous systems. As in nature, the network function is determined largely by the connections between elements. We can train a neural network to perform a particular function by adjusting the values of the connections (weights) between elements. Commonly neural networks are adjusted, or trained, so that a particular input leads to a specific target output. Such a situation is shown below. There, the network is adjusted, based on a comparison of the output and the target, until the network output matches the target. Typically many such input/target pairs are needed to train a network.

4.10.1 Artificial Neural Network

The Artificial neural network employs a mathematical simulation approach, just like human brain to process the acquired information and derive the output(s) after the network has been trained properly for pattern recognition. It has been found useful and efficient modelling tool, particularly in problems for which the characterization processes is difficult to describe through physical or statistical based equations. The rainfall runoff process lends itself well to ANN applications. The nonlinear nature of the relationships, non-availability of long historical records, and the complexity of the physical based models in this regard are some of the factors that have attracted researchers to consider alternative models in which, ANNs have been one of the viable alternative choices. The application of the method is being widely adopted in hydrology. Researchers (M.A. Kaltech 2008) have also compared the performance of developed ANN models with other methods successfully and demonstrated their approach. The merits and shortcomings of this methodology have also been discussed in review by the ASCE task committee on application of ANNs in hydrology (ASCE, 2000a, & b).

An artificial neural network is composed of a large number of interconnected processing elements (or nodes), arranged in an input layer, one or more hidden layers, an output layer and connection weights (Najjar and Ali, 1998a, & b; Najjar and Zang, 2000). The input layer interacts with the external environment to receive the input vector; the hidden layer transforms the information passed from the input layer by a

non-linear function. Following that, the output layer produces the desired response of the network (Chang *et al*., 2001).

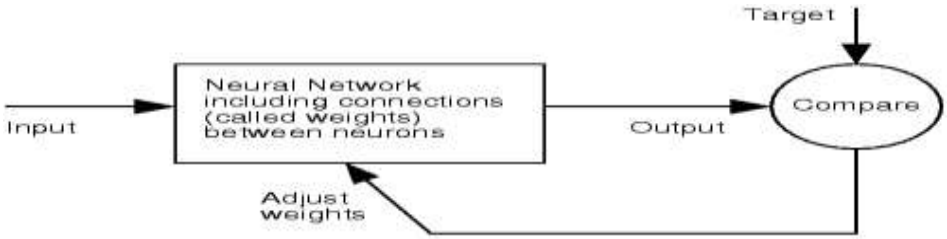

Figure 4.4 Depiction of Neural network

A one-layer network with R input elements and S neuron is as follows:

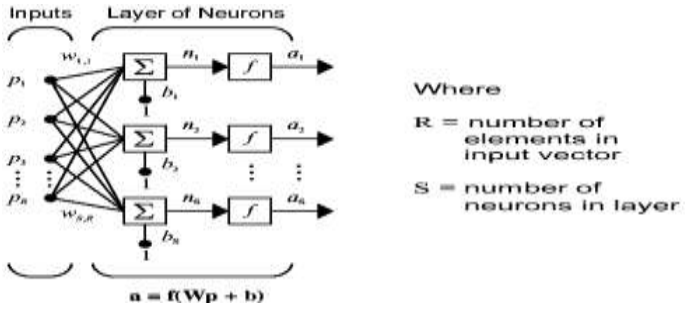

Figure 4.5 One-layer neural networks

In this network, each element of the input vector p is connected to each neuron input through the weight matrix W. The i^{th} neuron has a summer that gathers its weighted inputs and bias to form its own scalar output n (i). The various n (i) taken together form -element net input vector n. Finally, the neuron layer outputs form a column vector a.

CHAPTER –V

RESULTS AND DISCUSSION

5.1. Land use Land cover categorization:

5.1.1 Land use / land cover changes in the Ramganga River basin at Bareilly district:

This study attempts to assess the Land use Land cover change and their effects on the hydrological regime of Ramganga River basin at Bareilly district. Mapping of present and historical land use/ land cover conditions in the Ramganga River basin at Bareilly district was carried out for assessing the changes that have taken place mainly due to human induced activities. Satellite images were used as the prime source for mapping land cover dynamics. LANDSAT MSS (80 m. resolution), and TM (30 m. resolution) data were used to prepare land cover maps for three instances 1979, 1990, and 2009 respectively. Classification, categorization and quantification were performed on the basis of spectral characteristics using unsupervised classification technique (Isodata clustering) and visual interpretation. GCP's (ground control points) were utilized to improve and validate classification scheme. The overall accuracy and Kappa Coefficient were found to be 80% and 0.77 respectively. The analysis of the changes that has taken place from 1979 to 1990 and from 1990 to 2009 is presented in the beginning of this chapter, followed by recharge and runoff behavior with corresponding LULC change and rainfall patterns are presented subsequently in this chapter. Five classes of land use Land cover types were identified and mapped in the basin depending on the spatial resolution of the data and availability of the vegetation related parameters and are depicted in the Table5.1 and Figure 5.1. to 5.3.

Table. 5.1 Area covered by various LULC categories in hectares:

Classification symbol	LU/LC Classes	1979		1990		2009	
		Area (ha)	Area %	Area (ha)	Area %	Area (ha)	Area %
S	Settlement	16892	4.1	21012	5.1	26368	6.4
C	Crop Land	249672	60.6	314768	76.4	344432	83.6
F	Forest	116596	28.3	46144	11.2	24720	6
WL	Waste Land	20600	5	13596	3.3	8240	2
WB	Water Bodies	8240	2	16480	4	8240	2
	Total Area (Ha)	412000	100	412000	100	412000	100

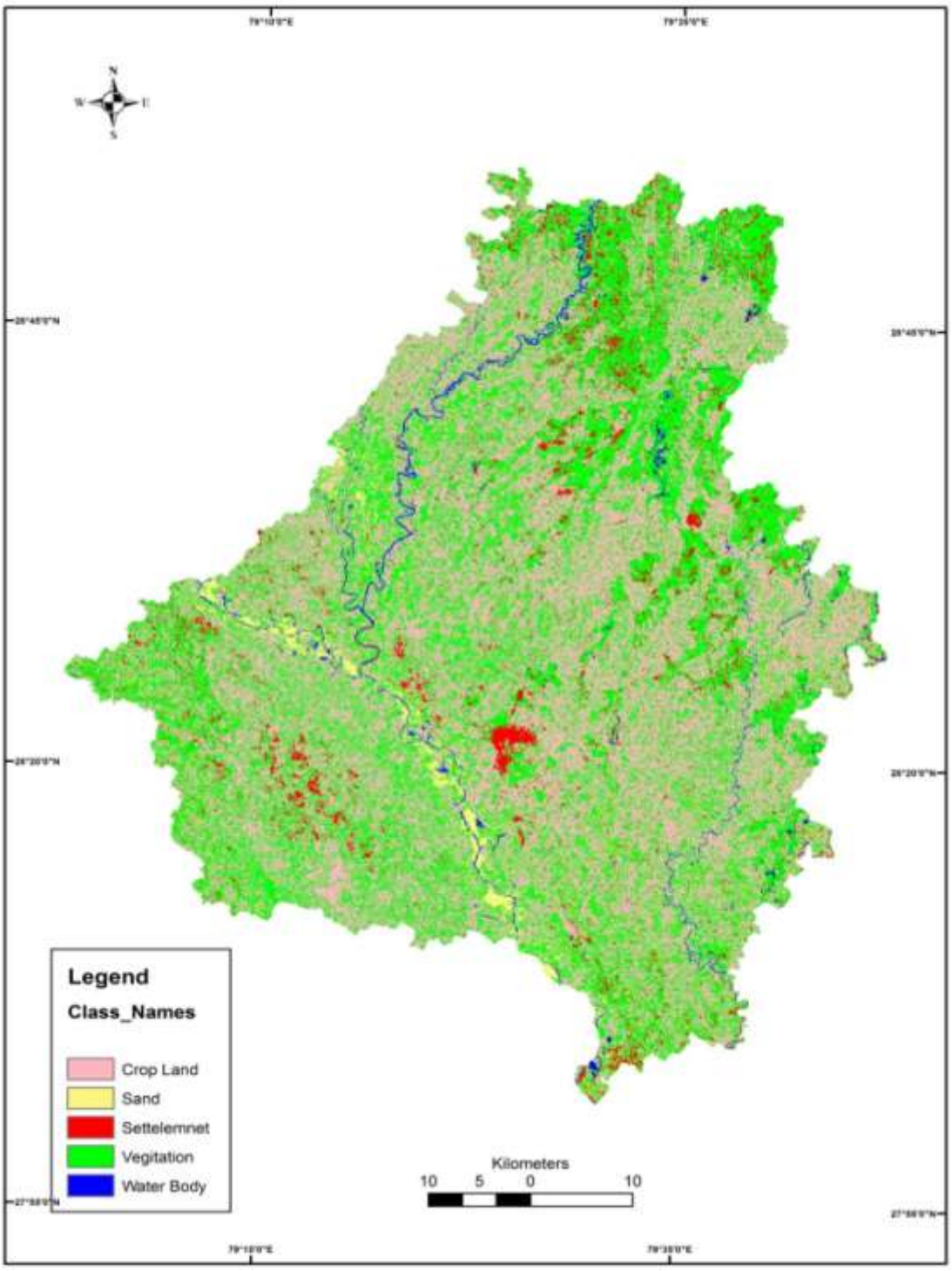

Fig.5.1: Land Use Land Cover map of the study area Bareilly District, 1979.

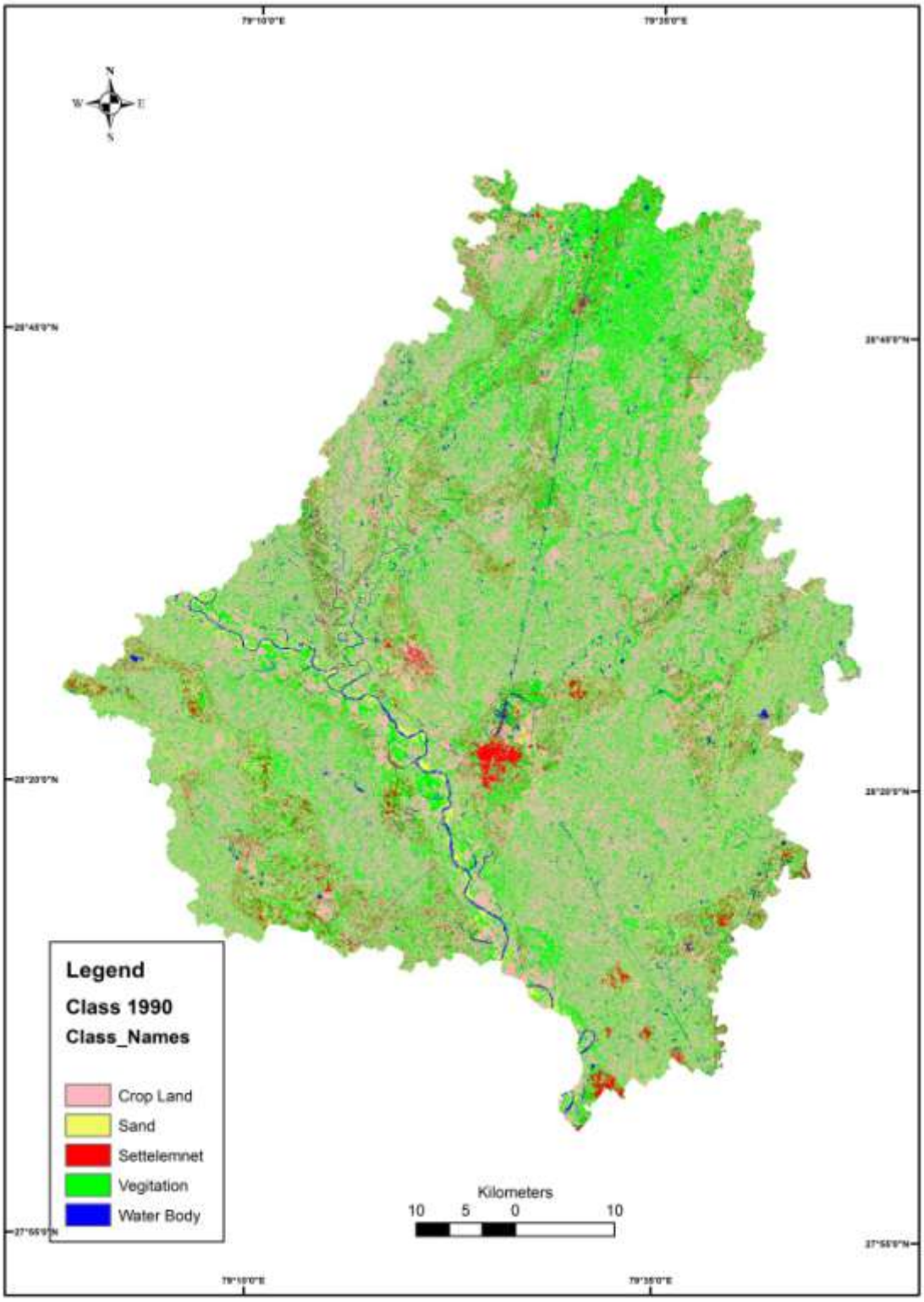

Fig.5.2: Land Use Land Cover map of the study area Bareilly District, 1990.

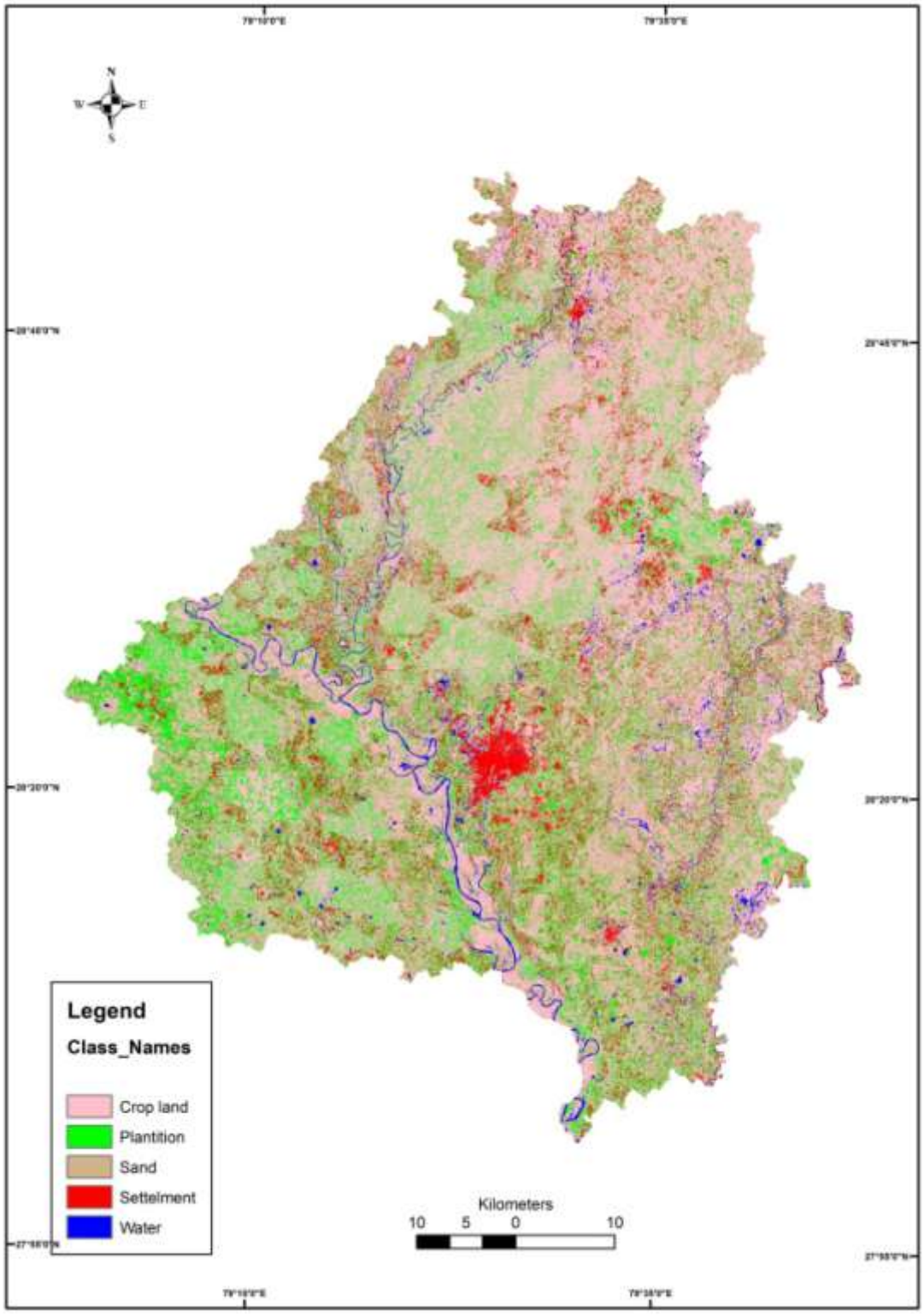

Fig.5.3: Land Use Land Cover map of the study area Bareilly District, 2009.

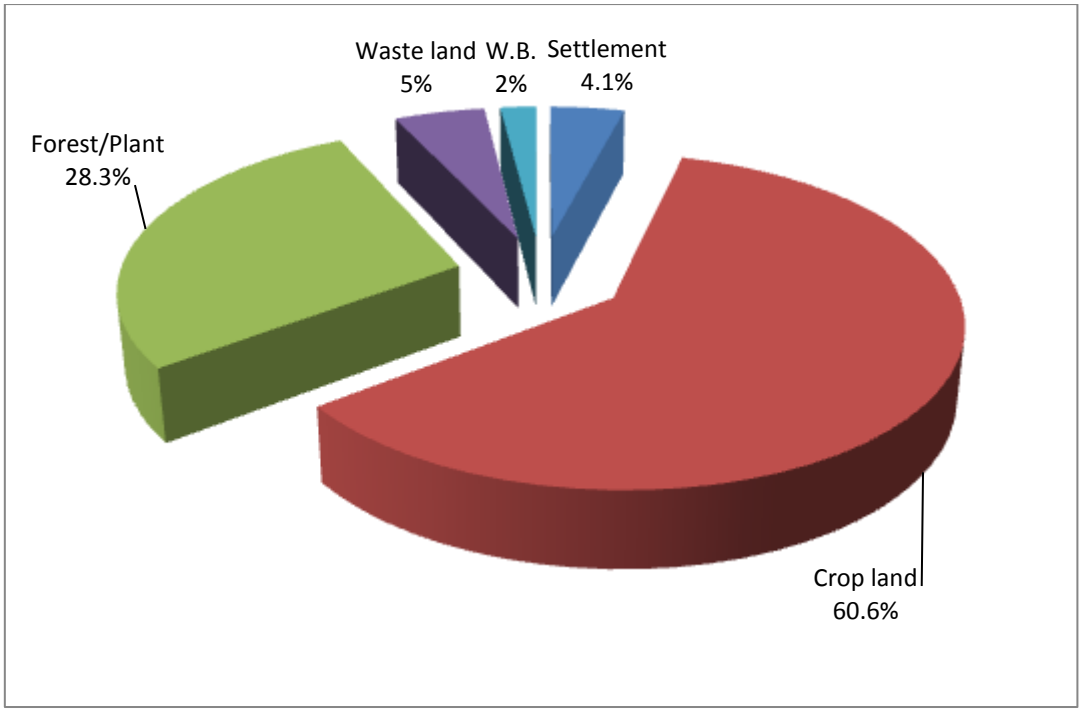

Figure 5.4 (a). Chart depicting % of LULC status in 1979.

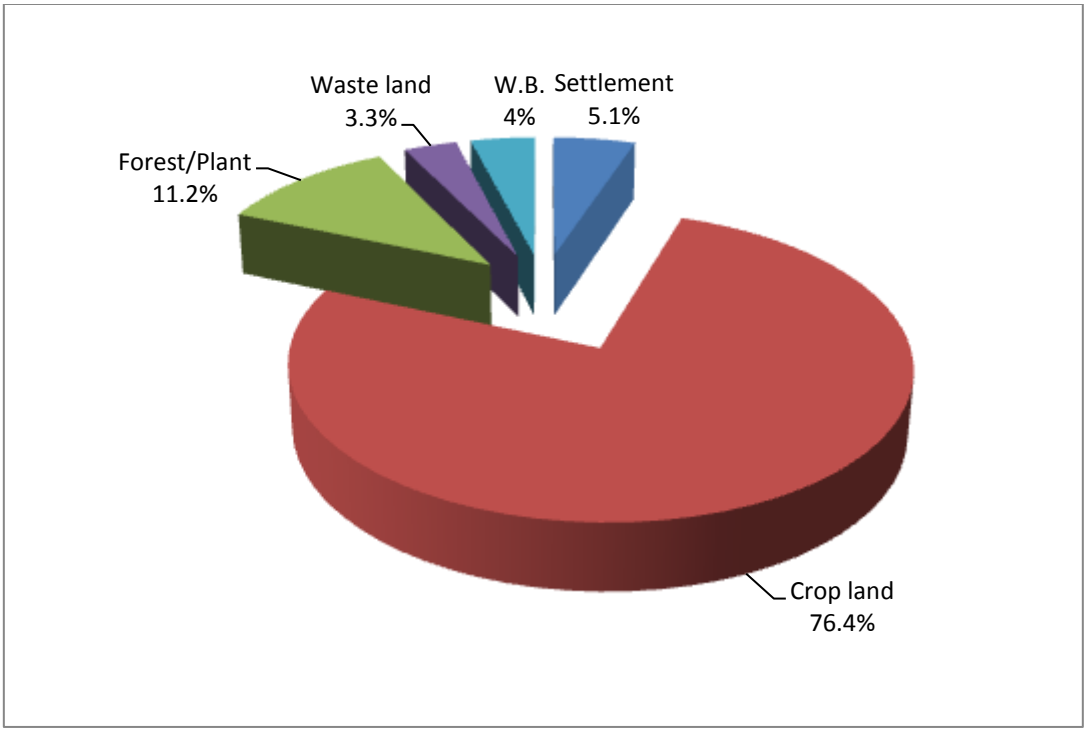

Figure 5.4(b): Chart depicting % of LULC status in 1990.

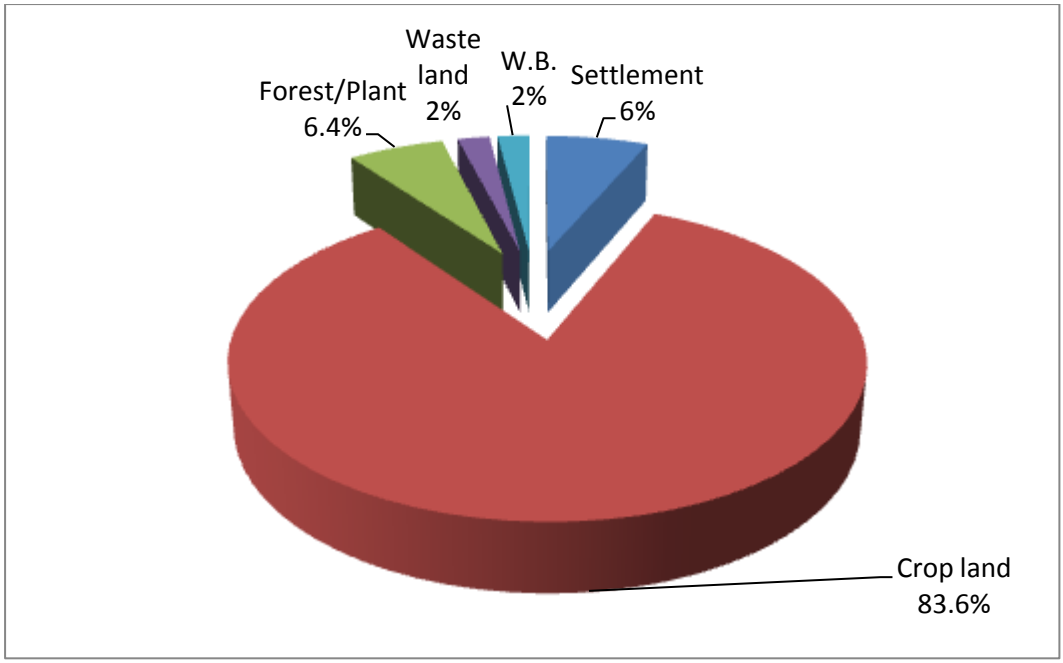

Figure 5.4 (c). Chart depicting % of LULC status in 2009.

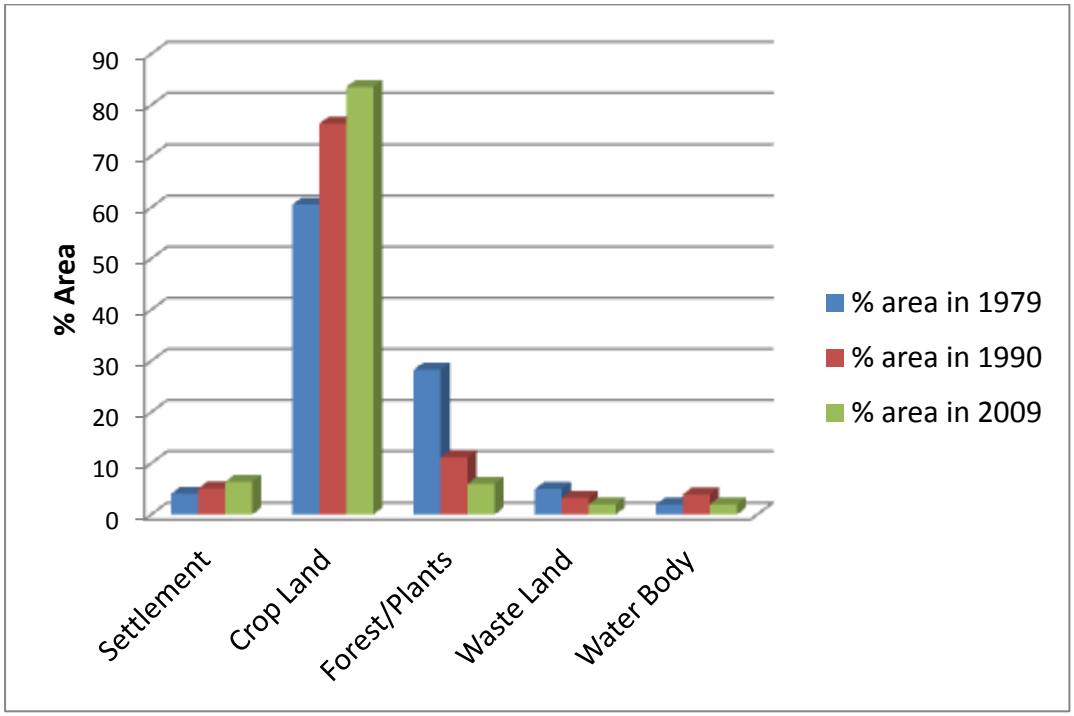

Figure 5.4 (d) LULC change status at three epochs: Year 1979, 1990 and 2009

The Land use Land cover analysis as shown in table 5.1, and Figure 5.4 (a), (b) (c) and (d) above, indicate that in the year 1979, a substantial portion of the study area (28.30 %) is under vegetation/plantation/forest cover. Similarly a major portion (60.60 %) of the study area is under agriculture crop land. The area under waste land is about 5% of the total geographical area. The area under settlements (Built up/ Roads etc) is merely 4.10 % of the total geographical area. The area under water bodies is 2% 0f the total geographical area. And after passage of about 11 years i.e. by 1990, the composition of land use land cover has changed significantly. Now the area under vegetation /plantation cover has decreased from 28.30 % to 11.20 %. The area under crop land has increased from 60.60% to 76.40 %. Similarly the area under settlements (Built-up, roads etc.) has also increased from mere 4.10 % to 5.10 %. The area under water bodies also increased from 2% to 4%. The area under Waste land has decreased from 5% to 3.3%. The trend of land use land cover transformation has continued further, which is evident from the Table 5.1 and Figure 5.4 (c). After passage of about 31 years i.e. by the year 2009, the land use land cover over the study area has experienced more significant changes. Now the area under vegetation/plantation/forest cover has decreased from 28.3% to mere 6%. This reduction in the vegetation/plantation/forest cover area has been the result of conversion of such area into crop land, Settlements, and waste land. Consequently, the area under Crop land has increased from 60.60 % in 1979, to 83.60 % in 2009. Similarly the area under Settlements has increased from mere 4.10 % to 6.40 %. The area under Waste land has also decreased from 5% in 1979 to 2 %.in 2009.

The study thus, shows a substantial loss of vegetation and plantation/forest area which has been ultimately converted to crop land and settlement (Built-up, Roads etc) area. The major land area being shifted to settlement land is of great concern as it poses risk of soil loss through erosion caused by surface runoff. It also reduces infiltration and percolation characteristics thus again posing risk of reduced groundwater replenishment from rainfall. This type of land area loss is of great concern and major bottleneck for soil loss and crop production. The area under water bodies has increased from 2% in 1979 to 4% in 1990. This increase in the area under water bodies indicates some kind of positive human intervention undertaken during 1979 to 1990. This is because of massive work undertaken by the then state government during 1978 to 1980 for the restoration/rejuvenation of water bodies in the village

level throughout the state of Uttar Pradesh including Bareilly district. It would be pertinent to mention here that during the year 1977 and 1978 the rainfall occurrence in the study area was poor (882mm and 872 mm respectively). The situation was further aggravated in the succeeding year 1979 causing severe drought as the rainfall occurrence was very less (mere 489 mm) this year. There was shortage of food thorough out the state. In order to mitigate the shortage of food, the state government had launched a massive employment cum food security programme (Food for Work Programme). Through this programme every/any person was given food for doing earth excavation work in the form of de-silting of village ponds, tanks, wells and construction of new ponds, tanks, including de-silting of canals, and construction of earthen roads in the villages. And this effort of the then government helped the poor and needy to earn food for themselves and simultaneously in improving the hydrologic regime of the basins. This rejuvenation/restoration of silted and encroached tanks, ponds, and other water bodies have been reflected as increased area under water bodies in the classified image of 1990. The analysis of classified images of 1990 and 2009 [Figure 5.2, 5.3, 5.4 (c) and table 5.1] indicates the reverse trend where in the area under water bodies has decreased from 4% in 1990 to 2% in 2009. This may be due to human encroachment for settlements in urban and sub-urban areas and for crop land in the rural areas.

5.2 Observed and normalized rainfall pattern:

Table 5.2 Relational statistical analysis of observed and normalized rainfall:

(1977-2013)	MEAN	STDEV	SKEW	KURT	VAR
January	12.96143	10.29251	0.531467	-0.88304	105.9358
February	16.31797	15.71682	1.196349	0.868557	247.0184
March	12.42049	12.48124	1.054671	0.184387	155.7813
April	9.018135	9.045636	1.608843	2.534586	81.82353
May	22.05154	15.09661	0.459508	-0.54376	227.9075
June	106.4869	77.77322	1.457188	3.040692	6048.674
July	251.3847	121.8522	0.179806	-0.74361	14847.97
August	257.2835	92.85591	0.539541	-0.61185	8622.221
September	150.541	89.98531	1.109767	1.419239	8097.356
October	22.12573	27.1968	1.592024	2.453131	739.6662
November	3.614622	5.713451	1.663099	1.657954	32.64352
December	5.631676	7.338619	1.771059	2.701842	53.85532

Data normalization is a necessary process required when working with mathematical models. The data need to be normalized so as to provide a definite distribution shape and make it suitable for analysis. The computer models are the most useful tools, which can be applied for hydrological management in the study area. Application of specific method for rainfall-runoff studies, water balance studies and recharge estimation depends on availability of data. Groundwater recharge is likely to vary in space even over a short-distance as variations in soil and vegetative parameters can significantly affect the rate of recharge (Cook *et al.,* 1989).

The normalized and observed rainfall data of Bareilly district for January to December months of 1977-2009 has been depicted in Fig. 5.5. to 5.16.

Fig. 5.5 shows the normalized and observed rainfall data of Bareilly district for the month of January. The maximum rainfall (normalized) of 23.05 mm is seen in the year 2013 followed by 22.90 mm in the year 2012, and the minimum rainfall of 14.03 mm was found in year 2006, 2008, and 2009. The observed rainfall data were collected for the period 1977-2009. The maximum observed rainfall of 34.2 mm was

recorded in year 2013 followed by 31.8 mm in the year 2012 and there was no (0.0 mm) rainfall during the month of January in the year 2006, 2008 and 2009.

Fig. 5.6 shows the normalized and observed rainfall data of Bareilly district for February. The highest normalized rainfall of 31.9 mm was found in the year 2007 followed by 31.8 mm in the year 2013 and the lowest rainfall of 18.6 mm was seen in the years 2003, 2004, 2005 and 2012 . The observed rainfall data were collected for the period 1977-2009, the maximum observed rainfall of 56.2 mm was recorded in 2003, followed by 53.1 mm in 1990, and the minimum observed rainfall was recorded in years 2003, 2004, 2006 and 2012 as Zero (0.0mm).

Fig. 5.7 represents the normalized and observed rainfall data of Bareilly district for the months of March. The highest normalized rainfall is seen in the year 1978 (24.79 mm) followed by in the year 1982 (24.76 mm) and the lowest in the years 1999, 2003, 2004, 2008 and 2012 (14.41 mm). The observed rainfall data were collected from 1977-2009. The maximum observed rainfall was recorded in 1978 (42.15 mm) followed by 1982 (41.05 mm) and the minimum observed rainfall was recorded in the years 1999, 2003, 2004, 2008 and 2012 (0.0 mm).

Fig. 5.8 shows the normalized and observed rainfall of Bareilly district for the months of April. The highest normalized rainfall is seen in the year 1983 (18.05 mm) followed by 1984 (17.87 mm) and the lowest was found in the years 1999 and 2003 (10.45mm). The observed rainfall data were collected from 1977-2009, the maximum observed rainfall was recorded in 1983 (38.2 mm) followed by 2004 (30.9 mm) and the minimum observed rainfall was recorded in the years 1999 and 2003 (0.0 mm).

Fig. 5.9 shows the normalized and observed rainfall of Bareilly district for the months of May. The highest normalized rainfall is seen in the year 2007 (44.8mm) followed by in the year 2006 (36.98 mm) and the lowest rainfall was seen in 1994 (36.87mm). The observed rainfall data were collected for 1977-2009. The maximum observed rainfall was recorded in 2007 (56.70 mm) followed by 2006 (53.70 mm) and the minimum observed rainfall was recorded in the year 2012 (0.20 mm).

Fig. 5.10 shows the normalized and observed rainfall of Bareilly district for the months of June. The highest normalized rainfall is seen in the year 2013 (184.23 mm) followed by in the year 2008 (183.81 mm) and the lowest rainfall was seen in 2010

(114.67 mm). The observed rainfall data were collected for 1977-2009. The highest observed rainfall was recorded in 2013 (371.10 mm) followed 2008 (302.90 mm) and the lowest observed rainfall was recorded in the year 2010 (9.10 mm).

Fig. 5.11 represents the normalized and observed rainfall of Bareilly district for the months of July. The highest normalized rainfall is seen in the year 2010 (370.99 mm) followed by in the year 1980 (366.52 mm) and the lowest rainfall was seen 1991 (254.20 mm). The observed rainfall data were collected from 1977-2009, the maximum observed rainfall was recorded in the year 2010 (505.80 mm) followed by in the year 2008 (437.80 mm) and the minimum observed rainfall was recorded in the year 1991 (8.63 mm).

Fig. 5.12 represents the normalized and observed rainfall of Bareilly district for the months of August. The highest normalized rainfall is seen in year 1982 (348.20 mm) followed by in the year 2011 (347.37 mm) and the lowest was in 2005 (260.81 mm). The observed rainfall data were collected for 1990-2006. The maximum observed rainfall was recorded in the year 1982 (446.51 mm) followed by in the year 2011 (432.30 mm) and the minimum observed rainfall was recorded in the year 2005 (92.50 mm).

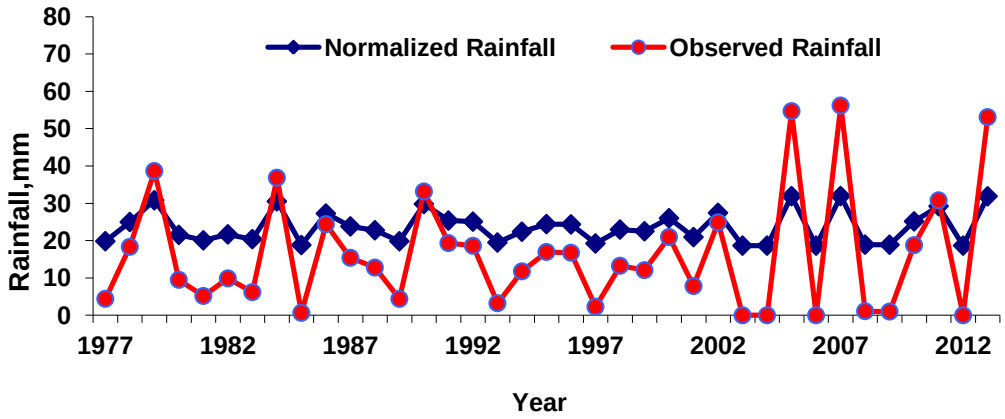

Fig. 5.6. Observed and Normalized Rainfall for Bareilly February

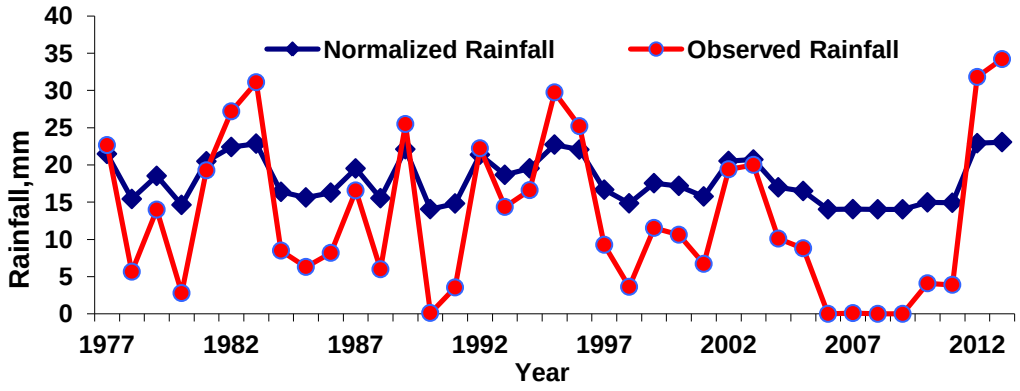

Fig. 5.5. Observed and Normalized Rainfall for Bareilly January

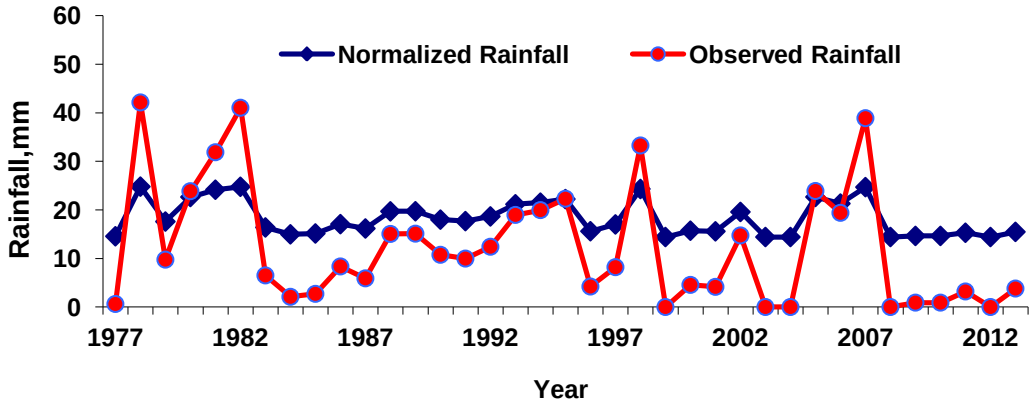

Fig. 5.7. Observed and Normalized Rainfall for Bareilly March

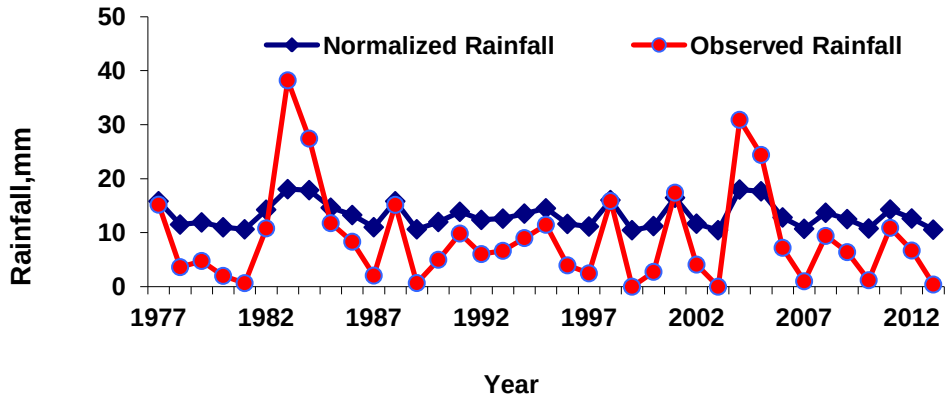

Fig. 5.8. Observed and Normalized Rainfall for Bareilly
April

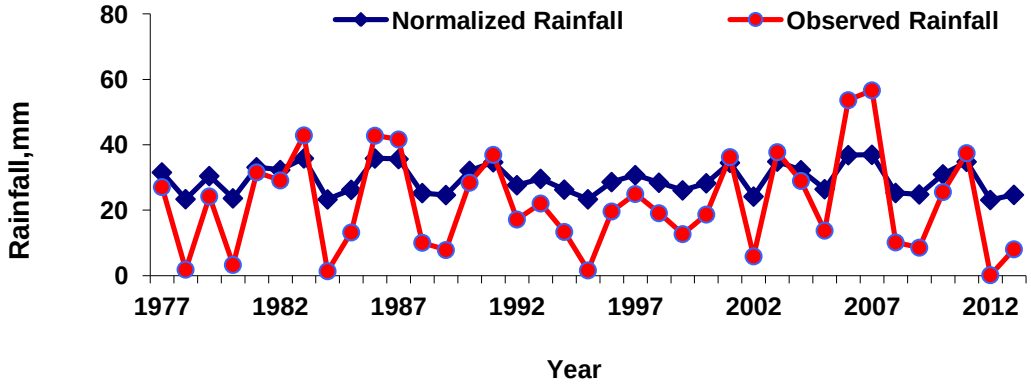

Fig. 5.9. Observed and Normalized Rainfall for Bareilly
May

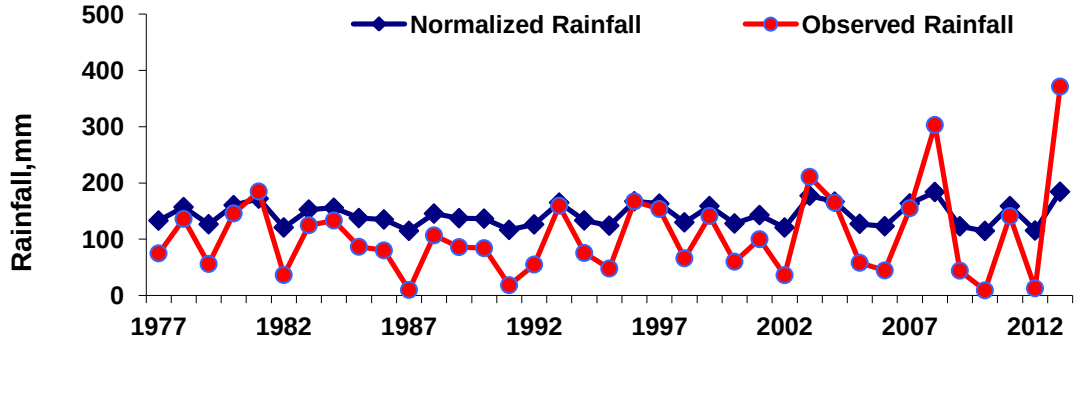

Fig. 5.10. Observed and Normalized Rainfall for Bareilly
June

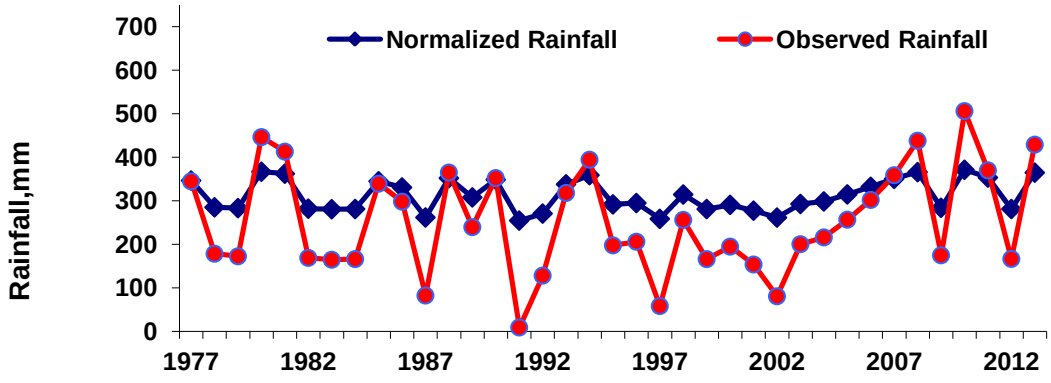

Fig. 5.11. Observed and Normalized Rainfall for Bareilly July

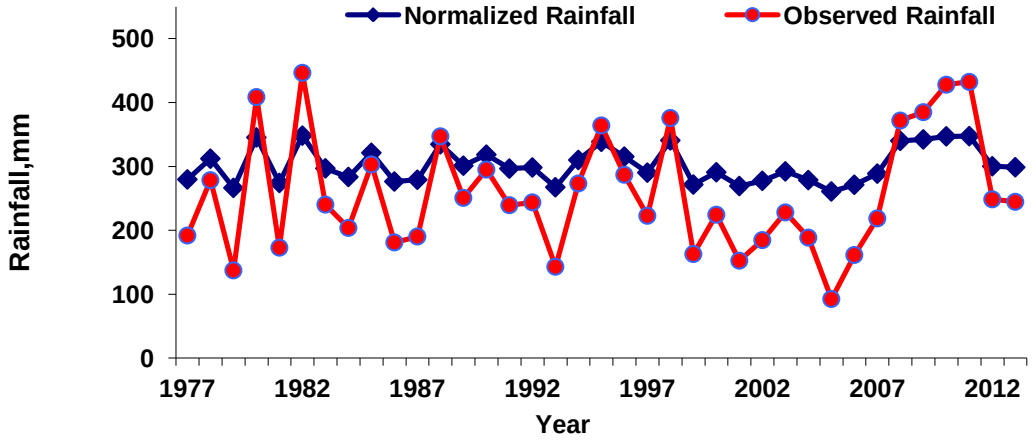

Fig. 5.12. Observed and Normalized Rainfall for Bareilly August

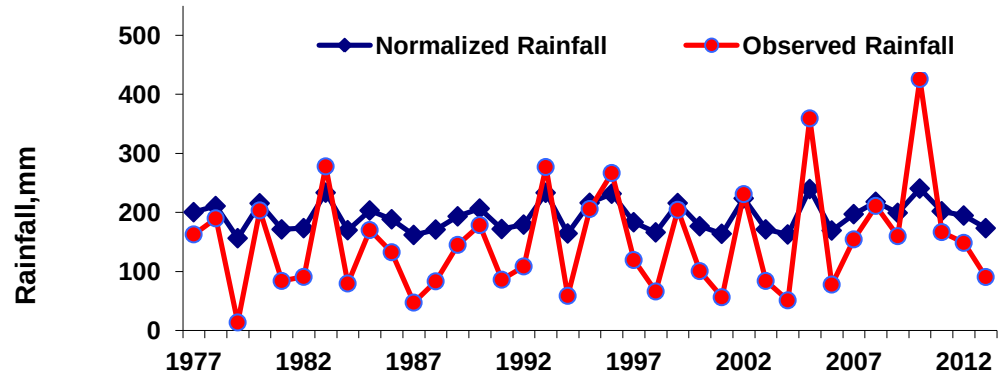

Fig. 5.13. Observed and Normalized Rainfall for Bareilly September

Fig. 5.13 represents the normalized and observed rainfall of Bareilly district for the months of September. The highest normalized rainfall was seen in the year 2010 (240.42 mm) followed by in the year 2005 (239.61mm) and the lowest normalized rainfall is seen in the year 1987 (161.84 mm). The observed rainfall data were collected for 1977-2009. The maximum observed rainfall was recorded in the year 2010 (425.9 mm) followed by in the year 2005 (359.3 mm) and the minimum observed rainfall was recorded in the year 1979 (13.69 mm).

Fig. 5.14 shows the normalized and observed rainfall of Bareilly district for the months of October. The highest normalized rainfall was seen in the year 1985 (49.30 mm) followed by in the year 2009 (49.20 mm) and the lowest normalized rainfall was seen in the years 2003, 2005, 2007, and 2011 (27.78 mm). The observed rainfall data were collected for 1977-2009. The maximum observed rainfall was recorded in the year 1985 (108.45 mm) followed by in the year 1990 (93.3 mm) and the minimum observed rainfall was recorded in the year 2003, 2005, 2007 and 2011 (0.0 mm).

Fig. 5.15 shows the normalized and observed rainfall of Bareilly district for the months of November. The highest normalized rainfall was seen in the year 1981 and 2009 (9.30 mm) followed by in the year 1992 (9.21 mm) and the lowest normalized rainfall was seen in 1992, 1993, 1994, 1996, 1999 ,2000 ,2003, 2004, 2005, 2007, 2008, 2011 and 2012 (5.12mm). The observed rainfall data were collected from 1979-2009. The maximum observed rainfall was recorded in the year 2009 (19.20 mm) followed by in the year 1981 (18.90 mm) and the minimum observed rainfall was recorded in the year 1977, 1983,1984, 1985, 1987, 1993, 1994, 1996, 1999, 2000, 2003, 2004, 2005, 2007, 2008, 2001 and 2012 (0.0 mm).

Fig. 5.16 shows the normalized and observed rainfall of Bareilly district for the months of December. The highest normalized rainfall was seen in the year 1986 (12.96 mm) followed by in the year 1985 (12.88 mm) and the lowest normalized rainfall was seen in the years 1992, 1993, 1996, (5.12mm). The observed rainfall data were collected for 1979-2009. The maximum observed rainfall was recorded in the year 1986 (29.77 mm) followed by in the year 1985 (22.44 mm) and the minimum observed rainfall was recorded in the year 1992, 2000, 2003, 2004, 2008 and 2011 (0.0 mm).

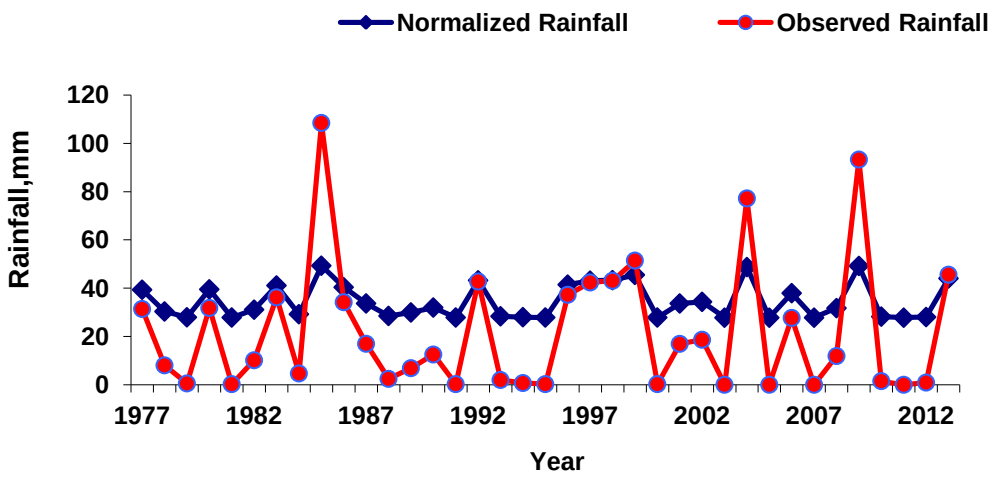

Fig. 5.14. Observed and Normalized Rainfall for Bareilly October

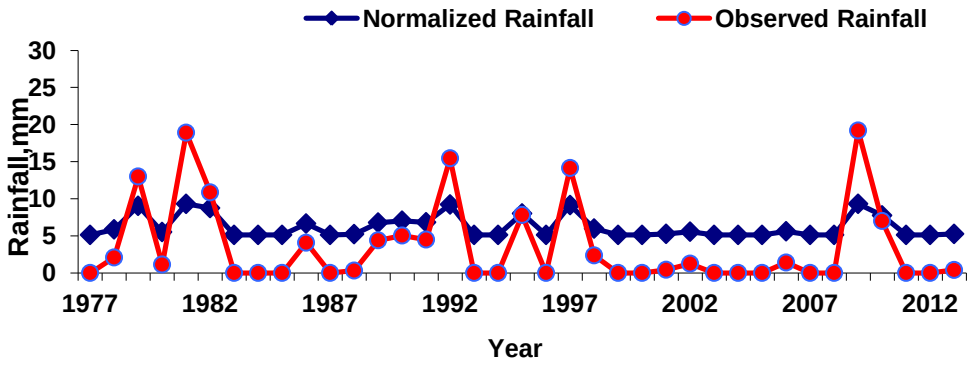

Fig. 5.15. Observed and Normalized Rainfall for Bareilly November

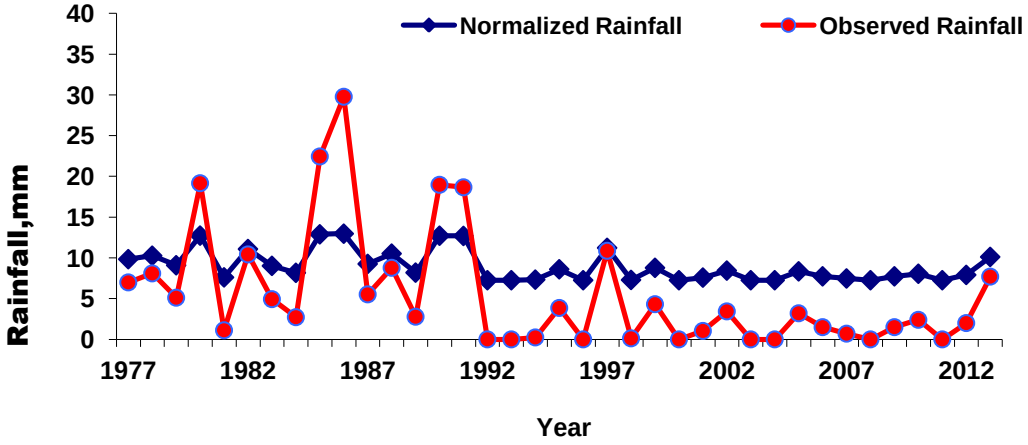

Fig. 5.16. Observed and Normalized Rainfall for Bareilly December

5.3. Rainfall pattern in the study area:

Table. 5.3. Monthly Rainfall during 2004-2013 at various rain gauge stations in mm:

Month	Bareilly Sadar	Baheri	Aonla	Nawabganj	Faridpur	Mirganj	Average
June	129.25	204.87	25.61	130.42	126.78	128.43	
July	278.45	512.29	64.03	271.6	302.79	306.56	
Aug.	247.62	536.3	67.04	253.67	226.03	291.16	
Sep.	188.49	293.5	36.69	175.3	164.67	205.55	
Oct.	17.47	50.46	6.31	25.05	18.15	22.19	
Nov.	1.16	4.12	0.52	4.41	3.65	1.8	
Dec.	1.41	1.2	0.15	2.05	0.35	2.47	
Jan.	5.54	11.8	1.47	3.8	3.6	8.3	
Feb.	16.75	37.24	4.66	13.24	8.99	23.04	
March	5.5	15.8	1.98	11.08	7.5	9.41	
April	5.99	11.35	1.42	11.83	5.64	6.65	
May	27.45	55.28	6.91	19.4	14.41	13.03	
Total	925.09	1734.21	216.27	921.85	882.56	1018.59	949.76

(Source: Nazarat, collectorate, Bareilly; and Hydromet Division, I.M.D.)

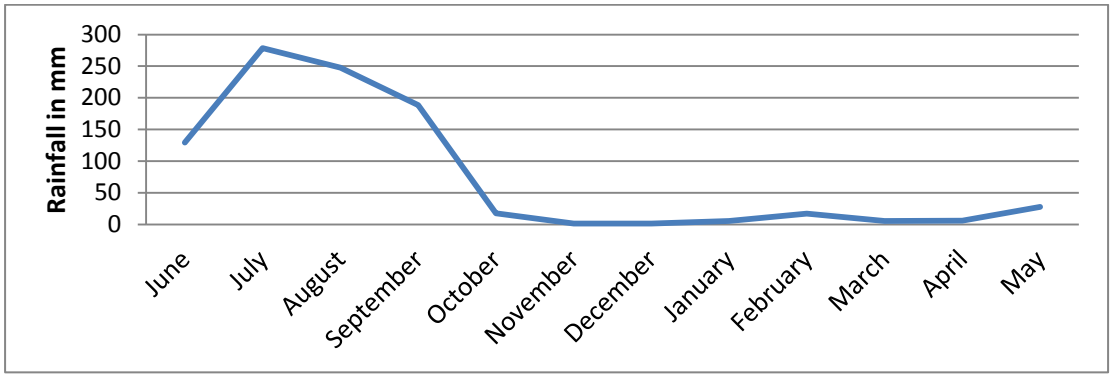

Figure. 5. 17 (a). Monthly pattern of rainfall at Bareilly Sadar raingauge station

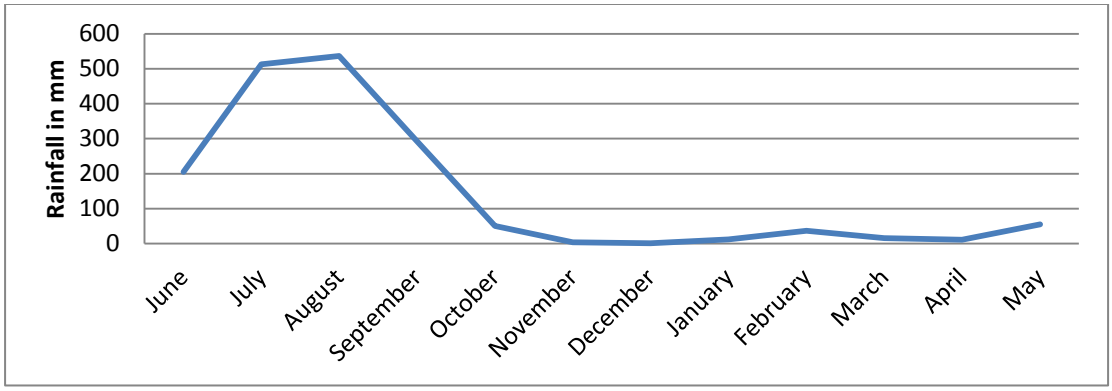

Figure 5. 17 (b). Monthly pattern of rainfall at Baheri raingauge station

5.3.1. Pattern of seasonal variation and distribution of rainfall:

Monthly rainfall pattern in the study area shows a similar trend at all the six rain gauge stations. Table. 5.3 and [Figure.5.18 (a) to Figure. 5.18 (f)]. It is observed from the figures that almost entire (about 92-95 %) rainfall occurs in four months of Monsoon season (mid June to mid October). The balance amount of rainfall (about 5-8% only) is received during the months of November to May [Table.5.3. and Figure.5.18 (g) and 5.18 (h)]. It is also observed from Table.5.3 and Figure. 5.18 (h) that the Baheri station which is located in the northern portion of the study area regularly receives maximum rainfall (1734.21 mm) and Aonla station located in the southern part of the study area receives minimum rainfall (216.27 mm). The other four rain gauge stations namely Mirganj, Bareilly Sadar, Nawabganj, and Faridpur, receive equally moderate amount (1018.59, 925.09, 921.85, and 882.56 mm respectively) of rainfall.

5.3.2. Spatial distribution pattern of rainfall at various rain gauge stations:

It is observed from table. 5.6. and figure. 5.19 (b) that rainfall received at Baheri raingauge station is always higher than the district average during all the months except in December and January months, (monsoon and non monsoon) of the study period (2004-2013). It is also observed from the figure. 5.19 (c) that Aonla raingauge station always received less than the average rainfall during the entire period of study (2004-2013). The rain gauge station at Mirganj also received good amount of rainfall during the monsoon season. The rainfall received at this station was higher than the study area average in the months of June, July, August and September figure 5.19(f). The rain gauge station at Bareilly sadar, Nawabganj and Faridpur experienced similar pattern of rainfall occurrences. It is evident from the figure.5.19 (a), 5.19 (d) and 5.19 (e) that these three stations received higher than the average rainfall during June, July and September while they received less than the average rainfall during the month of August.

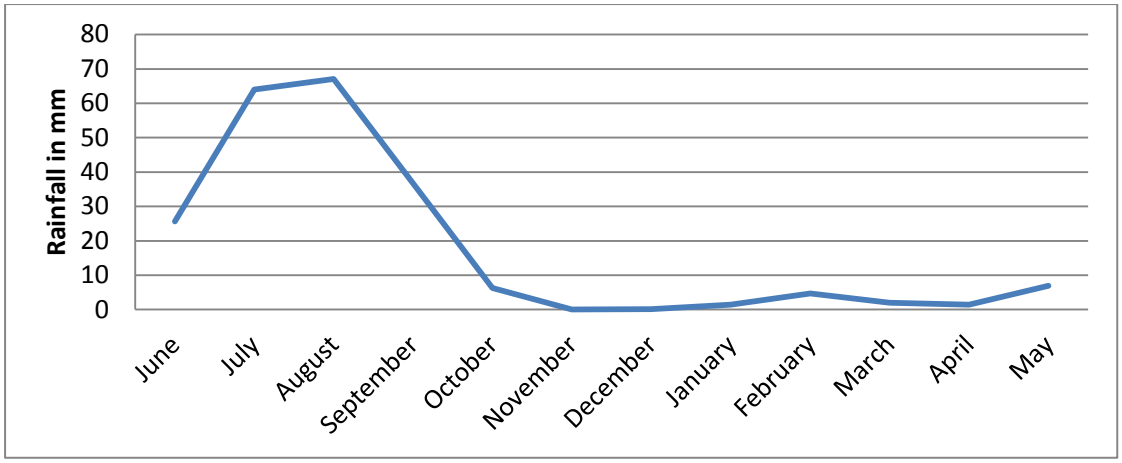

Figure 5.17 (c). Monthly pattern of rainfall at Aonla raingauge station

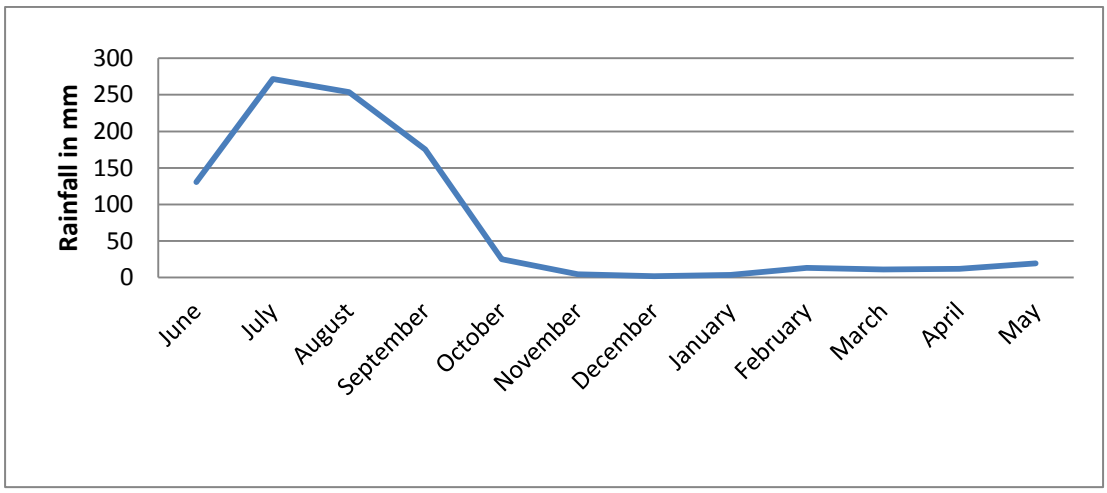

Figure 5.17 (d). Monthly pattern of rainfall at Nawabganj raingauge station

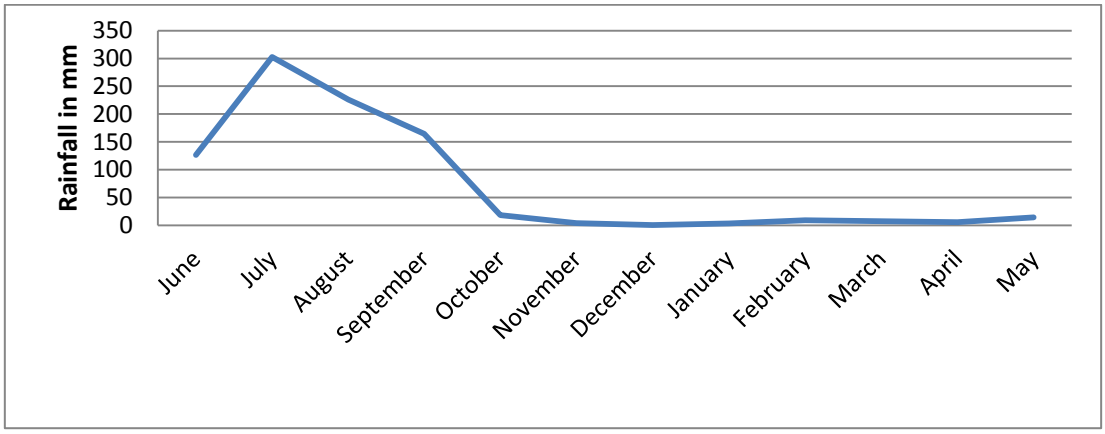

Figure 5.17 (e). Monthly pattern of rainfall at Faridpur raingauge station

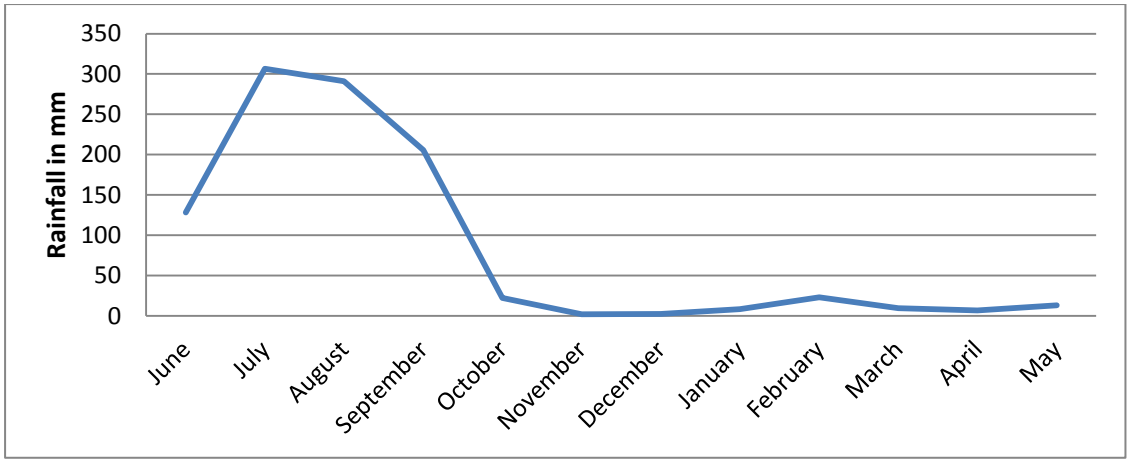

Figure. 5.17 (f). Monthly pattern of rainfall at Mirganj raingauge station

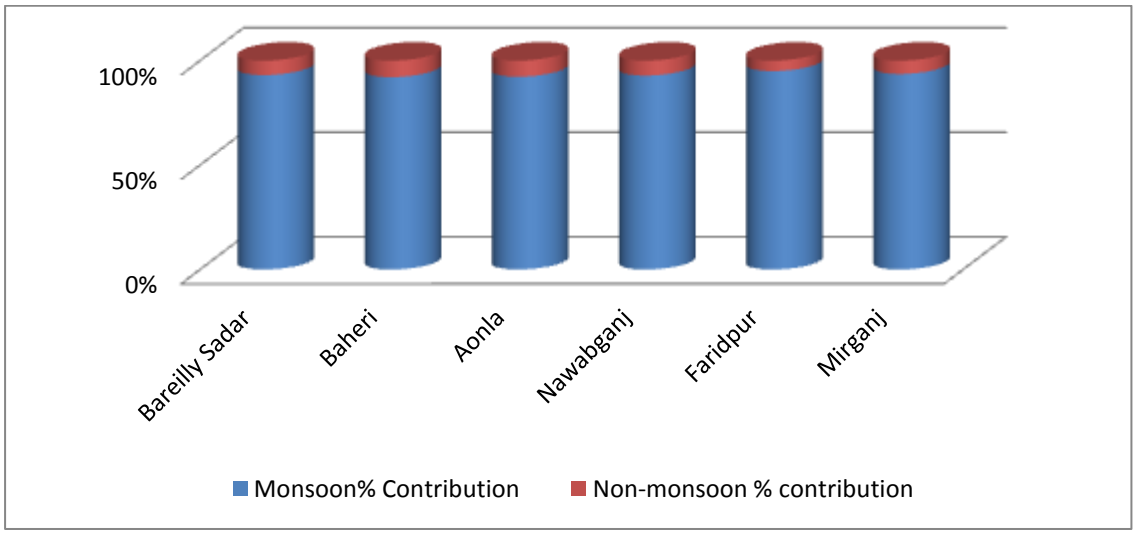

Figure. 5.18 (a). Percentage contributions by Monsoon and Non-monsoon rains on total annual rainfall

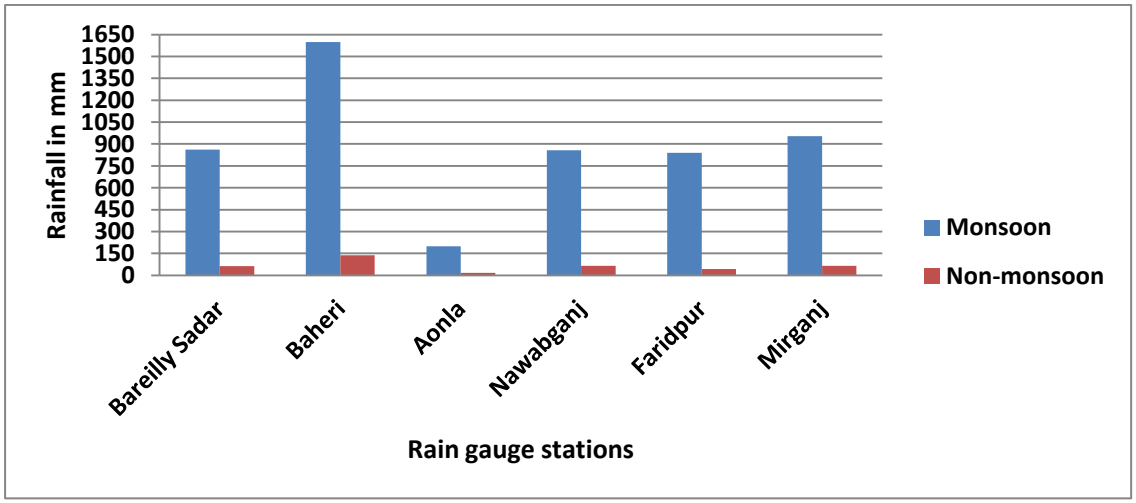

Figure. 5. 18 (b). Seasonal (Monsoon and Non-monsoon) and Tehsil-wise variation of rainfall

Table. 5.4. Percentage contribution of rainfall by Monsoon and Non-monsoon rain in the study area (2004-13)

Sl.No.	Raingauge Station	Monsoon Rainfall (mm)	contribution By monsoon rain (%)	Non-monsoon Rainfall (mm)	% contribution By Non-monsoon rain (%)
1	Bareilly Sadar	861.29	93.1	63.8	6.9
2	Baheri	1597.42	92.11	136.79	7.89
3	Aonla	199.68	92.3	17.11	7.7
4	Nwabganj	856.04	92.86	65.81	7.14
5	Faridpur	838.42	95	44.14	5
6	Mirganj	953.89	93.65	64.7	6.35

Table. 5.5. Long term (1984-2013) average monthly rainfall of the study area:

	Jan	Feb	Mar	Apr	May	Jun	Jul	Aug	Sep	Oct	Nov	Dec
Average	11.9	17.05	10.12	8.61	21.85	106.04	247.16	254.8	151.57	23.34	2.93	5.08

(Source: Nazarat, (Collectorate), Bareilly; and Hydro met Division, India Meteorological Department)

Table. 5.6. Monthly variation of rainfall from long term (1984-2013) monthly average:

Station	Jan	Feb	Mar	Apri	May	June	July	Aug	Sep	Oct	Nov	Dec
Bareilly Sadar	-6.36	-0.30	-4.62	-2.62	5.6	23.21	31.29	-7.18	36.92	-5.87	-1.76	-3.67
Baheri	-0.1	20.19	5.68	2.74	33.43	98.83	265.13	281.5	141.93	27.12	1.2	-3.88
Aonla	-10.43	-12.39	-8.14	-7.19	-14.94	-80.43	-183.13	-187.76	-114.88	-17.03	-2.4	-4.93
Nawab Ganj	-8.1	-3.81	0.96	3.22	-2.45	24.38	24.44	-1.13	23.73	1.71	1.49	-3.03
Faridpur	-8.3	-8.06	-2.62	-2.97	-7.44	20.74	55.63	-28.77	13.1	-5.19	0.73	-4.73
Mirganj	-3.6	5.99	-0.71	-1.96	-8.82	22.39	59.4	36.36	53.98	-1.15	-1.12	-2.61

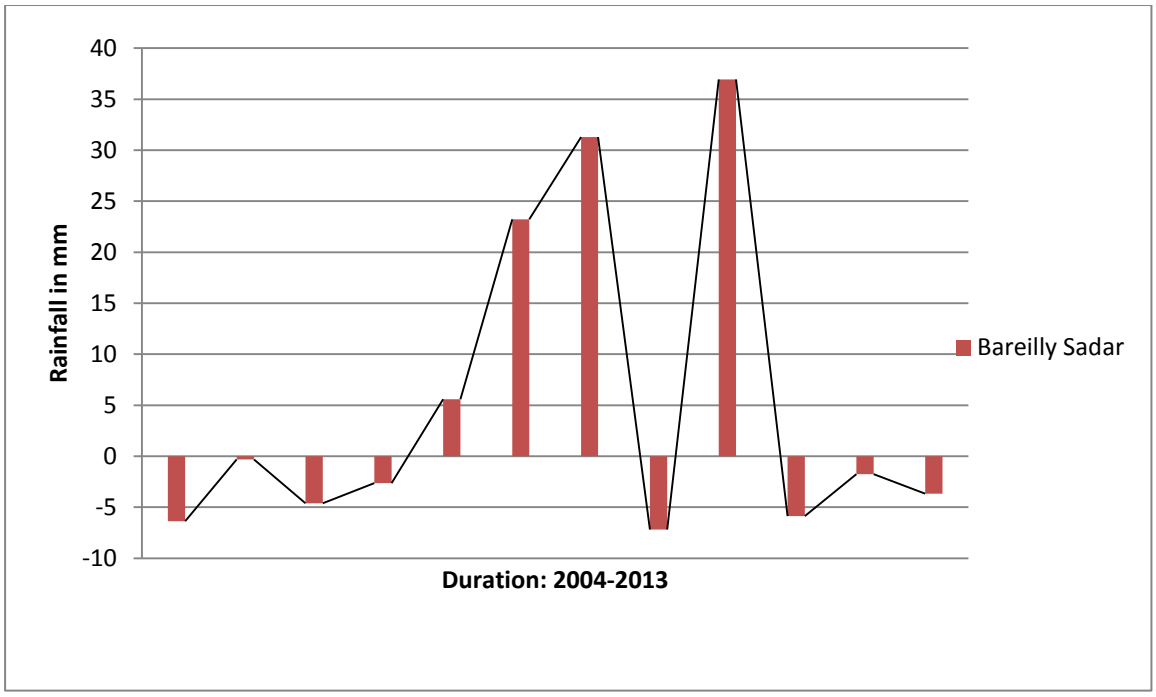

Figure 5.19 (a). Monthly variation of rainfall at Bareilly Sadar rain gauge station

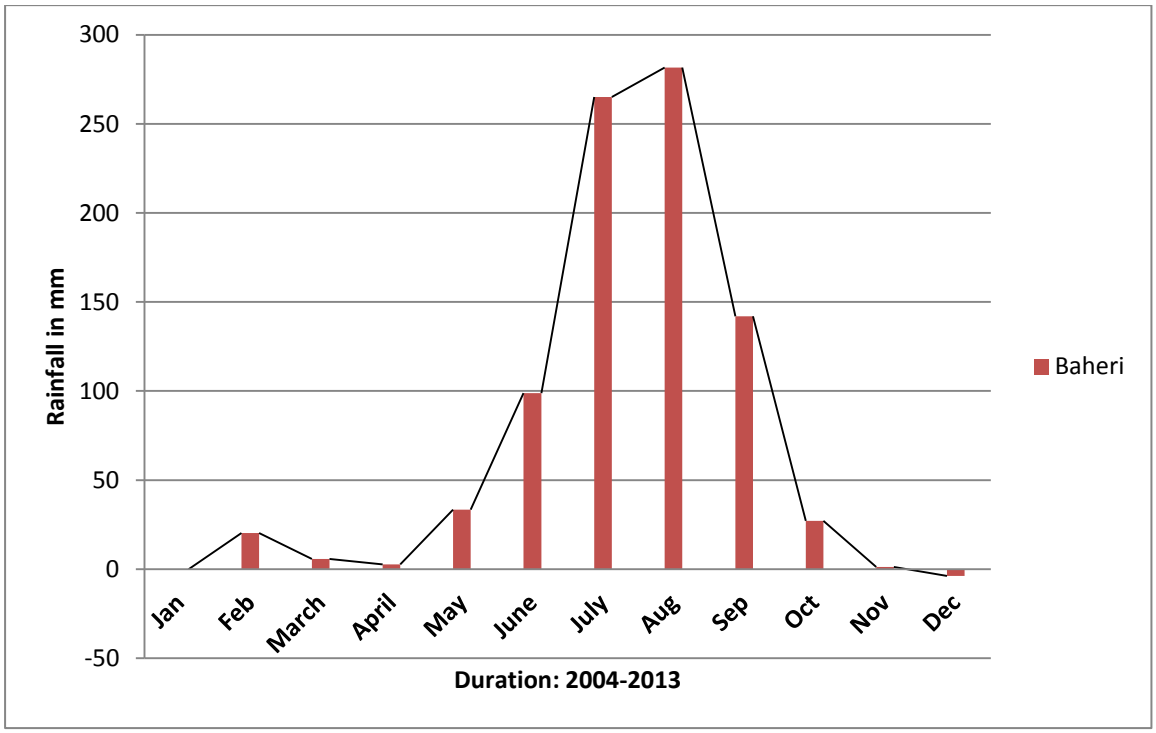

Figure. 5.19. (b). Monthly variation of rainfall from its long term monthly average at Baheri rain gauge station

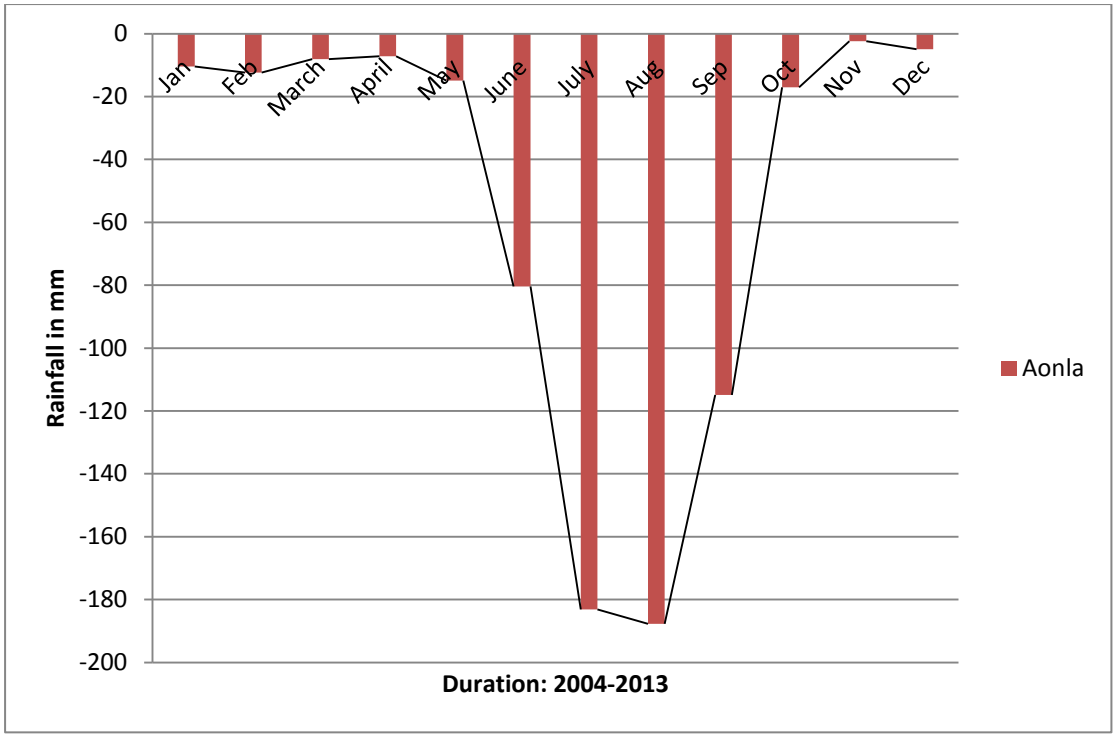

Figure. 5.19. (c). Monthly variation of rainfall from its long term monthly average at Aonla rain gauge station

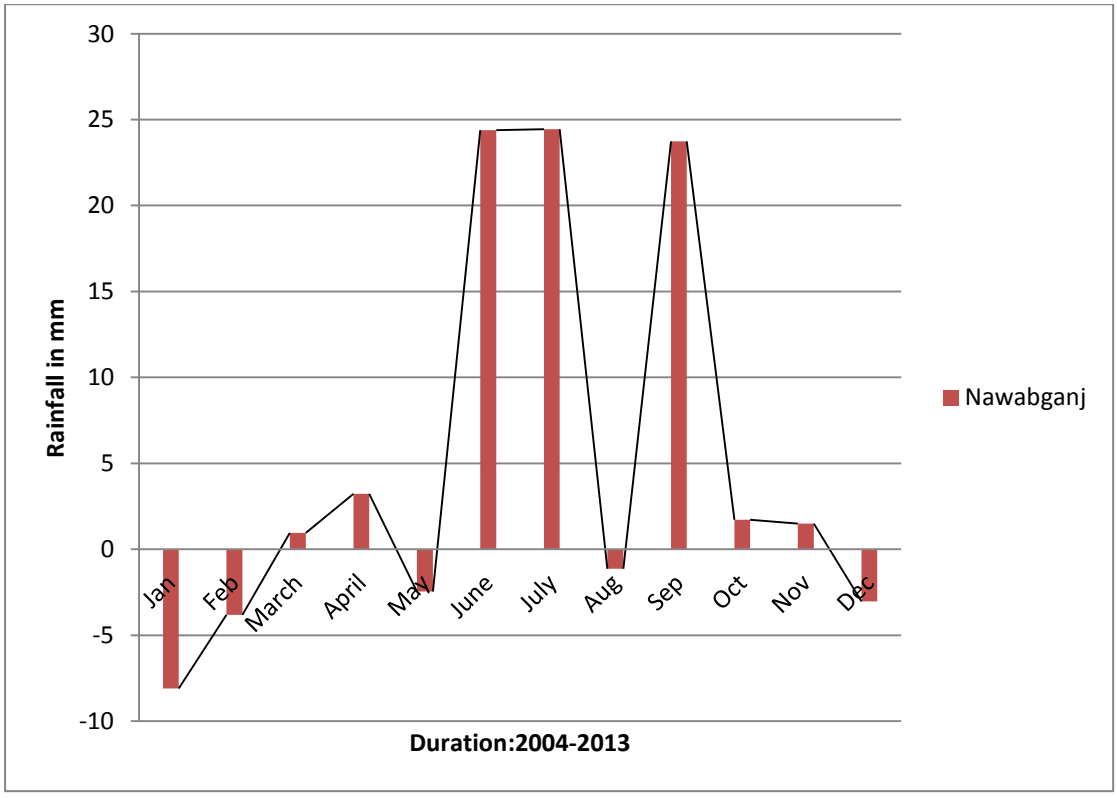

Figure. 5.19. (d). Monthly variation of rainfall from its long term monthly average at at Nawabganj rain gauge station

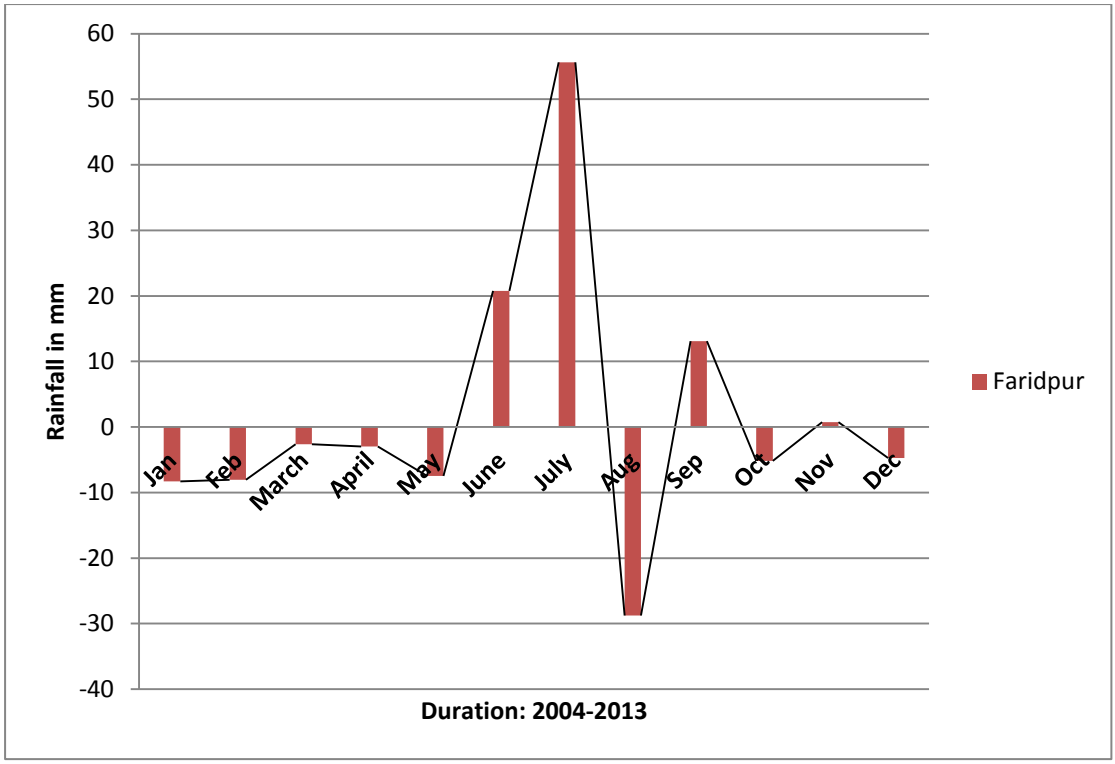

Figure. 5.19. (e). Monthly variation of rainfall from its long term monthly average at Faridpur rain gauge station

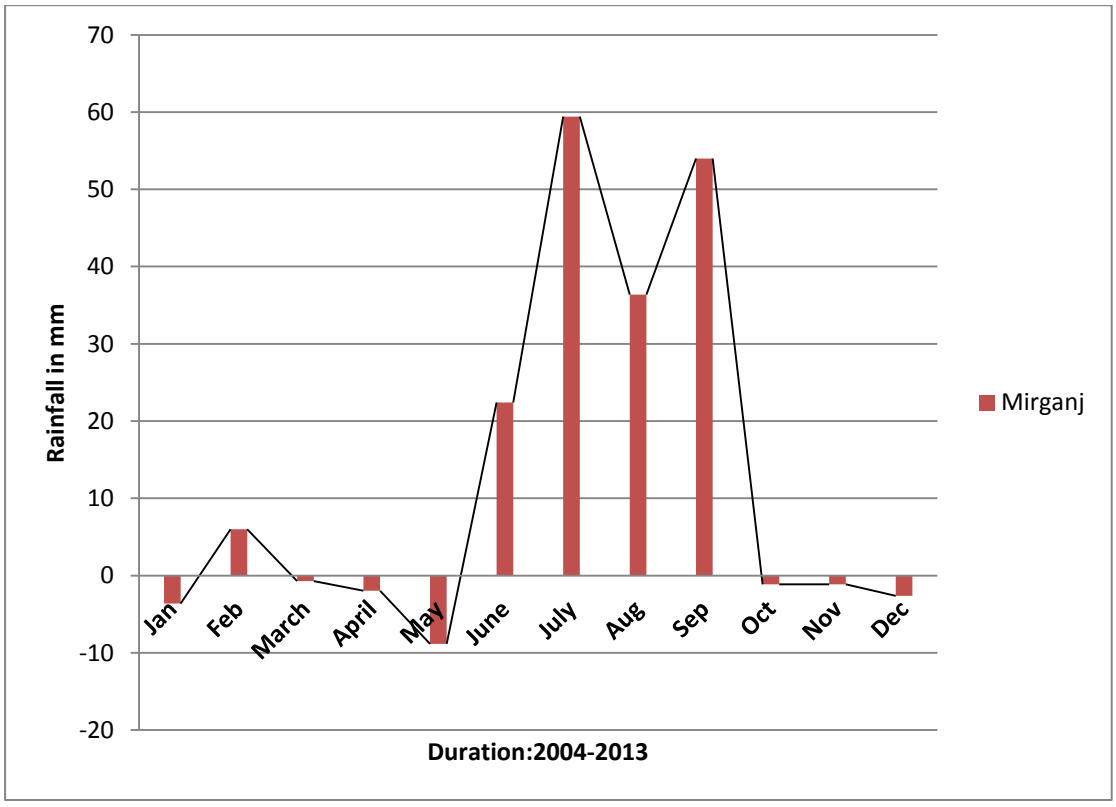

Figure. 5. 19. (f) Monthly variation of rainfall from its long term monthly average at Mirganj rain gauge station

5.4 Observed and normalized pre and post monsoon water table fluctuations:

The fluctuation of water table is largely due to changes in the infiltration and hydraulic conductivity properties of the land caused by Land use Land cover changes occurred in the area. In the present study, the observed water table data for the period 1998-2013 recorded at different observation wells situated at six tehsils i.e. Bareilly Sadar, Baheri, Aonla, Nawabganj, Faridpur and Mirganj was normalized for removing inaccuracies possibly due to human error in data recording.

Figure 5.20. shows that at Bareilly Sadar observatory, the observed pre-monsoon water table varied from 4.05 m (shallowest) in the year 1998 to 6.0 m (deepest) in the year 2010. The observed mean value was 5.37 m, which is a little lower than the normalized mean value of 5.73 m. The normalized pre-monsoon water table varies from 5.388 m (shallowest) in the year 1998 to 5.927 m (deepest) in the year 2010.

Figure 5.21. The trend of water table fluctuation during post-monsoon period at Bareilly Sadar observation well is shown in figure 5.21. It is seen that the value of deepest observed water table is 6.0 m in the year 2013 followed by 5.65 m in the year 2006. The observed (shallowest) water table is 3.12 m in the year 1998. Similarly the corresponding normalized value of 5.45 m as deepest in the year 2013 and shallowest water table of 4.67 m in the year 1998 have been calculated. The fluctuation is higher in the observed values than that in the normalized water table values.

Fig. 5.22. shows that at Baheri observatory, the observed pre-monsoon water table varied from 2.00 m (shallowest) in the year 2004 to 3.73 m (deepest) in the year 2010. The observed mean value was 2.85 m, which is a little higher than the normalized mean value of 3.07 m. The normalized pre-monsoon water table varies from 2.86 m (shallowest) in the year 2004 to 3.29 m (deepest) in the year 2010.The fluctuation is more pronounced in case of observed values than that of normalized values.

Fig.5.23. depicts the observed post-monsoon water table trend at Baheri observatory. It varied from 0.60 m (shallowest) in the year 1998 to 2.65 m (deepest) in the year 2009. The observed mean value for post-monsoon water table was 1.52 m, which is a little lower than the normalized mean value of 1.80 m. The normalized post-monsoon

water table varies from 1.555 m (shallowest) in the year 1998 to 2.097 m (deepest) in the year 2009.

Fig.5.24. depicts the trend of pre-monsoon water table fluctuations at Aonla observation station. The water table varied from 8.79 m (shallowest) in the year 2001 to 13.6 m (deepest) in the year 2013. The observed mean value for pre-monsoon water table was 10.65 m, which is a little lower than the normalized mean value of 11.36 m. The normalized pre-monsoon water table varies from 10.798 m (shallowest) in the year 2001 to 12.074 m (deepest) in the year 2013.

Fig.5.25. depicts the trend of post-monsoon water table fluctuations at Aonla observation station. The observed water table varied from 8.02 m (shallowest) in the year 2000 to 11.96 m (deepest) in the year 2013. The observed mean value for post-monsoon water table was 9.93 m, which is a little lower than the normalized mean value of 10.56 m. The normalized post-monsoon water table varies from 10.004 m (shallowest) in the year 2000 to 11.097 m (deepest) in the year 2013.

Fig.5.26. depicts the trend of pre-monsoon water table fluctuations at Nawabganj observation well. The water table varied from 3.21 m (shallowest) in the year 2000 to 5.64 m (deepest) in the year 2012. The observed mean water table value for pre-monsoon period was 4.37 m, which is a little lower than the normalized mean value of 4.62 m. The normalized pre-monsoon water table varies from 4.379 m (shallowest) in the year 2000 to 4.870 m (deepest) in the year 2012.

Fig.5.27. depicts the trend of post-monsoon water table fluctuations at Nawabganj observation station. The observed water table varied from 1.17 m (shallowest) in the year 2011 to 3.72 m (deepest) in the year 2012. The observed mean value for post-monsoon water table was 2.62 m, which is a little lower than the normalized mean value of 3.04 m. The normalized post-monsoon water table varies from 2.646 m (shallowest) in the year 2011 to 3.347 m (deepest) in the year 2012.

Fig.5.28. depicts the trend of pre-monsoon water table fluctuations at Faridpur observation well. The water table varied from 4.30 m (shallowest) in the year 2004 to 7.85 m (deepest) in the year 2008 and 2009. The observed mean water table value for pre-monsoon period was 5.62 m, which is a little lower than the normalized mean

value of 6.01 m. The normalized pre-monsoon water table varies from 5.65 m (shallowest) in the year 2004 to 6.595 m (deepest) in the year 2008 and 2009.

Fig.5.29. depicts the trend of post-monsoon water table fluctuations at Faridpur observation well. The observed water table varied from 2.78 m (shallowest) in the year 2013 to 6.04 m (deepest) in the year 2009. The observed mean value for post-monsoon water table was 2.62 m, which is a little lower than the normalized mean value of 3.04 m. The normalized post-monsoon water table varies from 4.523 m (shallowest) in the year 2013 to 5.469 m (deepest) in the year 2009

Fig.5.30. depicts the trend of pre-monsoon water table fluctuations at Mirganj observation well. The observed water table varied from 5.03 m (shallowest) in the year 2001 to 7.1 m (deepest) in the year 2012. The observed mean value for pre-monsoon water table was 2.62 m, which is a little lower than the normalized mean value of 3.04 m. The normalized pre-monsoon water table varies from 5.971 m (shallowest) in the year 2001 to 6.561 m (deepest) in the year 2012.

Fig.5.31. depicts the trend of post-monsoon water table fluctuations at Mirganj observation well. The water table varied from 2.28 m (shallowest) in the year 2000 to 6.7 m (deepest) in the year 2012. The observed mean water table value for pre-monsoon period was 5.62 m, which is a little lower than the normalized mean value of 6.01 m. The normalized pre-monsoon water table varies from 4.58 m (shallowest) in the year 2000 to 5.548 m (deepest) in the year 2012.

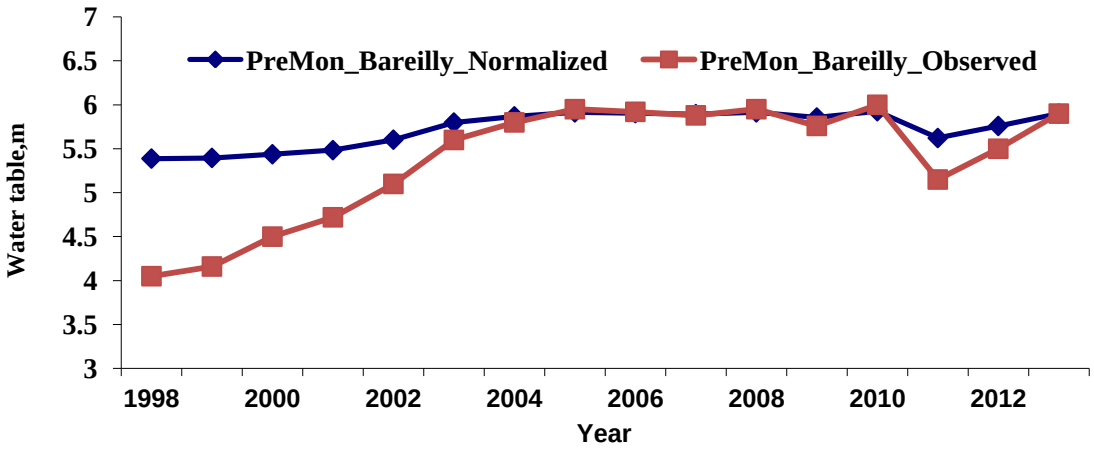

Fig. 5.20. Observed and Normalized Pre monsoon Water Table at Bareilly

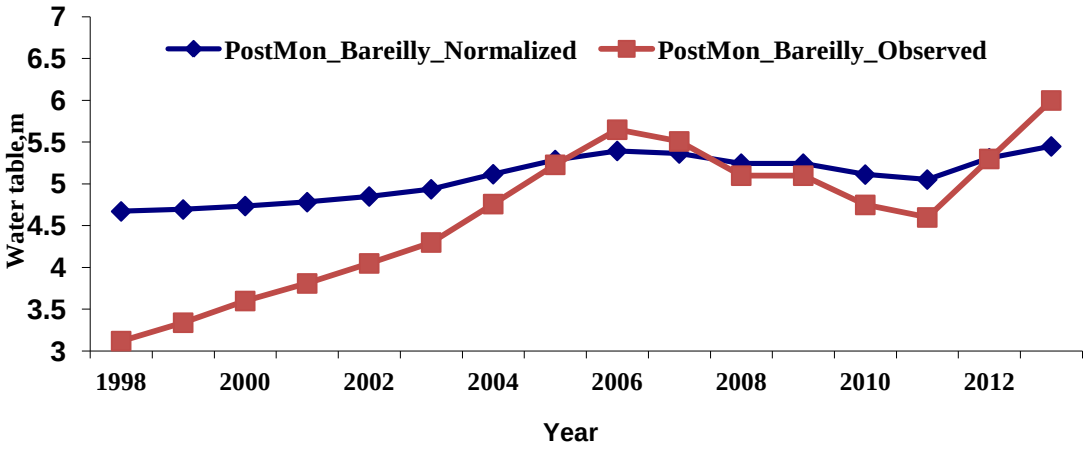

Fig. 5.21. Observed and Normalized Post monsoon Water Table at Bareilly

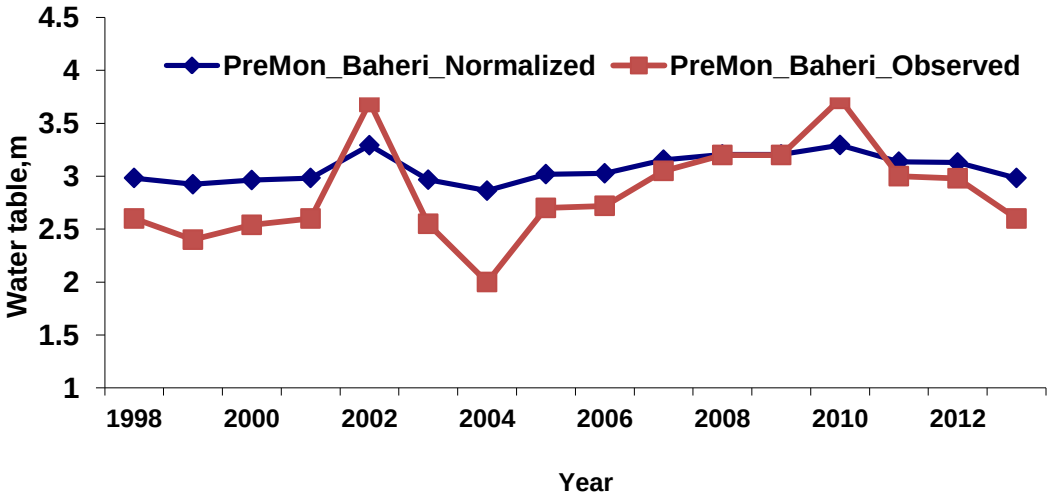

Fig. 5.22. Observed and Normalized Pre monsoon Water Table at Baheri

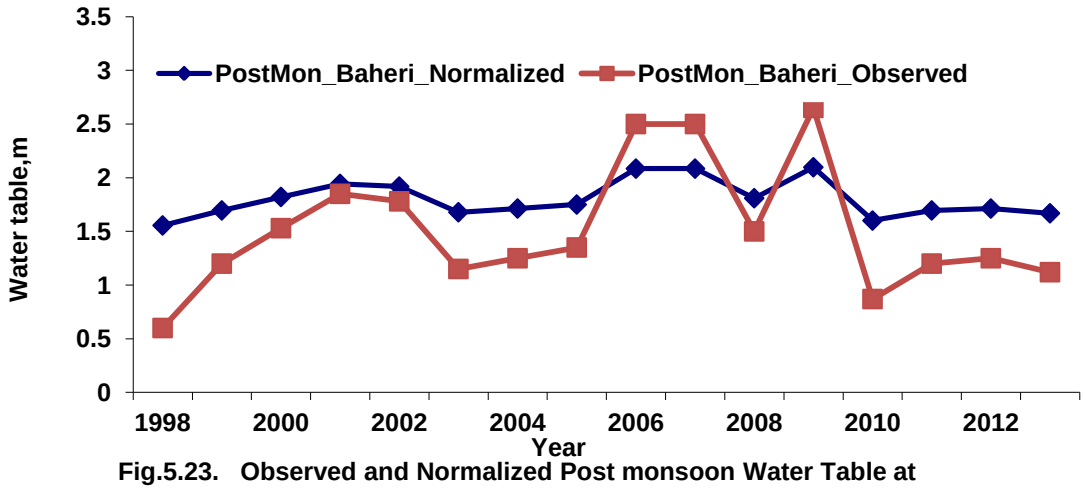

Fig.5.23. Observed and Normalized Post monsoon Water Table at Baheri

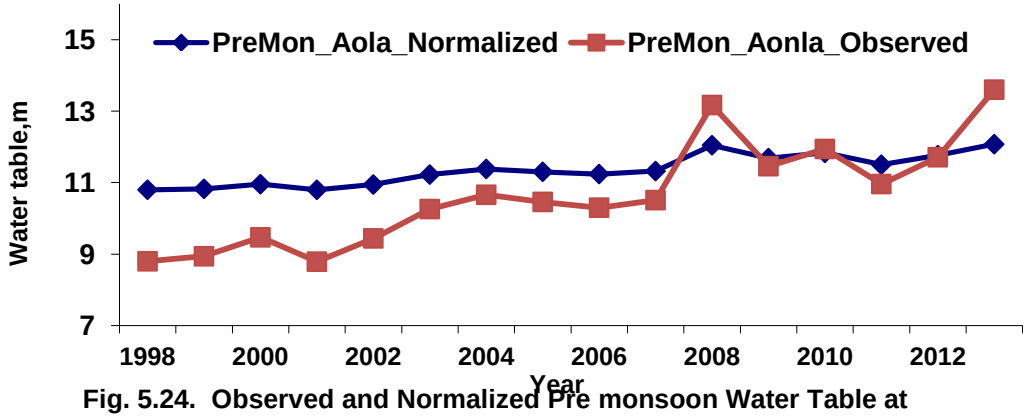

Fig. 5.24. Observed and Normalized Pre monsoon Water Table at Aonla

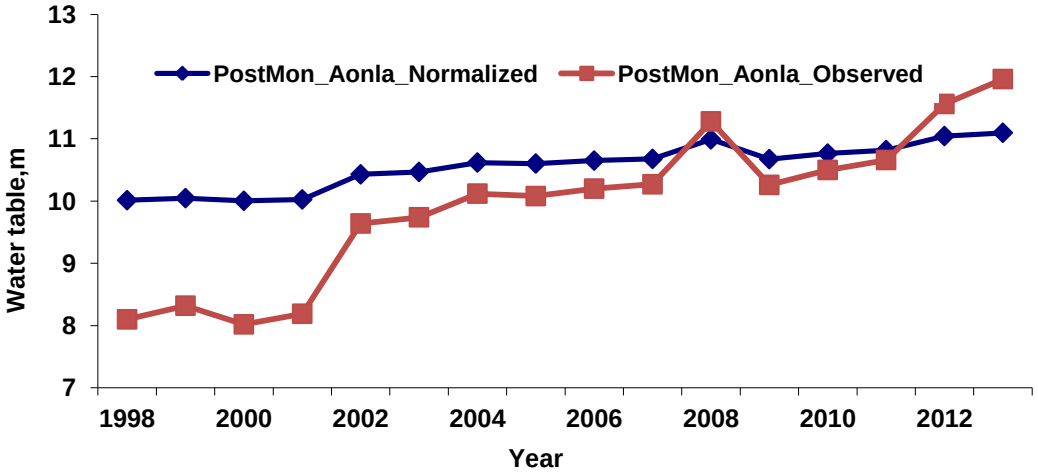

Fig. 5.25. Observed and Normalized Post monsoon Water Table at Aonla

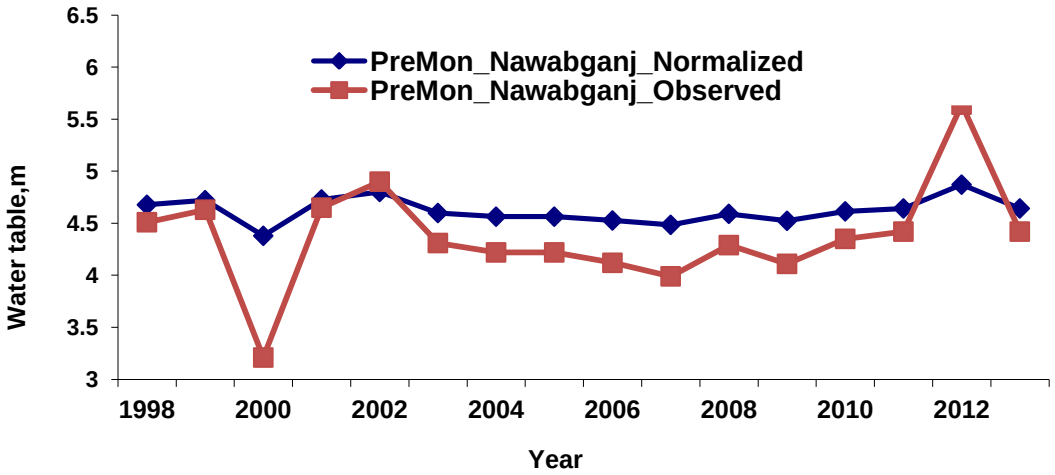

Fig. 5.26. Observed and Normalized Pre monsoon Water Table at Nawabgaanj

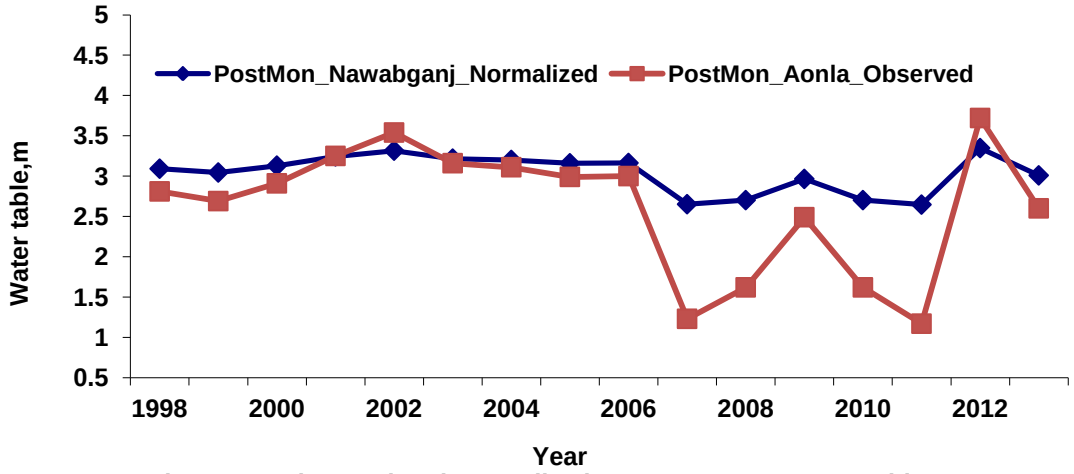

Fig. 5.27. Observed and Normalized Post monsoon Water Table at Nawabganj

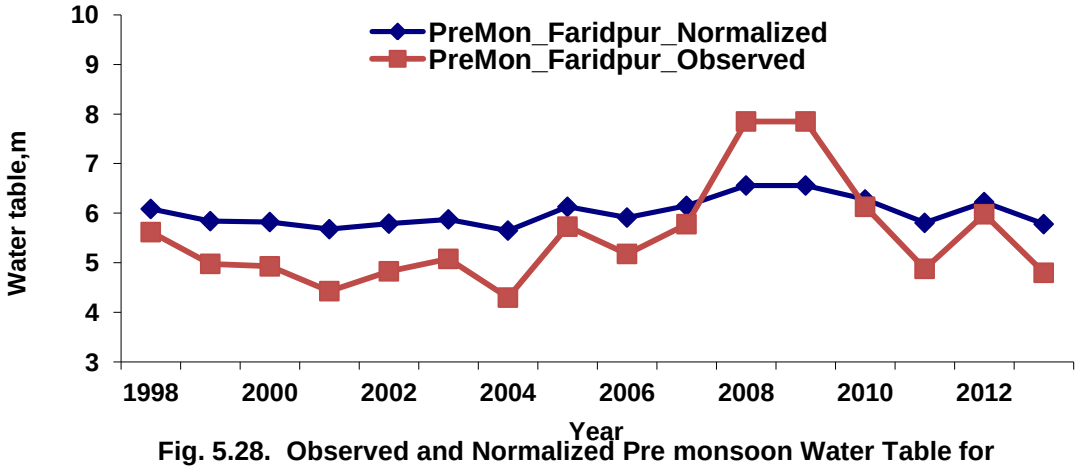

Fig. 5.28. Observed and Normalized Pre monsoon Water Table for Faridpur

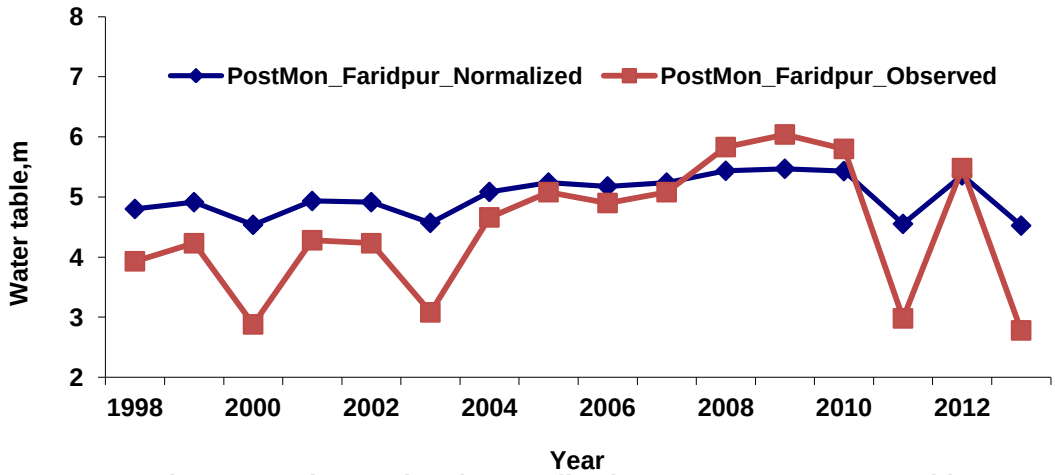

Fig. 5.29. Observed and Normalized Post monsoon Water Table at Faridpur

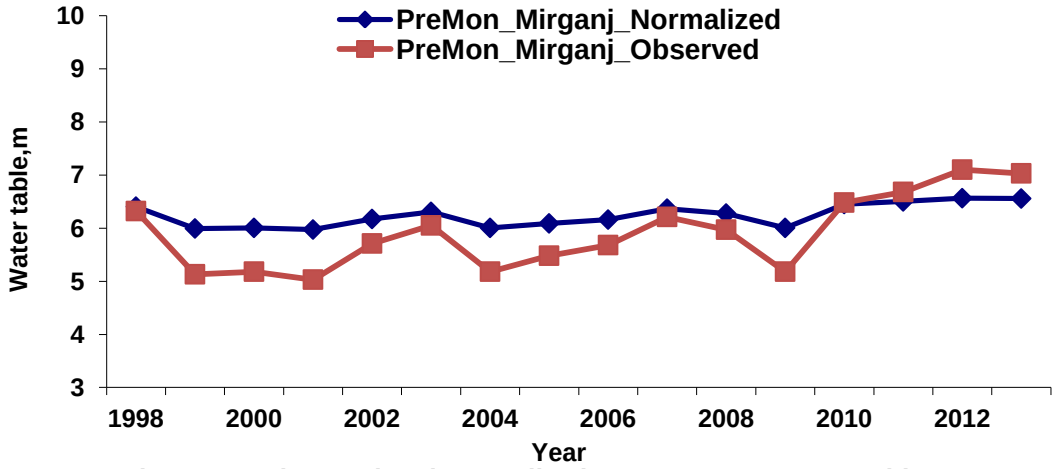

Fig. 5.30. Observed and Normalized Pre monsoon Water Table at Mirganj

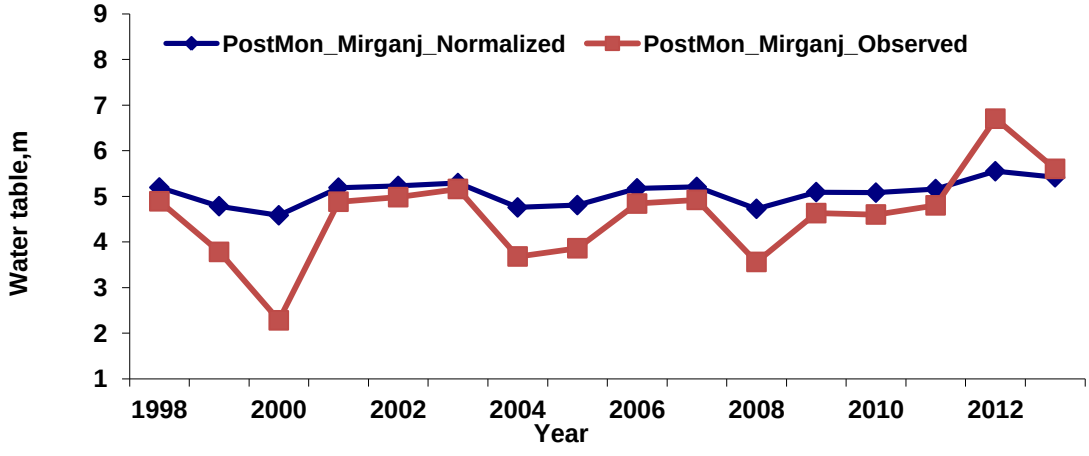

Fig. 5.31. Observed and Normalized Post monsoon Water Table at Mirganj

5.5. Groundwater Table analysis:

From the table.5.7. and figure. 5.32, it is observed that the pre-monsoon water table of the study area ranges from 2.981m (shallowest) at Baheri station to 11.477 m (Deepest) at Aonla station. Similarly post monsoon water table ranges from 1.619 m at Baheri station to 10.689m at Aonla station. It is also evident from table. 5.8. and figure. 5.33, that minimum fluctuations of 0.581m is at Bareilly sadar station followed by Aonla (0.788m), Faridpur (0.985m), Baheri (1.299m) and Mirganj station (1.38m). Highest fluctuations of ground water table (2.023m) was recorded at Nawabganj station followed by Mirganj and Baheri station. The all above three stations represent the areas which are not dominated by settlements but by water intensive cropped area. The crops grown are Paddy, Sugarcane Mentha and wheat. To meet out the water requirements of these crops the ground water draft is very high causing lowering of water table particularly in the non monsoon period. Also recharging of water table is very high as these areas receive very high amount of rainfall over negligible built up area and maximum crop cultivated area which are favourable for better infiltration and ground water recharge. The lower fluctuation in the water table observed at Bareilly Sadar station indicates the higher drafts with lesser recharge as this area is mainly dominated by city settlements forcing higher draft with lower recharge conditions. The water table depth at Aonla station is highest because of very less groundwater recharge as this area receives very less rainfall. The regular pattern of receiving lesser rainfall have compelled the farmers to grow less water consuming crops thus avoiding over pumping of groundwater , which is evident from the table. 5.8 and figure. 5.34 that in spite of very less rainfall the fluctuation of water level is still less than other stations except Bareilly Sadar station. From table. 5.9. and figure.5.36 the entire study area shows positive fluctuations in the ground water table. It is clear from the Figure that for more rainfall during monsoon season there is more groundwater recharge as reflected through more rise in Groundwater table. From figure. 5.36 it is also evident that the ground water table in the entire study area is depleting though, moderately but steadily.

Table.5.7. Tehsil-wise groundwater level status in the study area:

Observation well station name	Pre-Monsoon Water level (Meter)	Post-Monsoon Water level (Meter)	Fluctuation (Pre-Post) (Meter)
Bareilly Sadar	5.781	5.2	0.581
Baheri	2.918	1.619	1.299
Aonla	11.477	10.689	0.788
Nawabganj	4.378	2.355	2.023
Faridpur	5.848	4.863	0.985
Mirganj	6.099	4.719	1.38

(Source: Senior Hydro geologist's office, Bareilly, and Groundwater information system, NIC.)

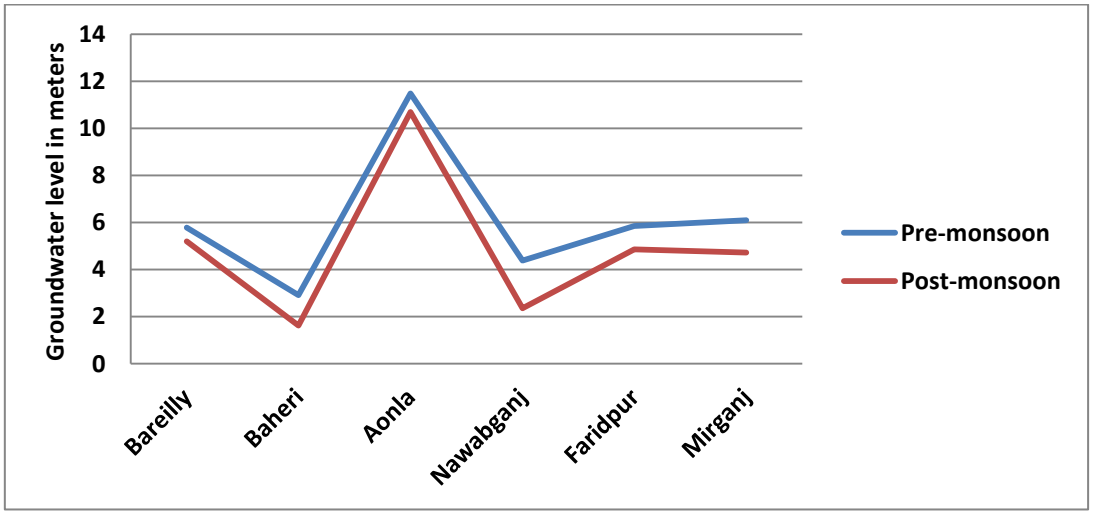

Figure. 5. 32. Tehsil-wise groundwater table (Pre & Post-monsoon) status in the area

Table.5.8. Tehsil-wise groundwater level fluctuation in the study period (2004-2013):

Station Name	Groundwater level Fluctuation in meters
Bareilly	+ 0.581
Baheri	+ 1.299
Aonla	+ 0.788
Nawabganj	+ 2.023
Faridpur	+ 0.985
Mirganj	+ 1.38

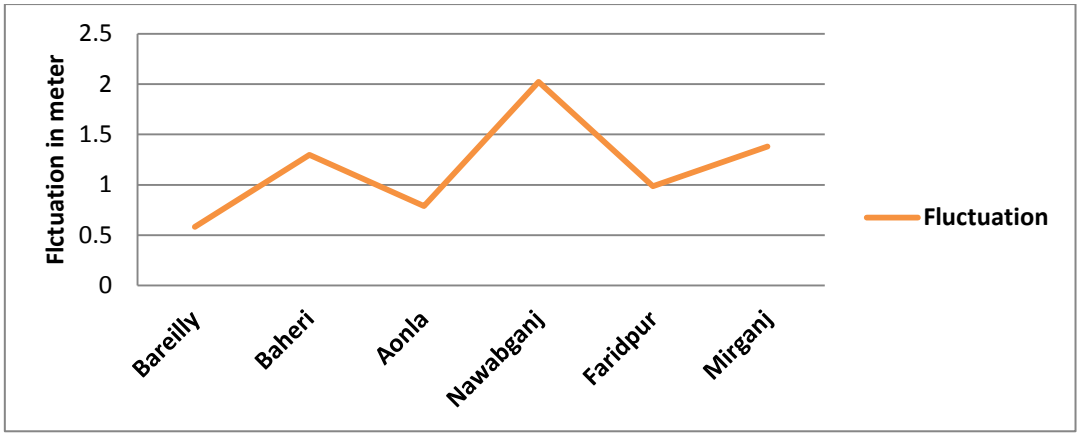

Figure. 5.33. Tehsil-wise groundwater level fluctuation in the study area

Table. 5.9. Pre & Post Monsoon water table and average water table fluctuation

Year	Average Pre-Monsoon groundwater table (Meter)	Average Post-Monsoon groundwater table (Meter)	Average Groundwater table fluctuation (Meter)
2004	5.36	4.59	+0.77
2005	5.75	4.76	+0.99
2006	5.65	5.18	+0.47
2007	5.9	4.92	+0.98
2008	6.74	4.81	+1.93
2009	6.26	5.19	+1.07
2010	6.44	4.69	+1.75
2011	5.85	4.23	+1.62
2012	6.48	5.67	+0.81
2013	6.39	5.01	+1.38

(Source: Senior Hydro-geologist[s] office, Bareilly, and Groundwater information system, NIC, GOI.)

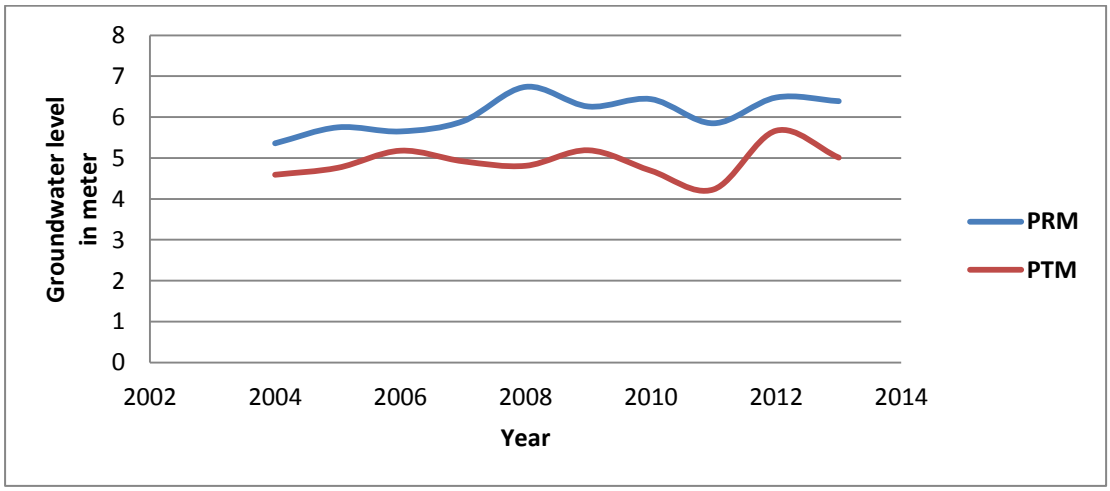

Figure. 5.34. Year-wise variation in Pre & Post-monsoon water level in the study area

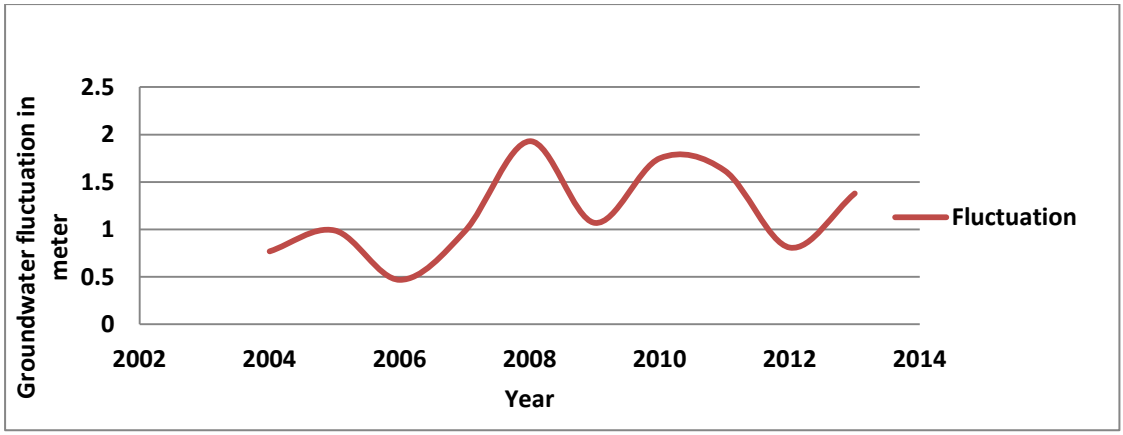

Figure. 5.35. Year-wise average water fluctuation in meters in the study area

Table. 5.10. Average annual rainfall and Post-monsoon water table during 2004-2013:

Year	Annual Rainfall (mm)	Post-monsoon groundwater level (mm)
2004	767.4	4596.67
2005	895	4765
2006	696.3	5181.67
2007	1040.1	4918.33
2008	1356.2	4815
2009	894.2	5195
2010	1430.2	4690
2011	1196.1	4235
2012	617.5	5668.33
2013	1288.5	5010

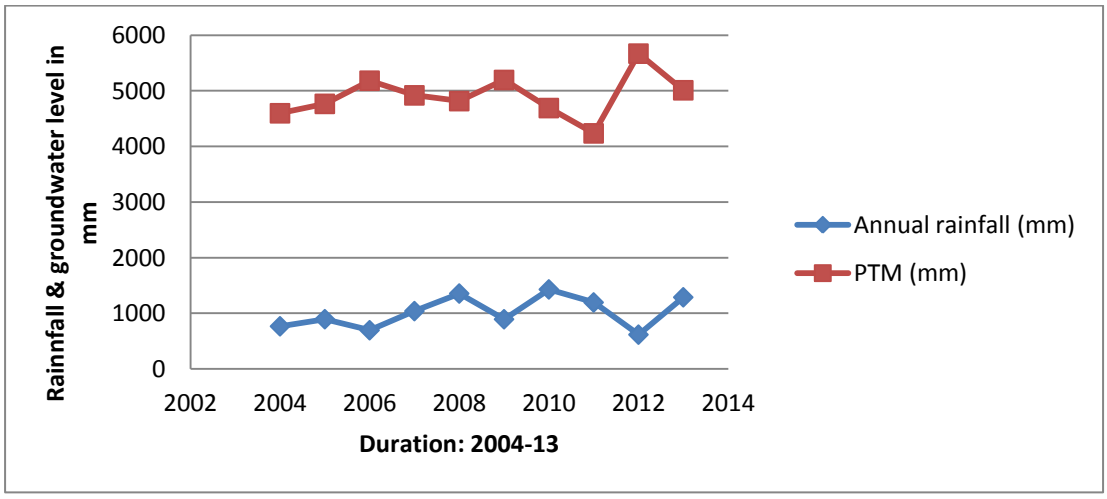

Figure. 5.36. Rainfall and groundwater table variation at the study area

5.6 Precipitation and Run-off/Recharge pattern in the study area:

5.6.1. Land Use Land Cover Change and Runoff Pattern:

The runoff response during three epochs 1979, 1990 and 2009 due to change in LULC over the study area has been depicted below:

From the Table 5.12 and Figure 5.37(a), it is evident that the LULC in the study area has been altered significantly from 1979 to 2009. The wetted Curve Number (CN) value of the area in 1979 was only 75.63, but after passage of 11 years, by 1990, the CN value of the same area became 76.65. Again after passage of 19 more years, by 2009, the CN value became 78.40. Consequently the runoff response over the study area also enhanced accordingly. It was observed that with a small (2.77 point) increase in curve number value (from 75.63 to 78.40) of the study area, the runoff volume increased from 214.37 ha-m in 1979 to a whooping 5851 ha-m in 2009, reflecting clearly the effect of LULC change dynamics prevailed in the study area. The table 5.11 and Figure No. 5.37(b), (c), and (d) show the pattern of monthly runoff occurrences over the study area during three epochs. In 1979, the maximum runoff (189 ha-m) was observed during the month of July followed by 25.29 ha-m in the month of August. It was also observed that no runoff occurred during the month of June, September and October in 1979. Likewise, in the year 1990, maximum runoff (1442 ha-m) was observed during the month of August, followed by 944 ha-m in July, 166.70 ha-m in September, and 48.76 ha-m in June. No runoff was observed during month of October, 1990. In the year 2009, highest runoff (4268 ha-m) was observed during the month of August, followed by 818.20 ha-m in October, 715.54 ha-m in September and 49.38 ha-m in July. It was also observed that no runoff occurred during the month of June, 2009.

From Table 5.13 and Fig. 5.37(e), it is evident that in the year 1979 runoff from the settlement land occurred only during the month of July (189 ha-m) and August (25 ha-m). In the year 1990, i.e., after a passage of about 11 years, the volume of runoff from the settlement land was observed to be quite high. It was observed as 1442 ha-m in August followed by 1944 ha-m in July, 165 ha-m in September and 49 ha-m in June. No runoff was observed in the month of October 1990. It was also observed that again after a passage of another 20 years, i.e. , 1990 to 2009, the volume of runoff occurred was further increased manifold. The maximum runoff 4268 ha-m was

observed in August followed by 818 ha-m in October, 716 ha-m in September and 49 ha-m in July. It was observed in general that runoff volume in 1979 was very low but it was found to be increasing rapidly in 1990 and 2009. The low volume of runoff in 1979 may be due to lesser area under settlement together with low storm events (lesser precipitation of 489.27 mm only in comparison to 1023.5 mm in 1990 and 1040.1 mm in 2009).

The Table 5.13 and Figure 5.37(f) indicate that out of all the land classes maximum runoff occurred from the cropland which was obvious as area under cropland was maximum throughout. The maximum run off volume (55752 ha-m) occurred during August in 2009 followed by 21608 ha-m and 14145 ha-m during the months of August and July respectively.

The Table 5.13 and Figure 5.17(g) indicate that runoff from the forest land is maximum (7189 ha-m) in 1990 followed by 1829 ha-m in 2009 and 1478 ha-m in 1979. The less runoff volume in 1979 was partially due to very poor annual rainfall (489.27 mm) together with good land cover conditions prevailing then, though area was maximum.

From Table 5.13 and Figure 5.37(h), it is evident that runoff was observed to be maximum (1334 ha-m) in August 2009 followed by 933 mm in August 1990, 611 mm in July 1990 and 15 mm in July 2009 from the waste land.

5.6.2 Rainfall and Runoff Pattern:

From Table 5.12 and Figure 5.38(a) it is evident that the runoff response from the rainfall during the three epochs 1979, 1990 and 2009 is quite clear and significant. The percentage runoff corresponding to rainfall was a mere 2.95% in the year 1979, which rose to 12.09% in 1990 and to 26.25% in 2009. It clearly indicated the effect of LULC changes that had taken place in favour of high runoff producing cropland at the cost of forest land.

From Figure 5.38 (b), and (c), it was observed that between1979 to 1990, the response of runoff due to rainfall was almost linear. But from 1990 onwards, the response became too intense with positive exponential increase as the curve change its direction between 1990 and 2009 with a positive trend. This phenomena indicated the alteration of LULC favouring bigger runoff volume generation with respect to rainfall

(y= 0.016x – 32.81, R^2= 0.882; y= 0.006x- 13.40, R^2= 0.964; y= 0.36x- 172.20, R^2= 0.94)

Figure 5.39(a), (b), and (c) indicate the runoff patter during the monsoon months of June-October in the year 1979. It is evident from the figure that the runoff is highest (11.19 mm) in July followed by 1.49 mm in August. It is also clear that no runoff occurred during the months of June, September and October 1979.

From Figure 5.40 (a), (b) and (c), it maybe deduced that there was good normal rainfall in June, July, August, September months of 1990. The runoff during the month of July was less than that during August though incident rainfall was more in July month than August month. This may be due to poor AMC conditions in July as compared to the conditions in the month of August. Highest runoff was observed during the month of August as 67.56 mm followed by 44.94mm in July and 7.84 mm in September 1990. It is to be emphasized here that rainfall during September month was about twice than that during June month but runoff was more than thrice during the corresponding months in 1990.

Figure 5.41(a), (b) and (c) indicate the pattern of runoff and rainfall in 2009. It is evident from the figure that volume of runoff occurred in August is almost equal to the value of rainfall occurred in the September month. It was due to heavy downpour (384.9 mm) occurring in the month of August preceded by fair (174.5 mm) and moderate (44.1 mm) rainfalls occurring in the July and June months respectively and thus creating better AMC conditions favourable for higher runoff generation. Also, contribution of enhanced CN value of the changed LULC classes for the study area was another contributing factor for higher runoff generation.

Table 5.12 and Figure 5.42 depict the rainfall and recharge pattern in the study area during three epochs 1979, 1990 and 2009. It is evident from the figure 5.42 that with increase in rainfall, the recharge also increases. Figure 5.43(a), (b) and (c) indicate the pattern of recharge over settlement lands during 1979, 1990 and 2009 under changing LULC dynamics together with rainfall occurrences.

Figure 5.44(a), (b) and (c) depicts the pattern of recharge over the crop land during 1979, 1990 and 2009. The recharge from cropland in 1979 is lower than that in 1990 and 2009. This may be due to the area under cropland in 1979 being lesser than that in

1990 and 2009. However, it is also evident that recharge volume has declining trend from 1990 and 2009 and beyond. The recharge in the year 1990 is 167.21 mm whereas it has declined by 2009 and it was observed to be 151.13 mm only. This may be because of changed LULC in favour of more cropland with lower recharge properties at the cost of forest and plantation land which had higher recharge characteristics.

Figure 5.45 (a) and (b) depict the recharge pattern over forest and plantation land during 1979, 1990 and 2009. The general trend indicates that the recharge through these areas is continuously declining. However, the rate of decline from 1979 to 1990 was slower than that from 1990 to 2009. This may be primarily due to reduction in the area in the successive years together with LULC changes favouring more to runoff process than recharge process.

Figure 5.46 (a) and (b) depicts the overall trend of recharge over the wastelands during 3 epochs 1979, 1990 and 2000. It is clearly evident that recharge is continuously declining. This is due to the reduction in the wasteland area together with deterioration of LULC conditions over these lands.

Table 5.12 and Figure 5.47(a) and (b) depict the relation between rainfall and resultant runoff and recharge that had occurred during the 3 epochs 179, 1990 and 2009 over the study area under changing LULC conditions. While runoff was found to be increasing from 2.59% in 1979 to 12.09% in 1990 and to 26.25% in 2009 of the incident rainfall in the respective years. But at the same time, recharge was found to be declining from 17.59% in 1990 to 17.46% in 2009 of the incident rainfall in the respective years. It is also evident from Figure 5.47(a) that during 1979 and 1990, the recharge was more than the runoff. But in 2009 it was observed that recharge is reduced from its 1990 value and also runoff in 2009 has exceeded significantly than the recharge. The recharge was only 17.46% of the incident rainfall where as the corresponding runoff was as high as 26.25% of the same rainfall in the year 2009. This clearly indicates that LULC has changed significantly favouring higher runoff and lower recharge conditions. It is further stated that from Figure 5.47(b), it was found that process of more runoff than recharge began between 1999- 2000 and the trend is continuously rising upward.

Table.5.11 Runoff Pattern month-wise over the study area:

Sl. No.	Year	Runoff Volume in ha-m					
		June	July	Aug	Sep	Oct	Total
1	1979	0	189.0215	25.29025	0	0	214.3117
2	1990	48.76838	944.1992	1442.434	164.7054	0	2600.107
3	2009	0	49.38734	4268.062	715.5422	818.2077	5851.199

Table. 5.12 Rainfall/Runoff/Recharge Pattern over the study area:

Sl.No.	Year	CN Value	Rainfall (Annual) (mm)	Rainfall (Monsoon) (mm)	Runoff (mm)	% Runoff	Recharge (mm)	% Recharge
1	1979	75.63	489.27	403.984	12.68789	2.59	29.26	7.24
2	1990	76.65	1023.5	950.52	123.7439	12.09	167.21	17.59
3	2009	78.40	1040.1	865.2	221.9053	26.25	151.132	17.46

Table. 5.13. Runoff Pattern month-wise and LULC category –wise, over the area.

LU/LC Class	Runoff Volume in ha-m									
	1979		1990				2009			
	July	Aug	une	July	Aug	Sep	uly	Aug	Sep	Oct
ettlement	189	25	49	944	1442	165	49	4268	716	818
CL	2793	374	731	4145	1608	2467	645	55752	9347	10688
Forest/Plant	1304	174	107	2074	3168	362	46	4001	671	767
WL	230	31	31	611	933	106	15	1334	224	256

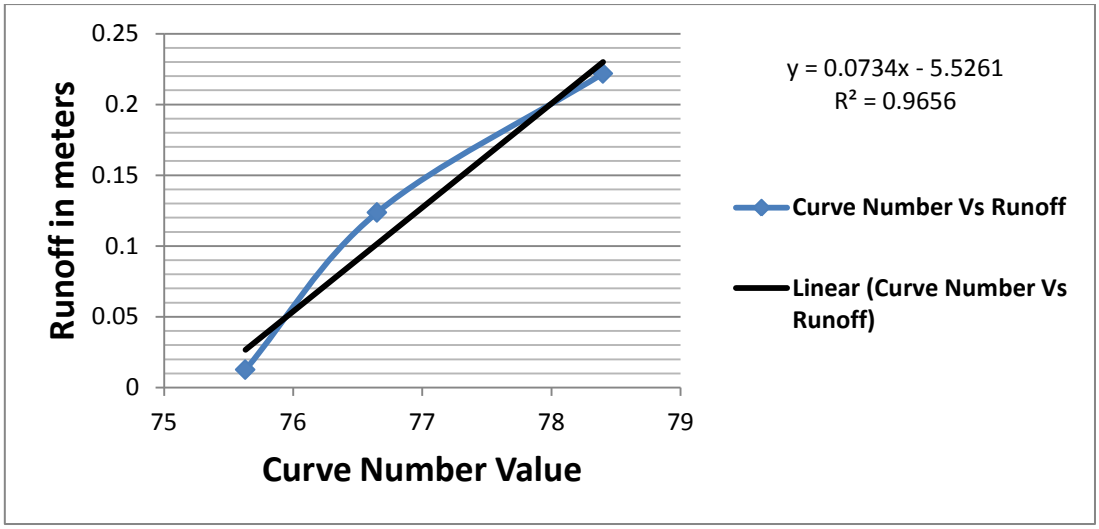

Fig. 5.37 (a). Curve number and Runoff response during three Epochs (1979, 1990 and 2009)

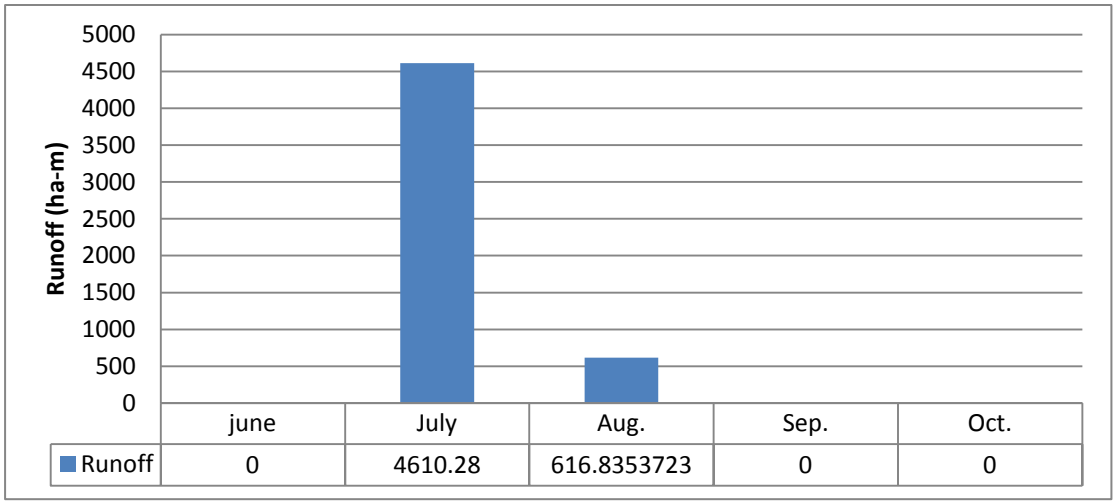

Fig. 5.37(b). Runoff Pattern month-wise in 1979, over the study area.

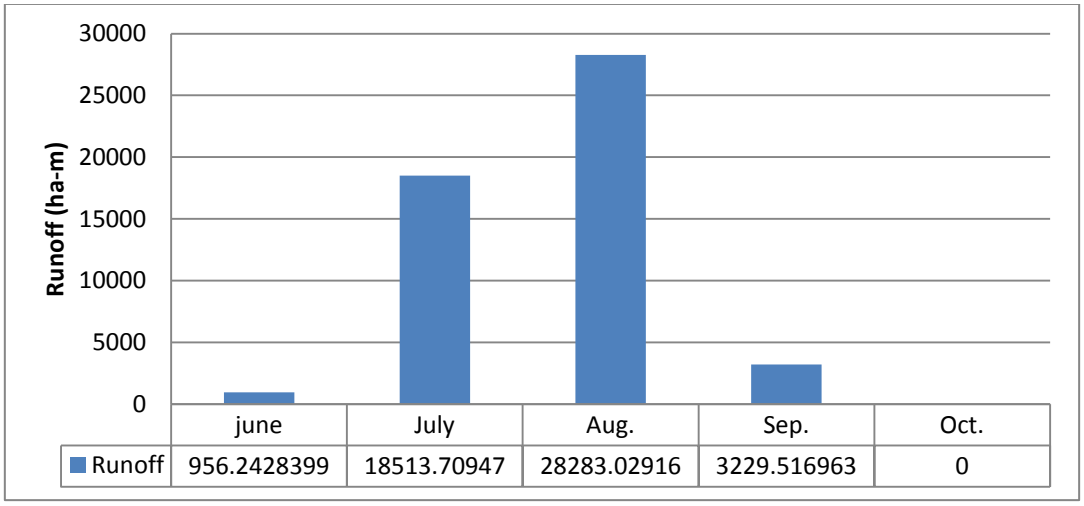

Fig. 5.37 (c). Runoff Pattern month-wise in 1990, over the study area.

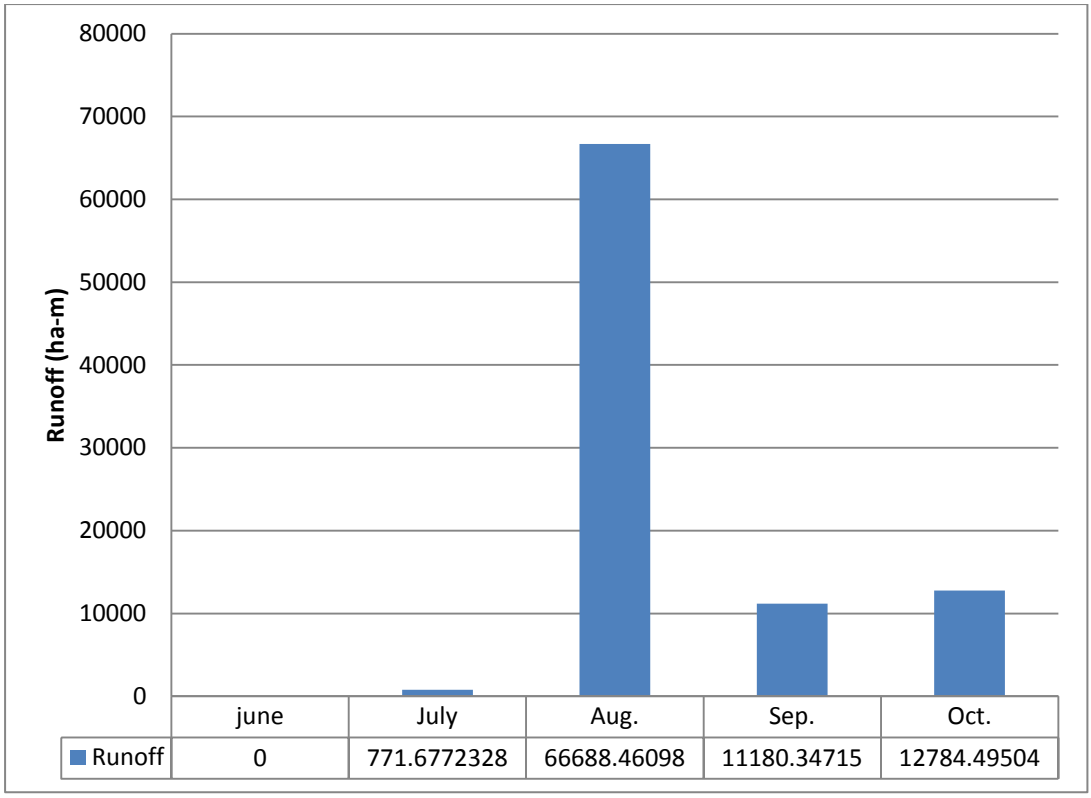

Fig. 5.37(d). Runoff Pattern month-wise in 2009, over the study area.

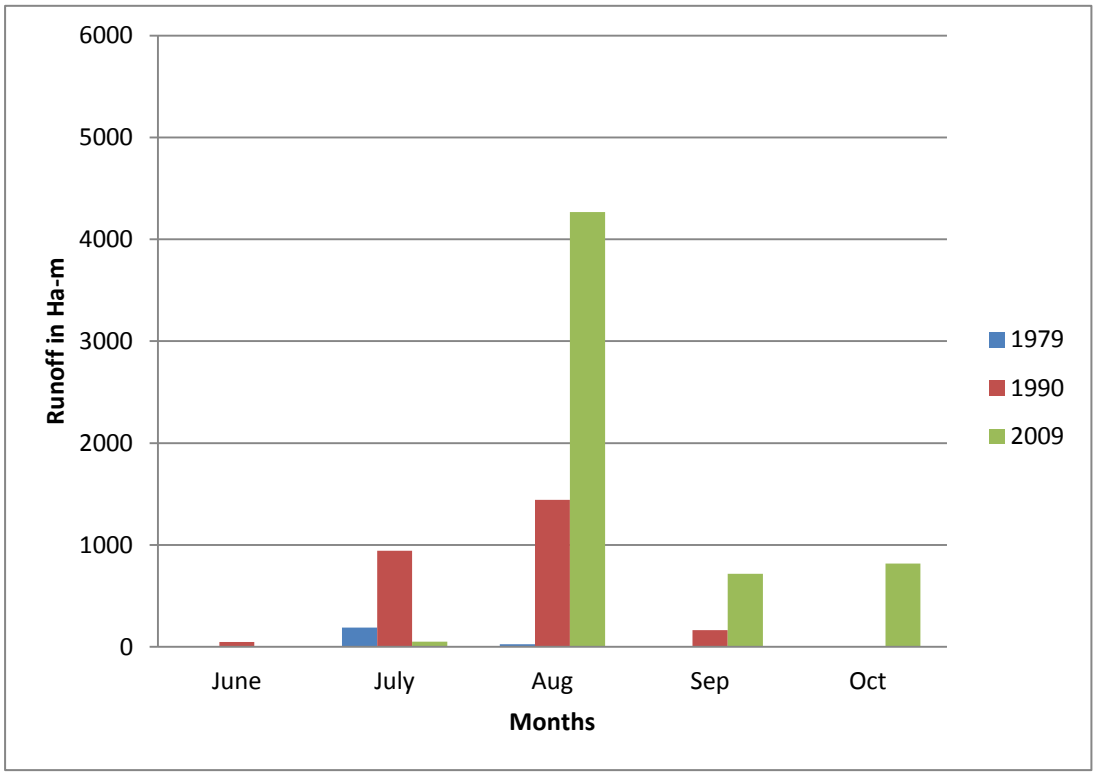

Fig. 5.37 (e). Runoff Pattern month-wise over the Settlement Land.

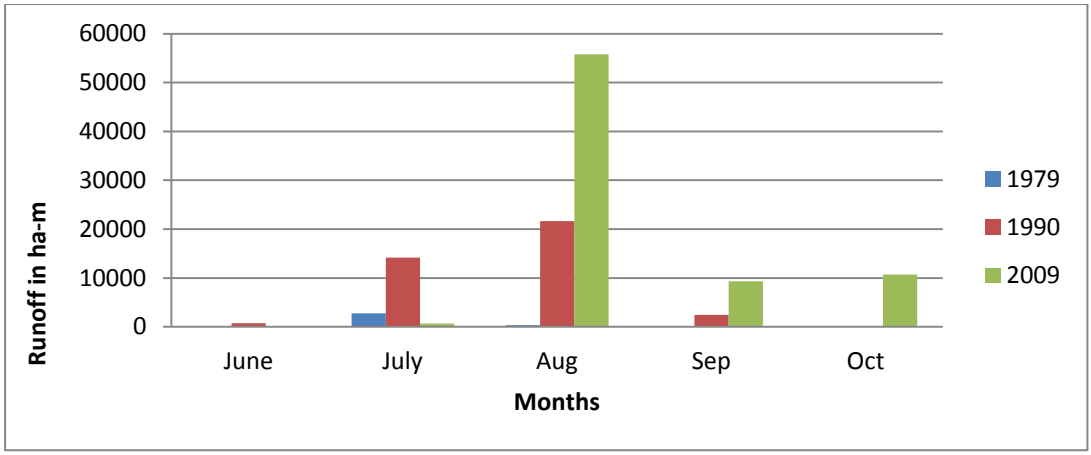

Fig. 5.37(f). Runoff Pattern month-wise over the Crop Land.

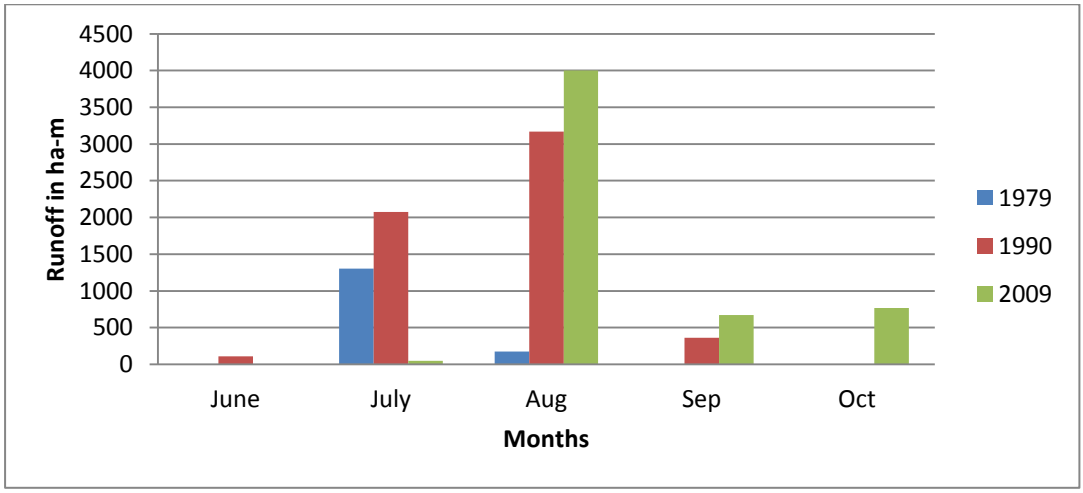

Fig. 5.37(g). Runoff Pattern month-wise over the Forest Land.

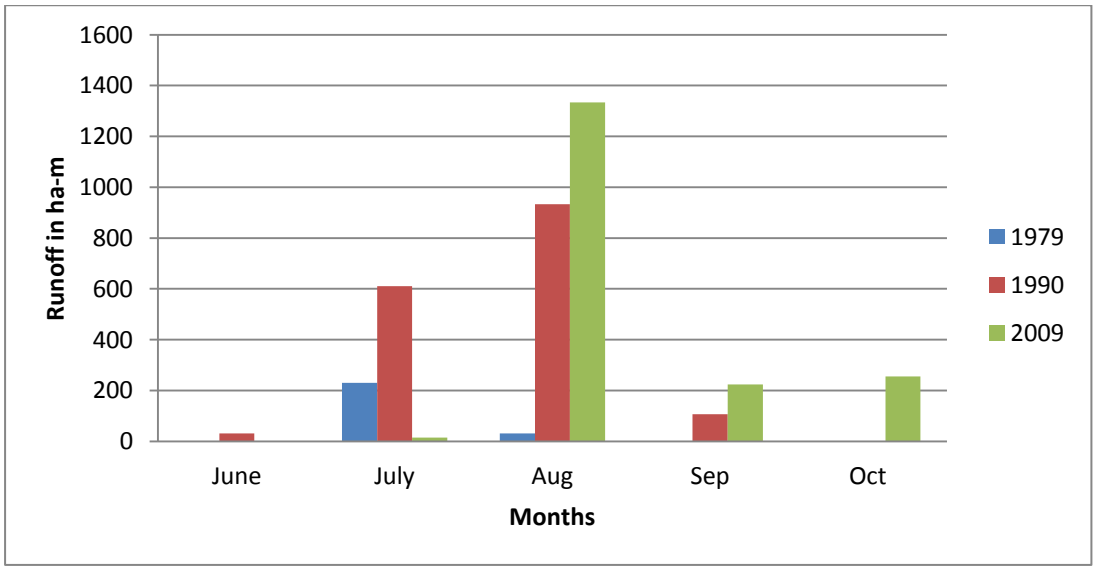

Fig. 5.37 (h). Runoff Pattern month-wise over the Waste Land.

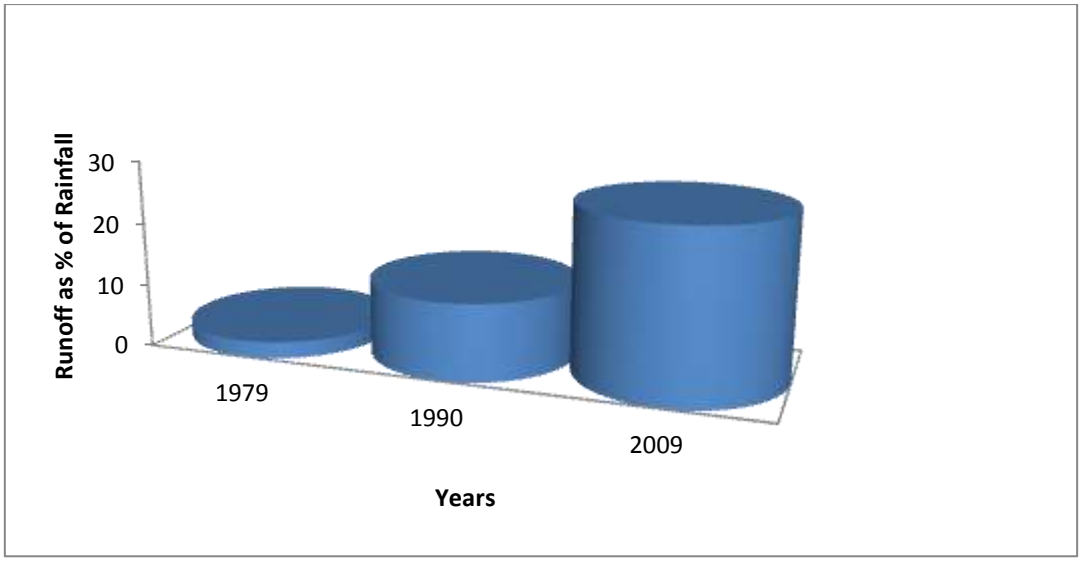

Fig. 5.38 (a). Runoff as % of Rainfall during three Epochs: 1979, 1990 and 2009

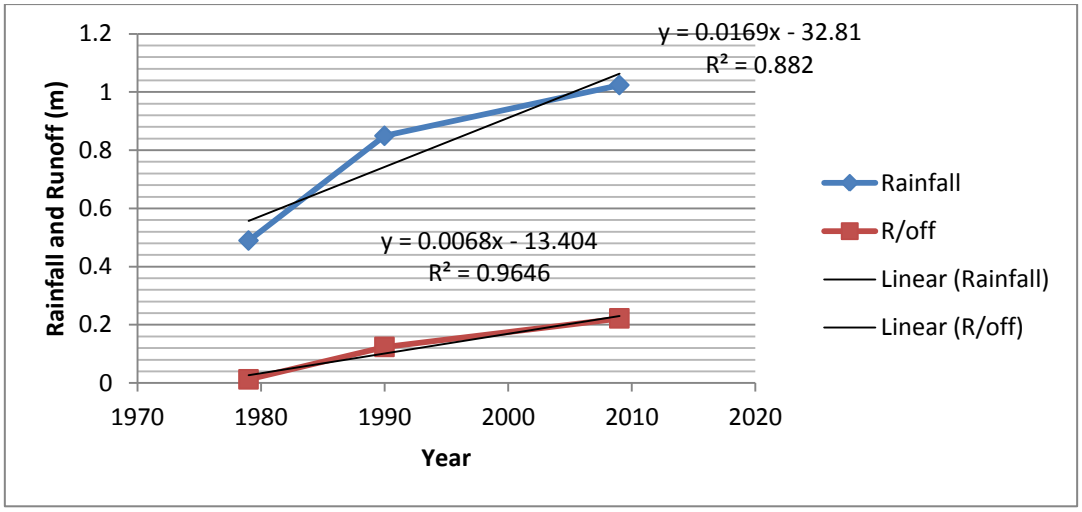

Fig. 5.38 (b). Rainfall Vs Runoff over the study area during three Epochs: 1979, 1990 and 2009

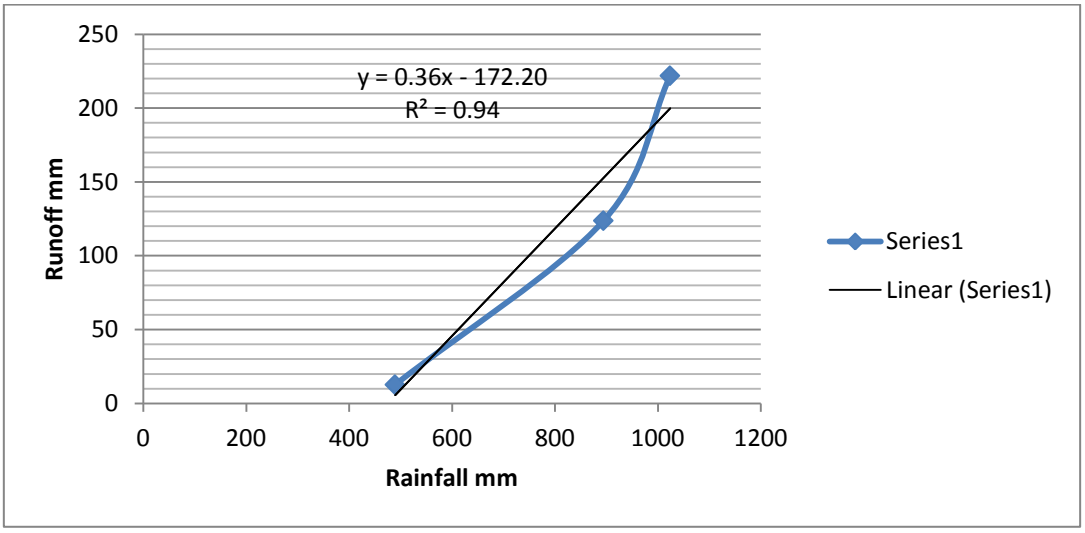

Fig. 5.38(c). Rainfall and Runoff Pattern over three epochs: 1979, 1990 and 2009.

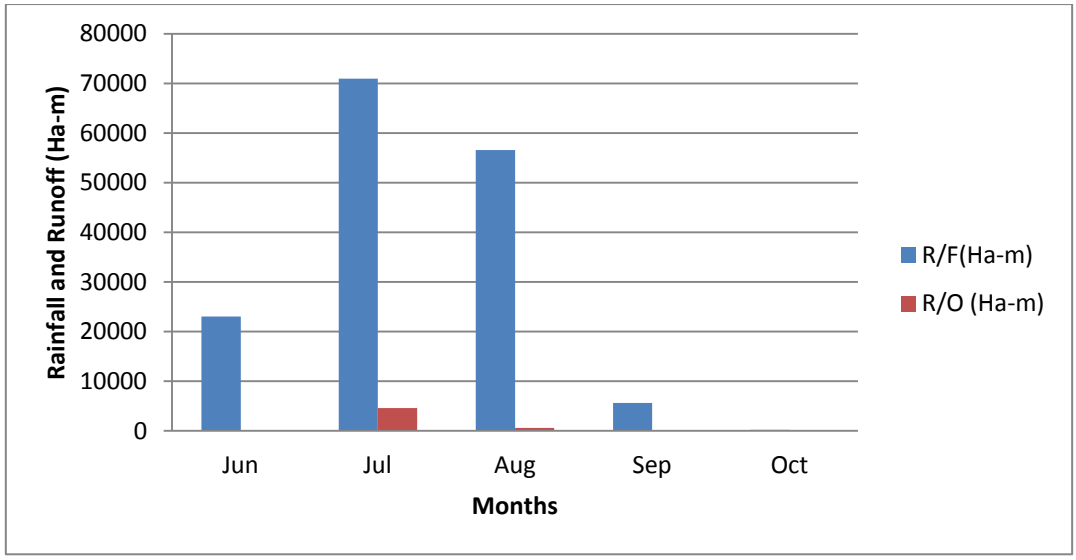

Fig. 5.39 (a). Rainfall Vs Runoff Pattern during June to October, 1979.

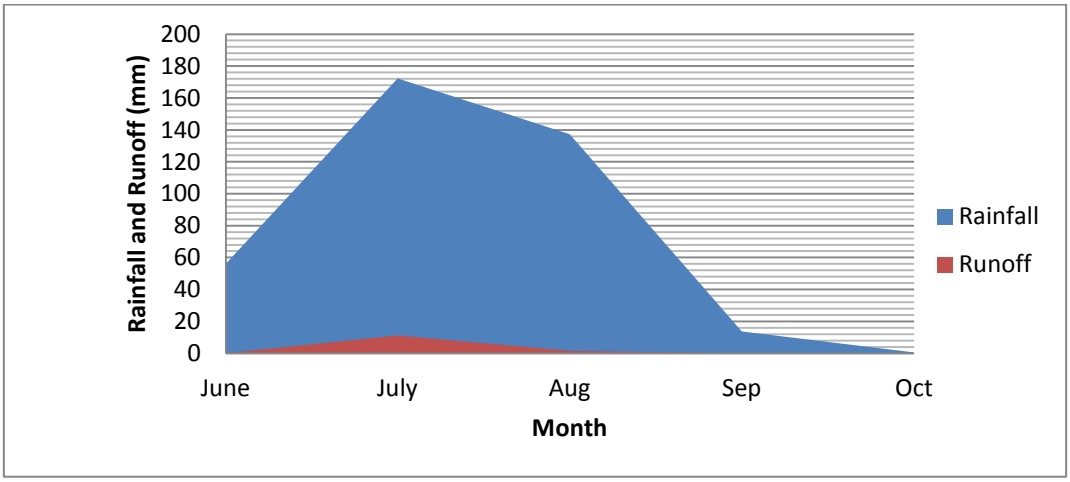

5.39 (b). Rainfall Vs Runoff Pattern during June to October, 1979.

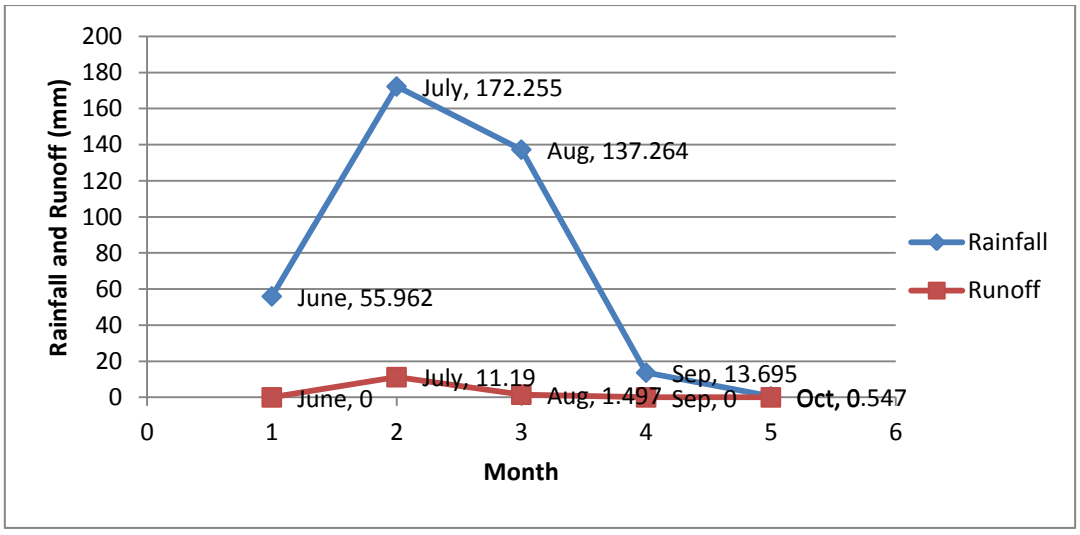

Fig. 5.39 (c). Rainfall Vs Runoff pattern during June to October, 1979.

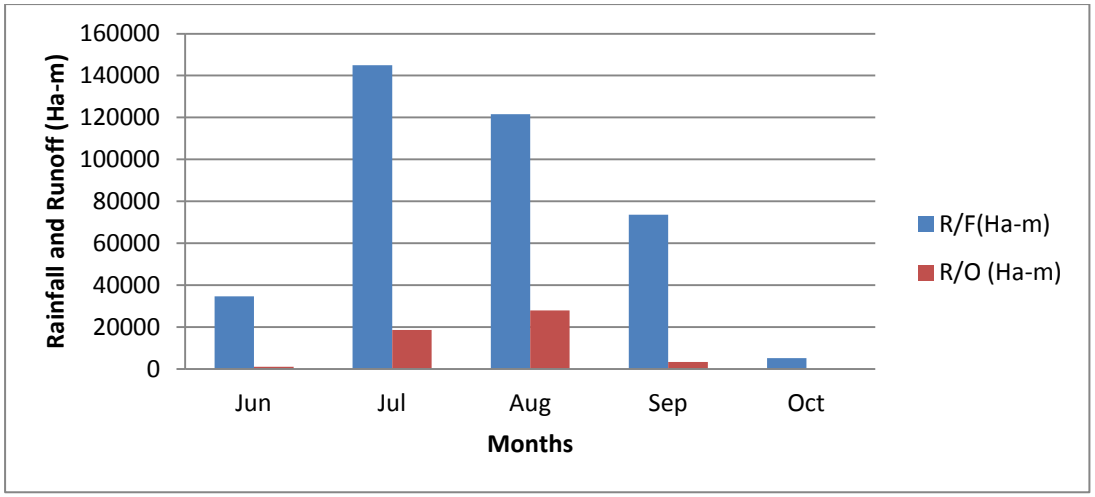

Fig. 5.40(a). Rainfall Vs Runoff pattern during June to October, 1990.

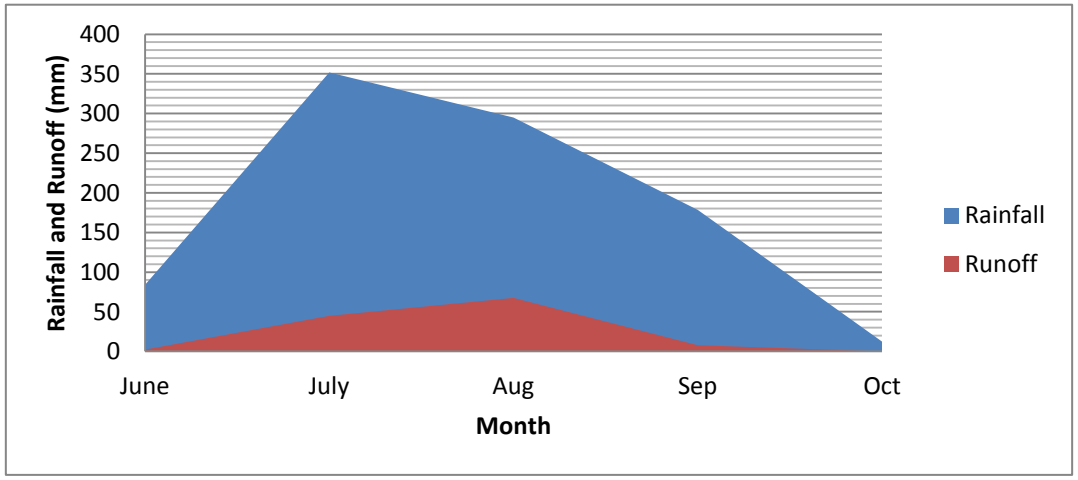

Fig. 5.40(b). Rainfall Vs Runoff pattern during June to October, 1990.

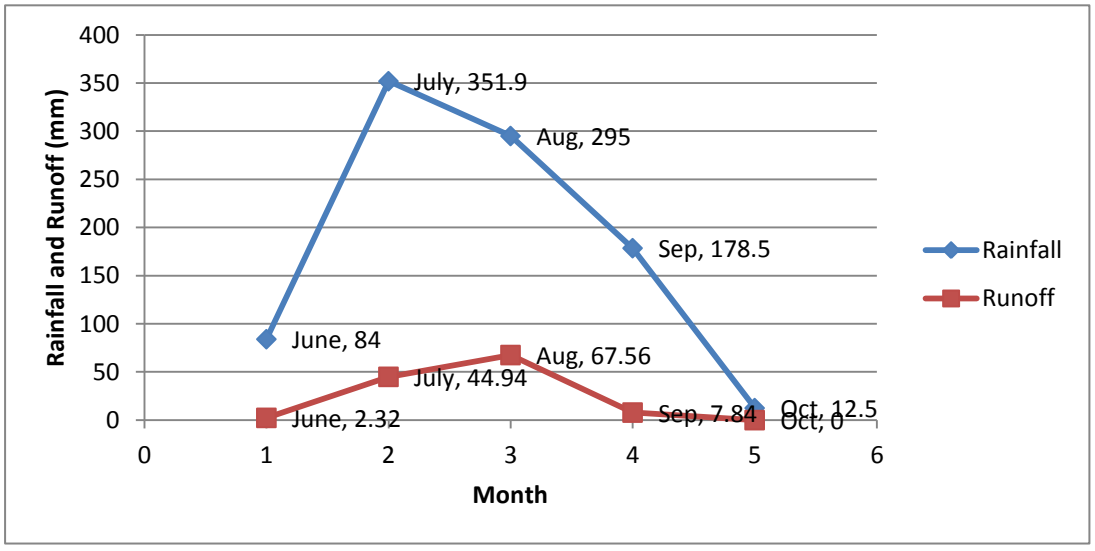

Fig. 5.40(c). Rainfall Vs Runoff pattern during June to October, 1990.

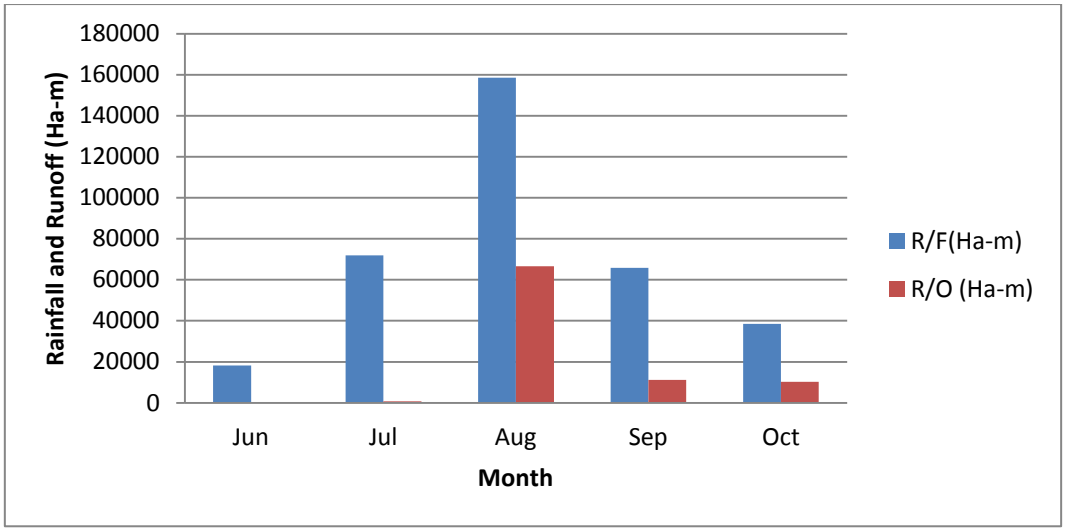

Fig. 5.41(a). Rainfall Vs Runoff pattern during June to October, 2009.

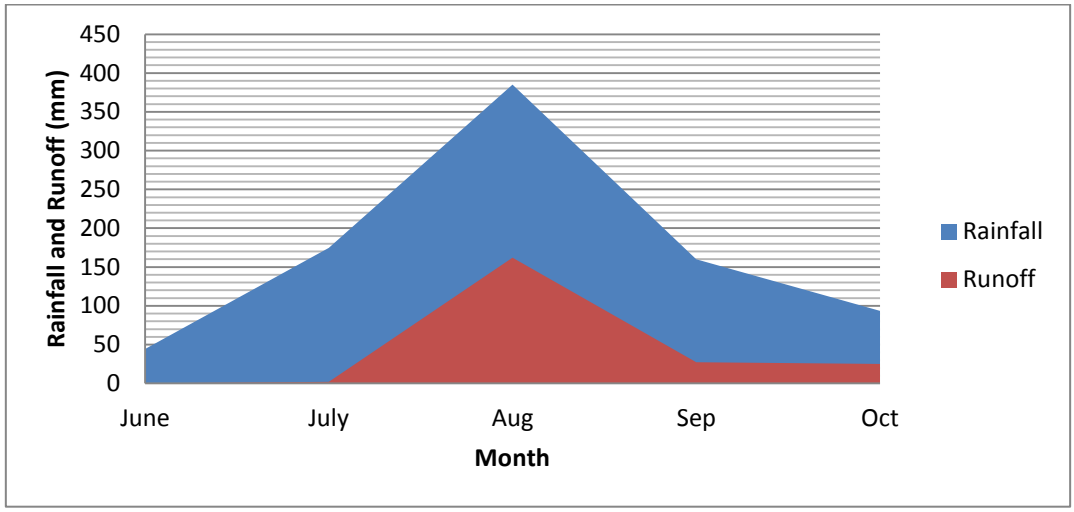

Fig. 5.41(b). Rainfall Vs Runoff pattern during June to October, 2009.

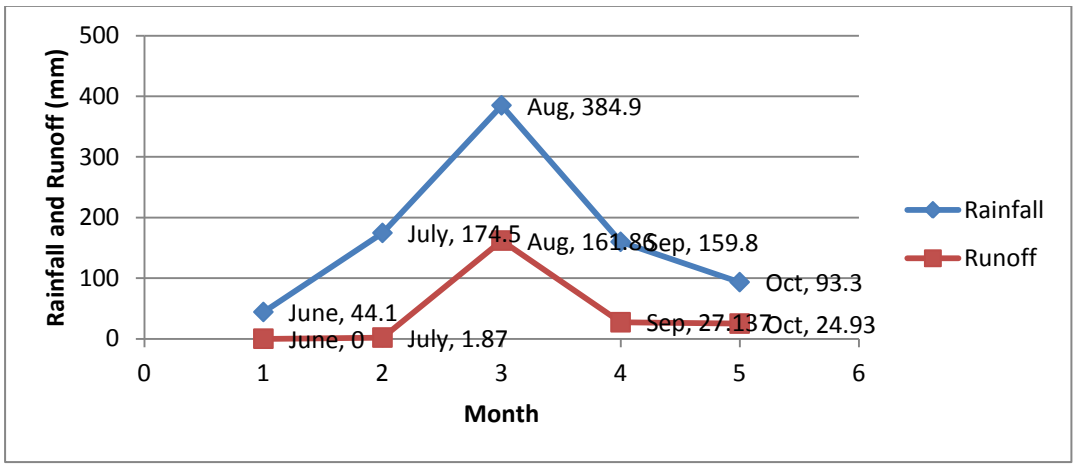

Fig. 5.41(c). Rainfall Vs Runoff pattern during June to October, 2009.

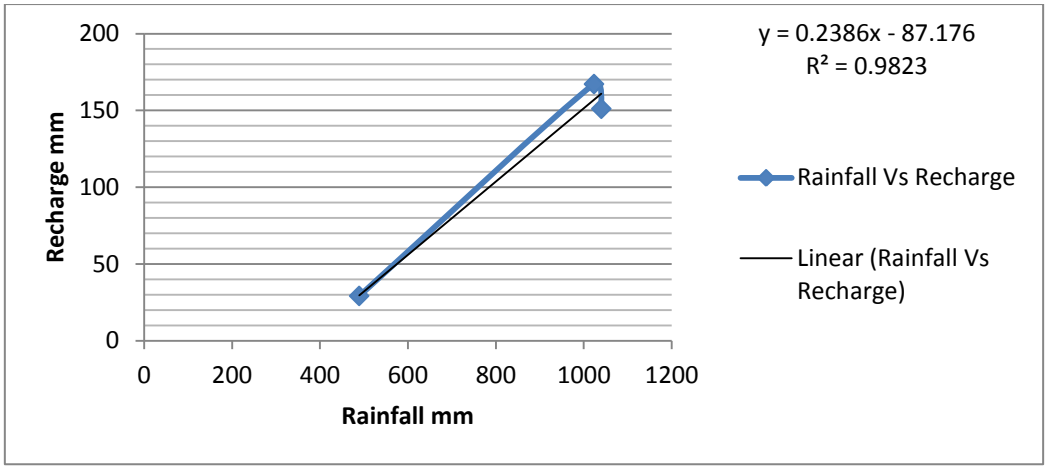

Fig. 5.42. Rainfall Vs Recharge Pattern in the study area during 1979 to 1990 to 2009.

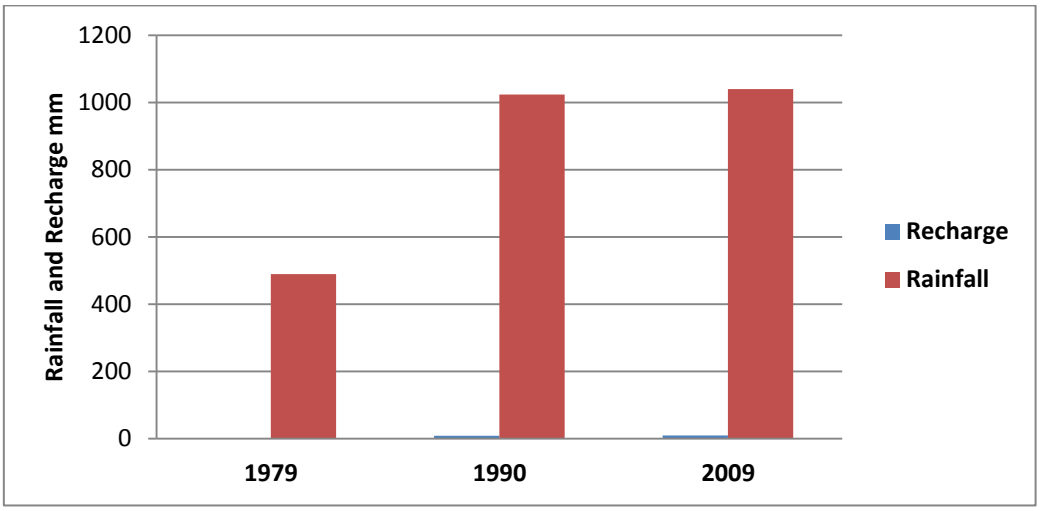

Fig. 5.43(a). Recharge pattern through Settlement Land during 1979, 1990 and 2009

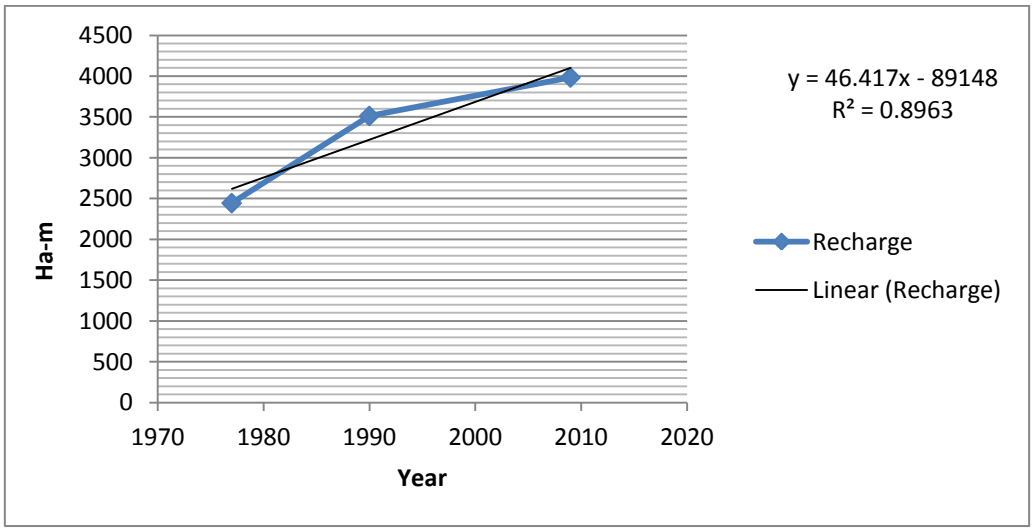

Fig. 5.43(b). Recharge Trend through Settlement Land during 1979, 1990 and 2009

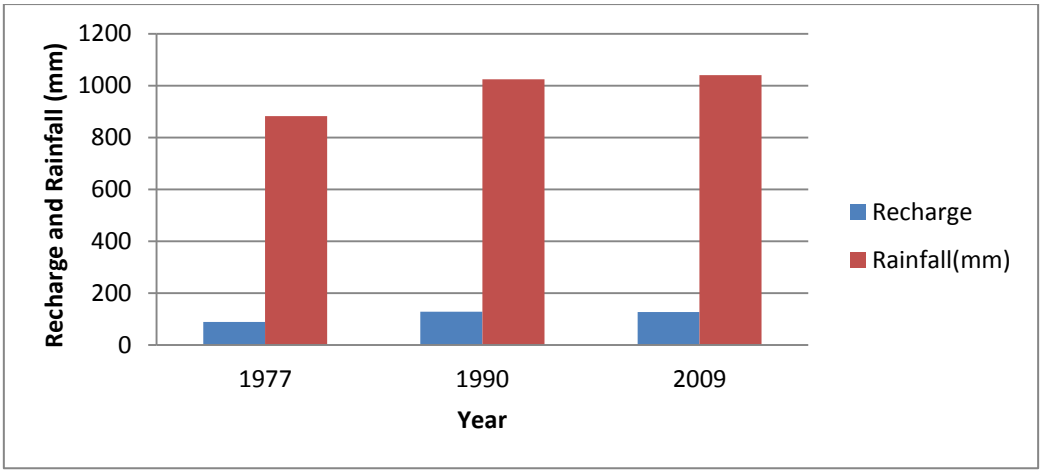

Fig. 5.44(a). Recharge pattern through Crop Land during 1979, 1990 and 2009

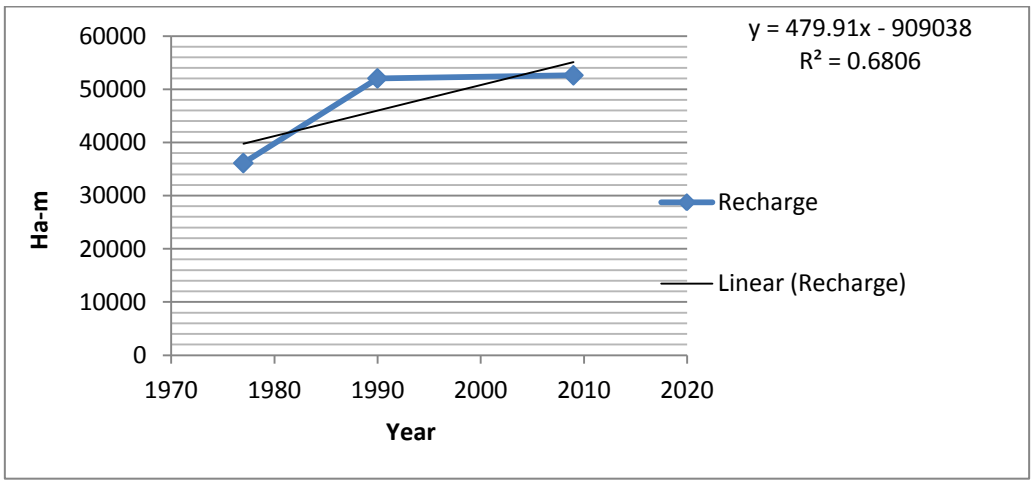

Fig. 5.44(b). Recharge Trend through Crop Land during three Epochs: 1979, 1990 and 2009.

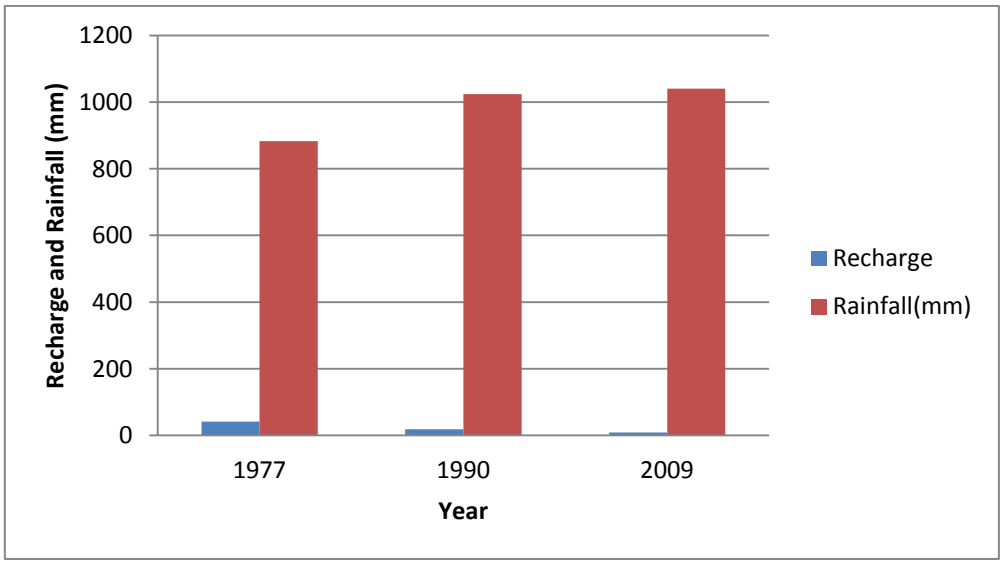

Fig. 5.45(a). Recharge pattern through Forest Land during 1979, 1990 and 2009.

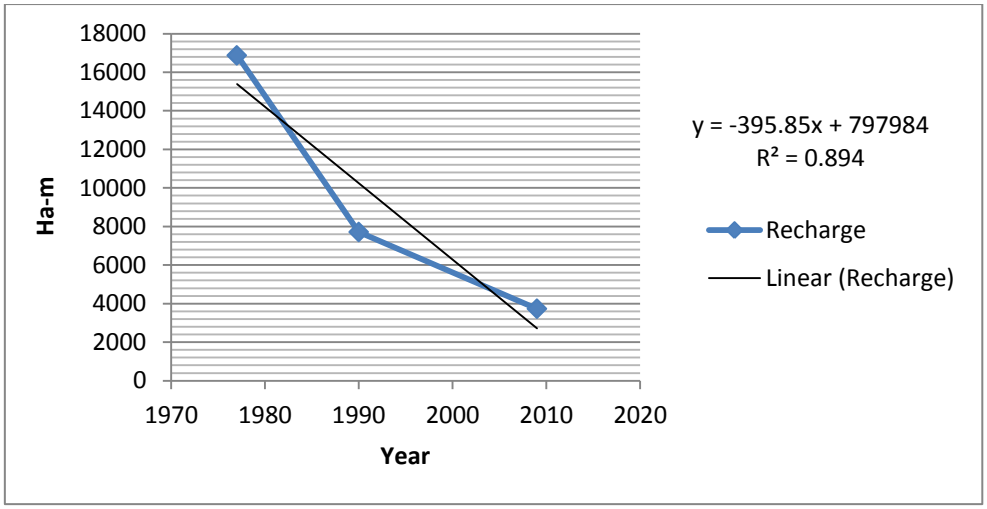

Fig. 5.45(b). Recharge Trend through Forest Land during 1979, 1990 and 2009.

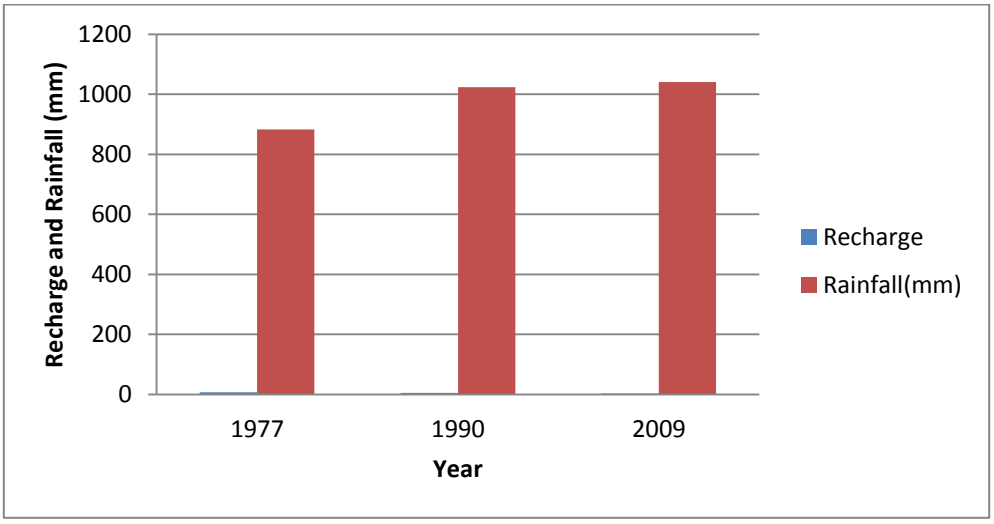

Fig. 5.46(a). Recharge pattern through Waste Land during 1979, 1990 and 2009.

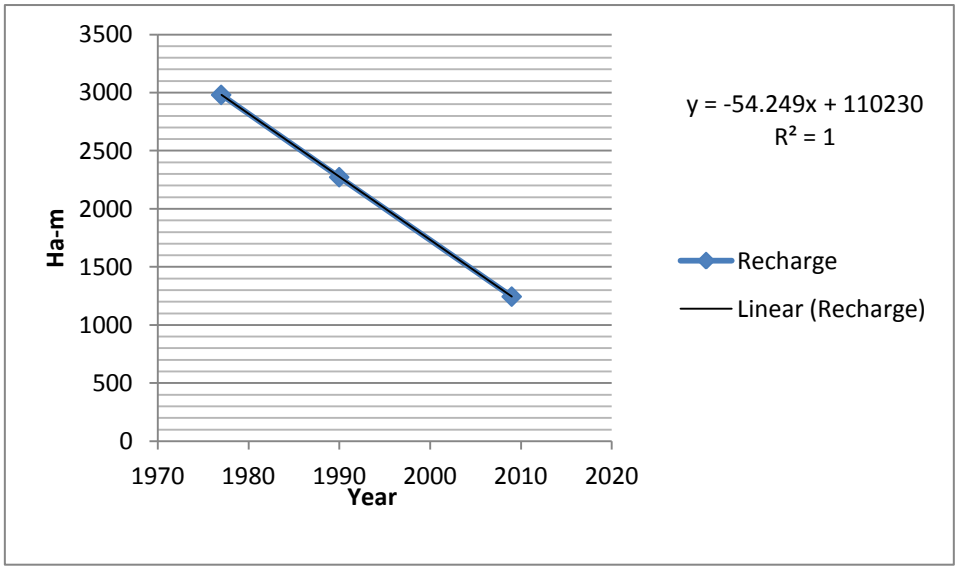

Fig. 5.46(b). Recharge Trend through Waste Land during 1979, 1990 and 2009.

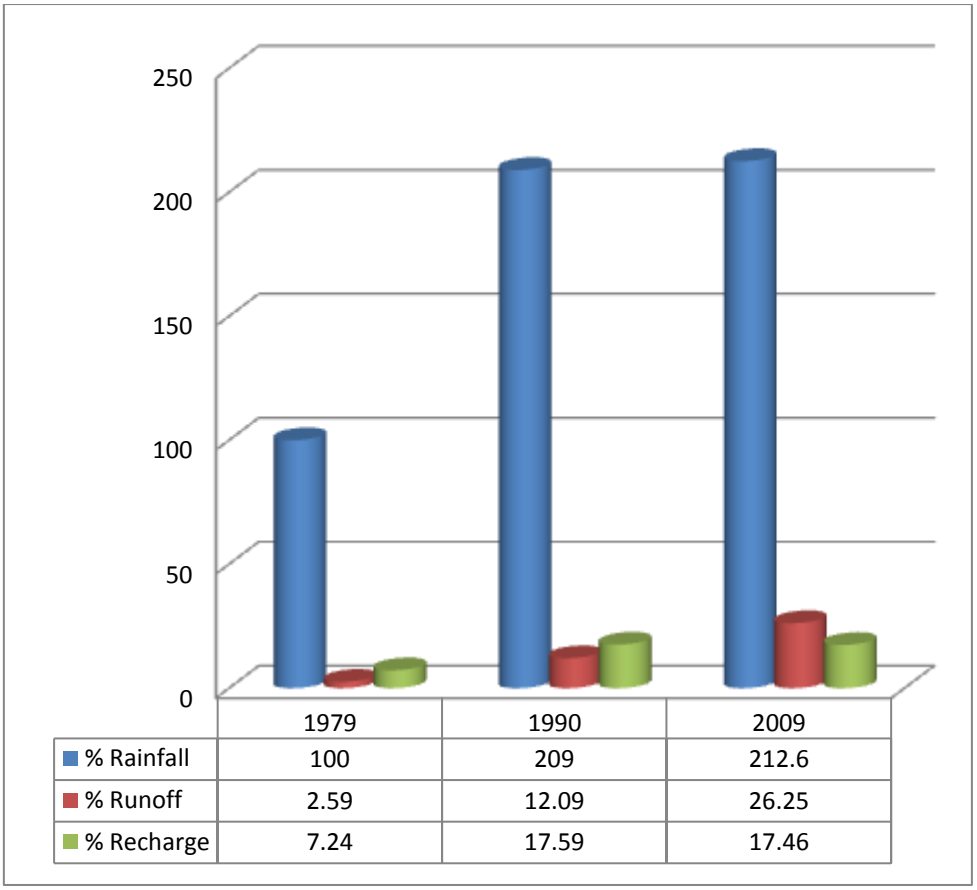

	1979	1990	2009
% Rainfall	100	209	212.6
% Runoff	2.59	12.09	26.25
% Recharge	7.24	17.59	17.46

Fig. 5.47(a) Rainfall Vs Runoff and Recharge Response during 1979, 1990 and 2009

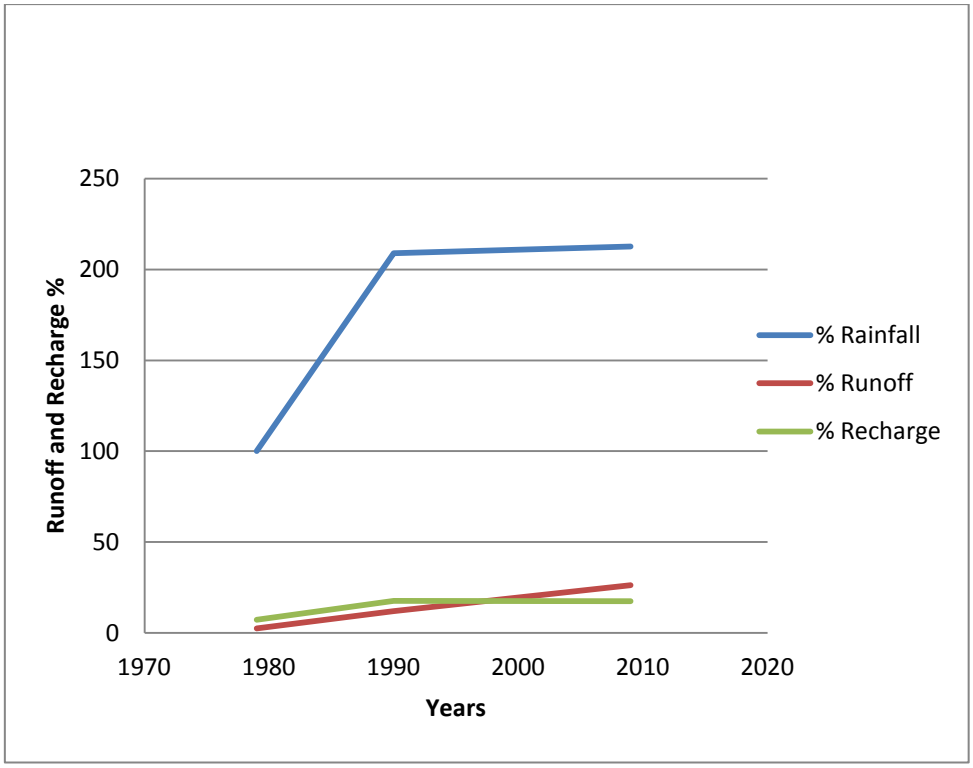

Fig. 5.47(b) Rainfall Vs Runoff and Recharge Response during 1979 to 1990 to 2009.

5.7 Artificial Neural Network Modelling:

The application of Artificial Neural Network Modelling for developing LULC-Runoff, LULC-Recharge and Runoff-Recharge relationships for various land uses in the study area district Bareilly was evaluated and investigated for two layer multi-perceptron NN model techniques. Standard back propagation (SBP) training algorithm was used.

The database compiled represents daily/monthly sets of rainfall, water table and LULC data (between1979-2009) and Secondary data generated for Runoff and recharge at the Ramganga River basin. The recorded data were taken for model development using various input variables (rainfall and LULC) and output runoff/discharge. The secondary data were used to validate the model performance. For development of ANN model, the available data were used as 70 percent for training, 15 percent for testing and 15 percent for validation. Inputs and outputs have been normalized in the range of (0–1) as NN works efficiently within this range. The neural network model has been developed using output and input data of the same period with an equivalent step time in the MATLAB Neural Network Toolbox.

The goal of the training process is to reach an optimal solution based on some performance measurements such as mean square error (MSE) and coefficient of determination (R). The training process of ANN is terminated when the overall error on the testing dataset was minimal. The validation sets are usually used to select the best performing network model. The behaviour of model during training, testing and validating for Runoff as well as Recharge, at Settlement Land, Crop Land, Forest and Wasteland, for the study area district Bareilly is represented in table 5.14 to 5.15 and figures 5.48 to 5.57, which shows its capability to predict the process input output relationship efficiently. Higher the correlation coefficient value (R), better the model predicts. The predicted results using ANN model shows that the model performed well with observed LULC, recharge and runoff data.

5.7.1. Recharge at Settlement Land

The Table 5.14, 5.15 and figures 5.52 (a), 5.57 (a), 5.58 (a), and 5.59 generated through Neural Network analysis depicts the pattern of recharge at settlement land from year 1979 to 2009 and simulated results up to year 2039. It is evident from the figures that there exists a great degree of conformity between the actual and modelled

values of recharge. The figures also depict simulated recharge pattern at settlement land even beyond year 2009 and up to year 2039 with a positive increasing trend predicted. This is mainly due to continuous increase in the settlement land coupled with water harvesting structures created through MNREGA in the study area.

5.7.2. Recharge at Crop Land

The Table 5.14, 5.15 and figures 5.52 (b), 5.57 (b), 5.58 (b), and 5.59 generated through Neural Network analysis depicts the pattern of recharge at Crop Land from year 1979 to 2009 and simulated results up to year 2039. It is evident from the figure that there exists a great degree of conformity between the actual and modelled values of recharge. The figures also depict simulated recharge pattern at crop land even beyond year 2019 and up to year 2039 with a decreasing trend predicted. This is mainly due to no scope of further increment in the crop land area together with prevailing land cover conditions causing reduction in net-recharge.

5.7.3. Recharge at Forest Land

The Table 5.14, 5.15 and figures 5.52 (c), 5.57 (c), 5.58 (c), and 5.59 generated through Neural Network analysis depicts the pattern of recharge at forest land from year 1979 to 2009 and simulated results up to year 2039. It is evident from the figure that there exists a great degree of conformity between the actual and modelled values of recharge. The figures also depict simulated recharge pattern at forest land even beyond year 2009 and up to year 2039 with a decreasing trend predicted. This is mainly due to continuous decrease in the forest land coupled with thinning of forest area, causing unfavourable conditions for better infiltration and recharge.

5.7.4. Recharge at Waste Land

The Table 5.14, 5.15 and figures 5.52 (d), 5.57 (d), 5.58 (d), and 5.59 generated through Neural Network analysis depicts the pattern of recharge at waste land from year 1979 to 2009 and simulated results up to year 2039. It is evident from the figure that there exists a great degree of conformity between the actual and modelled values of recharge. The figures also depict simulated recharge pattern at waste land even beyond year 2009 and up to year 2039 with a decreasing trend predicted. This is mainly due to continuous decrease in the waste land area, coupled with deteriorating land cover conditions.

Table 5.14.(a) Land use Land cover Vs Runoff Models

Sl. No.	Model	Neural Network model
1	LULC Vs Runoff at Settlement Land	$Y= 5.5e^{-11}*X^3-3.5e^{-6}*X^2+0.073*X-5.1e^{+2}$
2	LULC Vs Runoff at Crop Land	$Y= 7.3e^{-9}*X^2-0.0041*X+6.2e^2$
3	LULC Vs Runoff at Forest Land	$Y= -1.8e^{-13}*X^3+3.7e^{-8}*X^2-0.0021*X+41$
4	LULC Vs Runoff at Waste Land	$Y = -1.7e^{-11}*X^3+7.6e^{-7}*X^2-0.01*X+48$

Table 5.14.(b) Runoff Vs Recharge Models

Sl. No.	Model	Neural Network model
1	Runoff Vs Recharge at Settlement Land	$Y= 0.073*X^3-2.4*x^2+22*x+1.1e^{+2}$
2	Runoff Vs Recharge at Crop Land	$Y= - 0.0017*X^2+0.64*X+1.3e^{+2}$
3	Runoff Vs Recharge at Forest Land	$Y= 0.00027*X^3-0.048*X^2+2.5*X+1.4e^{+2}$
4	Runoff Vs Recharge at Waste Land	$Y = 0.41*X^3-5.6*X^2+28*X+1.2e^{+2}$

Table 5.14.(c) LULC Vs Recharge Models

Sl. No.	Model	Neural Network model
1	LULC Vs Recharge at Settlement Land	$Y= -0.05* X^3+0.082* x^2-4.4*X+7.9$
2	LULC Vs Recharge at Crop Land	$Y= 2.78e^{-05}X^2+0.0015*x+0.019$
3	LULC Vs Recharge at Forest Land	$Y= -0.00042* x^2+0.16X+0.028$
4	LULC Vs Recharge at Waste Land	$Y= 0.016*X^2-0.094*X+0.26$

Table 5.15 Training, Testing and Validation results of the models.

			Sample	Runoff Vs Recharge		LULC Vs Runoff		LULC Vs Recharge(Estimated)	
				MSE	R	MSE	R	MSE	R
1.	Settlement Land	Training	21	$23.026e^{-0}$	$9.41e^{-1}$	$2.319e^{-0}$	7.53^{e-1}	4.792^{e-4}	7.718^{e-1}
		Validation	5	$4.585e^{-0}$	$9.87\ e^{-1}$	$6.99\ e^{-1}$	$8.57\ e^{-}$	3.888^{e-4}	7.397^{e-1}
		Testing	5	$76.63\ e^{-0}$	$7.39\ e^{-1}$	$53.13\ e^{-0}$	$2.79\ e^{-1}$	1.54^{e-3}	5.493^{e-1}
2	Crop Land	Training	21	$18.54\ e^{-0}$	$9.32\ e^{-1}$	$196e^{-0}$	8.16^{e-1}	2.728^{e-4}	7.466^{e-1}
		Validation	5	$35.07\ e^{-0}$	$9.43\ e^{-1}$	$1757\ e^{-0}$	$8.36e^{-2}$	2.592^{e-3}	5.619^{e-2}
		Testing	5	$45.60\ e^{-0}$	$9.71\ e^{-1}$	$12949\ e^{-0}$	3.12^{e-1}	4.249^{e-3}	1.8^{e-1}
3	Forest	Training	21	$71.75\ e^{-0}$	$7.72\ e^{-1}$	$11.4\ e^{-0}$	8.85^{e-1}	2.264^{e-4}	7.538^{e-1}
		Validation	5	$112.6\ e^{-0}$	$7.13\ e^{-1}$	$39.5\ e^{-0}$	8.04^{e-1}	5.047^{e-4}	8.677^{e-2}
		Testing	5	$176.2\ e^{-0}$	$7.39\ e^{-1}$	$218\ e^{-0}$	-2.5^{e-1}	7.992^{e-4}	6.944^{e-1}
4	Waste Land	Training	21	$31.47\ e^{-0}$	$9.24\ e^{-1}$	$9.92\ e^{-1}$	8.14^{e-1}	1.604^{e-4}	9.095^{e-1}
		Validation	5	$131.4\ e^{-0}$	$5.24\ e^{-1}$	$2.31\ e^{-0}$	4.14^{e-1}	3.877^{e-4}	9.363^{e-1}
		Testing	5	$29.8\ e^{-0}$	$9.06\ e^{-1}$	$11.05\ e^{-0}$	3.65^{e-1}	4.785^{e-3}	-5.651^{e-1}

5.8 Model Validation and testing:

Figures 5.48 (a) and 5.50(a), show the validation performance of the model for the runoff occurring at settlement land of the study area. The best validation performance was witnessed at epoch 6 with minimum error of 0.69913. The training of the model continued further for 6 more iteration. It was terminated automatically after a total of 12 iterations as the error value were on an ever increasing trend. The figure does not indicate any major problem with the training and the validation except some over fitting that occurred at the beginning.

Figures 5.48(b) and 5.50(b), show the validation performance of the model for the runoff occurring at crop land of the study area. The best validation performance was witnessed at epoch 14 with minimum mean square error of 1757.5547. The training of the model continued further for 6 more iteration. It was terminated automatically after a total of 20 iterations as the error value were found to be on an ever increasing trend. The figure does not indicate any major problem with the training and the validation except some over fitting that occurred at the beginning.

Figures 5.48(c) and 5.50(c), show the validation performance of the model for the runoff occurring at forest land of the study area. The best validation performance was witnessed at epoch 9 with minimum mean square error of 39.5027. The training of the model continued further for 6 more iteration. It was terminated automatically after a total of 15 iterations. The figure indicates best fitted performance throughout.

Figures 5.48(d) and 5.50(d), show the validation performance of the model for the runoff occurring at waste land of the study area. The best validation performance was witnessed at epoch 4 with minimum mean square error of 2.3132. The training of the model continued further for 6 more iteration. It was terminated automatically after a total of 10 iterations. The figure indicates best fitted performance throughout.

Figures 5.49(a) and 5.51(a), present the regression plot by the model for the runoff occurring at settlement land of the study area. The figure depicts the relationship between output of neural network model and its targets. The training output shows the slight variation from the targeted having R value of 0.75336. The validation results are also found to be better fit with R value of 0.85773. The output-target relationship

for test run as well as for overall system run shows a non linear relationship with R values of 0.27939 and 0.42482 respectively.

Figures 5.49 (b) and 5.51 (b), present the regression plot by the model for the runoff occurring at crop land of the study area. The figure depicts the relationship between output of neural network model and its targets. The training output shows the slight variation from the targeted having R value of 0.81616. The validation results show a non-linear relationship with R vale of 0.08361. The output-target relationship for test run as well as for overall system run shows a non linear relationship with R values of 0.31238 and 0.21525 respectively.

Figures 5.49(c) and 5.51(c), present the regression plot by the model for the runoff occurring at forest land of the study area. The figure depicts the relationship between output of neural network model and its targets. The training output shows the slight variation from the targeted having R value of 0.88513. The validation results are also found to be better fit with marginal deviation having R value of 0.85773. The output-target relationship for test run shows a non linear relationship with R values of -0.25126 and for overall system run it depicts satisfactorily linear relationship having R value of 0.53425.

Figures 5.49(d) and 5.51(d), present the regression plot by the model for the runoff occurring at settlement land of the study area. The figure depicts the relationship between output of neural network model and its targets. The training output shows the slight variation from the targeted value having R value of 0.81469. The validation results are also found to be better fit with R value of 0.41465. The output-target relationship for test run as well as for overall system run shows a linear relationship with R values of 0.27939 and 0.42482 respectively.

Figures 5.52 (a), (b), (c), and (d) depict the mathematical relationship (model) between runoff and corresponding different land use land cover classes i.e.; settlement land, crop land, forest land and waste land in the study area.

Figures 5.53 (a), and 5.55 (a) show the validation performance of the model for the recharge occurring at settlement land in the study area. The best validation performance was witnessed at epoch 20 with minimum mean square error of 4.5851.

The training of the model continued further for 6 more iteration. It was terminated after a total of 26 iterations. The figure indicates best fitted performance throughout.

Figures 5.53(b) and 5.55(b) show the validation performance of the model for the recharge occurring at crop land of the study area. The best validation performance was witnessed at epoch 17 with minimum mean square error of 35.0787. The training of the model continued further for 6 more iteration. It was terminated after a total of 23 iterations. The figure indicates best fitted performance throughout.

Figures 5.53(c) and 5.55(c) show the validation performance of the model for the recharge occurring at forest land of the study area. The best validation performance was witnessed at epoch 9 with minimum mean square error of 112.6871. The training of the model continued further for 6 more iteration. It was terminated after a total of 15 iterations. The figure indicates best fitted performance throughout.

Figures 5.53(d) and 5.55(d) show the validation performance of the model for the runoff occurring at waste land of the study area. The best validation performance was witnessed at epoch 2 with minimum mean square error of 131.4189. The training of the model continued further for 6 more iteration. It was terminated after a total of 20 iterations. The figure indicate satisfactory performance with the training and the validation and testing except some over fitting that occurred at the beginning only.

Figures 5.54(a) and 5.56(a), present the regression plot by the model for the recharge occurring at settlement land of the study area. The figure depicts the satisfactory relationship between output of neural network model and its targets. The training output shows the nearly fitted values from the targeted having R value of 094172. The validation results are also found to be best fit with R value of 0.98709. The output-target relationship for test run as well as for overall system run shows a linear relationship with R values of 0.73987 and 0.92326 respectively.

Figures 5.54(b) and 5.56(b) presents the regression plot by the model for the recharge occurring at crop land of the study area. The figure depicts the satisfactory relationship between output of neural network model and its targets also. The training output shows the nearly fitted values from the targeted having R value of 0.93222. The validation results are also found to be best fit with R value of 0.94331. The

output-target relationship for test run as well as for overall system run shows a linear relationship with R values of 0.97123 and 0.93071 respectively.

Figures 5.54(c) and 5.56(c) presents the regression plot by the model for the recharge occurring at forest land of the study area. The figure depicts a satisfactory relationship between output of neural network model and its targets. The training output shows the slight variation from the targeted having R value of 0.77259. The validation results show a linear relationship with R vale of 0.71313. The output-target relationship for test run as well as for overall system run shows a linear relationship with R values of 0.73977 and 0.70403 respectively.

Figures 5.54(d) and 5.56(d), presents the regression plot by the model for the recharge occuring at waste land of the study area. The figure depicts a satisfactory relationship between output of neural network model and its targets. The training output shows the almost nil variation from the targeted having R value of 0.92458. The validation results show poor linear relationship with R vale of 0.52422. The output-target relationship for test run as well as for overall system run shows a linear relationship with satisfactory R values of 0.90648 and 0.86699 respectively.

Figures 5.57 (a), (b), (c), and (d) depict the mathematical relationship (models) between recharge and corresponding different land use land cover classes i.e.; settlement land, crop land, forest land and waste land in the study area.

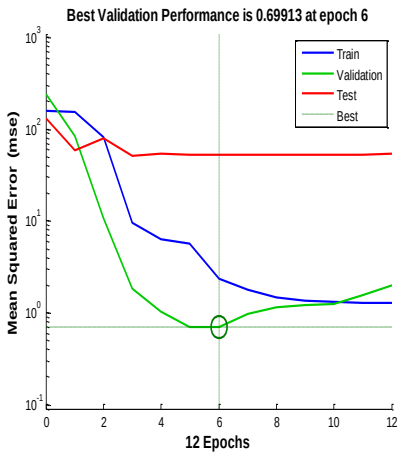

Fig.5.48(a) Performance relationship between Settlement Land Use and Runoff

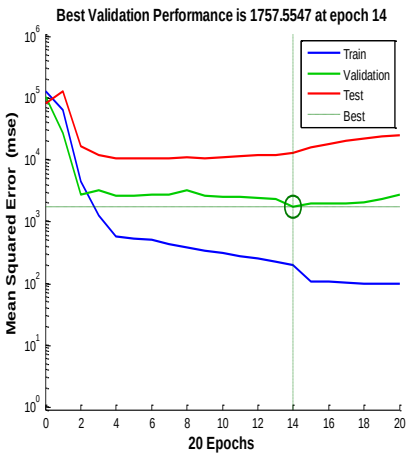

Fig.5.48(b) Performance relationship between Cultivable Land Use and Runoff

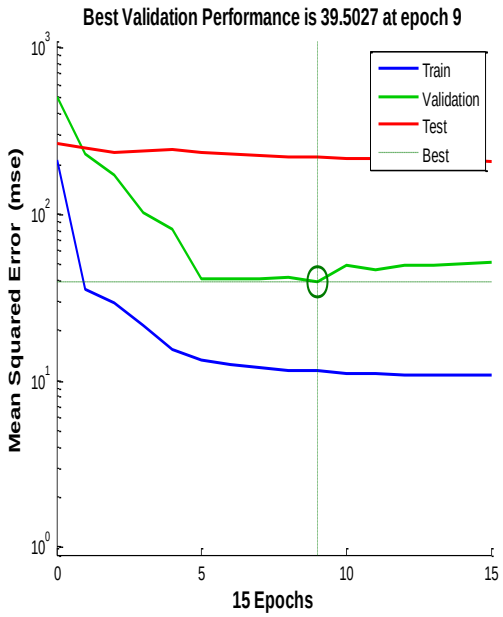

Fig.5.48(c) Performance relationship between Forest Land Use and Runoff

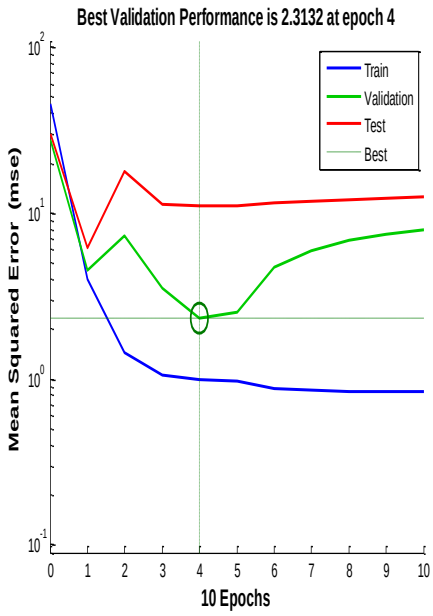

Fig.5.48(d) Performance relationship between Waste Land Use and Runoff

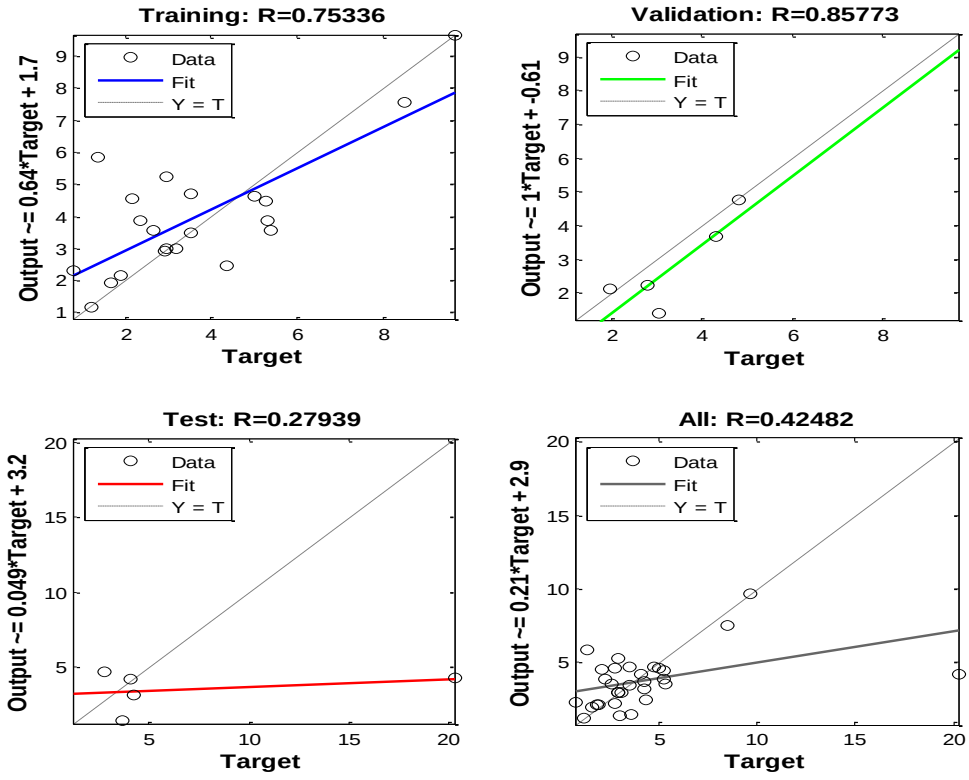

Fig.5.49(a) Regression relationship between Settlement Land Use and Runoff

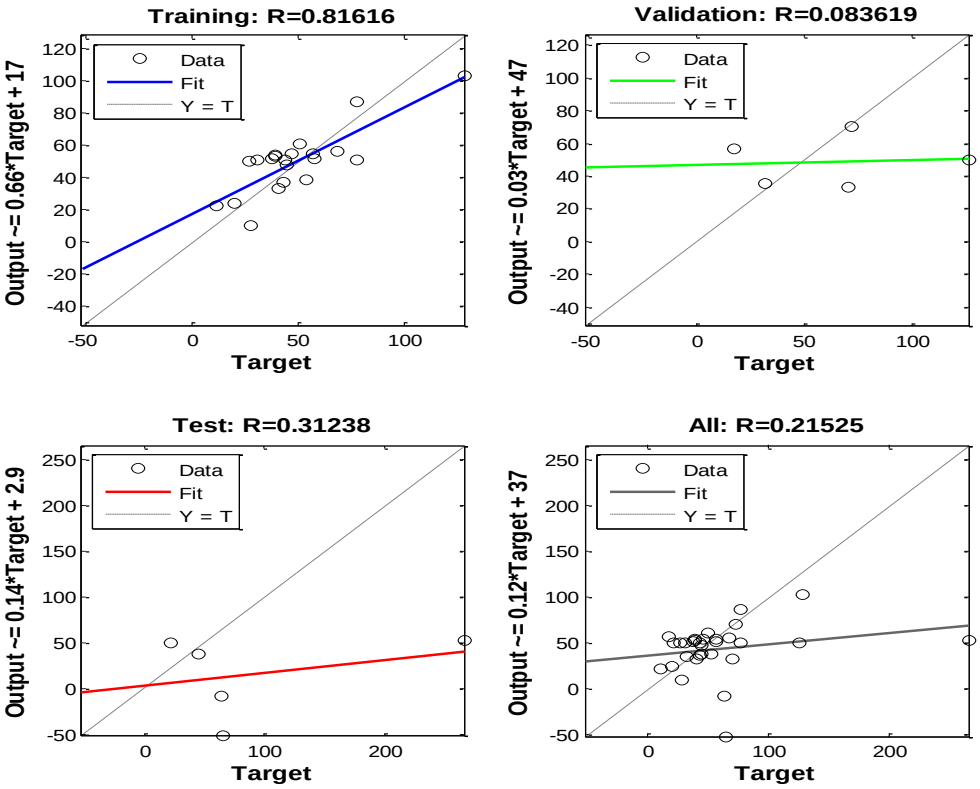

Fig.5.49(b) Regression relationship between Cultivable Land Use and Runoff

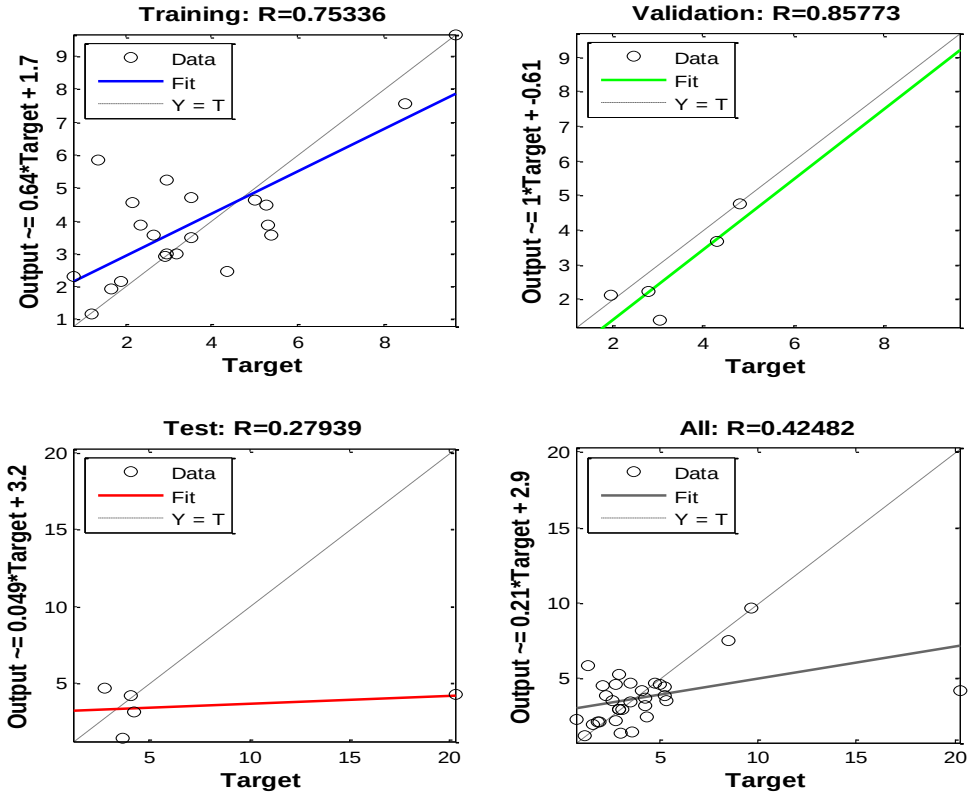

Fig.5.49(c) Regression relationship between Forest Land Use and Runoff

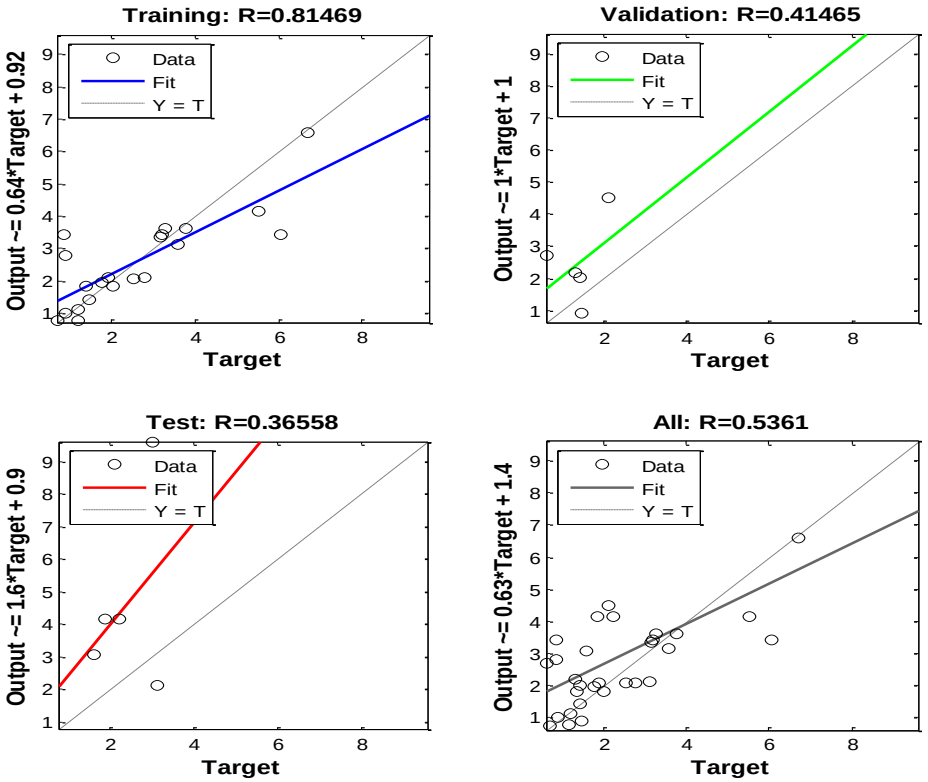

Fig.5.49(d) Performance relationship between Waste Land Use and Runoff

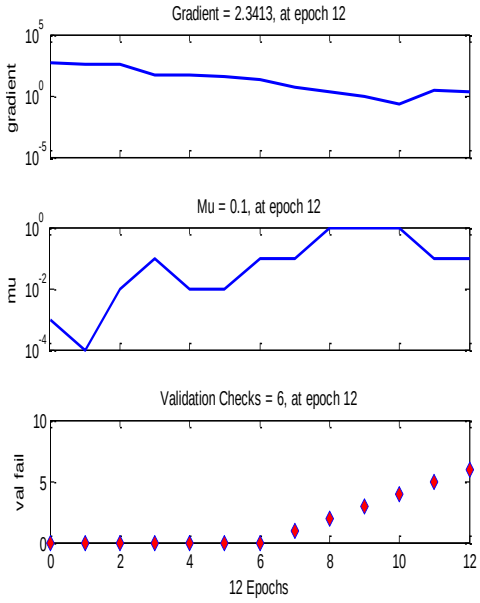

Fig.5.50(a) Model fitting analysis for settlement land use Vs Recharge

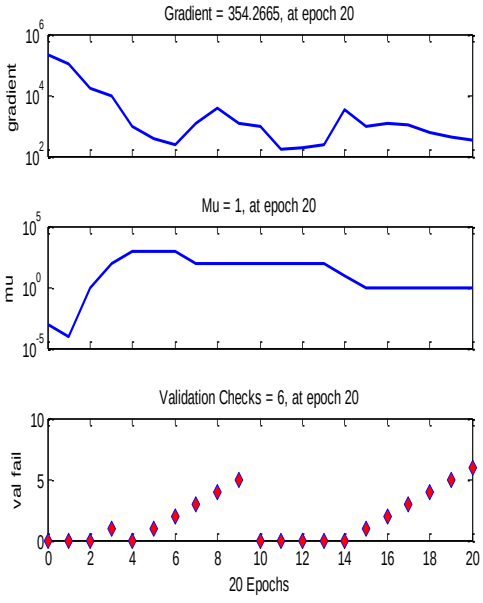

Fig.5.50(b) Model fitting analysis for crop land use Vs Recharge

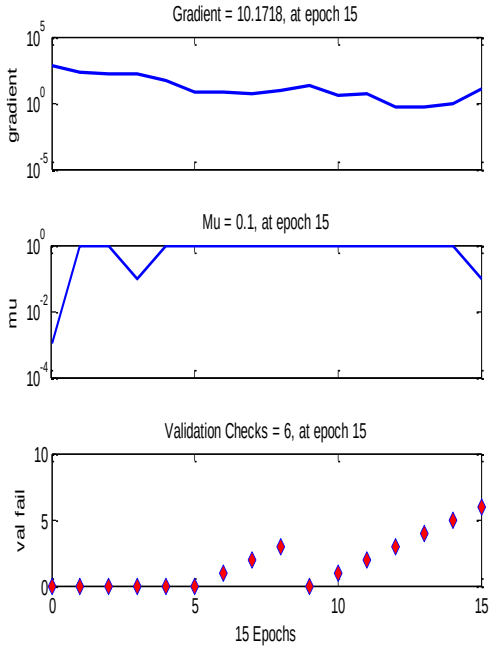

Fig.5.50(c) Model fitting analysis for forest land use Vs Recharge

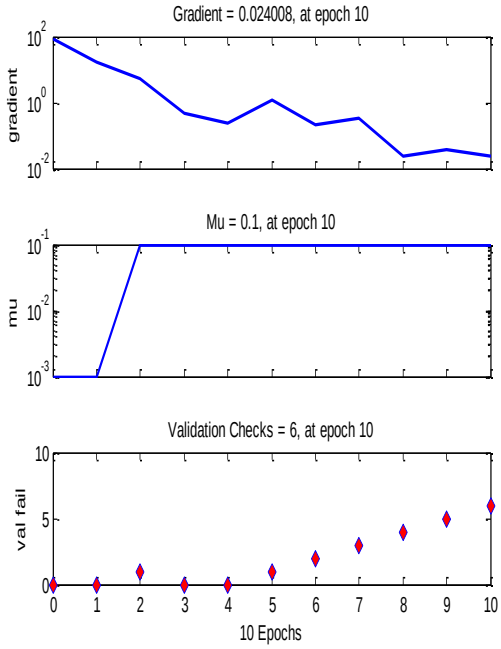

Fig.5.50(d) Model fitting analysis for waste land use Vs Recharge

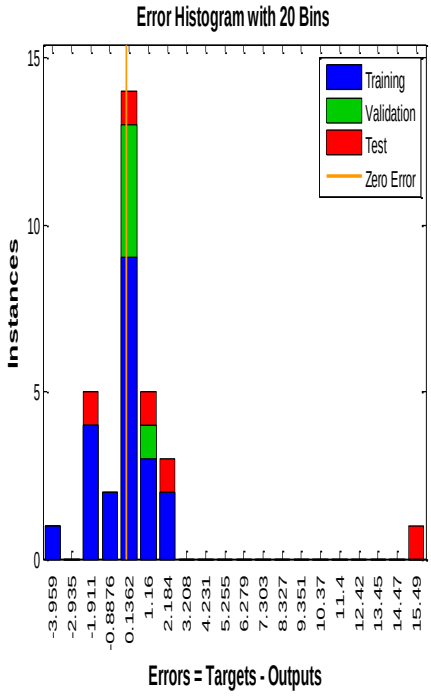

Fig.5.51(a) Error analysis of model For settlement Vs Recharge

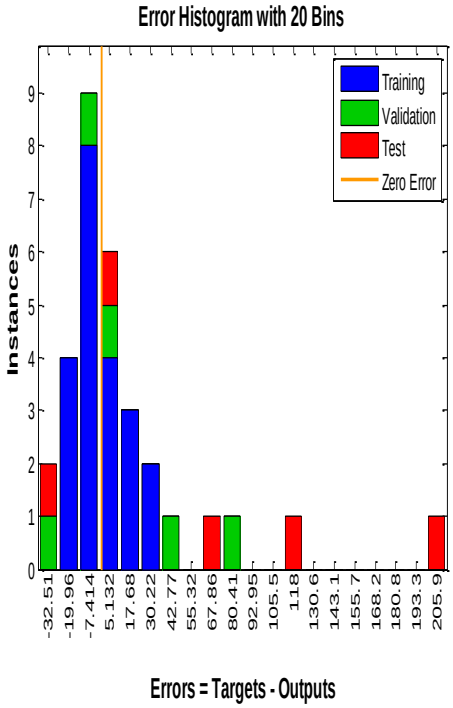

Fig.5.51(b) Error analysis of model for cropland area Vs Recharge

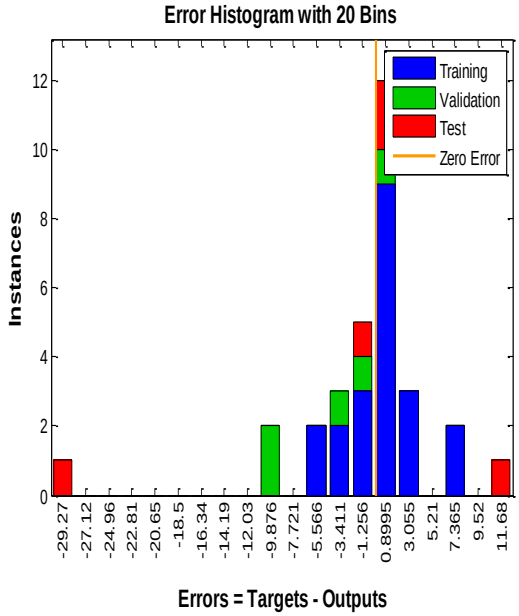

Fig.5.51(c) Error analysis of model for forest land area Vs Recharge

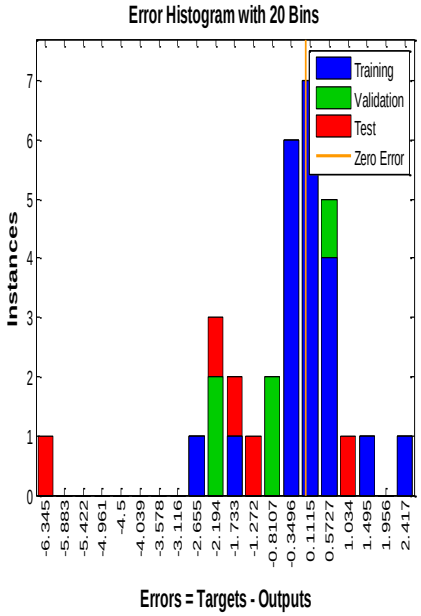

Fig.5.51(d) Error analysis of model for waste land area Vs Recharge

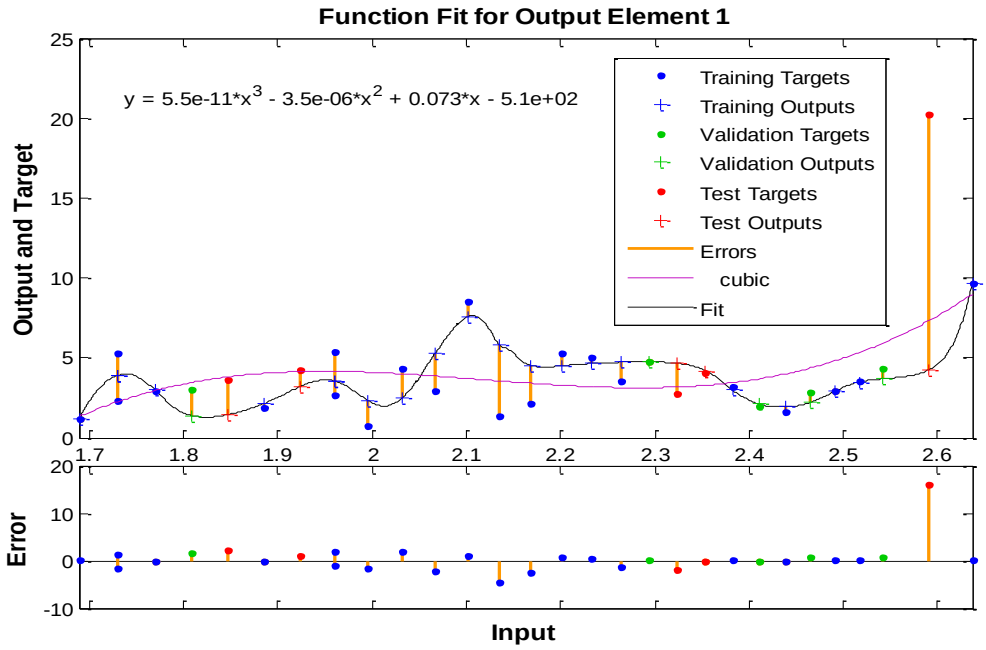

Fig. 5. 52(a) Model for Settlement land use Vs Recharge relationship

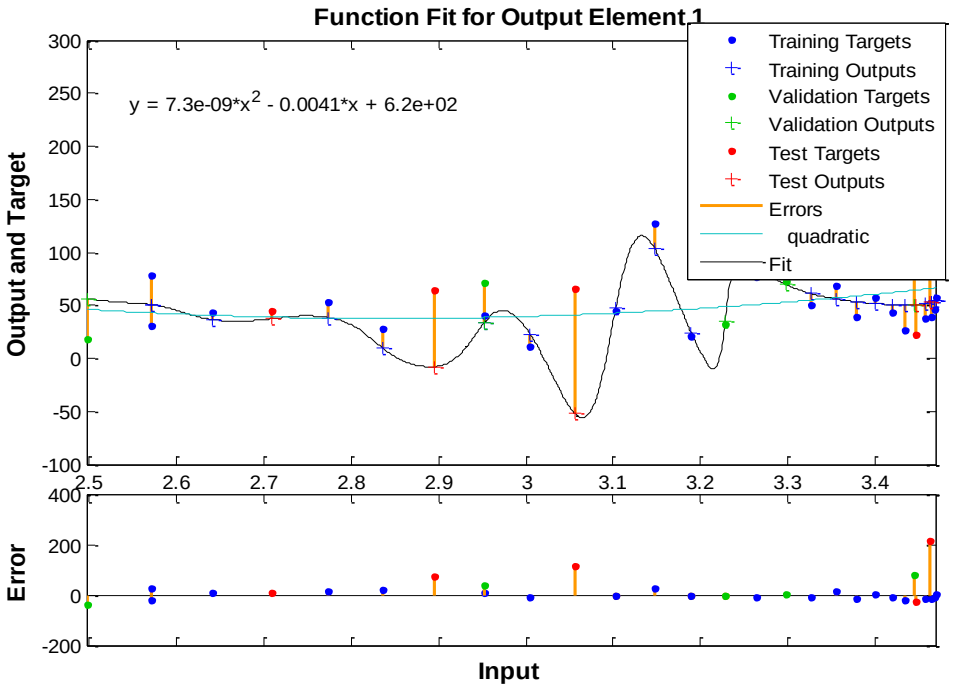

Fig. 5. 52(b) Model for crop land use Vs Recharge relationship

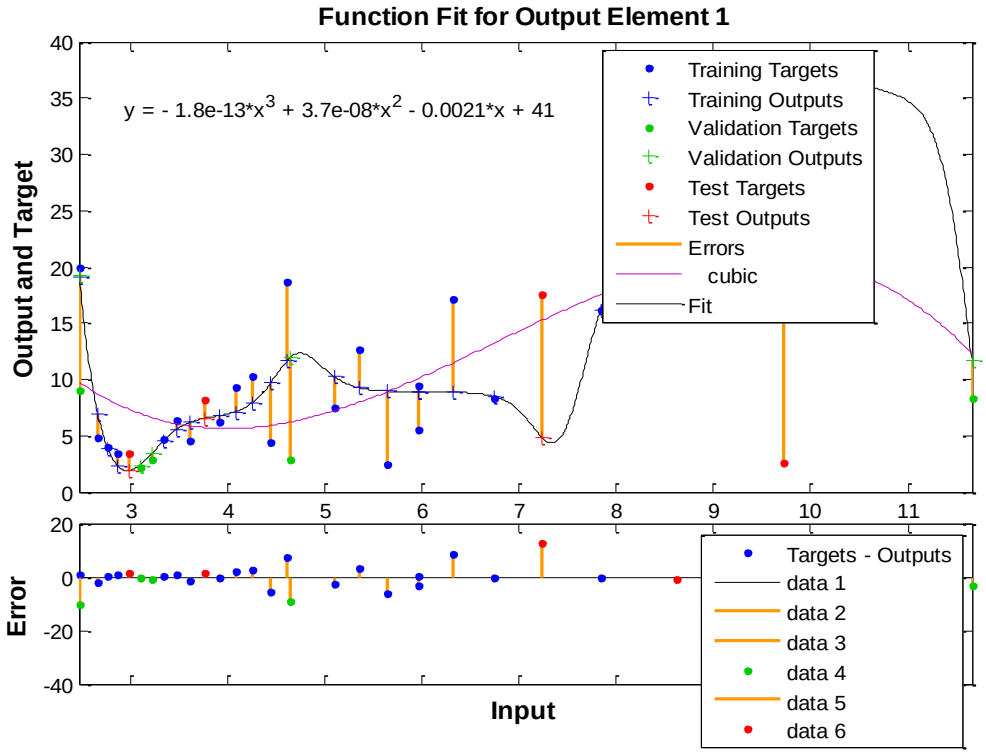

Fig. 5. 52(c) Model for forest land use Vs Recharge relationship

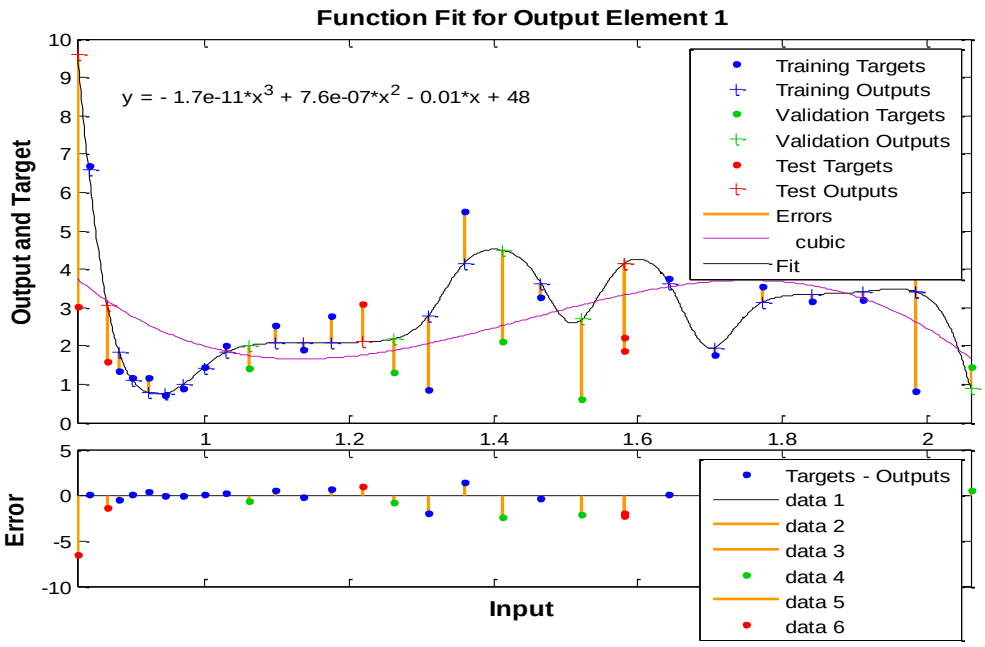

Fig. 5. 52(d) Model for waste land use Vs Recharge relationship

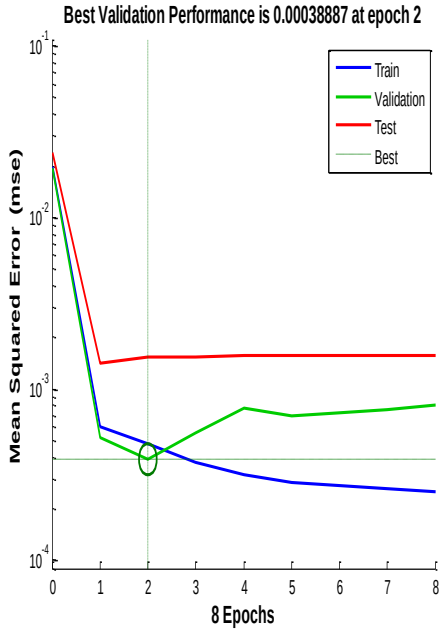

Fig. 5.53(a) **Performance relationship between estimated recharge Vs settlement land use area**

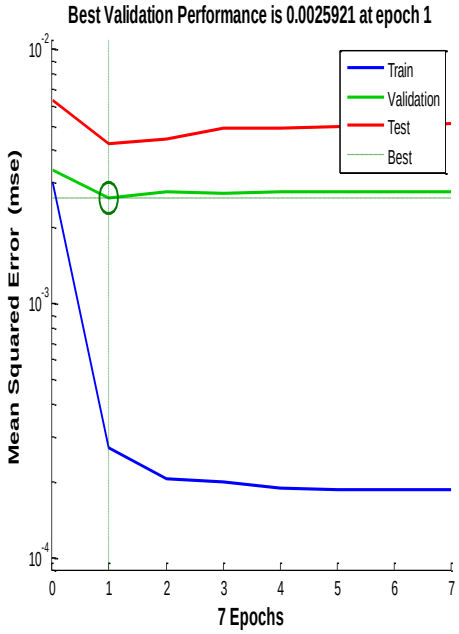

Fig. 5.53(b) **Performance relationship between estimated recharge Vs crop land area**

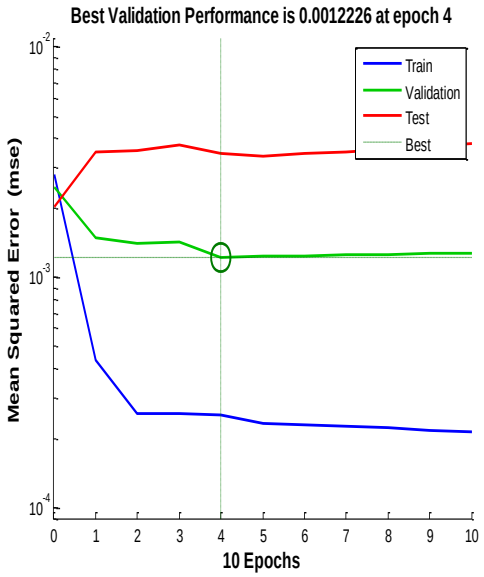

Fig. 5.53(c) Performance relationship between estimated recharge Vs forest land use area

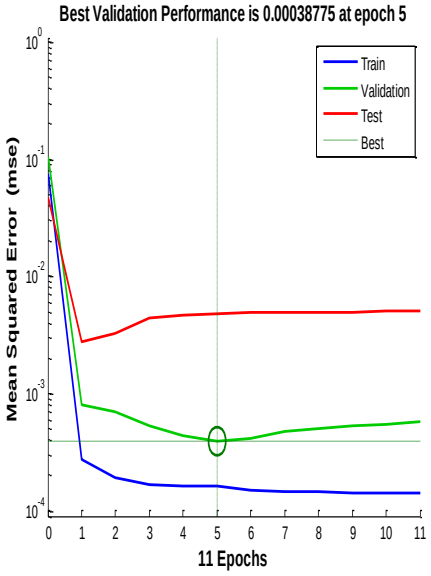

Fig. 5.53(d) Performance relationship between estimated recharge wasteland land use area

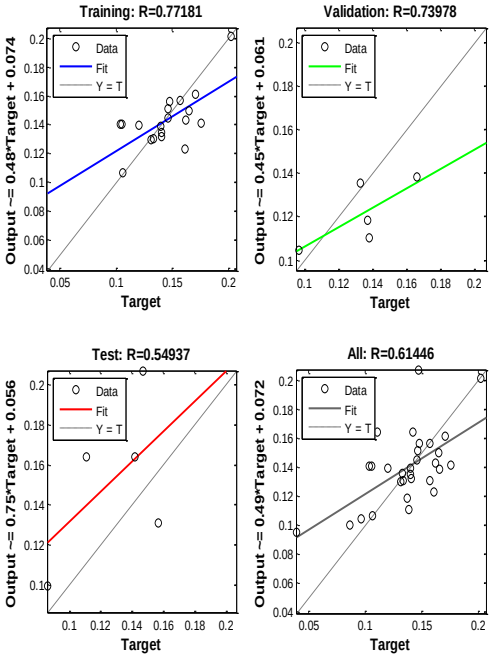

Fig.5.54(a) Performance relationship between Settlement Land Use and Recharge(Estimated)

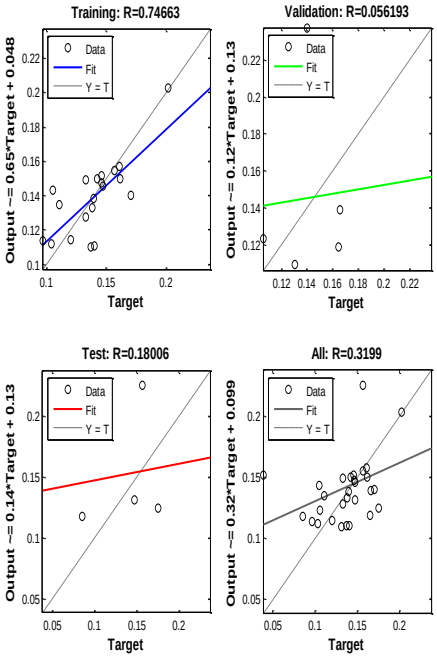

Fig.5.54(b) Performance relationship between Cropland Use and Recharge(Estimated)

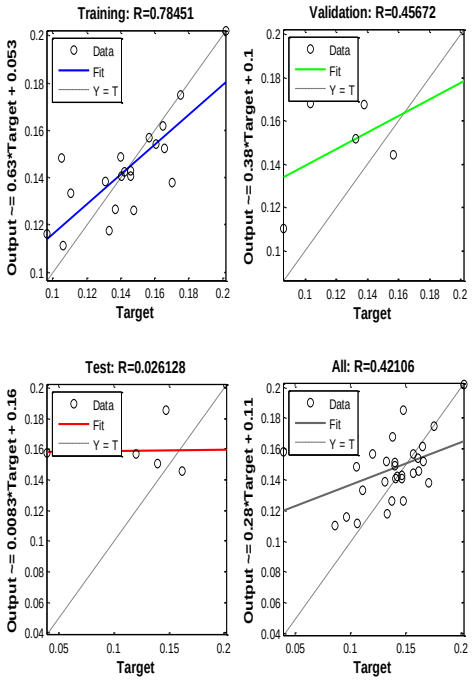

Fig.5.54(c) Performance relationship between Forest Land Use and Recharge(Estimated)

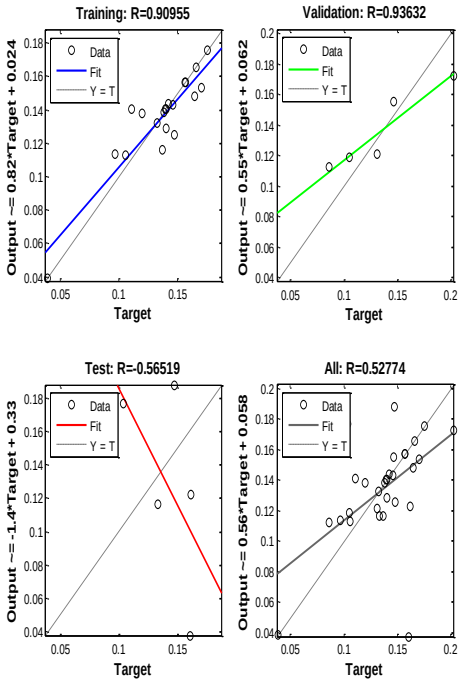

Fig.5.54(d) Performance relationship between Waste Land Use and Recharge(Estimated)

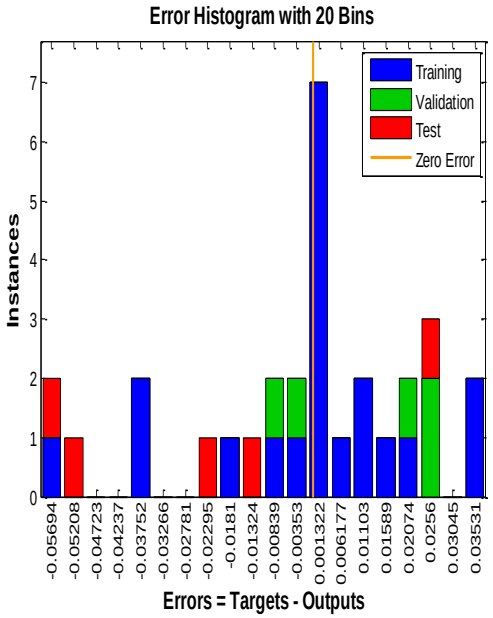

Fig.5.55(a) Error analysis of model for settlement land use Vs Recharge(Estimated)

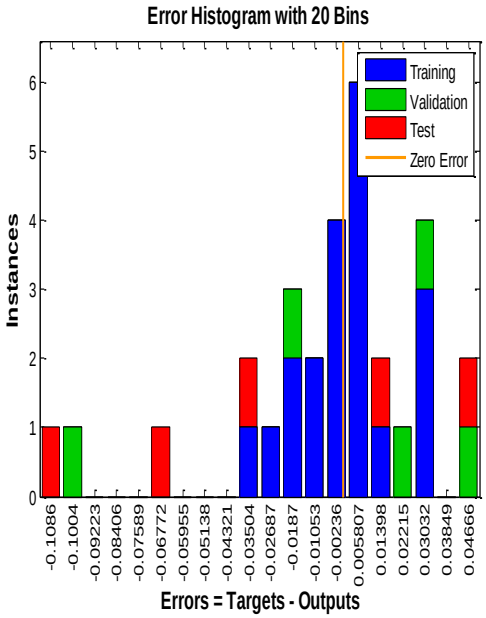

Fig.5.55(b) Error analysis of model for crop land use Vs Recharge(Estimated)

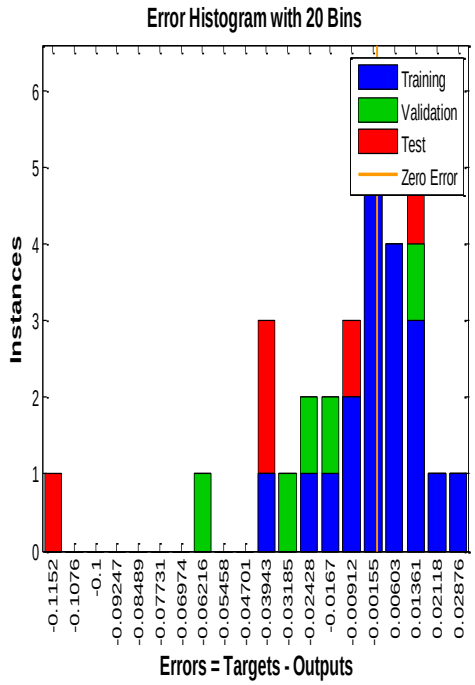

Fig.5.55(c) Error analysis of model for forest land use Vs Recharge(Estimated)

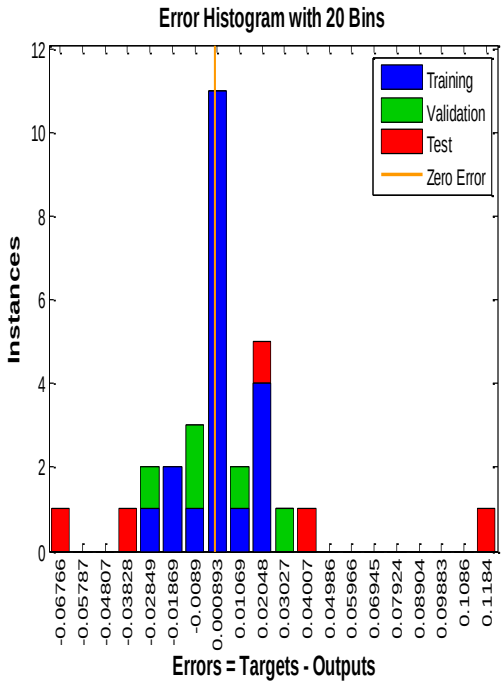

Fig.5.55(d) Error analysis of model for waste land use Vs Recharge(Estimated)

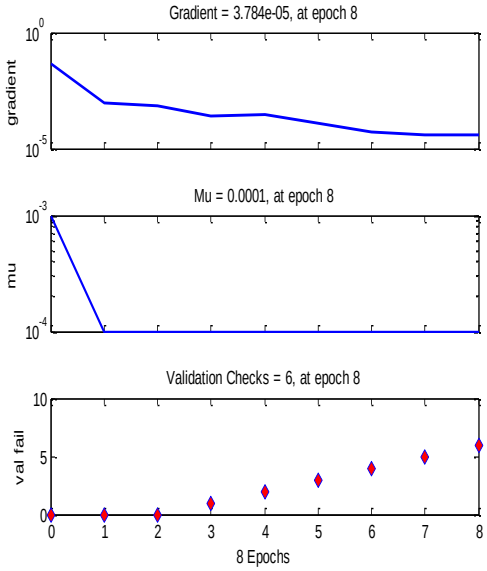

Fig.5.56(a) Model fitting analysis for settlement land use Vs Recharge(Estimated)

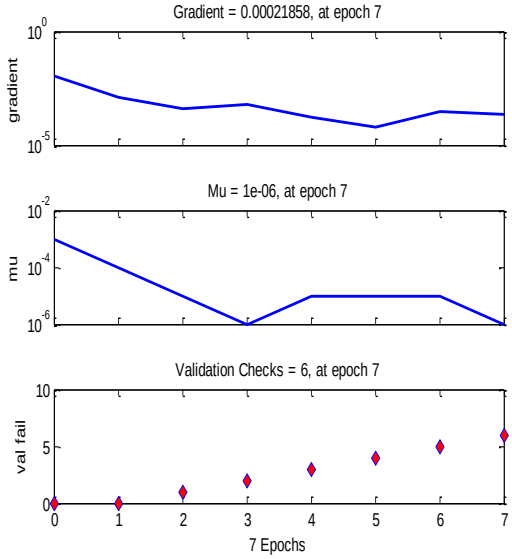

Fig.5.56(b) Model fitting analysis for crop land use Vs Recharge(Estimated)

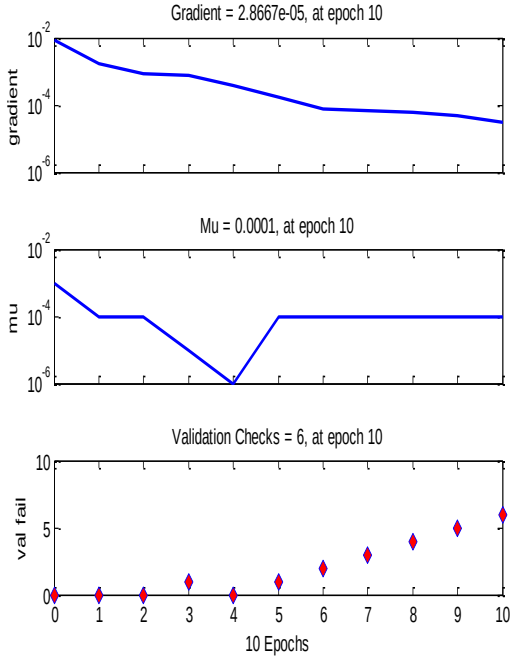

Fig.5.56(c) Model fitting analysis for forest land use Vs Recharge(Estimated)

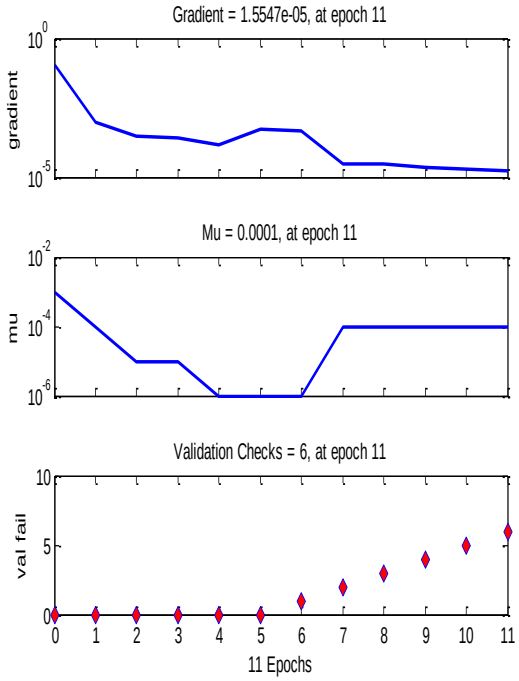

Fig.5.56(d) Model fitting analysis for waste land use Vs Recharge(Estimated)

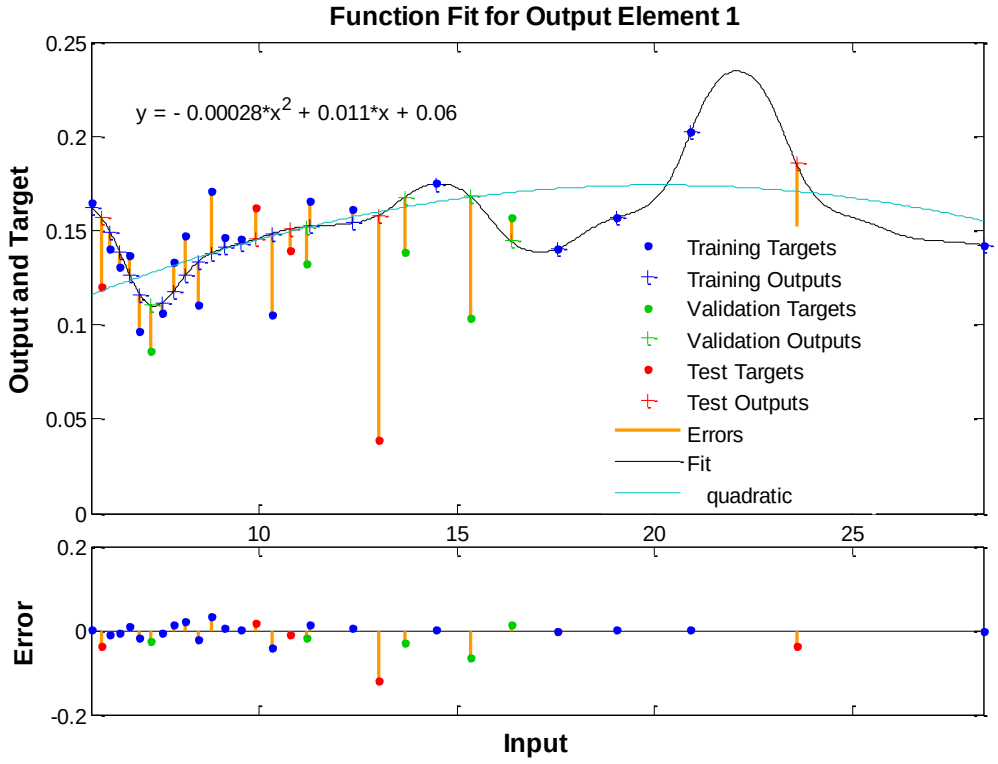

Fig.5.57(a) Model for settlement land use Vs Recharge(Estimated) relationship

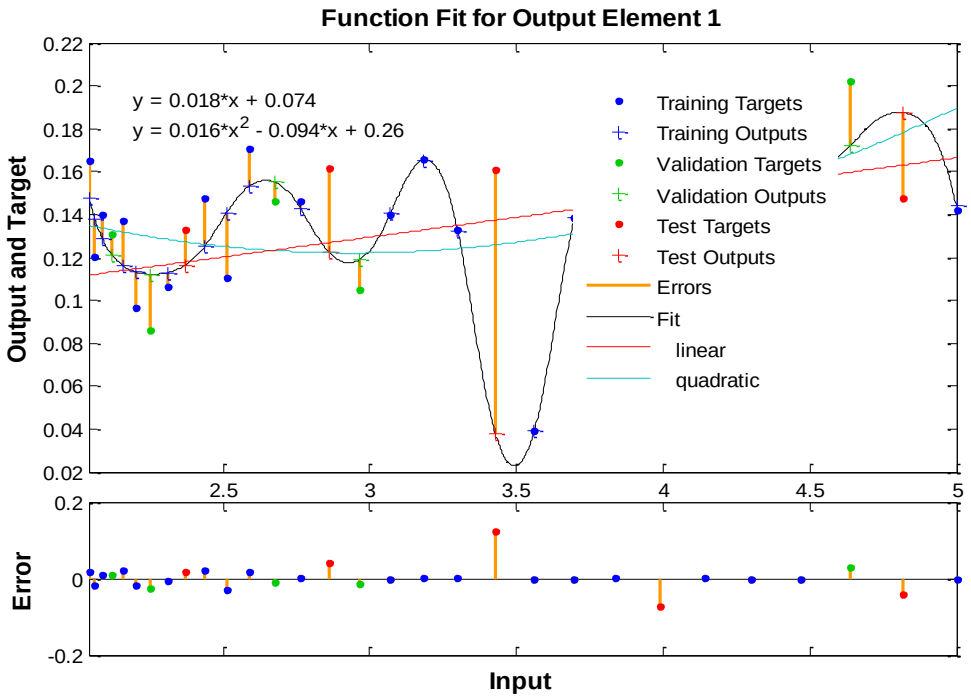

Fig.5.57(b) Model for crop land use Vs Recharge(Estimated) relationship

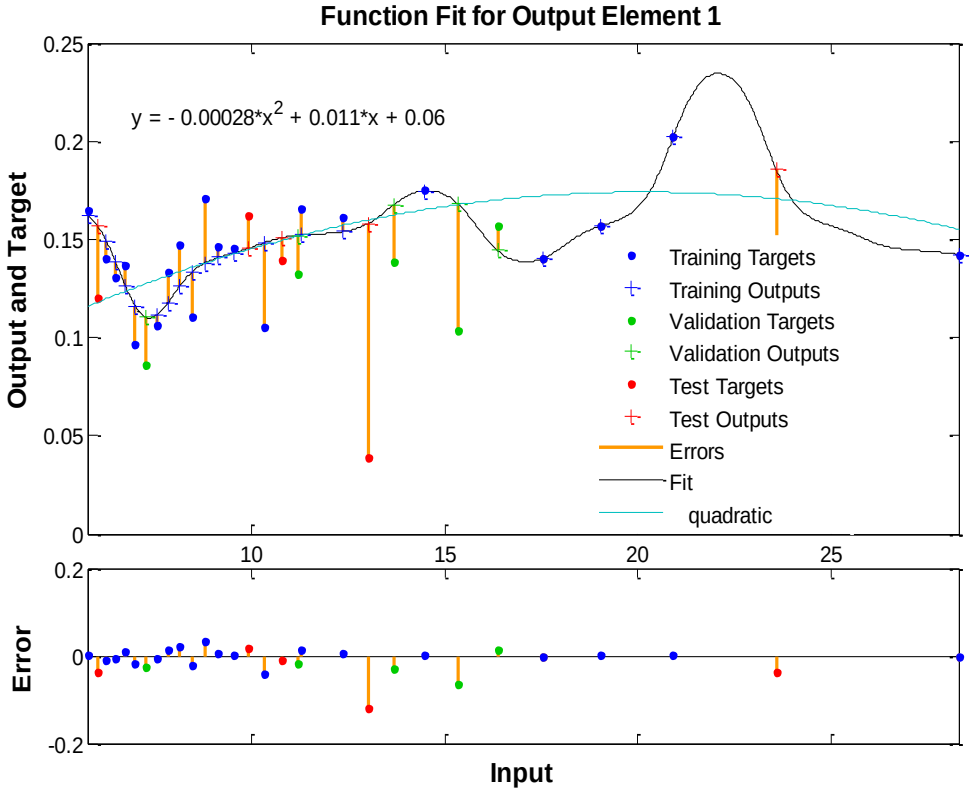

Fig.5.57(c) Model for forest land use Vs Recharge(Estimated) relationship

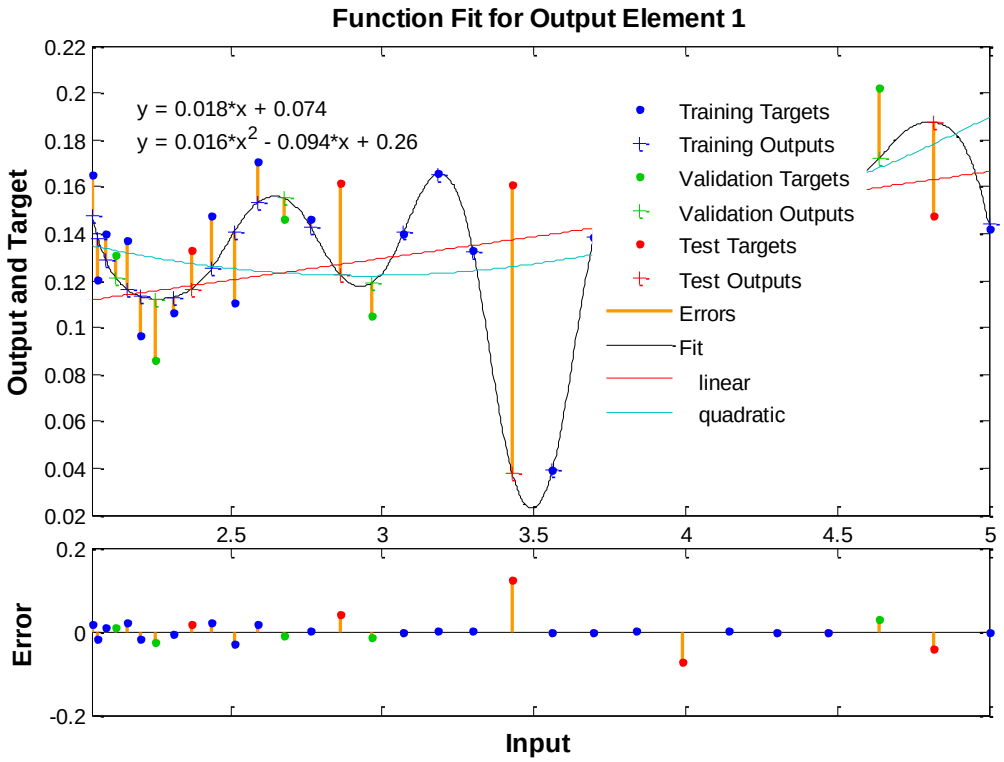

Fig.5.57(d) Model for waste land use Vs Recharge(Estimated) relationship

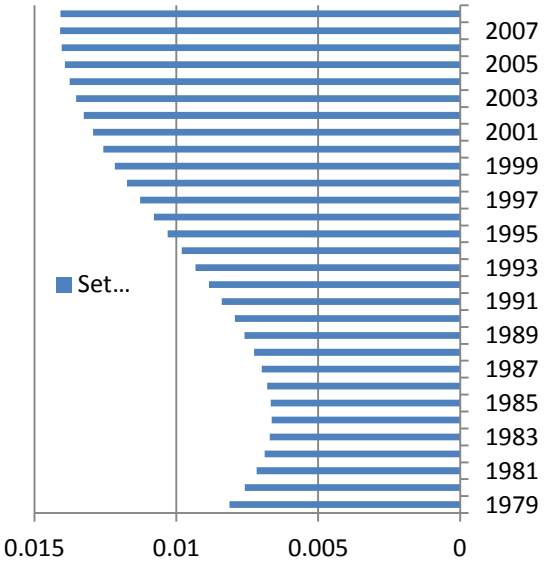

Fig. 5.58 (a)Recharge trend in settlement land use

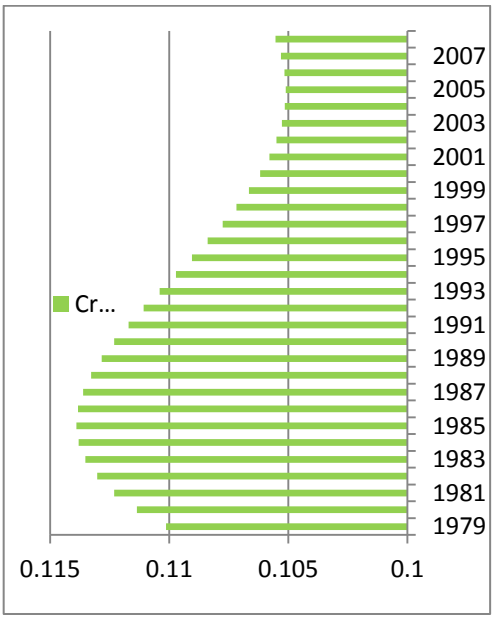

Fig. 5.58(b)Recharge trend in Crop land use area

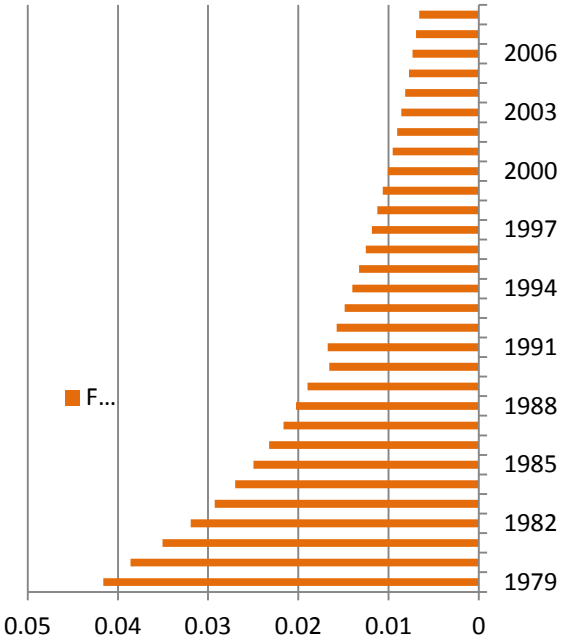

Fig. 5.58(c) Recharge trend in Forest land use area

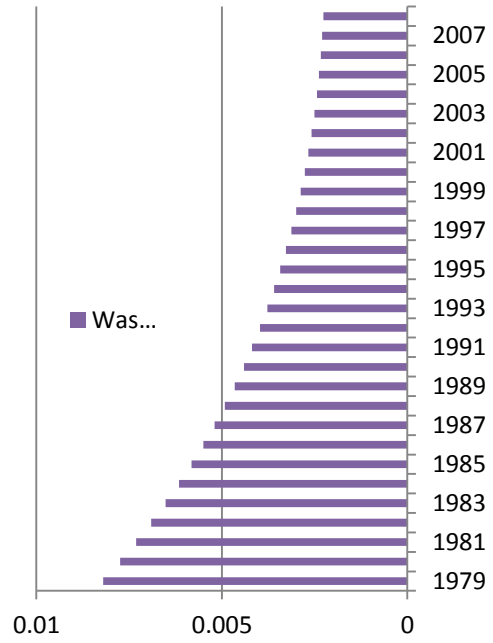

Fig. 5.58(d) Recharge trend in Wasteland use area

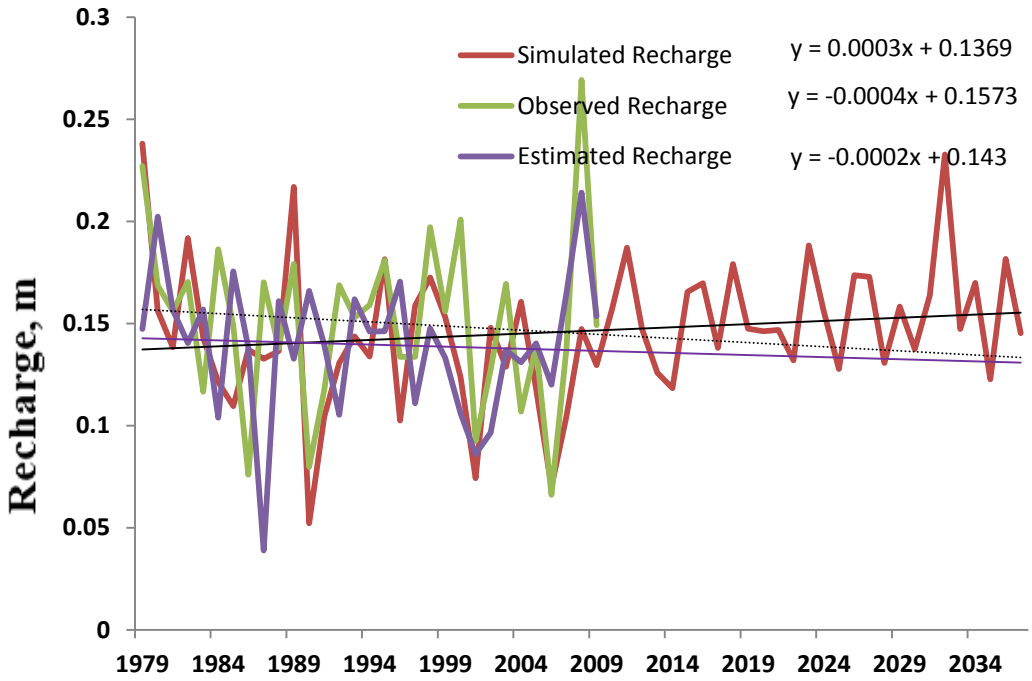

Fig. 5.59 Observed, Estimated and Simulated Recharge in the study area

Table 5.16. ARIMA Model Description for water table analysis

			Model Type
Model ID	VAR00002	Model_1	ARIMA(0,0,0)
	VAR00003	Model_2	ARIMA(0,0,0)
	VAR00004	Model_3	ARIMA(0,0,0)
	VAR00005	Model_4	ARIMA(0,0,0)
	VAR00006	Model_5	ARIMA(0,0,0)
	VAR00007	Model_6	ARIMA(0,0,0)

Table. 5.17. ARIMA Model Statistics

Model	Number of Predictor	Model Fit statistics								Ljung-Box Q(18)		
		Stationary R-squar	R-squared	RMSE	MAPE	MAE	MaxAPE	MaxAE	Normal BIC			
VAR2-Model_1	1	.026	.026	3.16	15.32	2.71	29.2	5.98	2.49	17.25	18	.50
VAR3-Model_2	1	.004	.004	4.43	15.59	3.65	29.08	8.0	3.17	18.0	18	.45
VAR4-Model_3	1	.092	.092	3.49	16.03	2.94	37.78	7.64	2.69	13.98	18	.73
VAR5-Model_4	1	.012	.012	2.40	14.75	1.95	27.91	5.02	1.95	23.78	18	.16
VAR6-Model_5	1	.000	.000	4.62	13.93	4.01	26.48	7.65	3.26	24.47	18	.14
VAR7-Model_6	1	.006	.006	21.23	12.96	18.37	26.89	38.6	6.30	13.48	18	.76

Table. 5.18. ARIMA Model Parameters

					Estimate	SE	t	Sig.
VAR00002-Model_1	VAR00002	No Transformation	Constant		112.598	97.216	1.158	.255
	VAR00001	No Transformation	Numerator	Lag 0	-.047	.049	-.974	.337
VAR00003-Model_2	VAR00001	No Transformation	Numerator	Lag 0	.026	.068	.383	.704
	VAR00003	No Transformation	Constant		-28.589	136.294	-.210	.835
VAR00004-Model_3	VAR00001	No Transformation	Numerator	Lag 0	-.101	.054	-1.878	.069
	VAR00004	No Transformation	Constant		219.686	107.256	2.048	.048
VAR00005-Model_4	VAR00001	No Transformation	Numerator	Lag 0	-.024	.037	-.655	.517
	VAR00005	No Transformation	Constant		61.633	73.961	.833	.410
VAR00006-Model_5	VAR00001	No Transformation	Numerator	Lag 0	-.006	.071	-.084	.934
	VAR00006	No Transformation	Constant		41.277	142.181	.290	.773
VAR00007-Model_6	VAR00001	No Transformation	Numerator	Lag 0	.155	.327	.474	.638
	VAR00007	No Transformation	Constant		-166.002	652.173	-.255	.801

CHAPTER – VI

SUMMARY AND CONCLUSION

The rapid population growth with economic development, urbanization and industrialization has created tremendous pressure on the limited natural resource base in the country. The riparian forest was converted to agricultural fields; agricultural fields converted to build up area for residential or industrial purpose. The land use/land cover resources are the bases for various development activities on the earth. The land use/land cover is one of the most important parameter to have meaningful plan for land resource management, such as development of cities, available water resources, mining activities, Agriculture, pasture, and environmental activities. It also enables the anticipation of the problems that may accompany with change in land use. The structural changes in ecosystem is the outcome of conversion of various land forms to other enhancing soil compaction, reducing infiltration, ground water recharge and exceeding peak flows in the form of runoff. This alteration in ecosystem is leading to offer negative influence on hydrology, bio-geochemical cycles and nutrient cycles.

The study of remotely sensed data showed that the study area Bareilly district has undergone significant change in land use land cover over last 30 years (Between 1979-2009). Classified image of year 1979 distinctively showed rich vegetation cover closely to half of the total area. But it is found converted mostly into cropland and built-up/settlement area with the passage of 30 years i.e. by year 2009. The above changes in the land use land cover has been mainly due demand of more food for growing population and need for the development of infrastructure. However, conversion of plantation/vegetation land to agriculture crop land and Agriculture crop land into built-up/settlement area need to be monitored and regulated judiciously for the preservation of natural resources and sustainability of the ecosystem.

The Land use Land cover analyses indicate that in the year 1979, a major portion of the study area (44%) is under vegetation/plantation/forest cover. Similarly an equal portion (44%) of the study area is under agriculture crop land. The area under waste land is about 5% of the total geographical area. The area under settlements (built-up/Roads etc) was merely 6% of the total geographical area. But after passage of about 30 years i.e. in 2009, the composition of land use land cover has changed

significantly. Now the area under vegetation/plantation/forest cover has decreased from 44% to mere 17%. This reduction in the vegetation/plantation/forest cover area has been the result of conversion of such area into crop land, Settlements, and waste land. Consequently, the area under Crop land has increased from 44% to 55%, Settlements from mere 6% to 17% and Waste land from 5% to 7%.

Rainfall is the main sources of water in the study area. The average rainfall over the study area is 949.76 mm and monsoon rainfall contributes to a large extent of about 93.17%. The annual minimum rainfall of 216.27 mm is received at Aonla rain gauge station and maximum rainfall of 1734.21 mm at Baheri rain gauge station. It is also evident that the rainfall is maximum on the northern side of the study area with a decreasing trend from north to south reaching minimum at Aonla. The main source of ground water occurring in the district is through rainfall and return flow from applied irrigation. Ground water level shows a seasonal pattern of fluctuation. The magnitude of fluctuation depends upon the amount of water recharge and draft. The Aonla area receives very little rainfall due to which groundwater table is lowest. The entire study area shows a declining trend of groundwater table though the other five areas (Tehsils) receive adequate amount of rain fall.

The excess withdrawal of groundwater from the earth for agricultural production has led to changes in hydrologic regime altering water budgeting components. The annual analysis of rainfall and water table fluctuation and pre and post-monsoon analysis of water table of the area were made to study the trend of water table movement at, Bareilly Sadar, Baheri, Aonla, Nawabganj, Faridpur, and Mirganj Tehsils. The study shows that all the areas have declining water table trend. The auto correlation function and partial auto correlation shows all the seasonal components are within the desired limit. The test parameters of model were also estimated and found within the desired limit (Table 5.16, 5.17 and 5.18).

The runoff study at different land use systems of the Study area shows that the highest runoff occurs in the August month in the region followed by July and September due to monsoon season and also due to saturated soil moisture regime after onset of monsoon. This precipitation is mainly responsible for overland flows in the area leading to erosion of top layer of soil. The crop land, settlement area and waste land has shown large runoff volumes generated in the successive years. This is mainly

because of temporal increase in the areas of crop land, settlement and waste land and their characteristics favouring runoff as compared to other land use (forest land).

The study shows the variation in runoff is highly dependent on rainfall occurrence and their temporal variations throughout the months. The rainfall pattern from 1979-1990 has changed in 1991 to 2009. These monsoon months have higher evaporation and also the high ET rate due to high temperature prevailing in these months leading to more losses in soil moisture and reduces replenishment trend in the area. Due to this change in temporal precipitation pattern, the runoff percentage occurring in the area has also been increasing throughout the study period from 1979 to 2009. The rainfall runoff study for the area shows that runoff occurred over the crop land, and settlement land has been continuously increasing while it was found to be decreasing over forest land and waste land. This is due the temporal change into their respective areas together with further deterioration of LULC conditions. The runoff which is the major component of outflow has also substantially increased due to increase in crop land and settlement lands and is flowing out from the area. The area needs attention to reduce the runoff flow and also measures to control soil moisture so that large amount of moisture loss inevitably occurring though transpiration can be compensated and overall inflow components can be balanced.

The further analysis of recharging at various land forms/uses shows that rate of recharge through settlement land during 1979-1990 periods is more than that of during 1990-2009. This was due to further compaction of such areas by use of heavy machineries, pakka roads, pavements, houses etc, though the quantum of recharge through settlement land had increased throughout. Similarly, the rate of recharge through crop land during 1979-1990 was found to be quite high due to increase in crop land. But during 1990-2000 periods in spite of substantial increase in crop land area the rate of recharge was found to be almost static i.e. rate of change in recharge was found to be almost zero.

CONCLUSION

1. Land use land cover of the study area, district Bareilly has been categorized into five categories i.e., Crop Land (C), Vegetation/Plantation/Forest Land (F), Waste Land (WL) Water Bodies (WB) and Structure/Settlement (S). The land use analysis shows that crop land and settlement land in the area has drastically increased with a substantial decrease in Vegetation/Forest/Plantation land. The forest in the area is almost disappeared or converted in to sparse trees land or orchard areas.

2. The CN (wetted) value of the study area was found to be altering due to human interventions as 75.63, 76.65 and 78.40 in 1979, 1990 and 2009 respectively.

3. The time series analysis shows that there was significant decrease in the water table. Though lowering of water table is moderate but may become alarming if adequate recharge majors are not made in place immediately and regularly.

4. Due to change in land uses, the runoff in the area has been substantially increased.

5. The simulation of recharge in the area has shown that recharging in the area after 1990 was decreased and there may not be significant replenishment of water leading to reduction in water table. The major outflow component in the area is runoff, and therefore area needs proper soil conservation and water management efforts to improve recharging.

6. The major portion of runoff was occurring on cropland and settlement.

7. The continuous decrease in recharging calls for more water management efforts and to reduce groundwater withdrawal for irrigation.

8. The neural network models developed for run-off and recharge shows that the recharge from the crop land, forest land and wasteland was critically low. It indicates the runoff occurring in the area is not conserved due to deteriorating land cover conditions and needs better water and soil moisture conservation measures.

9. The process of more runoff than recharge began between 1999- 2000 and the trend is continuously rising upward. This indicates due deterioration of LULC

conditions the runoff have increased far more than recharge causing tremendous impact on hydrologic regime in the study area.

10. The water resources planning, development and management is of paramount importance for the sustainable development of any region. Therefore, developing a model to effectively forecast the runoff and recharge was quite pertinent considering the fact that agriculture is the main activity in the study area. The behaviour of the developed model during training, testing and validation for Runoff as well as Recharge, at Settlement Land, Crop Land, Forest and Wasteland, for the study area has been found very responsive and satisfactory as it has provided satisfactory results in the form of mathematical equations/graphs .

11. In order to check the decline of groundwater table, cropping pattern should be moderated and area under crops having high water demand is to be reduced in favour of less water intensive crops besides other water conservation practices in the entire area.

REFERENCE

Agrawal S.P; Garg Vaibhav; Gupta Prasun K; R. Bhaskar; Nikam; and Thakur Praveen K. 2012; Climate and LULC change scenarios to study its impact on hydrological regime:international archives of the photogrammetry, remote sensing and spatial information sciences, Volume XXXIX-B8, 2012 XXII ISPRS Congress, 25 August – 01 September 2012, Melbourne, Australia.

Ahmad Sarfaraz , Zahoor Shahid, Farooq -Ul-Islam, Md. Abdullah Khan, Zaidi Wasi A. and Matloob Huma 2008; Impact of urbanization on hydrological regime in Indian cities: Journal of Environmental Research And Development Vol. 2 No. 4, April-June, 2008.

Akaike, H. 1974; A new look at the statistical model identification IEEE Trans. Automatic Control, AS-19: 716-723.

Alansi, A. W.; Amin, M. S. M.; Halim, G. Abdul; Shafri, H. Z. M.; Thamer, A. M.; Waleed, A. R. M.; Aimrun, W.; Ezrin, M. H 2009; The Effect of Development and Land Use Change on Rainfall-Runoff and Runoff-Sediment Relationships Under Humid Tropical Condition: Study of Bernam Watershed Malaysia: European Journal of Scientific Research;May2009, Vol. 31 Issue 1, p88.

Al-Jabari Samah; Sharkh Majed Abu; and Al-Mimi Ziad 2009; Estimation of runoff for agricultural watershed using SCS curve number and GIS: Thirteenth International Water Technology Conference, IWTC 13 2009, Hurghada, Egypt. Pp 1213-1229.

Anderson, R.L. 1942; Distribution of serial correlation coefficient. Annals of Mathematical Statistics, 13(1): 1-13.

Anderson, J.M., Burt, T.P., 1978. The role of topography in controlling through flow generation: Earth Surface Processes and Landforms 3, 331–344.

Anderson, M.P., Woessner, W.W., 1992. Applied Groundwater Modeling: Simulation of Flow and Advective Transport. Academic Press, Inc., San Diego, CA.

ASCE Task Committee 2000a. Artificial neural networks in hydrology—I: preliminary concepts. Journal of Hydrologic Engineering, American Society of Civil Engineers **5**(2): 115–123.

ASCE Task Committee 2000b. Artificial neural networks in hydrology—II: hydrologic applications. Journal of Hydrologic Engineering, American Society of Civil Engineers **5**(2): 124–137.

Ashagrie A. G, De P. J. M; Laat; De M. J. M; Wit; Tu M;, and Uhlenbrook S 2006: Detecting the influence of land use changes on discharges and floods in the Meuse River Basin – the predictive power of a ninety-year rainfall-runoff relation:

Axel Bronstert, Daniel Niehoff and Gerd B"urger, 2002; Effects of climate and use Change on storm runoff germination, present knowledge and modeling capabilities, hydrological process.16, 509-529 (2002).

Barkhordari 2003.: Assessing the effects of land use change on the hydrologic regime by RS and GS, a case study in the Minab catchment, Hormozgan Province, Iran: Thesis submitted to the international institute for geo-information science and earth observation.

Beven, K. J., Lamb, R., Quinn, P., Romanowicz, R., and Freer, J. 1995. `TOPMODEL', in Singh, V. P. (Ed.), Computer Models of Watershed Hydrology. Water Resource Publications, Colorado. pp. 627- 668.

Bicknell, B.R., Imhoffl, J.C., Kittle, J.L., Jr., Donigian, A.S., Jr., and Johanson, R.C., 1997, Hydrological Simulation Program-FORTRAN, User's manual for Version 11: Athens, Ga., U.S. Environmental Protection Agency Report No. EPA/600/R-97/080, 775 p.

Biren Baishya 2006; Modeling hydrological components and impact of land use/land cover change on hydrological regime, a thesis submitted to Andhra University, India.

Bosch, J.M., & Hewlett, J. D. 1982. A review of catchment experiments to determine the effect of vegetation changes on water yield and evapotranspiration. Journal of Hydrology, 55: 3-23.

Boulain, N. B., Cappelere, S. L., Gignous, J. and Peugeo, C. 2006; Hydrologic and land use impacts on vegetation growth and NPP at the watershed Scale in a Semi-arid environment.

Bouraoui, F., Vachaud, G., Haverkamp, R., Normand, B., 1997. A distributed physical approach for surface-subsurface water transport modeling in agricultural watersheds. Journal of Hydrology 203 (1/4), 79–92.

Boyd, D., Smith, A.F., Veale, B. 2000; Flood Management on the Grand River Basin. The Grand River Conservation Authority, 26 p.

Bowling, L.C., & Lettenmaier, D.P. 1997; Evaluation of the effects of forest roads on streamflow in Hard and Ware creeks, Washington. University of Washington, Seattle, WA, USA Water Resources Series Technical Report, No.155.

Box, G. E. P. and Cox, D. R. 1964; An Analysis of Transformations, J Royal. Statistical Society, 211-243, discussion 244-252.

Box, G.E.P. and Jenkins, G. 1970; 'Time series analysis, forecasting and control, First Ed. Hoden – Dey Inc., San Francisco.

Brooks, K.N., Ffolliott, P.F., Gregersen, H.M., and Thames, J.L. 1991. Hydrology and the management of watersheds. Ames, Iowa: Iowa State University Press.

Brown, D.G., Walker, R., Manson, S., Set, K., 2004. Modeling Land-Use and Land-Cover Change. Downloaded from: http://www-personal.umich.edu.

Bruijnzeel, L.A. 1990: Hydrology of moist tropical forests and effects of conversion: A state-of-knowledge review. Paris: UNESCO International Hydrological Programme.

Calder, I.R. 1993; Hydrologic effects of land- use change, Handbook of Hydrology, McGraw- Hill, New York, USA, 13(1): 13-50.

Calder, I.R. 1998: Water-resource and land use issues: SWIM Paper 3. Colombo: IIMI. Chang FJ, Hu HF, Chen YC. 2001. Counter propagation fuzzy neural network for stream-flow reconstruction: Hydrological Processes **15**(2):219–232.

Cho, J., Barone, V.A. and Mostaghimi, S., 2008. Simulation of land use impacts on groundwater levels and stream flow in a Virginia watershed. Agricultural Water Management 96 (2009) I-II.

Chomitz, K.M., and Kumari, K. 1996: The domestic benefits of tropical forests a critical review emphasizing hydrologic functions. World Bank Policy Research Working Paper, No. 1601.

Clark C.O., 1945. Storage and the unit hydrograph. Trans. ASCE 110, 1419–1446.

Clive A. Mc Alpine , Jozef I. Syktus , Ravinesh C. Deo , and Peter J. Lawrence , Hamish A. McGowan, Ian G. Watterson, Stuart R. Phinn.: Modeling impacts of

vegetation cover change on regional climate: Geophysical Research Letters, accepted Sept 2007.

Cook, P.G., Walker, G.R. and Jolly, I.D. 1989; Spatial variability of groundwater recharge in a semi-arid region. J. Hydrology, 111: 195-212.

Crawford Norman H. And Linsley Ray K. 1966; Digital simulation in hydrology, Stanford watershed model IV. Technical Report No. 39. July 1966.

Dams, J.; Woldeamlak, S.T. and Batelaan, O. 2008; Predicting land – use change and its impact on the groundwater system of the Kleine Nete Catchment, Belgium. Hydrology and Earth System Sciences, 12: 1369-1385.

De Fries, R. and Eshleman, K.N. 2004; Land-use change and hydrological processes: a major focus for the future. Hydrological Processes, 18: 2183-2186.

DHI 2000a; MIKE 11 a modelling system for rivers and channels. DHI Water and Environment, 82 p.

DHI 2000b; MIKE SHE Flow Modules, Technical Reference. DHI Water and Environment, 174 p.

DHI 2003; DHI Software. Modeling the world of water. URL: http://www.dhisoftware.com/index.htm.

Di Luzio, M., R. Srinivasan, and J. G. Arnold. 2002. Integration of watershed tools and SWAT model into BASINS. J. American Water Resour. Assoc. 38(4): 1127-1141.

Dimyati, P. 1995; Analysis of land use/land cover change using the combination of MSS and land use map. A case study of Yogyakarta, Indonesia. J. Remote Sensing, 17(5): 931-944.

Engineering Manual 2003. Remote sensing, Engineer Manual No. 1110-2-2907, Department of the Army, US Army Corps of Engineers Washington, DC.

Falkenmark, M., & Chapman, T.(eds). 1989; Comparative hydrology. An ecological approach to land and water resources, Paris: UNESCO.

FAO. 1987; Guidelines for economic appraisal of watershed management projects.Written by H.M. Gregersen, K.N. Brooks, J.A. Dixon and L.S. Hamilton. FAO Conservation Guide No. 16.

FAO. 1997; Seawater intrusion in coastal aquifers. Guidelines for study, monitoring and control. FAO Water Reports, No. 11.

FAO/Netherlands 1999; Water. Background Paper 6 of the Conference on the Multifunctional Character of Agriculture and Land. Maastricht.

Farley, K.A.; Jobbagy, E.G. and Jackson, R.B. 2005; Effects of afforestation on water yield: a global synthesis with implications for policy. Global change Biology, 11: 1565-1576.

Flannery,W.H., Teukolsky,B.P, S.A Vetterling, W.T. 1989; Numerical recipes in Pascal: the art of scientific computing. Cambridge University Press.

Fortin J-P., Turcotte, R., Massicotte, S., Moussa R., Fitzback J., Villeneuve, J-P. 2001; Distributed Watershed Model Compatible with Remote Sensing and GIS Data, I: Description of model. J. Hydrol. Eng., 6, 91-99.

Garg Vaibhav, Khwanchanok Ampha, Gupta Prasun K. Aggarwal S.P, Kiriwongwattana Komsan, Thakur Praveen K. and Nikam Bhaskar R. 2012: Urbanisation Effect on Hydrological Response: A Case Study of Asan River Watershed, India.: Journal of Environment and Earth Science, ISSN 2224-3216 (Paper) ISSN 2225-0948 (Online) Vol 2, No.9, 2012.

Geethalakshmi V. Nils-Otto Kitterod and Lakshmanan. 2008; Aliterature review on modelling of hydrological processes and feedback mechanism on climate: ISBN: 13 nr:978-82-17-00428-8 (Bioforsk report, volume 3).

GLOBE toolkit, 2003 in Landsat Multispectral Scanner (MSS) and Thematic Mapper (TM). (Available online http://iic.gis.umn.edu/finfo/land/landsat2.htm). (Accessed on December 2008.)

Gol, C ; Cakir, M ; Edis, S ; Yilmaz, H. (2010). The effect of Land-use/Land cover Change and demographic processes on soil properties in the Gokcay catchment, turkey. African Journal of agricultural research vol. 4(13), pp. 1670-1677.

Gregersen, B., Aalbaek, J., Lauridsen, P.E., Kaas, M., Lopdrup, U.,Veihe, A. and P van der Keur (2004). Land Use/Land Cover Changes and groundwater Potential Zoning in and around Raniganj coal mining area, Bardhaman District, West Bengal – A GIS and Remote Sensing Approach. J. Spatial Hydrology , Vol.4, No.2.

Griffiths, P. and Hill, I.D., Ellis Horwood (1985): Applied Statistics Algorithms, John Wiley and Sons, New York.

Hammersley, J.M. and Handscomb, D.C; 1964: Monte Carlo Methods, Methuen and Co, London; John Wiley and Sone, New York.)

Havard, P.L., Prasher, S.O., Bonnell, R.B., Madani, A., 1995. LINKFLOW, a water flow computer model for water table management. I. Model development. Transactions of the ASAE 38 (2), 481–488.

Hoang, T.M.T., Rahman, A., Weinmann, P.E., Laurenson, E.M. and Nathan, R.J. (1999): Joint Probability Description of Design Rainfalls. Proc. Water 99 Joint Congress – Brisbane, Inst. Of Engineers, Australia, pp 379-384.

Hofer, T. (1998a). Floods in Bangladesh. A highland-lowland interaction, Geographica Bernensia .G 48.

Hofer, T. (1998b). Do land use changes in the Himalayas affect downstream flooding: Traditional understanding and new evidences. Memoir Geological Society of India,: 119-141.

Homdee Tipaporn, Kobkiat Pongput, and Shinjiro Kanae impacts of land cover changes on hydrologic responses: a case study of Chi river basin, Thailand: Annual Journal of Hydraulic Engineering, JSCE, Vol.55, 2011.

Hope R, Jewitt G, Gowing, J. and Garratt, J., 2003. Linking the hydrological cycle and rural livelihoods: A case study in the Luvuvhu catchment, South Africa.

Hu, Wei ; Shao, Mingan ; Wang, Quanjiu ; Fan, Jun ; Horton, Robert. (2009). Temporal changes of soil hydraulic properties under different land-use. Geoderma 149 (2009) 355-366.

Hydrocomp (2002). Hydrocomp Forecast and Analysis Modeling. URL: http://www.hydrocomp.com/HFAMinfo.htm.

Idrissi Abdelkhalek, Ingrid Ruthy, Peou Hang, Mamik Vanclooster, and Etienne Persoons 2000: Impact of long term land use change on the hydrologic regime of the dyle watershed: International conference on agricultural effects on ground water and surface water, Wageningen The Netherlands, Oct.2000.

The India Water Portal, the Tyndall Centre for Climate Change Research

Ives, J.D., & Messerli, B.(1989). The Himalayan dilemma. Reconciling development and conservation. London: United Nations University Press.

Jakeman, A.J., I.G. Littlewood, and P.G. Whitehead 1990, 'Computation of the instantaneous unit hydrograph and identifiable component flows with application to two small upland catchments', Journal of Hydrology, vol 117, pp 275-300.

Jayalakshmi T, and Santakumaran A; (2011), Statistical Normalization and Back Propagationfor classification: International Journal of Computer theory and Engineering, Vol.3 pp 89-93, 1793-8201.

Jayatilaka, C.J., Storm, B., Mudgway, L.B., 1998. Simulation of water flow on irrigation bay scale with MIKE-SHE. Journal of Hydrology 208 (1/2), 108–130.

Julien, P. Y., Saghafian, B., F. L. Ogden (1995). Raster-Based Hydrologic Modeling of Spatially-Varied Surface Runoff", Water Resources Bulletin, AWRA, 31(3), p. 523-536.

Joshi, B.K. (2006). Vegetation Dynamics and its effect on soil loss under different land-use systems in Bhetagad Watershed, Indian Central Himalayas. J. Soil and Water Conservation, India, 5(2): 91-95.

Kaczmarek, Z., Dec., 1993, Water Balance Model for Climate Impact Analysis, ACTA Geophysica Polonica v.41 no. 4, 1- 16.

Kaltech, M.A. 2008. Rainfall-Runoff Modelling Using Artificial Neural Network modeling and understanding: Caspian Journal of Environmental Sciences, vol.6, pp.153-158.

Kiersch Benjamin, 2000: Land and Water Development Division Food and Agriculture Organization Rome, Italy workshop "Land-Water Linkages in Rural Watersheds" from 18 September to 27 October 2000.

Kouwen, N. (2001). WATFLOOD/SPL9 Hydrological Model & Flood Forecasting System. University of Waterloo, 192 p.

Kottegoda, N.T. and Horder, M.A. (1980). Daily flow model rainfall occurrences using pulse and a transfer function. J. Hydrology, 47: 215-234.

Kuczera, G., Lambert, M., Heneker, T., Jennings, S., Frost, A., Coombes, P. (2003): Joint Probability and design storms at the crossroads. Proc,28th Int. Hydrology and water resource. Symp. 10-14 Nov, Wollongong.

Kumar Arun 2009 ; Ground Water Resource Estimation Methodology: Report of the Ground Water Resource Estimation Committee, 1997, (Reprint 2009), Chairman & Addl.Secretary Central Ground Water Board Ministry of Water Resources Government of India.

Kumar B.M. 2005: Land use in Kerala: Changing scenarios and shifting paradigms: Journal of Tropical Agriculture 42 (1-2): 1-12, 2005.

Kumar C.P. 1993; Estimation of ground water recharge using soil moisture balance approach, NIH, Roorkee, India.

Kumar C.P. and Sethapathi P.V.: Assessment of Natural Ground water recharge in Upper Ganga Canal Command Area.

Kumar, P. Surendra., Praveen T.V., and Prasad M. Anjanaya; 2016. Artificial Neural Network Model for rainfall-runoff – A Case Study: International Journal of Hybrid Information Technology Vol.9, No.3 (2016), pp. 263-272

La Marche, J., & Lettenmaier, D.P. (1998). Forest road effects on flood flows in the Deschutes river basin, Washington. University of Washington, Seattle. Water Resources Series Technical Report, No.158.

Leavesley, G.H., Lichty, R.W., Troutman, B.M., and Saindon, L.G., 1983, Precipitation-runoff modeling system: User's manual: U.S. Geological Survey Water-Resources Investigations Report 83-4238, 207 p.

Lindstrom,G. Johanson, B. Persson, M. Gardelin, M. And Bergstrom, S. 1977. Development and test of the distributed HBV model: J. Hydro. 201, 272-288.

Loaiza Usuga,J.C. Jarauta-Bragulat, E. Porta J. R.M. Casanellas, Claret Poch (2010), assessing the effect of soil use changes on soil moisture regimes in mountain regions (catalan pre-pyrenees ne spain): Rev. Acad. Colomb. Cienc.: Volumen xxxiv, Número 132-septiembre De 2010.

Maidment, D.R. (Ed) (1993). Handbook of Hydrology, McGraw-Hill. Press, W.H.Flannery, Press, W.H., Teukolsky, S.A., Vetterling, W.T., Flannery, B.P (1993):

Numerical recipes in Fortran: the art of scientific computing. CambridgeUniversity Press.

Martinec, J., 1975: Snowmelt runoff model for river flow forecasts. Nordic Hydrology, 6, 145-154. Meyer, W.B. and Turner, B.L. (1994). Changes in land use and land cover. A Global Perspective. Cambridge University Press, Cambridge England; New York.

Math Works, Analyze Neural Network Performance after Training: Software developer for engineers and scientists; 1, Apple Hill Drive Natick MA 01760-2098, United States. Tax ID# 942960235. Phone: 508-647-7000.

Minns A.W. and Hall M.J. 1996; artificial neural networks as rainfall-runoff models: Hydrological Sciences Journal, 41:3, 399-417: Published online: 24 Dec 2009. http://dx.doi.org/10.1080/02626669609491511

Mishra Nitin, Khare Deepak, Gupta K.K; and Shukla Rituraj 2014: Impact of land use change on ground water – A review: Advances in water resource and protection (AWRP) Volume 2.

Mishra S.K; Rawat S.S; Pandey R.P; Chakraborti Shiulee; Jain M.K; and Chaube U.C.2014; Relation between Runoff Curve Number and PET: Journal of Hydruologic Engineering, February, 2014.

Mohan. S. and Shrestha M.N, 2000; A GIS based integrated model for assessment of hydrological changes due to land use modifications Lake 2000.

Morgan, D.S., Jones, J.L., 1995. Numerical model analysis of the effects of ground-water withdrawals on discharge to streams and springs in small basins typical of the Puget Sound Lowland. Washington. USGS Open-File Report 95-470.

Morgan, D.S., McFarland, W.D., 1994. Simulation analysis of the groundwater flow system in the Portland Basin, Oregon and Washington. USGS Open-File Report 94-505.

Morin, G. 2002: CEQUEAU. INRS-ETE, 89 p.

Mustard, J and Fisher, T. (2004). Land use and hydrology. In Gutman, G., Janetos, A., Jstice, C., Moran, E., Mustard, J., Rindfuss, R., Skole, D., Turner, B.L. and Cochrane, M. (Eds.), Land change Science: observing Monitoring and understanding

Trajectories of change on Earth's Surface (pp.257-276)., Kluwer Academic Publisher, Dordrecht, The Netherlands.

Mutie S.M; Mati B; Home P; Gadain H; and Gathenya J.2006: evaluating land use change effects on river flow Using usgs geospatial stream flow model in mara river Basin, kenya: Center for remote sensing of land surfaces, bonn, 28-30 september 2006.

Neitsch, S. L., J. G. Arnold, J. R. Kiniry, R. Srinivasan, and J. R.Williams. 2005b.: Soil and Water Assessment Tool Input/Output File Documentation, Version 2005. Temple, Tex.: USDA-ARS Grassland, Soil andWater Research Laboratory. Available at: www.brc.tamus.edu/swat/doc.html. Accessed 1 November 2006.

Najjar Y, Ali H. 1998a. On the use of BPNN in liquefaction potential assessment tasks: Artificial Intelligence and Mathematical Methods in Pavement and Geo-mechanical Systems. Attoh-Okine (ed); 55–63. Najjar Y, Ali H. 1998b. CPT-based liquefaction potential assessment: A Neuronet Approach: Geotechnical Special Publication No. 75, American Society of Civil Engineers: 542–553.
Najjar Y, Zhang X. 2000. Characterizing the 3D Stress-Strain Behavior of sandy Soils, A Neuro-Mechanistic Approach: Geotechnical Special Publication No. 96, American Society of Civil Engineers: USA; 43–57.

Ogden, F.L. (1998). CASC2D Reference Manual. Department of Civil and Environmental Engineering, U-37, University of Connecticut, 83 p.

Oke, M.O. , Martins, O. , Idowu, O.A. and Aiyelokun, O. (2015): Comparative analysis of groundwater recharge estimation value obtained using empirical methods in Ogun and Oshun river basins: Ife Journal of Science vol. 17, no. 1 (2015). https://www.researchgate.net/publication/277233312

Oldham, R.D., The Structure of the Himalayas and of the Gangetic Plain, Memoirs 0/the Geological Survey ofIndia, Vol. 43, pt. II, Delhi, 1939, p. 82.

Olorungemi, J.O. (1983). Monitoring urban land use in developed countries – An aerial photographic approach. Environmental Int., 9: 27-32.

Oluseyi O. Adeleke , Victor Makinde, Ayobami O. Eruola, Oluwaseun F. Dada , Akintayo O. Ojo and Taiwo J. Aluko (2015): Estimation of Groundwater Recharges Using Empirical Formulae in Odeda Local Government Area, Ogun State, Nigeria.:

Challenges 2015, 6, 271-281; doi:10.3390/challe6020271.
www.mdpi.com/journal/challenges.

Palamuleni Lobina, Gertrude Ndomba Preksedis, and Annegarn Harold John: Evaluating land cover change and its impact on hydrological regime in Upper Shire river catchment, Malawi: Springer- Verlag 2011.

Panahi Ali, Alijani Bohloul, Mohammadi Hosein 2010: The Effect of the Land Use/Cover Changes on the Floods of the Madarsu Basin of Northeastern Iran: J. Water Resourceand Protection, 2010, 2, 373-379 doi:10.4236/jwarp.2010.24043, Published Online April 2010.

Peters, N.E. & Meybeck, M. 2000; Water quality degradation effects on freshwater availability: Impacts of human activities. Water International, 25(2): 185-193.

Petchprayoon, Pakorn. Peter D. Blanken, Chaiwat Ekkawatpanit, and Khalid Hussein 2010; Hydrological impacts of land use/land cover change in a large river basin in central–northern Thailand: Internationa Journal of Climatology. Int. J. Climatol. 30: 1917–1930 (2010) Published online 30 March 2010 in Wiley Online Library (wileyonlinelibrary.com) DOI: 10.1002/joc.2131

Purandara B.K, Venkatesh B, and V.K.Chaube, 2010: Estimation of ground water recharge under various land covers in parts of Western ghat, Karnataka, India: RMZ-Materials and Geoenvironment, vol. 57, no.2,pp. 181-194.

Pucci Jr., A.A., Pope, D.A., 1995. Simulated effects of development on regional ground-water/surface-water interactions in the Northern Coastal Plain of New Jersey. Journal of Hydrology 167 (1–4), 241–262. (Amsterdam) [J. HYDROL. (AMST.)], vol. 167, no. 1-4, pp. 241-262, 1995.

Raghuwanshi, S. and Wallender, W.S. 2000; Forecasting Daily Evapotranspiration for a Grass Reference Crop.. Agricultural Engg. J., 9(1): 1-16.

Ramankutty Navin and Foley Jonathan 1999: Estimating historical changes in global land cover: croplands from 1700 to 1992: Global Bio-geochemical cycles, vol. 13, no 4, pages 997- 1027, December 1999.

Ramesh R, 2001: Effects of land-use change on groundwater quality In a coastal habitat of south India Impact of Human Activity on Groundwater Dynamics

(Proceedings of a symposium held during the Sixth IAHS Scientific Assembly at Maastricht, The Netherlands, July 2001). IAHS Publ. No. 269, 2001. 161

Ramireddygari, S.R., Sophocleous, M.A., Koelliker, J.K., Perkins, S.P., Govindaraju, R.S. 2000. Development and application of a comprehensive simulation model to evaluate impacts of watershed structures and irrigation water use on streamflow and groundwater: the case of Wet Walnut Creek Watershed, Kansas, USA: Journal of Hydrology 236 (3/4), 223–246.

Rao B. Bapuji, Sandeep V.M., Rao V.U.M., and Venkateswarulu B. Potential Evapotranspiration Estimation for Indian Conditions: Improving Accuracy through calibration Coefficients: Technical Bulletin No. 1/2012.

Richards, W.H. 2010; Estimating of groundwater recharge, University Cambridge Press, 245.

Riebsam, W.E., Mayer, W.B. and Turner, B.L.H. (1994). Monitoring temporal vegetation cover changes in Mediterranean and Arid ecosystems using a Judean Mountain and the Judean desert. J. Arid Environments, 33: 9-21.

Ross, M., Geurink, J., Said, A., Aly, A., Tara, P., 2005. Evapotranspiration conceptualization in the HSPFMODFLOW integrated models. Journal of the American Water Resources Association 41 (5), 1013–1025.

Safaa M. Soliman. 2013. Mitigation of Excessive Drawdowns via Rotational Groundwater Withdrawal (Case study: El Kharga Oases, Egypt): New York Science Journal 2013; 6(1) http://www.sciencepub.net/newyork.

Sahin, V. and Hall, M.J. 1996; The effect of afforestation and deforestation on water yields. J. Hydrology, 178: 293-309.

Salas, J.D. and Smith, R.A. 1986; Physical basis of stochastic models of annual flows. Water Resources Research, 17(2): 428-430.

Saucier, R. 2000; Computer generation of statistical distributions. Army Research Laboratory ARL-TR-2168.

Scanlon, R. B., Robert, R. C., David, A. S., David, E., Predict and Kevin Dennehy, F. 2005; Impact of land use and land cover change on groundwater recharge and quality in the southwestern US. Global Change Biology, 11:1577–1593.

Scanlon, Bridget, R., Kelley, K. E., Cheikh, G. B., Alan, L., Flint, W., Michael Edmunds Lorraine, E. Flint, and Ian Simmers (2006). Global synthesis of groundwater recharge in semiarid and arid regions Hydrological Processes Hydrol. Process. 20: 3335–3370.

Sharma U.C ; 2001; Effect of Farming systems type on insitu ground water recharge and quality in North East India : IAHS Publication No. 269, 2001.

Sikka AK, Samra JS, Sharda VN, Samraj P and Lakshmanam V. 2003: Low Flow andHigh Flow Responses to Converting Nautral Grassland into Bluegum (Eucalyptus globulus) in Nilgiris Watersheds of South India: Journal of Hydrology 270 12-26.

Sikazwe, K. 2008; The impact of land use change on Karst Groundwater quantity in Shentou Spring Basin, Shanxi Province, China. Environmental Research J., 2(5): 232-237.

Singh, A.K., Singh, J. and Gupta, A.P. 1991; Time series analysis of air temperature of Udaipur. Hydrol. J., 14: 16-23.

Singh R.D. 2013: Impacts of land cover land use change on water management in India: International Regional Science Meeting Land cover and land use changes dynamics and their impacts in South Asia 10-12 January 2013.

SMHI, Swedish Meteorological and Hydrological Institute 2003; SMHI Oceanography No. 73.

Snyder, F.F., 1938, Synthetic unit-graphs: Transactions, American Geophysical Union, vol. 19, p. 447-454.

Sophocleous, M., Perkins, S.P., 2000. Methodology and application of combined watershed and groundwater models in Kansas. Journal of Hydrology 236 (3/4), 185–201.

St-Hilaire, A., Morin, G., El-Jabi, N., Caissie, D. (2000). Water temperature modelling in a small forested stream: implication of forest canopy and soil temperature. Can. J. Civ. Eng., 27, 1095-1108.

Swingly Jeffry; Sumarauw Frans; and Ohgushi Koichiro 2002: Analysis on curve number,land use and land cover changes and the Impact to the peak flow in the Jobaru River Basin, Japan: International Journal of Civil & Environmental Engineering IJCEE-IJENS Vol: 12, No: 02

Syewoon hwang and wendy. graham, 2014: assessment of alternative methods for statistically downscaling daily gcm precipitation outputs to simulate regional streamflow: journal of the american water resources association (jawra) 1-23. doi: 10.1111/jawr.12154.

Tejwani, K.G.1993: Water management issues: Population, Agriculture and Forests – a focus on watershed management. In: Bonell M, Hufschmidt M.M, and Gladwell, J.S, Hydrology and water management in the humid tropics. Paris: UNESCO,pp 496-525.

Thanapakpawin P; Richey J; Thomas D; Rodda S; Campbell B; and Logsdon M 2006: Effects of landuse change on the hydrologic regime of the Mae Chaem river basin, NW Thailand: Journal of Hydrology 334, 215– 230.

Tian Hanqin, Banger Kamaljit, Bo Tao, and Dadhwal Vinay K; 2014: History of land use in India during 1880–2010: Large-scale land transformations reconstructed from satellite data and historical archives: Global and Planetary change, volume 121, October ,2014, page 78-88, www.elsevier.com/locate/gloplacha.

USGS-NPD 1991; SSARR Model Streamflow Synthesis and Reservoir Regulation, 426 p.

Vetterling, W.T., Teukolsky, S.A., Press, W.H. (1992): Numerical recipes example book (C).Press Syndicate of the University of Cambridge.

Victoria Ann Barone 2000, Modeling the Impacts of Land Use Activities on the Subsurface Flow Regime of the Upper Roanoke River Watershed: Virginia state university, January 2000.

Viessman, W.Jr, Lewis, G.L. and Knapp, J.W., 1989. Introduction to Hydrology:3rd edn., Harper and Row Publishers, Inc.pp 15-43.

Vijaindra, M. R. Sudha Ravindranath, and M. S. Nathawa 2009; GIS Application in Evaluating Land Use-Land Cover Change and its Impact on Hydrological Regime in Langat River Basin, Malaysia. Geospatial World – September 1, 2009.

Vose, D. 2000; Risk analysis: a quantitative guide. John Wiley and Sons Ltd, Chichester.

Wang, G., Yang, L., Chen, L. and Jumpei, K. 2005; Impacts of land use changes on ground water resources in the Heihe River Basin, Journal of Geographical Sciences 15, 4, 405-409.

WaterNet/Warfsa, Symposium: Water, Science, Technology & Policy Convergence and Action by All, 15-1, October 2003.

Weinmann PE, Rahman A, Hoang TMT, Laurenson EM, Nathan RJ. 2002; Monte Carlosimulation of flood frequency curves from rainfall - the way ahead. Australian Journal of Water Resources, IEAust, 6(1): 71-80.

Wetherhead E.K; and Howden N.J.K; 2009: The relationship between land use and surface water resources in the U.K.: Land use policy 26s 2009: s-243- s250. www.elsevier.com/locate/landusepol

Yates D.N. and Strzepek, K.M. 1994; Comparison of Models for Climate Change Assessment of River Basin Runof IIASA Working Paper, WP-94-45, Laxenburg, Austria.

Z. Yu 1998; Assessing the response of subgrid hydrologic processes to atmospheric forcing with a hydrologic model system: Global and Planetary Change 25 (2000) l-11. www.elsevier.com/locate/ gloplacha

Zamani Mojtaba , Sadoddin Amir, and Garizi Arash Zare 2013: Assessing Land Cover/LandUse Change and its Impacts on Surface Water Quality in the Ziarat Catchment: Hydrology current research 2013, 4:3

APPENDIX

Runoff in 1977:

Month	Day	Rainfall (mm)	Antecedent Rainfall(mm)	AMC	(S)	0.2 S	0.8 S	CN	Runoff (mm)
June	14	7.9	0	I	38.96	155.87	194.84	56.59	0
	15	22.4	7.9	I	38.96	155.87	194.84	56.59	0
	16	6.8	30.3	I	38.96	155.87	194.84	56.59	0
	27	13.6	0	I	38.96	155.87	194.84	56.59	0
	28	18.2	13.6	I	38.96	155.87	194.84	56.59	0
	30	5.9	31.8	I	38.96	155.87	194.84	56.59	0
July	1	24.6	37.7	II	16.37	65.472	81.84	75.63	0.751986
	2	14.7	62.3	III	7.12	28.472	35.59	87.71	1.330872
	3	28.4	63.4	III	7.12	28.472	35.59	87.71	7.962414
	7	32.3	43.1	II	16.37	65.472	81.84	75.63	2.595476
	8	12.4	60.7	III	7.12	28.472	35.59	87.71	0.68209
	10	18.5	44.7	II	16.37	65.472	81.84	75.63	0.054029
	13	13	30.9	I	38.96	155.87	194.84	56.59	0
	14	19.5	31.5	I	38.96	155.87	194.84	56.59	0
	17	27.2	32.5	I	38.96	155.87	194.84	56.59	0
	18	37.8	59.7	III	7.12	28.472	35.59	87.71	14.20302
	19	22.6	84.5	III	7.12	28.472	35.59	87.71	4.692011
	22	29.8	87.6	III	7.12	28.472	35.59	87.71	8.827265
	23	12.5	90.2	III	7.12	28.472	35.59	87.71	0.706443
	25	15.7	42.3	II	16.37	65.472	81.84	75.63	0
	27	12.9	68	III	7.12	28.472	35.59	87.71	0.807512
	29	14.7	28.6	I	38.96	155.87	194.84	56.59	0
	30	7.9	43.3	II	16.37	65.472	81.84	75.63	0
Aug.	7	10.8	0	I	38.96	155.87	194.84	56.59	0
	8	8.6	10.8	I	38.96	155.87	194.84	56.59	0
	10	17.9	19.4	I	38.96	155.87	194.84	56.59	0
	12	22.4	37.3	II	16.37	65.472	81.84	75.63	0.413794
	13	16.3	48.9	II	16.37	65.472	81.84	75.63	
	15	28.6	56.6	III	7.12	28.472	35.59	87.71	8.084357
	18	19	44.9	II	16.37	65.472	81.84	75.63	0.081884
	19	24	47.6	II	16.37	65.472	81.84	75.63	0.650672
	26	17.3	0	I	38.96	155.87	194.84	56.59	0
	27	12.9	17.3	I	38.96	155.87	194.84	56.59	0
	28	5.6	30.2	I	38.96	155.87	194.84	56.59	0
	31	8.5	35.8	II	16.37	65.472	81.84	75.63	0
Sep.	1	15.8	27	I	38.96	155.87	194.84	56.59	0
	2	12.4	24.3	I	38.96	155.87	194.84	56.59	0
	3	32.5	36.7	II	16.37	65.472	81.84	75.63	2.655625
	5	23.9	69.2	III	7.12	28.472	35.59	87.71	5.376316
	7	7.8	68.8	III	7.12	28.472	35.59	87.71	0.012748
	8	10.4	64.2	III	7.12	28.472	35.59	87.71	0.276765
	17	9.6	0	I	38.96	155.87	194.84	56.59	0
	19	13.7	9.6	I	38.96	155.87	194.84	56.59	0
	20	10.3	23.3	I	38.96	155.87	194.84	56.59	0
	28	26.4	0	I	38.96	155.87	194.84	56.59	0
Oct.	9	12.3	0	I	38.96	155.87	194.84	56.59	0
	10	6.2	12.3	I	38.96	155.87	194.84	56.59	0
	13	8.5	18.5	I	38.96	155.87	194.84	56.59	0
	20	4.4	0	I	38.96	155.87	194.84	56.59	0
									60.16528

Runoff in 1979:

Month	Day	Rainfall (mm)	Antecedent Rainfall(mm)	AMC	(S)	0.2 S	0.8 S	CN	Runoff (mm)
June	14	12.6	0	I	38.96	155.87	194.84	56.59	0
	15	20	12.6	I	38.96	155.87	194.84	56.59	0
	16	6.3	32.6	I	38.96	155.87	194.84	56.59	0
	29	6.2	0	I	38.96	155.87	194.84	56.59	0
	30	10.8	6.2	I	38.96	155.87	194.84	56.59	0
July	1	7.9	17	I	38.96	155.87	194.84	56.59	0
	2	19.3	24.9	I	38.96	155.87	194.84	56.59	0
	10	35.8	0	I	38.96	155.87	194.84	56.59	0
	11	27.4	35.8	II	16.37	65.472	81.84	75.63	1.309985
	14	18.4	63.2	III	7.12	28.472	35.59	87.71	2.714593
	15	16.9	81.6	III	7.12	28.472	35.59	87.71	2.108093
	16	12.5	98.5	III	7.12	28.472	35.59	87.71	0.706443
	18	17.9	111	III	7.12	28.472	35.59	87.71	2.506004
	19	16.2	128.9	III	7.12	28.472	35.59	87.71	1.845595
Aug.	4	21.5	0	I	38.96	155.87	194.84	56.59	0
	5	8.4	21.5	I	38.96	155.87	194.84	56.59	0
	6	7.3	29.9	I	38.96	155.87	194.84	56.59	0
	7	13.8	37.2	II	16.37	65.472	81.84	75.63	0
	13	5.6	0	I	38.96	155.87	194.84	56.59	0
	15	7.4	5.6	I	38.96	155.87	194.84	56.59	0
	16	8.3	13	I	38.96	155.87	194.84	56.59	0
	19	19.2	21.3	I	38.96	155.87	194.84	56.59	0
	20	16.8	40.5	II	16.37	65.472	81.84	75.63	0.002247
	21	15.2	57.3	III	7.12	28.472	35.59	87.71	1.494926
	28	7.5	0	I	38.96	155.87	194.84	56.59	0
	30	6.2	7.5	I	38.96	155.87	194.84	56.59	0
Total									**12.68789**

Runoff in 1990:

Month	Day	Rainfall (mm)	Antecedent Rainfall(mm)	AMC	(S)	0.2 S	0.8 S	CN	Runoff (mm)
June	12	5.5	0	I	36.84	147.39	184.23	57.96	0
	15	14.4	5.5	I	36.84	147.39	184.23	57.96	0
	16	15.2	19.9	I	36.84	147.39	184.23	57.96	0
	17	10.13	35.1	I	36.84	147.39	184.23	57.96	0
	18	5.8	39.73	II	15.47	61.9	77.37	76.65	1.381225
	19	7.4	45.53	II	15.47	61.9	77.37	76.65	0.939753
	22	15	23.33	I	36.84	147.39	184.23	57.96	0
	23	10.6	28.2	I	36.84	147.39	184.23	57.96	0
July	2	12.6	0	I	36.84	147.39	184.23	57.96	0
	3	16.9	12.6	I	36.84	147.39	184.23	57.96	0
	4	18.4	29.5	I	36.84	147.39	184.23	57.96	0
	7	32.4	47.9	II	15.47	61.9	77.37	76.65	3.039501
	8	27.8	67.7	III	6.73	26.92	33.65	88.3	8.113028
	9	14.8	78.6	III	6.73	26.92	33.65	88.3	1.561
	10	10.35	75	III	6.73	26.92	33.65	88.3	0.351607
	11	3.8	85.35	III	6.73	26.92	33.65	88.3	0.279456
	12	9.8	89.15	III	6.73	26.92	33.65	88.3	0.256669
	13	3.6	66.55	III	6.73	26.92	33.65	88.3	0.320999
	14	12.4	42.35	II	15.47	61.9	77.37	76.65	0.126849
	15	5.7	39.95	II	15.47	61.9	77.37	76.65	1.412025
	16	7.9	35.3	I	36.84	61.9	184.23	57.96	0
	17	3.3	39.4	II	15.47	61.9	77.37	76.65	2.271609
	20	14.7	16.9	I	36.84	61.9	184.23	57.96	0
	21	15.6	25.9	I	36.84	147.39	184.23	57.96	0
	22	6.7	33.6	I	36.84	147.39	184.23	57.96	0
	23	13.8	37	II	15.47	61.9	77.37	76.65	0.036841
	24	7.45	50.8	II	15.47	61.9	77.37	76.65	0.927475
	27	16.5	27.95	I	36.84	61.9	184.23	57.96	0
	28	31.9	37.5	II	15.47	61.9	77.37	76.65	2.877877
	29	24.9	55.85	III	6.73	26.92	33.65	88.3	6.371071
	30	40.6	73.3	III	6.73	26.92	33.65	88.3	16.99018
Aug.	4	1.2	65.5	III	6.73	26.92	33.65	88.3	1.087514
	8	2.4	1.2	I	36.84	26.92	184.23	57.96	0
	9	5.34	3.6	I	36.84	147.39	184.23	57.96	0
	13	6.1	7.74	I	36.84	147.39	184.23	57.96	0
	14	2.5	11.44	I	36.84	147.39	184.23	57.96	0
	15	16.8	8.6	I	36.84	147.39	184.23	57.96	0
	16	42.3	25.4	I	36.84	147.39	184.23	57.96	0
	17	31.9	67.7	III	6.73	26.92	33.65	88.3	10.77064
	18	38.7	99.6	III	6.73	26.92	33.65	88.3	15.57575
	19	58.4	132.2	III	6.73	26.92	33.65	88.3	31.29148
	22	22.4	129	III	6.73	26.92	33.65	88.3	4.978688
	23	14.7	119.5	III	6.73	26.92	33.65	88.3	1.526211
	24	6.6	95.5	III	6.73	26.92	33.65	88.3	0.000504
	26	12.2	59.1	III	6.73	26.92	33.65	88.3	0.764849
	27	13.1	71.3	III	6.73	26.92	33.65	88.3	1.013916
	30	5	40.7	II	15.47	61.9	77.37	76.65	1.638578
Sep.	3	13.7	5	I	36.84	61.9	184.23	57.96	0
	9	4.5	0	I	36.84	147.39	184.23	57.96	0
	10	17.2	4.5	I	36.84	147.39	184.23	57.96	0
	11	25.1	21.7	I	36.84	147.39	184.23	57.96	0
	12	6.4	46.8	II	15.47	61.9	77.37	76.65	1.204464
	14	2.3	53.2	II	15.47	61.9	77.37	76.65	2.701696
	16	4.8	33.8	I	36.84	61.9	184.23	57.96	0
	17	18.2	13.5	I	36.84	147.39	184.23	57.96	0
	18	15.9	25.3	I	36.84	147.39	184.23	57.96	0
	19	19.5	41.2	II	15.47	61.9	77.37	76.65	0.19952
	22	14.4	53.6	III	6.73	26.92	33.65	88.3	1.423739
	23	20.5	49.8	II	15.47	61.9	77.37	76.65	0.30705
	24	16	54.4	III	6.73	26.92	33.65	88.3	2.002164
Total									**123.7439**

Runoff in 2009:

Month	Day	Rainfall (mm)	Antecedent Rainfall(mm)	AMC	(S)	0.2 S	0.8 S	CN	Runoff (mm)
June		(mm)	Rainfall(mm)						(mm)
	5	0.87	0	I	33.33	133.34	166.67	60.38	**0**
	6	6.68	0.87	I	33.33	133.34	166.67	60.38	**0**
	7	7.85	7.55	I	33.33	133.34	166.67	60.38	**0**
	27	3.9	12.4	I	33.33	133.34	166.67	60.38	**0**
	29	11.2	19.3	I	33.33	133.34	166.67	60.38	**0**
	30	13.6	29.63	I	33.33	133.34	166.67	60.38	**0**
	1	0.33	36.55	II	14	55.98	69.98	78.4	**0**
July	9	6.7	29.03	I	33.33	133.34	166.67	60.38	**0**
	10	4	35.73	II	14	55.98	69.98	78.4	**0**
	12	11.37	35.83	II	14	55.98	69.98	78.4	**0**
	13	20.24	36	II	14	55.98	69.98	78.4	0.510858
	14	11.8	42.6	II	14	55.98	69.98	78.4	**0**
	15	8.32	54.11	III	6.08	24.35	30.43	89.3	0.153584
	16	11.1	55.73	III	6.08	24.35	30.43	89.3	0.710872
	17	1.35	62.83	III	6.08	24.35	30.43	89.3	**0**
	18	15.34	52.81	II	14	55.98	69.98	78.4	0.025177
	19	8.23	47.91	II	14	55.98	69.98	78.4	**0**
	20	19.94	44.34	II	14	55.98	69.98	78.4	0.464747
	22	6.57	55.96	III	6.08	24.35	30.43	89.3	0.007765
	23	2.07	51.43	III	6.08	24.35	30.43	89.3	**0**
	24	1.33	52.15	III	6.08	24.35	30.43	89.3	**0**
	25	2.67	38.14	II	14	55.98	69.98	78.4	**0**
	26	2.55	32.58	I	33.33	133.34	166.67	60.38	**0**
	28	15.4	15.19	I	33.33	133.34	166.67	60.38	**0**
	29	6.31	24.02	I	33.33	133.34	166.67	60.38	**0**
	30	10	28.26	I	33.33	133.34	166.67	60.38	**0**
	31	8.86	36.93	II	14	55.98	69.98	78.4	**0**
	1	4.43	43.12	II	14	55.98	69.98	78.4	**0**
	7	4.87	45	II	14	55.98	69.98	78.4	**0**
Aug.	8	9.98	34.47	I	33.33	133.34	166.67	60.38	**0**
	9	1.38	38.14	II	14	55.98	69.98	78.4	**0**
	11	4.98	29.52	I	33.33	133.34	166.67	60.38	**0**
	13	7.45	25.64	I	33.33	133.34	166.67	60.38	**0**
	14	5.37	28.66	I	33.33	133.34	166.67	60.38	**0**
	15	55.42	29.16	I	33.33	133.34	166.67	60.38	2.585124
	16	35.1	74.6	III	6.08	24.35	30.43	89.3	14.16586
	17	75.98	108.31	III	6.08	24.35	30.43	89.3	48.69939
	18	112.33	179.32	III	6.08	24.35	30.43	89.3	82.59484
	19	34.63	284.2	III	6.08	24.35	30.43	89.3	13.81998
	20	5.33	313.46	III	6.08	24.35	30.43	89.3	**0**
	22	5.08	263.37	III	6.08	24.35	30.43	89.3	**0**
	22	5.08	233.35	III	6.08	24.35	30.43	89.3	**0**
	25	5.42	162.45	III	6.08	24.35	30.43	89.3	**0**
	26	3.98	55.54	III	6.08	24.35	30.43	89.3	**0**
	28	1.17	24.89	I	33.33	119.13	152.46	60.38	**0**
	30	6.46	20.73	I	33.33	119.13	152.46	60.38	**0**
	31	5.53	22.11	I	33.33	119.13	152.46	60.38	**0**
	2	1.18	22.56	I	33.33	119.13	152.46	60.38	**0**
	3	1.8	18.32	I	33.33	119.13	152.46	60.38	**0**
Sep.	4	28.47	16.14	I	33.33	119.13	152.46	60.38	**0**
	5	3.65	43.44	II	14	55.98	69.98	78.4	**0**
	6	9.78	40.63	II	14	55.98	69.98	78.4	**0**
	7	8.43	44.88	II	14	55.98	69.98	78.4	**0**
	8	5.1	52.13	II	14	55.98	69.98	78.4	**0**
	9	24.71	55.43	III	6.08	24.35	30.43	89.3	7.074539
	10	9.38	51.67	II	14	55.98	69.98	78.4	**0**
	11	2.45	57.4	III	6.08	24.35	30.43	89.3	**0**
	12	62.82	50.07	II	14	55.98	69.98	78.4	20.06223
	13	2.03	104.46	III	6.08	24.35	30.43	89.3	**0**
	4	8.98	101.39	III	6.08	24.35	30.43	89.3	0.252325
	5	13.72	85.66	III	6.08	24.35	30.43	89.3	1.533218
Oct.	6	43.63	90	III	6.08	24.35	30.43	89.3	20.74143
	7	26.97	131.18	III	6.08	24.35	30.43	89.3	8.503353
Total									**221.9053**

Groundwater Recharge:

Year	Annual Rainfall (mm)	Monsoon Rainfall (mm)	Monsoon Rainfall (inch)	Recharge from Monsoon Rainfall (inch)		Recharge from Monsoon Rainfall (mm)		Average Recharge (mm)	% Recharge
				MCF	KSF	MCF	KSF		
1977	882.462	832.593	32.77	5.8502	5.5467	148.5958	140.8864	144.741	16.4019
1978	872.572	792.616	31.20	5.5997	5.1633	142.2326	131.1480	136.690	15.6652
1979	489.27	403.984	15.90	1.8632	0.4407	47.3261	11.1938	29.2600	7.24
1980	1297.34	1238.89	48.77	7.9610	9.0850	202.2102	230.761	216.485	16.6868
1981	963.295	886.268	34.89	6.1706	6.0487	156.7335	153.6378	155.185	16.1098
1982	891.935	781.728	30.77	5.5295	5.0573	140.4496	128.4564	134.453	15.0743
1983	973.447	886.514	34.90	6.1720	6.0510	156.7699	153.6955	155.232	15.9467
1984	666.071	588.485	23.16	4.0877	3.0273	103.8296	76.8950	90.3623	13.5664
1985	1064.42	1020.55	40.17	6.9073	7.2517	175.4466	184.1934	179.820	16.8936
1986	851.64	768.516	30.25	5.4431	4.9278	138.2552	125.1661	131.710	15.4655
1987	433.726	388.265	15.28	1.5309	0.0129	38.8857	0.3287	19.607	4.52066
1988	972.532	914.453	36.00	6.3324	6.3071	160.8435	160.2004	160.521	16.5054
1989	788.752	735.915	28.97	5.2238	4.6037	132.6605	116.9267	124.806	15.8232
1990	1023.57	950.528	37.42	6.5335	6.6326	165.9513	168.4784	167.215	16.3364
1991	455.456	389.581	15.33	1.5619	0.0722	39.6614	1.8341	20.7478	4.55539
1992	669.93	595.169	23.43	4.1460	3.1038	105.3096	78.8367	92.0729	13.7436
1993	964.373	921.165	36.26	6.3702	6.3682	161.8049	161.7506	161.777	16.7754
1994	873.416	815.834	32.11	5.7465	5.3870	145.9624	136.8306	141.396	16.1888
1995	909.153	817.014	32.16	5.7538	5.3986	146.1490	137.1174	141.633	15.5785
1996	1033.79	983.67	38.72	6.7130	6.928	170.511	175.971	173.241	16.757
1997	668.425	621.164	24.45	4.3651	3.395	110.875	86.251	98.563	14.745
1998	894.622	826.099	32.52	5.810	5.485	147.58	139.319	143.450	16.034
1999	766.499	738.555	29.07	5.241	4.6299	133.144	117.6	125.372	16.356
2000	637.4	598.489	23.56	4.174	3.141	106.036	79.795	92.915	14.577
2001	553.13	515.555	20.29	3.387	2.146	86.049	54.518	70.283	12.706
2002	624.639	556.803	21.92	3.799	2.656	96.509	67.466	81.987	13.125
2003	780.61	760.61	29.94	5.390	4.849	136.925	123.184	130.054	16.66
2004	767.4	726.4	28.59	5.158	4.507	131.014	114.487	122.751	15.995
2005	895	780	30.7	5.518	5.04	140.164	128.027	134.096	14.982
2006	696.3	666.8	26.25	4.725	3.89	120.024	98.807	109.416	15.713
2007	1040.1	943.2	37.13	6.493	6.567	164.92	166.807	165.867	15.947
2008	1356.2	1345.7	52.9	8.428	9.939	214.086	252.462	233.274	17.20
2009	894.2	865.2	34.06	6.046	5.853	153.59	148.674	151.132	16.901
2010	1430.2	1395.8	54.95	8.639	10.332	219.436	262.439	240.937	16.846
2011	1196.1	1147.3	45.16	7.536	8.331	191.439	211.624	201.531	16.849
2012	617.5	577	22.71	3.985	2.894	101.237	73.521	87.379	14.150
2013	1288.5	1188.9	46.80	7.732	8.676	196.404	220.380	208.392	16.173

Year	Total Rainfall (mm)	Total Runoff (mm)	Runoff (mm)			
			Settlements	C.L.	Forest/Plantation	W.L.
1979	489.27	12.68789	0.520203	7.688859	3.590672	0.634394
1990	894.2	123.744	5.073504	74.98886	35.01955	6.1872
2009	1023.573	234.707	9.622987	142.2324	66.42208	11.73535

Year	Total Rainfall(mm)	Runoff Volume (ha-m)			
		Settlements	C.L.	Forest/Plantation	W.L.
1979	489.27	8.787274	249672	116596	20600
1990	894.2	106.6045	314768	46144	13596
2009	1023.573	673.994	344432	24720	8240

Rainfall Data Statistics (1977-2013)

(1977-2013)	MEAN	STDEV	SKEW	KURT	VAR
January	12.96143	10.29251	0.531467	-0.88304	105.9358
February	16.31797	15.71682	1.196349	0.868557	247.0184
March	12.42049	12.48124	1.054671	0.184387	155.7813
April	9.018135	9.045636	1.608843	2.534586	81.82353
May	22.05154	15.09661	0.459508	-0.54376	227.9075
June	106.4869	77.77322	1.457188	3.040692	6048.674
July	251.3847	121.8522	0.179806	-0.74361	14847.97
August	257.2835	92.85591	0.539541	-0.61185	8622.221
September	150.541	89.98531	1.109767	1.419239	8097.356
October	22.12573	27.1968	1.592024	2.453131	739.6662
November	3.614622	5.713451	1.663099	1.657954	32.64352
December	5.631676	7.338619	1.771059	2.701842	53.85532

Rainfall ARIMA model statistics for Rainfall Data (1977-2013) analysed

Month→	Jan				Feb			
Year↓	Prid	LL	HL	Resid	Prid	LL	HL	Resid
1977	18.77377	12.34896	25.19858	2.698329	23.18203	14.17459	32.18946	-3.33624
1978	18.72631	12.3015	25.15112	-3.30579	23.20821	14.20077	32.21565	1.776183
1979	18.67885	12.25404	25.10367	-0.16111	23.2344	14.22696	32.24184	7.581511
1980	18.6314	12.20658	25.05621	-4.00778	23.26059	14.25315	32.26802	-1.71796
1981	18.58394	12.15913	25.00875	1.890096	23.28677	14.27933	32.29421	-3.20426
1982	18.53648	12.11167	24.96129	3.857927	23.31296	14.30552	32.3204	-1.63123
1983	18.48902	12.06421	24.91384	4.362664	23.33914	14.33171	32.34658	-2.93792
1984	18.44157	12.01675	24.86638	-2.0628	23.36533	14.35789	32.37277	7.166348
1985	18.39411	11.9693	24.81892	-2.77016	23.39152	14.38408	32.39896	-4.56499
1986	18.34665	11.92184	24.77146	-2.0786	23.4177	14.41027	32.42514	3.851897
1987	18.29919	11.87438	24.724	1.217274	23.44389	14.43645	32.45133	0.371261
1988	18.25173	11.82692	24.67655	-2.72836	23.47008	14.46264	32.47751	-0.6902
1989	18.20428	11.77947	24.62909	3.898103	23.49626	14.48883	32.5037	-3.65616
1990	18.15682	11.73201	24.58163	-4.10374	23.52245	14.51501	32.52989	6.283787
1991	18.10936	11.68455	24.53417	-3.29423	23.54864	14.5412	32.55607	1.831455
1992	18.0619	11.63709	24.48672	3.29848	23.57482	14.56738	32.58226	1.519031
1993	18.01445	11.58963	24.43926	0.646711	23.60101	14.59357	32.60845	-4.0962
1994	17.96699	11.54218	24.3918	1.564851	23.6272	14.61976	32.63463	-1.23789
1995	17.91953	11.49472	24.34434	4.802958	23.65338	14.64594	32.66082	0.781054
1996	17.87207	11.44726	24.29688	4.174357	23.67957	14.67213	32.68701	0.677122
1997	17.82462	11.3998	24.24943	-1.15787	23.70575	14.69832	32.71319	-4.46205
1998	17.77716	11.35235	24.20197	-2.94016	23.73194	14.7245	32.73938	-0.76355
1999	17.7297	11.30489	24.15451	-0.19044	23.75813	14.75069	32.76557	-1.24603

2000	17.68224	11.25743	24.10705	-0.50065	23.78431	14.77688	32.79175	2.225794
2001	17.63478	11.20997	24.0596	-1.87617	23.8105	14.80306	32.81794	-2.85785
2002	17.58733	11.16251	24.01214	2.931173	23.83669	14.82925	32.84412	3.60648
2003	17.53987	11.11506	23.96468	3.171477	23.86287	14.85544	32.87031	-5.19402
2004	17.49241	11.0676	23.91722	-0.51173	23.88906	14.88162	32.8965	-5.22021
2005	17.44495	11.02014	23.86977	-0.95329	23.91525	14.90781	32.92268	8.004796
2006	17.3975	10.97268	23.82231	-3.36606	23.94143	14.93399	32.94887	-5.27258
2007	17.35004	10.92523	23.77485	-3.30043	23.96762	14.96018	32.97506	7.979446
2008	17.30258	10.87777	23.72739	-3.27114	23.99381	14.98637	33.00124	-5.05966
2009	17.25512	10.83031	23.67993	-3.22368	24.01999	15.01255	33.02743	-5.11073
2010	17.20766	10.78285	23.63248	-2.243	24.04618	15.03874	33.05362	1.116289
2011	17.16021	10.7354	23.58502	-2.25016	24.07236	15.06493	33.0798	5.158363
2012	17.11275	10.68794	23.53756	5.795356	24.09855	15.09111	33.10599	-5.4297
2013	17.06529	10.64048	23.4901	5.987614	24.12474	15.1173	33.13218	7.758635
Month→	March				April			
Year↓	Prid	LL	HL	Resid	Prid	LL	HL	Resid
1977	20.07597	12.98762	27.16431	-5.50554	13.6255	8.737534	18.51346	2.19642
1978	19.975	12.88665	27.06335	4.819224	13.60121	8.713251	18.48918	-2.09119
1979	19.87403	12.78569	26.96238	-2.26906	13.57693	8.688968	18.46489	-1.67116
1980	19.77307	12.68472	26.86142	2.885081	13.55265	8.664685	18.44061	-2.5528
1981	19.6721	12.58376	26.76045	4.487514	13.52836	8.640402	18.41633	-2.90164
1982	19.57114	12.48279	26.65948	5.194559	13.50408	8.61612	18.39204	0.743944
1983	19.47017	12.38182	26.55852	-3.08391	13.4798	8.591837	18.36776	4.578316
1984	19.3692	12.28086	26.45755	-4.40149	13.45552	8.567554	18.34348	4.41877
1985	19.26824	12.17989	26.35659	-4.1245	13.43123	8.543271	18.3192	1.188187
1986	19.16727	12.07893	26.25562	-2.10021	13.40695	8.518988	18.29491	-0.14185
1987	19.06631	11.97796	26.15465	-2.89147	13.38267	8.494706	18.27063	-2.36713
1988	18.96534	11.87699	26.05369	0.73825	13.35838	8.470423	18.24635	2.454982
1989	18.86437	11.77603	25.95272	0.860275	13.3341	8.44614	18.22206	-2.70373
1990	18.76341	11.67506	25.85176	-0.76437	13.30982	8.421857	18.19778	-1.32465
1991	18.66244	11.5741	25.75079	-0.97074	13.28554	8.397574	18.1735	0.584035
1992	18.56148	11.47313	25.64982	0.096242	13.26125	8.373291	18.14922	-0.88653
1993	18.46051	11.37216	25.54886	2.698005	13.23697	8.349009	18.12493	-0.63355
1994	18.35954	11.2712	25.44789	3.135393	13.21269	8.324726	18.10065	0.323025
1995	18.25858	11.17023	25.34693	3.969726	13.18841	8.300443	18.07637	1.316931
1996	18.15761	11.06927	25.24596	-2.54843	13.16412	8.27616	18.05208	-1.54442
1997	18.05665	10.9683	25.14499	-1.04622	13.13984	8.251877	18.0278	-1.99993
1998	17.95568	10.86733	25.04403	6.354759	13.11556	8.227595	18.00352	2.91644
1999	17.85471	10.76637	24.94306	-3.43928	13.09127	8.203312	17.97924	-2.63134
2000	17.75375	10.6654	24.8421	-2.03398	13.06699	8.179029	17.95495	-1.83954
2001	17.65278	10.56444	24.74113	-2.06606	13.04271	8.154746	17.93067	3.422539
2002	17.55182	10.46347	24.64016	2.031302	13.01843	8.130463	17.90639	-1.35112
2003	17.45085	10.3625	24.5392	-3.03542	12.99414	8.10618	17.8821	-2.53421
2004	17.34988	10.26154	24.43823	-2.93445	12.96986	8.081898	17.85782	5.023532
2005	17.24892	10.16057	24.33727	5.420487	12.94558	8.057615	17.83354	4.715474
2006	17.14795	10.05961	24.2363	4.159019	12.92129	8.033332	17.80926	-0.10082
2007	17.04699	9.95864	24.13533	7.64333	12.89701	8.009049	17.78497	-2.18102
2008	16.94602	9.857674	24.03437	-2.53059	12.87273	7.984766	17.76069	0.820521

2009	16.84505	9.756708	23.9334	-2.20294	12.84845	7.960484	17.73641	-0.33758
2010	16.74409	9.655742	23.83244	-2.10198	12.82416	7.936201	17.71212	-2.05378
2011	16.64312	9.554776	23.73147	-1.35158	12.79988	7.911918	17.68784	1.486448
2012	16.54216	9.45381	23.6305	-2.12672	12.7756	7.887635	17.66356	-0.14942
2013	16.44119	9.352844	23.52954	-0.96424	12.75131	7.863352	17.63928	-2.19216
Month→	May				June			
Year↓	Prid	LL	HL	Resid	Prid	LL	HL	Resid
1977	29.51142	20.11495	38.90789	2.073473	140.3993	97.29839	183.5002	-7.31111
1978	29.50547	20.109	38.90193	-6.08443	140.5543	97.45337	183.6552	16.35271
1979	29.49951	20.10305	38.89598	0.978639	140.7093	97.60835	183.8102	-14.1599
1980	29.49356	20.0971	38.89003	-5.82057	140.8642	97.76334	183.9651	19.53234
1981	29.48761	20.09114	38.88408	3.684363	141.0192	97.91832	184.1201	31.03463
1982	29.48166	20.08519	38.87813	2.850151	141.1742	98.0733	184.2751	-20.3782
1983	29.47571	20.07924	38.87218	6.416063	141.3292	98.22829	184.4301	11.27667
1984	29.46976	20.07329	38.86623	-6.1261	141.4842	98.38327	184.5851	14.34686
1985	29.46381	20.06734	38.86027	-3.18677	141.6392	98.53825	184.7401	-4.1504
1986	29.45786	20.06139	38.85432	6.417139	141.7941	98.69323	184.895	-6.76588
1987	29.4519	20.05544	38.84837	6.236574	141.9491	98.84822	185.05	-27.1269
1988	29.44595	20.04948	38.84242	-4.16161	142.1041	99.0032	185.205	3.395938
1989	29.44	20.04353	38.83647	-4.76313	142.2591	99.15818	185.36	-4.957
1990	29.43405	20.03758	38.83052	2.649471	142.4141	99.31317	185.515	-5.87544
1991	29.4281	20.03163	38.82457	5.282755	142.5691	99.46815	185.67	-26.099
1992	29.42215	20.02568	38.81862	-1.7265	142.724	99.62313	185.8249	-16.4934
1993	29.4162	20.01973	38.81266	0.202182	142.879	99.77812	185.9799	22.08715
1994	29.41024	20.01378	38.80671	-3.07818	143.034	99.9331	186.1349	-9.70118
1995	29.40429	20.00783	38.80076	-6.02141	143.189	100.0881	186.2899	-19.1679
1996	29.39834	20.00187	38.79481	-0.74743	143.344	100.2431	186.4449	23.99943
1997	29.39239	19.99592	38.78886	1.377065	143.499	100.398	186.5999	19.61161
1998	29.38644	19.98997	38.78291	-0.94489	143.6539	100.553	186.7548	-13.7068
1999	29.38049	19.98402	38.77696	-3.27174	143.8089	100.708	186.9098	15.00972
2000	29.37454	19.97807	38.771	-1.0923	143.9639	100.863	187.0648	-16.076
2001	29.36859	19.97212	38.76505	5.171883	144.1189	101.018	187.2198	-1.32866
2002	29.36263	19.96617	38.7591	-5.15079	144.2739	101.173	187.3748	-23.5731
2003	29.35668	19.96021	38.75315	5.550633	144.4288	101.3279	187.5298	32.83793
2004	29.35073	19.95426	38.7472	2.926305	144.5838	101.4829	187.6847	22.07582
2005	29.34478	19.94831	38.74125	-2.88001	144.7388	101.6379	187.8397	-17.4926
2006	29.33883	19.94236	38.7353	7.537222	144.8938	101.7929	187.9947	-21.863
2007	29.33288	19.93641	38.72935	7.65127	145.0488	101.9479	188.1497	18.49358
2008	29.32693	19.93046	38.72339	-4.0113	145.2038	102.1029	188.3047	38.60708
2009	29.32097	19.92451	38.71744	-4.45458	145.3587	102.2578	188.4596	-22.4439
2010	29.31502	19.91856	38.71149	1.687522	145.5137	102.4128	188.6146	-30.8411
2011	29.30907	19.9126	38.70554	5.528064	145.6687	102.5678	188.7696	13.07084
2012	29.30312	19.90665	38.69959	-6.13616	145.8237	102.7228	188.9246	-30.4762
2013	29.29717	19.9007	38.69364	-4.5629	145.9787	102.8778	189.0796	38.25551
Month→	July				August			
Year↓	Prid	LL	HL	Resid	Prid	LL	HL	Resid

1977	305.3929	229.2335	381.5524	40.74659	297.8809	240.9701	354.7916	-18.2473
1978	305.7274	229.568	381.8869	-20.9741	298.1054	241.1946	355.0161	13.98862
1979	306.0619	229.9024	382.2214	-23.2341	298.3299	241.4191	355.2406	-31.9385
1980	306.3964	230.2369	382.5558	60.12999	298.5543	241.6436	355.4651	46.78571
1981	306.7309	230.5714	382.8903	55.20375	298.7788	241.8681	355.6896	-24.629
1982	307.0654	230.9059	383.2248	-25.4183	299.0033	242.0926	355.9141	49.20635
1983	307.3998	231.2404	383.5593	-27.0806	299.2278	242.3171	356.1386	-2.27698
1984	307.7343	231.5749	383.8938	-26.9619	299.4523	242.5416	356.3631	-15.9736
1985	308.0688	231.9094	384.2283	36.44293	299.6768	242.7661	356.5876	21.57907
1986	308.4033	232.2438	384.5628	21.97187	299.9013	242.9905	356.8121	-23.497
1987	308.7378	232.5783	384.8972	-47.3161	300.1258	243.215	357.0365	-20.9914
1988	309.0723	232.9128	385.2317	42.69238	300.3503	243.4395	357.261	34.30556
1989	309.4067	233.2473	385.5662	-1.93652	300.5748	243.664	357.4855	0.557407
1990	309.7412	233.5818	385.9007	38.55264	300.7993	243.8885	357.71	17.57025
1991	310.0757	233.9163	386.2352	-55.867	301.0238	244.113	357.9345	-4.44013
1992	310.4102	234.2507	386.5697	-40.0923	301.2482	244.3375	358.159	-2.91525
1993	310.7447	234.5852	386.9041	26.79316	301.4727	244.562	358.3835	-34.0507
1994	311.0792	234.9197	387.2386	47.45182	301.6972	244.7865	358.608	8.379408
1995	311.4137	235.2542	387.5731	-19.9702	301.9217	245.011	358.8325	36.6162
1996	311.7481	235.5887	387.9076	-17.2165	302.1462	245.2355	359.057	13.20557
1997	312.0826	235.9232	388.2421	-53.854	302.3707	245.46	359.2815	-12.1243
1998	312.4171	236.2577	388.5766	1.691453	302.5952	245.6844	359.506	38.16877
1999	312.7516	236.5921	388.9111	-31.9923	302.8197	245.9089	359.7304	-31.1793
2000	313.0861	236.9266	389.2455	-22.7003	303.0442	246.1334	359.9549	-12.1736
2001	313.4206	237.2611	389.58	-36.3758	303.2687	246.3579	360.1794	-33.9491
2002	313.7551	237.5956	389.9145	-52.5984	303.4932	246.5824	360.4039	-26.0386
2003	314.0895	237.9301	390.249	-21.6829	303.7177	246.8069	360.6284	-11.4978
2004	314.424	238.2646	390.5835	-16.1867	303.9421	247.0314	360.8529	-25.3252
2005	314.7585	238.599	390.918	-0.48729	304.1666	247.2559	361.0774	-43.3564
2006	315.093	238.9335	391.2524	16.73461	304.3911	247.4804	361.3019	-33.0962
2007	315.4275	239.268	391.5869	34.69597	304.6156	247.7049	361.5264	-15.9016
2008	315.762	239.6025	391.9214	49.79497	304.8401	247.9294	361.7509	35.20238
2009	316.0964	239.937	392.2559	-32.539	305.0646	248.1539	361.9754	37.21301
2010	316.4309	240.2715	392.5904	54.56351	305.2891	248.3783	362.1998	41.77928
2011	316.7654	240.606	392.9249	36.27077	305.5136	248.6028	362.4243	41.86547
2012	317.0999	240.9404	393.2594	-36.1964	305.7381	248.8273	362.6488	-5.52552
2013	317.4344	241.2749	393.5938	46.94413	305.9626	249.0518	362.8733	-7.29542
Month→	September				October			
Year↓	Prid	LL	HL	Resid	Prid	LL	HL	Resid
1977	188.0057	136.3057	239.7057	12.41378	34.33067	19.16705	49.49429	5.021758
1978	188.2961	136.5961	239.9961	22.48696	34.35107	19.18745	49.51469	-4.00281
1979	188.5866	136.8865	240.2866	-32.2721	34.37147	19.20785	49.53508	-6.43204
1980	188.877	137.177	240.577	26.60231	34.39187	19.22825	49.55548	5.118612
1981	189.1674	137.4674	240.8674	-17.9433	34.41226	19.24865	49.57588	-6.55635
1982	189.4578	137.7578	241.1578	-16.0864	34.43266	19.26905	49.59628	-3.34086
1983	189.7483	138.0482	241.4483	43.73264	34.45306	19.28944	49.61668	6.648873

1984	190.0387	138.3387	241.7387	-20.1059	34.47346	19.30984	49.63708	-5.26221
1985	190.3291	138.6291	242.0291	12.97063	34.49386	19.33024	49.65748	14.80826
1986	190.6195	138.9195	242.3195	-2.19575	34.51426	19.35064	49.67788	5.868445
1987	190.9099	139.2099	242.61	-29.0629	34.53466	19.37104	49.69827	-0.85668
1988	191.2004	139.5004	242.9004	-20.1803	34.55506	19.39144	49.71867	-6.04871
1989	191.4908	139.7908	243.1908	1.873555	34.57545	19.41184	49.73907	-4.63214
1990	191.7812	140.0812	243.4812	14.74935	34.59585	19.43224	49.75947	-2.6219
1991	192.0716	140.3716	243.7717	-20.1991	34.61625	19.45263	49.77987	-6.76034
1992	192.3621	140.662	244.0621	-12.9742	34.63665	19.47303	49.80027	8.598765
1993	192.6525	140.9525	244.3525	40.66702	34.65705	19.49343	49.82067	-6.29227
1994	192.9429	141.2429	244.6429	-28.559	34.67745	19.51383	49.84106	-6.68956
1995	193.2333	141.5333	244.9333	23.02666	34.69785	19.53423	49.86146	-6.84193
1996	193.5238	141.8237	245.2238	38.16812	34.71824	19.55463	49.88186	6.749695
1997	193.8142	142.1142	245.5142	-10.4435	34.73864	19.57503	49.90226	8.372568
1998	194.1046	142.4046	245.8046	-27.8879	34.75904	19.59542	49.92266	8.563329
1999	194.395	142.695	246.095	21.42216	34.77944	19.61582	49.94306	10.72285
2000	194.6854	142.9854	246.3855	-18.0879	34.79984	19.63622	49.96346	-6.94393
2001	194.9759	143.2759	246.6759	-31.1373	34.82024	19.65662	49.98385	-1.14814
2002	195.2663	143.5663	246.9663	28.56856	34.84064	19.67702	50.00425	-0.49738
2003	195.5567	143.8567	247.2567	-24.336	34.86103	19.69742	50.02465	-7.07963
2004	195.8471	144.1471	247.5472	-33.1975	34.88143	19.71782	50.04505	13.85821
2005	196.1376	144.4376	247.8376	43.47339	34.90183	19.73822	50.06545	-7.12042
2006	196.428	144.728	248.128	-27.0404	34.92223	19.75861	50.08585	3.010241
2007	196.7184	145.0184	248.4184	0.354307	34.94263	19.77901	50.10625	-7.16122
2008	197.0088	145.3088	248.7088	20.97819	34.96303	19.79941	50.12665	-3.22426
2009	197.2993	145.5992	248.9993	1.921713	34.98343	19.81981	50.14704	14.21848
2010	197.5897	145.8897	249.2897	42.83708	35.00383	19.84021	50.16744	-6.78304
2011	197.8801	146.1801	249.5801	4.065597	35.02422	19.86061	50.18784	-7.24281
2012	198.1705	146.4705	249.8705	-3.45103	35.04462	19.88101	50.20824	-7.00187
2013	198.4609	146.7609	250.161	-25.1516	35.06502	19.9014	50.22864	8.980406

Month→	November				December			
Year↓	Prid	LL	HL	Resid	Prid	LL	HL	Resid
1977	6.70321	3.644248	9.762171	-1.5832	10.55302	7.147222	13.95882	-0.71205
1978	6.674806	3.615844	9.733768	-0.80763	10.46482	7.059015	13.87062	-0.19888
1979	6.646402	3.587441	9.705364	2.394612	10.37661	6.970808	13.78241	-1.28277
1980	6.617999	3.559037	9.67696	-1.10822	10.2884	6.882602	13.6942	2.442562
1981	6.589595	3.530633	9.648557	2.717217	10.2002	6.794395	13.606	-2.5932
1982	6.561191	3.50223	9.620153	2.181423	10.11199	6.706189	13.51779	0.972918
1983	6.532788	3.473826	9.591749	-1.41278	10.02378	6.617982	13.42958	-1.00151
1984	6.504384	3.445422	9.563346	-1.38438	9.935576	6.529775	13.34138	-1.76678
1985	6.47598	3.417019	9.534942	-1.35597	9.84737	6.441569	13.25317	3.042379
1986	6.447577	3.388615	9.506538	0.20485	9.759163	6.353362	13.16496	3.207454
1987	6.419173	3.360211	9.478135	-1.29917	9.670956	6.265155	13.07676	-0.41372
1988	6.390769	3.331808	9.449731	-1.16579	9.58275	6.176949	12.98855	0.938204

1989	6.362366	3.303404	9.421327	0.418947	9.494543	6.088742	12.90034	-1.30396
1990	6.333962	3.275	9.392924	0.699798	9.406337	6.000536	12.81214	3.310366
1991	6.305558	3.246597	9.36452	0.515624	9.31813	5.912329	12.72393	3.374189
1992	6.277155	3.218193	9.336116	2.941609	9.229923	5.824122	12.63572	-1.97332
1993	6.248751	3.189789	9.307713	-1.12875	9.141717	5.735916	12.54752	-1.88512
1994	6.220347	3.161386	9.279309	-1.10034	9.05351	5.647709	12.45931	-1.72561
1995	6.191944	3.132982	9.250905	1.816567	8.965303	5.559502	12.3711	-0.36586
1996	6.16354	3.104578	9.222502	-1.04353	8.877097	5.471296	12.2829	-1.6205
1997	6.135136	3.076175	9.194098	3.006491	8.78889	5.383089	12.19469	2.437819
1998	6.106733	3.047771	9.165694	-0.13113	8.700683	5.294883	12.10648	-1.40669
1999	6.078329	3.019367	9.137291	-0.95832	8.612477	5.206676	12.01828	0.166428
2000	6.049925	2.990964	9.108887	-0.92992	8.52427	5.118469	11.93007	-1.26767
2001	6.021522	2.96256	9.080483	-0.75919	8.436064	5.030263	11.84186	-0.85473
2002	5.993118	2.934156	9.05208	-0.43887	8.347857	4.942056	11.75366	0.089694
2003	5.964714	2.905753	9.023676	-0.84471	8.25965	4.853849	11.66545	-1.00305
2004	5.936311	2.877349	8.995272	-0.8163	8.171444	4.765643	11.57724	-0.91484
2005	5.907907	2.848945	8.966869	-0.7879	8.083237	4.677436	11.48904	0.265113
2006	5.879503	2.820542	8.938465	-0.27003	7.99503	4.589229	11.40083	-0.25926
2007	5.8511	2.792138	8.910061	-0.73109	7.906824	4.501023	11.31262	-0.43472
2008	5.822696	2.763734	8.881658	-0.70269	7.818617	4.412816	11.22442	-0.56202
2009	5.794292	2.735331	8.853254	3.515568	7.730411	4.32461	11.13621	0.005364
2010	5.765889	2.706927	8.82485	1.980994	7.642204	4.236403	11.048	0.410013
2011	5.737485	2.678523	8.796447	-0.61748	7.553997	4.148196	10.9598	-0.2974
2012	5.709081	2.65012	8.768043	-0.58908	7.465791	4.05999	10.87159	0.443391
2013	5.680678	2.621716	8.739639	-0.42721	7.377584	3.971783	10.78338	2.737748

Time Series Modeler
Notes

Output Created		
Comments		03-Mar-2016 09:50:59
Input	Active Dataset	DataSet0
	Filter	<none>
	Weight	<none>
	Split File	<none>
	Date	<none>
Missing Value Handling	Definition of Missing	User-defined missing values are treated as missing.
	Cases Used	Only cases with valid data for the dependent variable are used in computing any statistics
Syntex		TSMODEL /MODELSUMMARY PRINT=[MODELFIT RESIDACF RESIDPACF] PLOT=[SRSQUARE RSQUARE RMSE MAPE MAXAPE MAXAE NORMBIC RESIDACF RESIDPACF] /MODELSTATISTICS DISPLAY=YES MODELFIT=[SRSQUARE RSQUARE RMSE MAPE MAE MAXAPE MAXAE NORMBIC] /MODELDETAILS PRINT=[PARAMETERS RESIDACF RESIDPACF FORECASTS] PLOT=[RESIDACF RESIDPACF] /SERIESPLOT OBSERVED FORECAST FIT FORECASTCI FITCI /OUTPUTFILTER ISPLAY=ALLMODELS /SAVE PREDICTED(Predicted) LCL(LCL) UCL(UCL) NRESIDUAL(NResidual) /AUXILIARY CILEVEL=95 MAXACFLAGS=40 /MISSING USERMISSING=EXCLUDE /MODEL DEPENDENT=VAR00002 VAR00003 VAR00004 VAR00005 VAR00006 VAR00007 INDEPENDENT=VAR00001 PREFIX='Model' /ARIMA AR=[0] DIFF=0 MA=[0] TRANSFORM=NONE CONSTANT=YES /TRANSFERFUNCTION VARIABLES=VAR00001 NUM=[0] DENOM=[0] DIFF=0 DELAY=0 TRANSFORM=NONE /AUTOOUTLIER DETECT=OFF.
Resources	Processor Time	00:00:04.204
	Elapsed Time	00:00:03.963
Variables Created or Modified	Predicted_VAR00002_Model_1	Predicted value from VAR00002-Model_1
	LCL_VAR00002_Model_1	LCL from VAR00002-Model_1
	UCL_VAR00002_Model_1	UCL from VAR00002-Model_1
	NResidual_VAR00002_Model_1	Noise residual from VAR00002-Model_1
	Predicted_VAR00003_Model_2	Predicted value from VAR00003-Model_2
	LCL_VAR00003_Model_2	LCL from VAR00003-Model_2
	UCL_VAR00003_Model_2	UCL from VAR00003-Model_2
	NResidual_VAR00003_Model_2	Noise residual from VAR00003-Model_2
	Predicted_VAR00004_Model_3	Predicted value from VAR00004-Model_3
	LCL_VAR00004_Model_3	LCL from VAR00004-Model_3
	UCL_VAR00004_Model_3	UCL from VAR00004-Model_3
	NResidual_VAR00004_Model_3	Noise residual from VAR00004-Model_3
	Predicted_VAR00005_Model_4	Predicted value from VAR00005-Model_4
	LCL_VAR00005_Model_4	LCL from VAR00005-Model_4
	UCL_VAR00005_Model_4	UCL from VAR00005-Model_4
	NResidual_VAR00005_Model_4	Noise residual from VAR00005-Model_4
	Predicted_VAR00006_Model_5	Predicted value from VAR00006-Model_5
	LCL_VAR00006_Model_5	LCL from VAR00006-Model_5
	UCL_VAR00006_Model_5	UCL from VAR00006-Model_5
	NResidual_VAR00006_Model_5	Noise residual from VAR00006-Model_5
	Predicted_VAR00007_Model_6	Predicted value from VAR00007-Model_6
	LCL_VAR00007_Model_6	LCL from VAR00007-Model_6
	UCL_VAR00007_Model_6	UCL from VAR00007-Model_6
	NResidual_VAR00007_Model_6	Noise residual from VAR00007-Model_6
Use	From	First observation
	To	Last observation
Predict	From	First observation
	To	Last observation

Model Description

			Model Type
Model ID	VAR00002	Model_1	ARIMA(0,0,0)
	VAR00003	Model_2	ARIMA(0,0,0)
	VAR00004	Model_3	ARIMA(0,0,0)
	VAR00005	Model_4	ARIMA(0,0,0)
	VAR00006	Model_5	ARIMA(0,0,0)
	VAR00007	Model_6	ARIMA(0,0,0)

Model Statistics

Model	Number of Predictors	Model Fit statistics								Ljung-Box Q(18)			Number of Outliers
		Stationary R-squared	R-squared	RMSE	MAPE	MAE	MaxAPE	MaxAE	Normalized BIC				
VAR00002-Model_1	1	.026	.026	3.165	15.324	2.719	29.202	5.988	2.499	17.258	18	.505	0
VAR00003-Model_2	1	.004	.004	4.437	15.590	3.659	29.084	8.005	3.175	18.007	18	.455	0
VAR00004-Model_3	1	.092	.092	3.492	16.033	2.946	37.786	7.643	2.696	13.982	18	.730	0
VAR00005-Model_4	1	.012	.012	2.408	14.754	1.956	27.919	5.024	1.953	23.784	18	.162	0
VAR00006-Model_5	1	.000	.000	4.629	13.932	4.012	26.487	7.651	3.260	24.476	18	.140	0
VAR00007-Model_6	1	.006	.006	21.231	12.969	18.378	26.895	38.607	6.306	13.489	18	.762	0

ARIMA Model Parameters

					Estimate	SE	t	Sig.
VAR00002-Model_1	VAR00002	No Transformation	Constant		112.598	97.216	1.158	.255
	VAR00001	No Transformation	Numerator	Lag 0	-.047	.049	-.974	.337
VAR00003-Model_2	VAR00001	No Transformation	Numerator	Lag 0	.026	.068	.383	.704
	VAR00003	No Transformation	Constant		-28.589	136.294	-.210	.835
VAR00004-Model_3	VAR00001	No Transformation	Numerator	Lag 0	-.101	.054	-1.878	.069
	VAR00004	No Transformation	Constant		219.686	107.256	2.048	.048
VAR00005-Model_4	VAR00001	No Transformation	Numerator	Lag 0	-.024	.037	-.655	.517
	VAR00005	No Transformation	Constant		61.633	73.961	.833	.410
VAR00006-Model_5	VAR00001	No Transformation	Numerator	Lag 0	-.006	.071	-.084	.934
	VAR00006	No Transformation	Constant		41.277	142.181	.290	.773
VAR00007-Model_6	VAR00001	No Transformation	Numerator	Lag 0	.155	.327	.474	.638
	VAR00007	No Transformation	Constant		-166.002	652.173	-.255	.801

Residual ACF

Model		1	2	3	4	5	6	7	8	9	10	11	12	13	14	15	16	17	18	19	20	21	22	23	24	25	26	27	28	29	30	31	32	33	34	35	36
VAR00002-Model_1	ACF	.241	-.054	-.175	-.216	-.251	-.024	.003	-.029	-.069	.211	-.048	-.082	.050	-.142	-.203	-.054	.067	.100	.103	.208	.114	-.107	-.010	-.049	-.068	-.008	-.105	-.088	.044	.159	.129	-.037	.067	-.075	-.012	.046
	SE	.164	.174	.174	.179	.186	.195	.195	.195	.195	.196	.202	.202	.203	.203	.206	.211	.212	.212	.213	.215	.220	.222	.223	.223	.223	.224	.224	.225	.226	.226	.229	.231	.232	.232	.233	.233
VAR00003-Model_2	ACF	-.418	.019	-.089	-.035	.034	.211	-.209	.128	-.077	-.140	.141	.060	-.077	-.120	.117	.014	-.008	-.096	-.012	-.107	.259	-.222	.245	-.125	-.123	.061	.132	-.061	.090	-.155	.018	.062	-.071	.046	.046	-.038
	SE	.164	.191	.191	.192	.192	.193	.199	.205	.207	.207	.210	.213	.213	.214	.216	.217	.217	.217	.218	.218	.220	.228	.234	.241	.242	.244	.244	.246	.247	.248	.250	.250	.251	.251	.252	.252
VAR00004-Model_3	ACF	.125	-.009	-.187	-.080	-.224	-.251	.005	-.020	.028	-.071	-.040	.198	.189	.023	-.076	.059	.059	-.093	-.096	.012	-.236	-.150	-.058	.160	.209	.123	.130	-.088	.018	-.163	-.024	.013	.017	-.001	.017	.012
	SE	.164	.167	.167	.172	.174	.181	.190	.190	.190	.191	.191	.191	.197	.202	.202	.203	.203	.204	.205	.206	.206	.213	.216	.216	.220	.225	.227	.229	.230	.230	.233	.233	.233	.233	.233	.233
VAR00005-Model_4	ACF	.095	-.293	.094	-.115	-.359	.018	.203	-.159	-.161	.256	.060	-.191	.095	-.012	-.173	.008	.046	.027	-.057	.084	.271	.079	-.053	-.081	-.122	-.101	.008	.074	.003	-.075	.005	.038	-.009	.036	.021	-.024
	SE	.164	.166	.179	.181	.183	.201	.201	.206	.210	.213	.221	.221	.226	.227	.227	.231	.231	.231	.231	.231	.232	.240	.241	.241	.242	.244	.245	.245	.246	.246	.246	.246	.246	.246	.247	.247
VAR00006-Model_5	ACF	-.052	-.393	-.036	.322	-.006	-.105	-.069	-.155	-.168	.259	-.078	-.270	-.040	.144	.031	.025	.062	-.034	-.055	.294	.028	-.203	-.104	.296	.050	-.214	-.098	.073	.002	.000	-.063	.006	-.013	.059	.020	-.013
	SE	.164	.165	.188	.189	.203	.203	.204	.205	.208	.212	.220	.221	.230	.230	.232	.232	.233	.233	.233	.233	.243	.243	.248	.249	.258	.259	.263	.264	.265	.265	.265	.265	.265	.265	.266	.266
VAR00007-Model_6	ACF	-.190	-.268	.042	.106	.086	-.161	-.029	-.013	-.120	.120	-.030	.031	-.181	-.009	.164	-.047	-.118	.074	.034	.088	-.112	-.093	.186	-.006	.007	-.117	.101	-.016	-.098	.106	-.107	.004	.103	-.072	.054	-.018
	SE	.164	.170	.181	.182	.183	.184	.188	.188	.188	.190	.192	.192	.193	.197	.197	.201	.201	.203	.204	.204	.205	.206	.208	.212	.212	.212	.214	.215	.215	.216	.218	.219	.219	.220	.221	.221

Residual

PACF

Model		1	2	3	4	5	6	7	8	9	10	11	12	13	14	15	16	17	18	19	20	21	22	23	24	25	26	27	28	29	30	31	32	33	34	35	36
VAR00002-Model_1	PACF	.241	-.119	-.141	-.157	-.209	.028	-.098	-.123	-.146	.206	-.233	-.087	.069	-.287	-.139	-.151	-.062	.069	-.095	.001	.067	-.160	-.059	.055	-.044	.063	-.243	-.086	.028	-.057	-.081	-.028	.095	-.071	.124	-.079
	SE	.164	.164	.164	.164	.164	.164	.164	.164	.164	.164	.164	.164	.164	.164	.164	.164	.164	.164	.164	.164	.164	.164	.164	.164	.164	.164	.164	.164	.164	.164	.164	.164	.164	.164	.164	.164
VAR00003-Model_2	PACF	-.418	-.189	-.198	-.210	-.135	.189	-.036	.088	.067	-.182	-.057	.056	-.014	-.273	.021	.145	-.075	.164	-.077	.294	-.015	-.136	.113	.024	-.074	.045	.005	-.019	-.013	-.030	-.034	.097	-.096	-.106	-.054	-.009
	SE	.164	.164	.164	.164	.164	.164	.164	.164	.164	.164	.164	.164	.164	.164	.164	.164	.164	.164	.164	.164	.164	.164	.164	.164	.164	.164	.164	.164	.164	.164	.164	.164	.164	.164	.164	.164
VAR00004-Model_3	PACF	.125	-.024	-.186	-.036	-.223	-.262	.020	-.148	-.109	-.176	-.239	.106	.075	-.140	-.091	.030	.090	.025	-.052	.026	-.326	-.118	-.006	-.058	.034	-.115	-.005	-.100	-.047	-.117	-.015	-.089	-.028	.052	.112	-.111
	SE	.164	.164	.164	.164	.164	.164	.164	.164	.164	.164	.164	.164	.164	.164	.164	.164	.164	.164	.164	.164	.164	.164	.164	.164	.164	.164	.164	.164	.164	.164	.164	.164	.164	.164	.164	.164
VAR00005-Model_4	PACF	.095	-.305	.177	-.281	-.249	-.075	.061	-.244	-.178	.068	-.061	-.121	-.059	-.235	-.034	-.128	-.246	-.048	-.262	-.128	.132	.016	-.082	-.127	-.072	-.024	.049	-.116	-.052	-.004	-.140	-.040	-.018	-.066	.035	.018
	SE	.164	.164	.164	.164	.164	.164	.164	.164	.164	.164	.164	.164	.164	.164	.164	.164	.164	.164	.164	.164	.164	.164	.164	.164	.164	.164	.164	.164	.164	.164	.164	.164	.164	.164	.164	.164
VAR00006-Model_5	PACF	-.052	-.397	-.101	.185	-.012	.086	-.057	-.298	-.341	.081	-.234	-.135	-.058	-.243	-.106	.027	-.035	-.072	-.101	.024	-.131	-.106	-.235	.076	.021	-.076	-.037	-.098	-.047	-.093	-.090	.066	.050	-.070	-.035	.029
	SE	.164	.164	.164	.164	.164	.164	.164	.164	.164	.164	.164	.164	.164	.164	.164	.164	.164	.164	.164	.164	.164	.164	.164	.164	.164	.164	.164	.164	.164	.164	.164	.164	.164	.164	.164	.164
VAR00007-Model_6	PACF	-.190	-.315	-.098	.010	.123	-.077	-.032	-.121	-.225	.005	-.058	.081	-.189	-.113	-.050	-.059	-.128	.029	-.044	.064	-.085	-.218	.057	-.034	.097	-.130	.083	-.156	-.081	-.072	-.120	.024	.072	-.049	-.091	.044
	SE	.164	.164	.164	.164	.164	.164	.164	.164	.164	.164	.164	.164	.164	.164	.164	.164	.164	.164	.164	.164	.164	.164	.164	.164	.164	.164	.164	.164	.164	.164	.164	.164	.164	.164	.164	.164

Model Summary

Model Fit

Fit Statistic	Mean	SE	Minimum	Maximum	Percentile						
					5	10	25	50	75	90	95
Stationary R-squared	.023	.035	.000	.092	.000	.000	.003	.009	.043	.092	.092
R-squared	.023	.035	.000	.092	.000	.000	.003	.009	.043	.092	.092
RMSE	6.560	7.234	2.408	21.231	2.408	2.408	2.976	3.964	8.779	21.231	21.231
MAPE	14.767	1.142	12.969	16.033	12.969	12.969	13.692	15.039	15.700	16.033	16.033
MaxAPE	29.562	4.178	26.487	37.786	26.487	26.487	26.793	28.502	31.348	37.786	37.786
MAE	5.612	6.296	1.956	18.378	1.956	1.956	2.528	3.302	7.603	18.378	18.378
MaxAE	12.153	13.011	5.024	38.607	5.024	5.024	5.747	7.647	15.655	38.607	38.607
Normalized BIC	3.315	1.541	1.953	6.306	1.953	1.953	2.363	2.936	4.021	6.306	6.306

Residual ACF Summary

Lag	Mean	SE	Minimum	Maximum	Percentile						
					5	10	25	50	75	90	95
Lag 1	-.033	.241	-.418	.241	-.418	-.418	-.247	.022	.154	.241	.241
Lag 2	-.166	.173	-.393	.019	-.393	-.393	-.318	-.161	-.002	.019	.019
Lag 3	-.058	.114	-.187	.094	-.187	-.187	-.178	-.062	.055	.094	.094
Lag 4	-.003	.191	-.216	.322	-.216	-.216	-.141	-.058	.160	.322	.322
Lag 5	-.120	.181	-.359	.086	-.359	-.359	-.278	-.115	.047	.086	.086
Lag 6	-.058	.158	-.251	.211	-.251	-.251	-.184	-.065	.040	.211	.211
Lag 7	-.016	.133	-.209	.203	-.209	-.209	-.104	-.013	.054	.203	.203
Lag 8	-.041	.107	-.159	.128	-.159	-.159	-.156	-.025	.022	.128	.128
Lag 9	-.095	.073	-.168	.028	-.168	-.168	-.163	-.099	-.045	.028	.028
Lag 10	.106	.173	-.140	.259	-.140	-.140	-.089	.166	.257	.259	.259
Lag 11	.001	.083	-.078	.141	-.078	-.078	-.055	-.035	.080	.141	.141
Lag 12	-.042	.173	-.270	.198	-.270	-.270	-.211	-.026	.094	.198	.198
Lag 13	.006	.132	-.181	.189	-.181	-.181	-.103	.005	.119	.189	.189
Lag 14	-.019	.104	-.142	.144	-.142	-.142	-.126	-.010	.053	.144	.144
Lag 15	-.023	.152	-.203	.164	-.203	-.203	-.181	-.022	.129	.164	.164
Lag 16	.001	.043	-.054	.059	-.054	-.054	-.048	.011	.033	.059	.059
Lag 17	.018	.072	-.118	.067	-.118	-.118	-.036	.052	.064	.067	.067
Lag 18	-.004	.084	-.096	.100	-.096	-.096	-.094	-.004	.081	.100	.100
Lag 19	-.014	.073	-.096	.103	-.096	-.096	-.067	-.033	.051	.103	.103
Lag 20	.096	.142	-.107	.294	-.107	-.107	-.018	.086	.229	.294	.294
Lag 21	.054	.203	-.236	.271	-.236	-.236	-.143	.071	.262	.271	.271
Lag 22	-.116	.108	-.222	.079	-.222	-.222	-.208	-.129	-.050	.079	.079
Lag 23	.034	.145	-.104	.245	-.104	-.104	-.069	-.032	.201	.245	.245
Lag 24	.032	.162	-.125	.296	-.125	-.125	-.092	-.027	.194	.296	.296
Lag 25	-.008	.127	-.123	.209	-.123	-.123	-.123	-.030	.089	.209	.209
Lag 26	-.043	.125	-.214	.123	-.214	-.214	-.142	-.054	.076	.123	.123
Lag 27	.028	.110	-.105	.132	-.105	-.105	-.100	.054	.130	.132	.132
Lag 28	-.018	.076	-.088	.074	-.088	-.088	-.088	-.038	.074	.074	.074
Lag 29	.010	.062	-.098	.090	-.098	-.098	-.023	.010	.055	.090	.090
Lag 30	-.021	.134	-.163	.159	-.163	-.163	-.157	-.038	.119	.159	.159
Lag 31	-.007	.081	-.107	.129	-.107	-.107	-.074	-.010	.046	.129	.129
Lag 32	.010	.035	-.037	.062	-.037	-.037	-.019	.005	.044	.062	.062
Lag 33	-.007	.064	-.071	.103	-.071	-.071	-.068	-.011	.038	.103	.103
Lag 34	-.001	.059	-.075	.059	-.075	-.075	-.073	.017	.050	.059	.059
Lag 35	.024	.023	-.012	.054	-.012	-.012	.009	.021	.048	.054	.054
Lag 36	-.006	.030	-.038	.046	-.038	-.038	-.027	-.015	.021	.046	.046

Residual PACF Summary

Lag 1	-.033	.241	-.418	.241	-.418	-.418	-.247	.022	.154	.241	.241
Lag 2	-.225	.139	-.397	-.024	-.397	-.397	-.335	-.247	-.096	-.024	-.024
Lag 3	-.091	.138	-.198	.177	-.198	-.198	-.189	-.121	-.029	.177	.177
Lag 4	-.081	.169	-.281	.185	-.281	-.281	-.227	-.096	.054	.185	.185
Lag 5	-.117	.146	-.249	.123	-.249	-.249	-.229	-.172	.022	.123	.123
Lag 6	-.019	.156	-.262	.189	-.262	-.262	-.123	-.023	.112	.189	.189
Lag 7	-.024	.056	-.098	.061	-.098	-.098	-.067	-.034	.030	.061	.061
Lag 8	-.141	.133	-.298	.088	-.298	-.298	-.258	-.136	-.069	.088	.088
Lag 9	-.156	.135	-.341	.067	-.341	-.341	-.254	-.162	-.065	.067	.067
Lag 10	.000	.153	-.182	.206	-.182	-.182	-.178	.036	.113	.206	.206
Lag 11	-.147	.097	-.239	-.057	-.239	-.239	-.235	-.147	-.057	-.057	-.057
Lag 12	-.017	.109	-.135	.106	-.135	-.135	-.124	-.016	.087	.106	.106
Lag 13	-.029	.098	-.189	.075	-.189	-.189	-.091	-.036	.071	.075	.075
Lag 14	-.215	.072	-.287	-.113	-.287	-.287	-.276	-.239	-.133	-.113	-.113
Lag 15	-.066	.058	-.139	.021	-.139	-.139	-.115	-.070	-.020	.021	.021
Lag 16	-.023	.112	-.151	.145	-.151	-.151	-.134	-.016	.058	.145	.145
Lag 17	-.076	.111	-.246	.090	-.246	-.246	-.158	-.068	-.004	.090	.090
Lag 18	-.050	.072	-.164	.029	-.164	-.164	-.095	-.058	.026	.029	.029
Lag 19	-.105	.080	-.262	-.044	-.262	-.262	-.141	-.086	-.050	-.044	-.044
Lag 20	-.051	.136	-.294	.064	-.294	-.294	-.170	.013	.035	.064	.064
Lag 21	-.060	.162	-.326	.132	-.326	-.326	-.180	-.050	.083	.132	.132
Lag 22	-.120	.078	-.218	.016	-.218	-.218	-.175	-.127	-.075	.016	.016
Lag 23	-.035	.122	-.235	.113	-.235	-.235	-.120	-.032	.071	.113	.113
Lag 24	-.010	.077	-.127	.076	-.127	-.127	-.075	-.005	.060	.076	.076
Lag 25	-.006	.068	-.074	.097	-.074	-.074	-.072	-.011	.050	.097	.097
Lag 26	-.060	.064	-.130	.045	-.130	-.130	-.119	-.070	-.006	.045	.045
Lag 27	-.025	.115	-.243	.083	-.243	-.243	-.089	-2.156E-5	.057	.083	.083
Lag 28	-.096	.045	-.156	-.019	-.156	-.156	-.126	-.099	-.070	-.019	-.019
Lag 29	-.035	.038	-.081	.028	-.081	-.081	-.059	-.047	-.003	.028	.028
Lag 30	-.062	.041	-.117	-.004	-.117	-.117	-.099	-.064	-.024	-.004	-.004
Lag 31	-.080	.048	-.140	-.015	-.140	-.140	-.125	-.085	-.029	-.015	-.015
Lag 32	-.028	.064	-.097	.066	-.097	-.097	-.091	-.034	.034	.066	.066
Lag 33	-.019	.070	-.096	.072	-.096	-.096	-.095	-.023	.055	.072	.072
Lag 34	-.052	.054	-.106	.052	-.106	-.106	-.079	-.068	-.024	.052	.052
Lag 35	.015	.090	-.091	.124	-.091	-.091	-.063	.000	.115	.124	.124
Lag 36	-.018	.063	-.111	.044	-.111	-.111	-.087	.005	.033	.044	.044

Time Series Modeler

Notes

Output Created		**03-Mar-2016 10:30:45**
Comments		
Input	**Active Dataset**	**DataSet0**
	Filter	**<none>**
	Weight	**<none>**
	Split File	**<none>**
	Date	**<none>**
Missing Value Handling	**Definition of Missing**	**User-defined missing values are treated as missing.**
	Cases Used	**Only cases with valid data for the dependent variable are used in computing any statistics**
Syntex		**TSMODEL /MODELSUMMARY PRINT=[MODELFIT RESIDACF RESIDPACF] PLOT=[SRSQUARE RSQUARE RMSE MAPE MAXAPE MAXAE NORMBIC RESIDACF RESIDPACF] /MODELSTATISTICS DISPLAY=YES MODELFIT=[SRSQUARE RSQUARE RMSE MAPE MAE MAXAPE MAXAE NORMBIC] /MODELDETAILS PRINT=[PARAMETERS RESIDACF RESIDPACF FORECASTS] PLOT=[RESIDACF RESIDPACF] /SERIESPLOT OBSERVED FORECAST FIT FORECASTCI FITCI /OUTPUTFILTER ISPLAY=ALLMODELS /SAVE PREDICTED(Predicted) LCL(LCL) UCL(UCL) NRESIDUAL(NResidual) /AUXILIARY CILEVEL=95 MAXACFLAGS=40 /MISSING USERMISSING=EXCLUDE /MODEL DEPENDENT=VAR00002 VAR00003 VAR00004 VAR00005 VAR00006 VAR00007 INDEPENDENT=VAR00001 PREFIX='Model' /ARIMA AR=[0] DIFF=0 MA=[0] TRANSFORM=NONE CONSTANT=YES /TRANSFERFUNCTION VARIABLES=VAR00001 NUM=[0] DENOM=[0] DIFF=0 DELAY=0 TRANSFORM=NONE /AUTOOUTLIER DETECT=OFF.**
Resources	**Processor Time**	**00:00:04.437**
	Elapsed Time	**00:00:04.258**
Variables Created or Modified	**Predicted_VAR00002_Model_1**	**Predicted value from VAR00002-Model_1**
	LCL_VAR00002_Model_1	**LCL from VAR00002-Model_1**
	UCL_VAR00002_Model_1	**UCL from VAR00002-Model_1**
	NResidual_VAR00002_Model_1	**Noise residual from VAR00002-Model_1**
	Predicted_VAR00003_Model_2	**Predicted value from VAR00003-Model_2**
	LCL_VAR00003_Model_2	**LCL from VAR00003-Model_2**
	UCL_VAR00003_Model_2	**UCL from VAR00003-Model_2**
	NResidual_VAR00003_Model_2	**Noise residual from VAR00003-Model_2**
	Predicted_VAR00004_Model_3	**Predicted value from VAR00004-Model_3**
	LCL_VAR00004_Model_3	**LCL from VAR00004-Model_3**
	UCL_VAR00004_Model_3	**UCL from VAR00004-Model_3**
	NResidual_VAR00004_Model_3	**Noise residual from VAR00004-Model_3**
	Predicted_VAR00005_Model_4	**Predicted value from VAR00005-Model_4**
	LCL_VAR00005_Model_4	**LCL from VAR00005-Model_4**
	UCL_VAR00005_Model_4	**UCL from VAR00005-Model_4**
	NResidual_VAR00005_Model_4	**Noise residual from VAR00005-Model_4**
	Predicted_VAR00006_Model_5	**Predicted value from VAR00006-Model_5**
	LCL_VAR00006_Model_5	**LCL from VAR00006-Model_5**
	UCL_VAR00006_Model_5	**UCL from VAR00006-Model_5**

	NResidual_VAR00006_Model_5	**Noise residual from VAR00006-Model_5**
	Predicted_VAR00007_Model_6	**Predicted value from VAR00007-Model_6**
	LCL_VAR00007_Model_6	**LCL from VAR00007-Model_6**
	UCL_VAR00007_Model_6	**UCL from VAR00007-Model_6**
	NResidual_VAR00007_Model_6	**Noise residual from VAR00007-Model_6**
Use	**From**	**First observation**
	To	**Last observation**
Predict	**From**	**First observation**
	To	**Last observation**

Model Description

			Model Type
Model ID	VAR00002	Model_1	ARIMA(0,0,0)
	VAR00003	Model_2	ARIMA(0,0,0)
	VAR00004	Model_3	ARIMA(0,0,0)
	VAR00005	Model_4	ARIMA(0,0,0)
	VAR00006	Model_5	ARIMA(0,0,0)
	VAR00007	Model_6	ARIMA(0,0,0)

Model Statistics

Model	Number of Predictors	Model Fit statistics								Ljung-Box Q(18)			Number of Outliers
		Stationary R-squared	R-squared	RMSE	MAPE	MAE	MaxAPE	MaxAE	Normalized BIC	Statistics	DF	Sig.	
VAR00002-Model_1	1	.009	.009	37.515	10.671	33.010	21.977	60.130	7.445	17.682	18	.477	0
VAR00003-Model_2	1	.008	.008	28.033	7.774	23.590	16.624	49.206	6.862	20.080	18	.328	0
VAR00004-Model_3	1	.015	.015	25.467	11.257	21.638	20.646	43.733	6.670	38.279	18	.004	0
VAR00005-Model_4	1	.001	.001	7.469	18.751	6.516	30.036	14.808	4.217	16.930	18	.528	0
VAR00006-Model_5	1	.041	.041	1.507	18.635	1.210	37.762	3.516	1.015	9.545	18	.946	0
VAR00007-Model_6	1	.250	.250	1.678	13.859	1.289	34.090	3.374	1.230	12.363	18	.828	0

ARIMA Model Parameters

					Estimate	SE	t	Sig.
VAR00002-Model_1	VAR00002	No Transformation	Constant		-355.884	1.152E3	-.309	.759
	VAR00001	No Transformation	Numerator	Log 0	.334	.578	.579	.566
VAR00003-Model_2	VAR00001	No Transformation	Numerator	Log 0	.224	.432	.520	.606
	VAR00003	No Transformation	Constant		-145.939	861.135	-.169	.866
VAR00004-Model_3	VAR00001	No Transformation	Numerator	Log 0	.290	.392	.741	.464
	VAR00004	No Transformation	Constant		-386.161	782.289	-.494	.625

VAR00005-Model_4	VAR00001	No Transformation	Numerator	Log 0	.020	.115	.177	.860
	VAR00005	No Transformation	Constant		-5.997	229.445	-.026	.979
VAR00006-Model_5	VAR00001	No Transformation	Numerator	Log 0	-.028	.023	-1.224	.229
	VAR00006	No Transformation	Constant		62.857	46.286	1.358	.183
VAR00007-Model_6	VAR00001	No Transformation	Numerator	Log 0	-.088	.026	-3.415	.002
	VAR00007	No Transformation	Constant		184.938	51.534	3.589	.001

Model Summary

Model Fit

Fit Statistic	Mean	SE	Minimum	Maximum	Percentile						
					5	10	25	50	75	90	95
Stationary R-squared	.054	.097	.001	.250	.001	.001	.006	.012	.093	.250	.250
R-squared	.054	.097	.001	.250	.001	.001	.006	.012	.093	.250	.250
RMSE	16.945	15.362	1.507	37.515	1.507	1.507	1.635	16.468	30.404	37.515	37.515
MAPE	13.491	4.470	7.774	18.751	7.774	7.774	9.947	12.558	18.664	18.751	18.751
MaxAPE	26.856	8.348	16.624	37.762	16.624	16.624	19.640	26.006	35.008	37.762	37.762
MAE	14.542	13.350	1.210	33.010	1.210	1.210	1.269	14.077	25.945	33.010	33.010
MaxAE	29.128	24.907	3.374	60.130	3.374	3.374	3.480	29.270	51.937	60.130	60.130
Normalized BIC	4.573	2.893	1.015	7.445	1.015	1.015	1.176	5.443	7.008	7.445	7.445

Residual ACF Summary

Lag	Mean	SE	Minimum	Maximum	Percentile						
					5	10	25	50	75	90	95
Lag 1	-.067	.155	-.343	.081	-.343	-.343	-.187	-.017	.043	.081	.081
Lag 2	-.024	.150	-.153	.267	-.153	-.153	-.118	-.060	.041	.267	.267
Lag 3	.044	.199	-.122	.430	-.122	-.122	-.086	-.011	.145	.430	.430
Lag 4	-.165	.187	-.366	.156	-.366	-.366	-.302	-.218	-.008	.156	.156
Lag 5	.050	.162	-.159	.218	-.159	-.159	-.111	.078	.192	.218	.218
Lag 6	-.021	.139	-.146	.191	-.146	-.146	-.132	-.079	.135	.191	.191
Lag 7	-.093	.118	-.212	.117	-.212	-.212	-.199	-.098	-.026	.117	.117
Lag 8	-.092	.129	-.253	.090	-.253	-.253	-.234	-.066	.000	.090	.090
Lag 9	-.090	.113	-.273	.068	-.273	-.273	-.161	-.087	-.009	.068	.068
Lag 10	-.014	.079	-.116	.112	-.116	-.116	-.086	-.009	.040	.112	.112
Lag 11	-.105	.196	-.300	.152	-.300	-.300	-.288	-.135	.091	.152	.152
Lag 12	.063	.138	-.064	.262	-.064	-.064	-.042	.004	.219	.262	.262
Lag 13	.063	.129	-.155	.170	-.155	-.155	-.057	.110	.168	.170	.170
Lag 14	-.029	.081	-.147	.081	-.147	-.147	-.095	-.031	.044	.081	.081
Lag 15	-.007	.108	-.127	.150	-.127	-.127	-.116	-.007	.081	.150	.150
Lag 16	.012	.110	-.170	.136	-.170	-.170	-.091	.053	.085	.136	.136
Lag 17	.005	.113	-.208	.098	-.208	-.208	-.077	.054	.075	.098	.098
Lag 18	-.033	.125	-.168	.152	-.168	-.168	-.136	-.046	.067	.152	.152
Lag 19	.026	.116	-.113	.187	-.113	-.113	-.095	.024	.136	.187	.187
Lag 20	-.042	.110	-.197	.123	-.197	-.197	-.131	-.046	.049	.123	.123
Lag 21	-.037	.098	-.133	.148	-.133	-.133	-.091	-.072	.023	.148	.148
Lag 22	.017	.117	-.108	.200	-.108	-.108	-.061	-.032	.139	.200	.200
Lag 23	-.032	.106	-.230	.086	-.230	-.230	-.080	-.014	.030	.086	.086
Lag 24	-.031	.101	-.141	.152	-.141	-.141	-.114	-.038	.026	.152	.152

Residual PACF Summary

Lag	Mean	SE	Minimum	Maximum	Percentile						
					5	10	25	50	75	90	95
Lag 1	-.067	.155	-.343	.081	-.343	-.343	-.187	-.017	.043	.081	.081
Lag 2	-.055	.183	-.307	.262	-.307	-.307	-.157	-.069	.036	.262	.262
Lag 3	.017	.165	-.137	.320	-.137	-.137	-.095	-.030	.123	.320	.320
Lag 4	-.163	.172	-.298	.143	-.298	-.298	-.293	-.227	-.020	.143	.143
Lag 5	.027	.165	-.205	.227	-.205	-.205	-.138	.047	.178	.227	.227
Lag 6	-.061	.134	-.157	.132	-.157	-.157	-.156	-.138	.101	.132	.132
Lag 7	-.058	.127	-.205	.137	-.205	-.205	-.187	-.060	.049	.137	.137
Lag 8	-.162	.139	-.319	.024	-.319	-.319	-.307	-.159	-.037	.024	.024
Lag 9	-.195	.111	-.338	-.106	-.338	-.338	-.337	-.134	-.116	-.106	-.106
Lag 10	-.100	.106	-.217	.059	-.217	-.217	-.201	-.102	-.017	.059	.059
Lag 11	-.099	.103	-.239	.063	-.239	-.239	-.158	-.128	-.008	.063	.063
Lag 12	-.064	.089	-.218	.014	-.218	-.218	-.147	-.021	-.005	.014	.014
Lag 13	-.015	.130	-.150	.165	-.150	-.150	-.148	-.034	.124	.165	.165
Lag 14	-.057	.108	-.219	.090	-.219	-.219	-.134	-.066	.039	.090	.090
Lag 15	-.065	.122	-.195	.102	-.195	-.195	-.170	-.076	.037	.102	.102
Lag 16	-.093	.064	-.175	-.012	-.175	-.175	-.155	-.096	-.027	-.012	-.012
Lag 17	-.053	.069	-.149	.044	-.149	-.149	-.114	-.047	-.003	.044	.044
Lag 18	-.097	.096	-.200	.025	-.200	-.200	-.168	-.134	.020	.025	.025
Lag 19	-.014	.053	-.067	.088	-.067	-.067	-.046	-.029	.016	.088	.088
Lag 20	-.068	.109	-.200	.077	-.200	-.200	-.182	-.053	.018	.077	.077
Lag 21	-.046	.108	-.160	.099	-.160	-.160	-.128	-.088	.083	.099	.099
Lag 22	-.065	.088	-.139	.079	-.139	-.139	-.138	-.090	.010	.079	.079
Lag 23	-.049	.050	-.113	.028	-.113	-.113	-.086	-.060	.000	.028	.028
Lag 24	-.040	.041	-.087	.029	-.087	-.087	-.071	-.049	-.006	.029	.029

Rainfall during October months (1977-2013) Normalized

Time Series Modeler

Notes

Output Created		03-Mar-2016 09:04:13
Comments		
Input	Active Dataset	DataSet0
	Filter	<none>
	Weight	<none>
	Split File	<none>
	Date	<none>
Missing Value Handling	Definition of Missing	User-defined missing values are treated as missing.
	Cases Used	Only cases with valid data for the dependent variable are used in computing any statistics
Syntex		TSMODEL /MODELSUMMARY PRINT=[MODELFIT RESIDACF RESIDPACF] PLOT=[SRSQUARE RSQUARE RMSE MAPE MAXAPE MAXAE NORMBIC RESIDACF RESIDPACF] /MODELSTATISTICS DISPLAY=YES MODELFIT=[SRSQUARE RSQUARE RMSE MAPE MAE MAXAPE MAXAE NORMBIC] /MODELDETAILS PRINT=[PARAMETERS RESIDACF RESIDPACF FORECASTS] PLOT=[RESIDACF RESIDPACF] /SERIESPLOT OBSERVED FORECAST FIT FORECASTCI FITCI /OUTPUTFILTER ISPLAY=ALLMODELS /SAVE PREDICTED(Predicted) LCL(LCL) UCL(UCL) NRESIDUAL(NResidual) /AUXILIARY CILEVEL=95 MAXACFLAGS=40 /MISSING USERMISSING=EXCLUDE /MODEL DEPENDENT=VAR00002 VAR00003 VAR00004 VAR00005 VAR00006 VAR00007 INDEPENDENT=VAR00001 PREFIX='Model' /ARIMA AR=[0] DIFF=0 MA=[0] TRANSFORM=NONE CONSTANT=YES /TRANSFERFUNCTION VARIABLES=VAR00001 NUM=[0] DENOM=[0] DIFF=0 DELAY=0 TRANSFORM=NONE /AUTOOUTLIER DETECT=OFF.
Resources	Processor Time	00:00:04.422
	Elapsed Time	00:00:04.299
Variables Created or Modified	Predicted_VAR00002_Model_1	Predicted value from VAR00002-Model_1
	LCL_VAR00002_Model_1	LCL from VAR00002-Model_1
	UCL_VAR00002_Model_1	UCL from VAR00002-Model_1
	NResidual_VAR00002_Model_1	Noise residual from VAR00002-Model_1
Use	From	First observation
	To	Last observation
Predict	From	First observation
	To	Last observation

[DataSet0]

Warnings The forecast table is not created because no forecasts could be calculated.

Model Description

			Model Type
Model ID	VAR00002	Model_1	ARIMA(0,0,0)

Model Statistics

Model	Number of Predictors	Model Fit statistics								Ljung-Box Q(18)			Number of Outliers
		Stationary R-squared	R-squared	RMSE	MAPE	MAE	*MaxAPE*	MaxAE	Normalized BIC	Statistics	DF	Sig.	
VAR00002-Model_1	1	.001	.001	7.469	18.751	6.516	30.036	14.808	4.217	16.930	18	.528	0

ARIMA Model Parameters

					Estimate	SE	t	Sig.
VAR00002-Model_1	VAR00002	No Transformation	Constant		-5.997	229.445	-.026	.979
	VAR00001	No Transformation	Numerator	Lag 0	.020	.115	.177	.860

Residual ACF

Model		1	2	3	4	5	6	7	8	9	10	11	12	13	14	15	16	17	18	19	20	21	22	23	24	25	26	27	28	29	30	31	32	33	34	35	36
VAR00002-Model_1	ACF	-.135	-.034	-.122	-.247	.183	-.127	.117	-.228	-.064	.011	.026	.262	-.024	.032	-.127	.041	.098	-.123	.119	-.197	.148	-.042	.011	.152	-.196	.001	-.022	.017	.057	-.010	-.026	.026	.044	.034	-.036	.023
	SE	.164	.167	.168	.170	.179	.184	.187	.189	.196	.197	.199	.197	.206	.206	.206	.208	.208	.208	.210	.212	.213	.218	.221	.221	.221	.224	.229	.229	.229	.229	.229	.229	.229	.230	.230	.230

Residual PACF

Model		1	2	3	4	5	6	7	8	9	10	11	12	13	14	15	16	17	18	19	20	21	22	23	24	25	26	27	28	29	30	31	32	33	34	35	36
VAR00002-Model_1	ACF	-.135	-.053	-.137	-.298	.089	-.156	.019	-.303	-.121	-.217	-.131	-.012	-.023	-.097	-.159	-.012	-.018	-.200	-.035	-.176	.099	-.128	.028	.029	-.057	-.215	.085	-.143	-.026	-.062	-.025	.052	-.016	-.100	-.091	-.057
	SE	.164	.164	.164	.164	.164	.164	.164	.164	.164	.164	.164	.164	.164	.164	.164	.164	.164	.164	.164	.164	.164	.164	.164	.164	.164	.164	.164	.164	.164	.164	.164	.164	.164	.164	.164	.164

Model Summary

Model Fit

Fit Statistic	Mean	SE	Minimum	Maximum	Percentile						
					5	10	25	50	75	90	95
Stationary R-squared	.001	.	.001	.001	.001	.001	.001	.001	.001	.001	.001
R-squared	.001	.	.001	.001	.001	.001	.001	.001	.001	.001	.001
RMSE	7.469	.	7.469	7.469	7.469	7.469	7.469	7.469	7.469	7.469	7.469
MAPE	18.751	.	18.751	18.751	18.751	18.751	18.751	18.751	18.751	18.751	18.751
MaxAPE	30.036	.	30.036	30.036	30.036	30.036	30.036	30.036	30.036	30.036	30.036
MAE	6.516	.	6.516	6.516	6.516	6.516	6.516	6.516	6.516	6.516	6.516
MaxAE	14.808	.	14.808	14.808	14.808	14.808	14.808	14.808	14.808	14.808	14.808
Normalized BIC	4.217	.	4.217	4.217	4.217	4.217	4.217	4.217	4.217	4.217	4.217

Residual ACF Summary

Lag	Mean	SE	Minimum	Maximum	Percentile						
					5	10	25	50	75	90	95
Lag 1	-.135	.	-.135	-.135	-.135	-.135	-.135	-.135	-.135	-.135	-.135
Lag 2	-.034	.	-.034	-.034	-.034	-.034	-.034	-.034	-.034	-.034	-.034
Lag 3	-.122	.	-.122	-.122	-.122	-.122	-.122	-.122	-.122	-.122	-.122
Lag 4	-.247	.	-.247	-.247	-.247	-.247	-.247	-.247	-.247	-.247	-.247
Lag 5	.183	.	.183	.183	.183	.183	.183	.183	.183	.183	.183
Lag 6	-.127	.	-.127	-.127	-.127	-.127	-.127	-.127	-.127	-.127	-.127
Lag 7	.117	.	.117	.117	.117	.117	.117	.117	.117	.117	.117
Lag 8	-.228	.	-.228	-.228	-.228	-.228	-.228	-.228	-.228	-.228	-.228
Lag 9	-.064	.	-.064	-.064	-.064	-.064	-.064	-.064	-.064	-.064	-.064
Lag 10	-.011	.	-.011	-.011	-.011	-.011	-.011	-.011	-.011	-.011	-.011
Lag 11	-.026	.	-.026	-.026	-.026	-.026	-.026	-.026	-.026	-.026	-.026
Lag 12	.262	.	.262	.262	.262	.262	.262	.262	.262	.262	.262
Lag 13	-.024	.	-.024	-.024	-.024	-.024	-.024	-.024	-.024	-.024	-.024
Lag 14	.032	.	.032	.032	.032	.032	.032	.032	.032	.032	.032
Lag 15	-.127	.	-.127	-.127	-.127	-.127	-.127	-.127	-.127	-.127	-.127
Lag 16	.041	.	.041	.041	.041	.041	.041	.041	.041	.041	.041
Lag 17	.098	.	.098	.098	.098	.098	.098	.098	.098	.098	.098
Lag 18	-.123	.	-.123	-.123	-.123	-.123	-.123	-.123	-.123	-.123	-.123
Lag 19	.119	.	.119	.119	.119	.119	.119	.119	.119	.119	.119
Lag 20	-.197	.	-.197	-.197	-.197	-.197	-.197	-.197	-.197	-.197	-.197
Lag 21	.148	.	.148	.148	.148	.148	.148	.148	.148	.148	.148
Lag 22	-.042	.	-.042	-.042	-.042	-.042	-.042	-.042	-.042	-.042	-.042
Lag 23	.011	.	.011	.011	.011	.011	.011	.011	.011	.011	.011
Lag 24	.152	.	.152	.152	.152	.152	.152	.152	.152	.152	.152
Lag 25	-.196	.	-.196	-.196	-.196	-.196	-.196	-.196	-.196	-.196	-.196
Lag 26	.001	.	.001	.001	.001	.001	.001	.001	.001	.001	.001
Lag 27	-.022	.	-.022	-.022	-.022	-.022	-.022	-.022	-.022	-.022	-.022
Lag 28	.017	.	.017	.017	.017	.017	.017	.017	.017	.017	.017
Lag 29	.057	.	.057	.057	.057	.057	.057	.057	.057	.057	.057
Lag 30	-.010	.	-.010	-.010	-.010	-.010	-.010	-.010	-.010	-.010	-.010
Lag 31	-.026	.	-.026	-.026	-.026	-.026	-.026	-.026	-.026	-.026	-.026
Lag 32	.026	.	.026	.026	.026	.026	.026	.026	.026	.026	.026
Lag 33	.044	.	.044	.044	.044	.044	.044	.044	.044	.044	.044
Lag 34	-.034	.	-.034	-.034	-.034	-.034	-.034	-.034	-.034	-.034	-.034
Lag 35	-.036	.	-.036	-.036	-.036	-.036	-.036	-.036	-.036	-.036	-.036
Lag 36	.023	.	.023	.023	.023	.023	.023	.023	.023	.023	.023

Residual PACF Summary

Lag	Mean	SE	Minimum	Maximum	Percentile						
					5	10	25	50	75	90	95
Lag 1	-.135	.	-.135	-.135	-.135	-.135	-.135	-.135	-.135	-.135	-.135
Lag 2	-.053	.	-.053	-.053	-.053	-.053	-.053	-.053	-.053	-.053	-.053
Lag 3	-.137	.	-.137	-.137	-.137	-.137	-.137	-.137	-.137	-.137	-.137
Lag 4	-.298	.	-.298	-.298	-.298	-.298	-.298	-.298	-.298	-.298	-.298
Lag 5	.089	.	.089	.089	.089	.089	.089	.089	.089	.089	.089
Lag 6	-.156	.	-.156	-.156	-.156	-.156	-.156	-.156	-.156	-.156	-.156
Lag 7	.019	.	.019	.019	.019	.019	.019	.019	.019	.019	.019
Lag 8	-.303	.	-.303	-.303	-.303	-.303	-.303	-.303	-.303	-.303	-.303
Lag 9	-.121	.	-.121	-.121	-.121	-.121	-.121	-.121	-.121	-.121	-.121
Lag 10	-.217	.	-.217	-.217	-.217	-.217	-.217	-.217	-.217	-.217	-.217
Lag 11	-.131	.	-.131	-.131	-.131	-.131	-.131	-.131	-.131	-.131	-.131
Lag 12	-.012	.	-.012	-.012	-.012	-.012	-.012	-.012	-.012	-.012	-.012
Lag 13	-.023	.	-.023	-.023	-.023	-.023	-.023	-.023	-.023	-.023	-.023
Lag 14	-.097	.	-.097	-.097	-.097	-.097	-.097	-.097	-.097	-.097	-.097
Lag 15	-.159	.	-.159	-.159	-.159	-.159	-.159	-.159	-.159	-.159	-.159
Lag 16	-.012	.	-.012	-.012	-.012	-.012	-.012	-.012	-.012	-.012	-.012
Lag 17	-.018	.	-.018	-.018	-.018	-.018	-.018	-.018	-.018	-.018	-.018
Lag 18	-.200	.	-.200	-.200	-.200	-.200	-.200	-.200	-.200	-.200	-.200
Lag 19	-.035	.	-.035	-.035	-.035	-.035	-.035	-.035	-.035	-.035	-.035
Lag 20	-.176	.	-.176	-.176	-.176	-.176	-.176	-.176	-.176	-.176	-.176
Lag 21	.099	.	.099	.099	.099	.099	.099	.099	.099	.099	.099
Lag 22	-.128	.	-.128	-.128	-.128	-.128	-.128	-.128	-.128	-.128	-.128
Lag 23	.028	.	.028	.028	.028	.028	.028	.028	.028	.028	.028
Lag 24	.029	.	.029	.029	.029	.029	.029	.029	.029	.029	.029
Lag 25	-.057	.	-.057	-.057	-.057	-.057	-.057	-.057	-.057	-.057	-.057
Lag 26	-.215	.	-.215	-.215	-.215	-.215	-.215	-.215	-.215	-.215	-.215
Lag 27	.085	.	.085	.085	.085	.085	.085	.085	.085	.085	.085
Lag 28	-.143	.	-.143	-.143	-.143	-.143	-.143	-.143	-.143	-.143	-.143
Lag 29	-.026	.	-.026	-.026	-.026	-.026	-.026	-.026	-.026	-.026	-.026
Lag 30	-.062	.	-.062	-.062	-.062	-.062	-.062	-.062	-.062	-.062	-.062
Lag 31	-.025	.	-.025	-.025	-.025	-.025	-.025	-.025	-.025	-.025	-.025
Lag 32	.052	.	.052	.052	.052	.052	.052	.052	.052	.052	.052
Lag 33	-.016	.	-.016	-.016	-.016	-.016	-.016	-.016	-.016	-.016	-.016
Lag 34	-.100	.	-.100	-.100	-.100	-.100	-.100	-.100	-.100	-.100	-.100
Lag 35	-.091	.	-.091	-.091	-.091	-.091	-.091	-.091	-.091	-.091	-.091
Lag 36	-.057	.	-.057	-.057	-.057	-.057	-.057	-.057	-.057	-.057	-.057

Water Table (Meter), (Pre-Monsoon), Observed and normalized, Statistics (Tehsil-wise)

(1998-2013)		Tehsils of Bareilly District					
PARAMETERS↓		Bareilly	Baheri	Aonla	Nawabganj	Faridpur	Mirganj
MEAN	Observed	5.37	2.85	10.65	4.37	5.52	5.90
	Normalized	5.73	3.07	11.36	4.62	6.01	6.24
STDEV	Observed	0.674644	0.458929	1.451105	0.499306	1.051749	0.689323
	Normalized	0.205919	0.132988	0.43056	0.122232	0.286639	0.2161
SKEW	Observed	-0.94766	0.471531	0.59510	0.326994	1.374954	0.374138
	Normalized	-0.69026	0.366071	0.26776	0.223707	0.775872	0.182777
KURT	Observed	-0.51525	0.224933	-0.1929	3.541234	1.463737	-1.06568
	Normalized	-1.25938	-1.02207	-1.0733	0.375762	-0.33483	-1.53807
VAR	Observed	0.455145	0.210616	2.10570	0.249306	1.106176	0.475166
	Normalized	0.042403	0.017686	0.18538	0.014941	0.082162	0.046699
CORRELATION		0.990497	0.983758	0.98858	0.962719	0.979659	0.993648
RSQ		0.981084	0.967781	0.97729	0.926828	0.959732	0.987336

Water Table (Meter), (Post-Monsoon), Observed and normalized, Statistics (Tehsil-wise)

(1998-2013)		Tehsils of Bareilly District					
PARAMETERS↓		Bareilly	Baheri	Aonla	Nawabganj	Faridpur	Mirganj
MEAN	Observed	4.64	1.52	9.93	2.62	4.45	4.57
	Normalized	5.08	1.80	10.56	3.04	5.01	5.08
STDEV	Observed	0.860084	0.595538	1.226131	0.793444	1.096776	0.991622
	Normalized	0.266342	0.174381	0.368595	0.237967	0.342664	0.270058
SKEW	Observed	-0.32497	0.765076	-0.28179	-0.75453	-0.22197	-0.27643
	Normalized	-0.267	0.637295	-0.35543	-0.65764	-0.18807	-0.30085
KURT	Observed	-0.90585	-0.16512	-0.70085	-0.5237	-1.16091	1.623558
	Normalized	-1.42359	-0.76954	-0.94242	-0.91741	-1.3959	-0.63506
VAR	Observed	0.739745	0.354665	1.503398	0.629553	1.202918	0.983313
	Normalized	0.070938	0.030409	0.135862	0.056628	0.117419	0.072931
CORRELATION		0.992914	0.992471	0.996704	0.994855	0.996902	0.970747
RSQ		0.985878	0.984999	0.993419	0.989736	0.993814	0.942349

Pre-Monsoon Water Table (Tehsil-Wise)

Year	Tehsils					
	Bareilly		Baheri		Aonla	
	Observed	Normalized	Observed	Normalized	Observed	Normalized
1998	4.05	5.388176	2.6	2.98322	8.8	10.80042
1999	4.16	5.395737	2.4	2.923582	8.94	10.82665
2000	4.5	5.437553	2.54	2.963309	9.47	10.95504
2001	4.72	5.484045	2.6	2.98322	8.79	10.79866
2002	5.1	5.603205	3.7	3.292501	9.44	10.94653
2003	5.6	5.798111	2.55	2.966516	10.26	11.22451
2004	5.8	5.86877	2	2.862947	10.66	11.38217
2005	5.95	5.914011	2.7	3.019507	10.46	11.30261
2006	5.92	5.90557	2.72	3.027132	10.3	11.23995
2007	5.88	5.893833	3.05	3.155603	10.51	11.32243
2008	5.95	5.914011	3.2	3.205346	13.17	12.04527
2009	5.76	5.855489	3.2	3.205346	11.46	11.68555
2010	6.0	5.927376	3.73	3.294513	11.94	11.83294
2011	5.15	5.621863	3	3.137091	10.96	11.50096
2012	5.5	5.759626	2.98	3.129485	11.71	11.76669
2013	5.9	5.89977	2.6	2.98322	13.6	12.07474

Year	Nawabganj		Faridpur		Mirganj	
	Observed	Normalized	Observed	Normalized	Observed	Normalized
1998	4.51	4.677476	5.62	6.086839	6.32	6.402821
1999	4.63	4.721722	4.98	5.840767	5.13	5.991475
2000	3.21	4.379293	4.93	5.823518	5.18	6.002587
2001	4.65	4.728648	4.43	5.679216	5.03	5.971827
2002	4.9	4.800664	4.83	5.790411	5.71	6.170196
2003	4.31	4.598417	5.08	5.876518	6.05	6.304415
2004	4.22	4.563408	4.3	5.65089	5.18	6.002587
2005	4.22	4.563408	5.73	6.130241	5.48	6.087338
2006	4.12	4.526771	5.18	5.913725	5.68	6.15875
2007	3.99	4.484574	5.78	6.149702	6.21	6.364688
2008	4.29	4.590527	7.85	6.5595	5.97	6.272916
2009	4.11	4.523285	7.85	6.5595	5.18	6.002587
2010	4.35	4.614308	6.13	6.27749	6.48	6.451867
2011	4.42	4.642204	4.88	5.806724	6.68	6.500954
2012	5.64	4.870872	5.98	6.224896	7.1	6.56173
2013	4.42	4.642204	4.8	5.780862	7.03	6.555019

Post-Monsoon Water Table (Tehsil-Wise)

Year	Tehsils					
	Bareilly		Baheri		Aonla	
	Observed	Normalized	Observed	Normalized	Observed	Normalized
1998	3.12	4.672047	0.6	1.555345	8.1	10.0142
1999	3.34	4.695101	1.2	1.695175	8.32	10.04701
2000	3.6	4.736434	1.53	1.821007	8.02	10.00424
2001	3.81	4.782927	1.85	1.942159	8.19	10.02663
2002	4.05	4.851037	1.78	1.917494	9.64	10.42921
2003	4.3	4.937065	1.15	1.678292	9.74	10.46833
2004	4.76	5.117004	1.25	1.712834	10.12	10.61932
2005	5.23	5.287335	1.35	1.750087	10.08	10.60351
2006	5.65	5.395757	2.5	2.084683	10.2	10.65068
2007	5.51	5.365062	2.5	2.084683	10.27	10.67776
2008	5.1	5.244352	1.5	1.80904	11.28	10.99104
2009	5.1	5.244352	2.65	2.097168	10.26	10.67391
2010	4.75	5.113051	0.87	1.600934	10.5	10.76333
2011	4.6	5.053338	1.2	1.695175	10.66	10.8188
2012	5.3	5.308756	1.25	1.712834	11.56	11.04454
2013	6	5.450028	1.12	1.668568	11.96	11.0973

Year	Nawabganj		Faridpur		Mirganj	
	Observed	Normalized	Observed	Normalized	Observed	Normalized
1998	2.81	3.09142	3.93	4.800869	4.89	5.192844
1999	2.69	3.044235	4.23	4.91349	3.78	4.782811
2000	2.91	3.129498	2.88	4.536732	2.28	4.582805
2001	3.25	3.243524	4.28	4.933111	4.88	5.189047
2002	3.54	3.315253	4.23	4.91349	4.98	5.226418
2003	3.16	3.216187	3.08	4.569117	5.16	5.28967
2004	3.11	3.200039	4.66	5.083938	3.68	4.755007
2005	2.99	3.158749	5.08	5.239039	3.86	4.806739
2006	3	3.162316	4.9	5.175374	4.84	5.173748
2007	1.23	2.651087	5.08	5.239039	4.92	5.204157
2008	1.62	2.701828	5.83	5.435614	3.56	4.724827
2009	2.49	2.964711	6.04	5.469311	4.63	5.091237
2010	1.62	2.701828	5.8	5.430073	4.6	5.07928
2011	1.17	2.646252	2.98	4.551935	4.8	5.15828
2012	3.72	3.347202	5.48	5.358903	6.7	5.548298
2013	2.6	3.008368	2.78	4.523392	5.6	5.41532

Time Series Modeler Notes

Output Created		03-Mar-2016 13:07:00
Comments		
Input	Active Dataset	DataSet0
	Filter	<none>
	Weight	<none>
	Split File	<none>
	Date	<none>
Missing Value Handling	Definition of Missing	User-defined missing values are treated as missing.
	Cases Used	Only cases with valid data for the dependent variable are used in computing any statistics.
Syntax		TSMODEL /MODELSUMMARY PRINT=[MODELFIT RESIDACF RESIDPACF] PLOT=[SRSQUARE RSQUARE RMSE MAPE MAE MAXAPE MAXAE NORMBIC RESIDACF RESIDPACF] /MODELSTATISTICS DISPLAY=YES MODELFIT=[SRSQUARE RSQUARE RMSE MAPE MAE MAXAPE MAXAE NORMBIC] /MODELDETAILS PRINT=[PARAMETERS RESIDACF RESIDPACF FORECASTS] PLOT=[RESIDACF RESIDPACF] /SERIESPLOT OBSERVED FORECAST FIT FORECASTCI FITCI /OUTPUTFILTER DISPLAY=ALLMODELS /SAVE PREDICTED(Predicted) LCL(LCL) UCL(UCL) NRESIDUAL(NResidual) /AUXILIARY CILEVEL=95 MAXACFLAGS=24 /MISSING USERMISSING=EXCLUDE /MODEL DEPENDENT=VAR00002 VAR00003 VAR00004 VAR00005 VAR00006 VAR00007 NDEPENDENT=VAR00001 PREFIX='Model' /ARIMA AR=[0] DIFF=0 MA=[0] TRANSFORM=NONE CONSTANT=YES /TRANSFERFUNCTION VARIABLES=VAR00001 NUM=[0] DENOM=[0] DIFF=0 DELAY=0 TRANSFORM=NONE /AUTOOUTLIER DETECT=OFF.
Resources	Processor Time	00:00:04.484
	Elapsed Time	00:00:04.248
Variables Created or Modified	Predicted_VAR00002_Model_1	Predicted value from VAR00002-Model_1
	LCL_VAR00002_Model_1	LCL from VAR00002-Model_1
	UCL_VAR00002_Model_1	UCL from VAR00002-Model_1
	NResidual_VAR00002_Model_1	Noise residual from VAR00002-Model_1
	Predicted_VAR00003_Model_2	Predicted value from VAR00003-Model_2
	LCL_VAR00003_Model_2	LCL from VAR00003-Model_2
	UCL_VAR00003_Model_2	UCL from VAR00003-Model_2
	NResidual_VAR00003_Model_2	Noise residual from VAR00003-Model_2
	Predicted_VAR00004_Model_3	Predicted value from VAR00004-Model_3
	LCL_VAR00004_Model_3	LCL from VAR00004-Model_3
	UCL_VAR00004_Model_3	UCL from VAR00004-Model_3
	NResidual_VAR00004_Model_3	Noise residual from VAR00004-Model_3
	Predicted_VAR00005_Model_4	Predicted value from VAR00005-Model_4
	LCL_VAR00005_Model_4	LCL from VAR00005-Model_4
	UCL_VAR00005_Model_4	UCL from VAR00005-Model_4
	NResidual_VAR00005_Model_4	Noise residual from VAR00005-Model_4
	Predicted_VAR00006_Model_5	Predicted value from VAR00006-Model_5
	LCL_VAR00006_Model_5	LCL from VAR00006-Model_5
	UCL_VAR00006_Model_5	UCL from VAR00006-Model_5
	NResidual_VAR00006_Model_5	Noise residual from VAR00006-Model_5
	Predicted_VAR00007_Model_6	Predicted value from VAR00007-Model_6
	LCL_VAR00007_Model_6	LCL from VAR00007-Model_6
	UCL_VAR00007_Model_6	UCL from VAR00007-Model_6
	NResidual_VAR00007_Model_6	Noise residual from VAR00007-Model_6
Use	From	First observation
	To	Last observation
Predict	From	First observation
	To	Last observation

Model Description

			Model Type
Model ID	VAR00002	Model_1	ARIMA(0,0,0)
	VAR00003	Model_2	ARIMA(0,0,0)
	VAR00004	Model_3	ARIMA(0,0,0)
	VAR00005	Model_4	ARIMA(0,0,0)
	VAR00006	Model_5	ARIMA(0,0,0)
	VAR00007	Model_6	ARIMA(0,0,0)

Model Statistics

Model	Number of Predictors	Model Fit statistics								Ljung-Box Q(18)			Number of Outliers
		Stationary R-squared	R-squared	RMSE	MAPE	MAE	MaxAPE	MaxAE	Normalized BIC	Statistics	DF	Sig.	
VAR00002-Model_1	1	.675	.675	.157	2.280	.117	5.496	.294	-3.353	.	0	.	0
VAR00003-Model_2	1	.001	.001	.180	7.895	.144	15.241	.291	-3.079	.	0	.	0
VAR00004-Model_3	1	.879	.879	.133	.952	.100	2.288	.251	-3.691	.	0	.	0
VAR00005-Model_4	1	.174	.174	.224	5.912	.175	13.356	.446	-2.647	.	0	.	0
VAR00006-Model_5	1	.093	.093	.338	5.187	.255	14.408	.652	-1.824	.	0	.	0
VAR00007-Model_6	1	.185	.185	.252	4.182	.210	8.728	.412	-2.407	.	0	.	0

ARIMA Model Parameters

					Estimate	SE	t	Sig
VAR00002-Model_1	VAR00002	No Transformation	Constant		-87.076	17.103	-5.091	.000
	VAR00001	No Transformation	Numerator	Lag 0	.046	.009	5.388	.000
VAR00003-Model_2	VAR00001	No Transformation	Numerator	Lag 0	.001	.010	.125	.902
	VAR00003	No Transformation	Constant		-.659	19.621	-.034	.974
VAR00004-Model_3	VAR00001	No Transformation	Numerator	Lag 0	.073	.007	10.078	.000
	VAR00004	No Transformation	Constant		-135.000	14.444	-9.347	.000
VAR00005-Model_4	VAR00001	No Transformation	Numerator	Lag 0	-.021	.012	-1.716	.108
	VAR00005	No Transformation	Constant		44.819	24.352	1.840	.087
VAR00006-Model_5	VAR00001	No Transformation	Numerator	Lag 0	.022	.018	1.195	.252
	VAR00006	No Transformation	Constant		-38.912	36.748	-1.059	.308
VAR00007-Model_6	VAR00001	No Transformation	Numerator	Lag 0	.024	.014	1.781	.097
	VAR00007	No Transformation	Constant		-43.807	27.453	-1.596	.133

Residual ACF

Model		1	2	3	4	5	6	7	8	9	10	11	12	13	14	15
VAR00002- Model_1	ACF	.746	.290	-.113	-.453	-.591	-.498	-.279	-.069	.058	.116	.125	.109	.059	.006	-.005
	SE	.250	.363	.378	.380	.412	.462	.495	.504	.505	.505	.507	.509	.510	.511	.511
VAR00003- Model_2	ACF	.215	.016	-.224	-.380	.078	-.009	.058	-.104	-.174	-.101	-.182	.081	.072	.081	.074
	SE	.250	.261	.261	.273	.304	.306	.306	.306	.309	.315	.317	.323	.324	.325	.327
VAR00004- Model_3	ACF	.234	.038	-.249	-.045	-.198	-.107	-.431	-.149	.079	.219	.091	.017	.001	.001	.000
	SE	.250	.263	.264	.278	.278	.287	.290	.327	.331	.333	.342	.343	.343	.343	.343
VAR00005- Model_4	ACF	.230	-.137	.099	-.204	-.548	-.251	-.075	.037	.088	.158	.162	.092	-.045	-.088	-.018
	SE	.250	.263	.267	.270	.279	.340	.351	.352	.352	.354	.358	.363	.364	.364	.366
VAR00006- Model_5	ACF	-.044	.286	-.026	-.146	-.237	-.250	-.194	-.024	-.161	.077	.137	-.080	.167	-.024	.019
	SE	.250	.250	.270	.270	.275	.288	.301	.309	.309	.314	.315	.319	.320	.325	.326
VAR00007- Model_6	ACF	.071	-.428	-.131	.118	.166	-.104	-.349	-.026	.128	.033	.133	-.115	-.128	.082	.052
	SE	.250	.251	.293	.297	.300	.306	.308	.332	.332	.335	.335	.338	.341	.344	.345

Residual PACF

Model		1	2	3	4	5	6	7	8	9	10	11	12	13	14	15
VAR00002- Model_1	PACF	.746	-.601	-.038	-.464	.179	-.196	.113	-.389	.037	-.246	.186	-.241	-.066	-.168	.041
	SE	.250	.250	.250	.250	.250	.250	.250	.250	.250	.250	.250	.250	.250	.250	.250
VAR00003- Model_2	PACF	.215	-.032	-.232	-.314	.256	-.117	-.093	-.205	-.004	-.154	-.252	-.003	-.006	-.114	-.121
	SE	.250	.250	.250	.250	.250	.250	.250	.250	.250	.250	.250	.250	.250	.250	.250
VAR00004- Model_3	PACF	.234	-.018	-.269	.085	-.212	-.095	-.431	-.092	.106	-.113	-.037	-.166	-.038	-.221	-.148
	SE	.250	.250	.250	.250	.250	.250	.250	.250	.250	.250	.250	.250	.250	.250	.250
VAR00005- Model_4	PACF	.230	-.201	.201	-.363	-.405	-.182	-.189	.127	-.208	-.129	-.191	-.088	-.095	-.202	-.051
	SE	.250	.250	.250	.250	.250	.250	.250	.250	.250	.250	.250	.250	.250	.250	.250
VAR00006- Model_5	PACF	-.044	.285	-.005	-.249	-.279	-.200	-.098	.073	-.188	-.151	.078	-.212	-.070	-.056	-.117
	SE	.250	.250	.250	.250	.250	.250	.250	.250	.250	.250	.250	.250	.250	.250	.250
VAR00007- Model_6	PACF	.071	-.436	-.071	-.064	.093	-.129	-.289	-.078	-.195	-.099	.160	-.180	-.078	-.142	-.138
	SE	.250	.250	.250	.250	.250	.250	.250	.250	.250	.250	.250	.250	.250	.250	.250

Model Summary

Model Fit

Fit Statistic	Mean	SE	Minimum	Maximum	Percentile						
					5	10	25	50	75	90	95
Stationary R-squared	.334	.355	.001	.879	.001	.001	.070	.179	.726	.879	.879
R-squared	.334	.355	.001	.879	.001	.001	.070	.179	.726	.879	.879
RMSE	.214	.075	.133	.338	.133	.133	.151	.202	.274	.338	.338
MAPE	4.401	2.512	.952	7.895	.952	.952	1.948	4.684	6.408	7.895	7.895
MaxAPE	9.919	5.282	2.288	15.241	2.288	2.288	4.694	11.042	14.616	15.241	15.241
MAE	.167	.058	.100	.255	.100	.100	.113	.160	.221	.255	.255
MaxAE	.391	.148	.251	.652	.251	.251	.281	.353	.498	.652	.652
Normalized BIC	-2.833	.679	-3.691	-1.824	-3.691	-3.691	-3.438	-2.863	-2.261	-1.824	-1.824

Residual ACF Summary

Lag	Mean	SE	Minimum	Maximum	Percentile						
					5	10	25	50	75	90	95
Lag 1	.242	.271	-.044	.746	-.044	-.044	.042	.223	.362	.746	.746
Lag 2	.011	.272	-.428	.290	-.428	-.428	-.210	.027	.287	.290	.290
Lag 3	-.108	.129	-.249	.099	-.249	-.249	-.230	-.122	.005	.099	.099
Lag 4	-.185	.211	-.453	.118	-.453	-.453	-.399	-.175	-.004	.118	.118
Lag 5	-.222	.311	-.591	.166	-.591	-.591	-.559	-.217	.100	.166	.166
Lag 6	-.203	.172	-.498	-.009	-.498	-.498	-.313	-.179	-.080	-.009	-.009
Lag 7	-.212	.181	-.431	.058	-.431	-.431	-.370	-.237	-.042	.058	.058
Lag 8	-.056	.066	-.149	.037	-.149	-.149	-.115	-.047	-.008	.037	.037
Lag 9	.003	.134	-.174	.128	-.174	-.174	-.164	.069	.098	.128	.128
Lag 10	.084	.111	-.101	.219	-.101	-.101	.000	.096	.173	.219	.219
Lag 11	.078	.129	-.182	.162	-.182	-.182	.023	.129	.144	.162	.162
Lag 12	.017	.095	-.115	.109	-.115	-.115	-.088	.049	.096	.109	.109
Lag 13	.021	.102	-.128	.167	-.128	-.128	-.066	.030	.095	.167	.167
Lag 14	.010	.065	-.088	.082	-.088	-.088	-.040	.003	.081	.082	.082
Lag 15	.020	.036	-.018	.074	-.018	-.018	-.008	.009	.058	.074	.074

Residual PACF Summary

Lag	Mean	SE	Minimum	Maximum	Percentile						
					5	10	25	50	75	90	95
Lag 1	.242	.271	-.044	.746	-.044	-.044	.042	.223	.362	.746	.746
Lag 2	-.167	.318	-.601	.285	-.601	-.601	-.477	-.117	.058	.285	.285
Lag 3	-.069	.170	-.269	.201	-.269	-.269	-.241	-.054	.047	.201	.201
Lag 4	-.228	.203	-.464	.085	-.464	-.464	-.388	-.281	-.027	.085	.085
Lag 5	-.061	.272	-.405	.256	-.405	-.405	-.310	-.060	.198	.256	.256
Lag 6	-.153	.045	-.200	-.095	-.200	-.200	-.197	-.156	-.111	-.095	-.095
Lag 7	-.165	.186	-.431	.113	-.431	-.431	-.325	-.143	-.042	.113	.113
Lag 8	-.094	.188	-.389	.127	-.389	-.389	-.251	-.085	.086	.127	.127
Lag 9	-.075	.138	-.208	.106	-.208	-.208	-.198	-.096	.054	.106	.106
Lag 10	-.149	.052	-.246	-.099	-.246	-.246	-.177	-.140	-.110	-.099	-.099
Lag 11	-.010	.183	-.252	.186	-.252	-.252	-.206	.020	.166	.186	.186
Lag 12	-.148	.088	-.241	-.003	-.241	-.241	-.219	-.173	-.066	-.003	-.003
Lag 13	-.059	.032	-.095	-.006	-.095	-.095	-.082	-.068	-.030	-.006	-.006
Lag 14	-.151	.060	-.221	-.056	-.221	-.221	-.207	-.155	-.100	-.056	-.056
Lag 15	-.089	.072	-.148	.041	-.148	-.148	-.141	-.119	-.028	.041	.041

Time Series Modeler

Notes

Output Created		03-Mar-2016 12:50:44
Comments		
Input	Active Dataset	DataSet0
	Filter	<none>
	Weight	<none>
	Split File	<none>
	Date	<none>
Missing Value Handling	Definition of Missing	User-defined missing values are treated as missing.
	Cases Used	Only cases with valid data for the dependent variable are used in computing any statistics.
Syntax		TSMODEL /MODELSUMMARY PRINT=[MODELFIT RESIDACF RESIDPACF] PLOT=[SRSQUARE RSQUARE RMSE MAPE MAE MAXAPE MAXAE NORMBIC RESIDACF RESIDPACF] /MODELSTATISTICS DISPLAY=YES MODELFIT=[SRSQUARE RSQUARE RMSE MAPE MAE MAXAPE MAXAE NORMBIC] /MODELDETAILS PRINT=[PARAMETERS RESIDACF RESIDPACF FORECASTS] PLOT=[RESIDACF RESIDPACF] /SERIESPLOT OBSERVED FORECAST FIT FORECASTCI FITCI /OUTPUTFILTER DISPLAY=ALLMODELS /SAVE PREDICTED(Predicted) LCL(LCL) UCL(UCL) NRESIDUAL(NResidual) /AUXILIARY CILEVEL=95 MAXACFLAGS=24 /MISSING USERMISSING=EXCLUDE /MODEL DEPENDENT=VAR00002 VAR00003 VAR00004 VAR00005 VAR00006 VAR00007 INDEPENDENT=VAR00001PREFIX='Model /ARIMA AR=[0] DIFF=0 MA=[0] TRANSFORM=NONE CONSTANT=YES /TRANSFERFUNCTION VARIABLES=VAR00001 NUM=[0] DENOM=[0] DIFF=0 DELAY=0 TRANSFORM=NONE /AUTOOUTLIER DETECT=OFF.
Resources	Processor Time	00:00:04.422
	Elapsed Time	0:00:04.375
Variables Created or Modified	Predicted_VAR00002_Model_1	Predicted value from VAR00002-Model_1
	LCL_VAR00002_Model_1	LCL from VAR00002-Model_1
	UCL_VAR00002_Model_1	UCL from VAR00002-Model_1
	NResidual_VAR00002_Model_1	Noise residual from VAR00002-Model_1
	Predicted_VAR00003_Model_2	Predicted value from VAR00003-Model_2
	LCL_VAR00003_Model_2	LCL from VAR00003-Model_2
	UCL_VAR00003_Model_2	UCL from VAR00003-Model_2
	NResidual_VAR00003_Model_2	Noise residual from VAR00003-Model_2
	Predicted_VAR00004_Model_3	Predicted value from VAR00004-Model_3
	LCL_VAR00004_Model_3	LCL from VAR00004-Model_3
	UCL_VAR00004_Model_3	UCL from VAR00004-Model_3
	NResidual_VAR00004_Model_3	Noise residual from VAR00004-Model_3
	Predicted_VAR00005_Model_4	Predicted value from VAR00005-Model_4
	LCL_VAR00005_Model_4	LCL from VAR00005-Model_4
	UCL_VAR00005_Model_4	UCL from VAR00005-Model_4
	NResidual_VAR00005_Model_4	Noise residual from VAR00005-Model_4
	Predicted_VAR00006_Model_5	Predicted value from VAR00006-Model_5
	LCL_VAR00006_Model_5	LCL from VAR00006-Model_5
	UCL_VAR00006_Model_5	UCL from VAR00006-Model_5
	NResidual_VAR00006_Model_5	Noise residual from VAR00006-Model_5
	Predicted_VAR00007_Model_6	Predicted value from VAR00007-Model_6
	LCL_VAR00007_Model_6	LCL from VAR00007-Model_6
	UCL_VAR00007_Model_6	UCL from VAR00007-Model_6
	NResidual_VAR00007_Model_6	Noise residual from VAR00007-Model_6
Use	From	First observation
	To	Last observation
Predict	From	First observation
	To	Last observation

Model Description

			Model Type
Model ID	VAR00002	Model_1	ARIMA(0,0,0)
	VAR00003	Model_2	ARIMA(0,0,0)
	VAR00004	Model_3	ARIMA(0,0,0)
	VAR00005	Model_4	ARIMA(0,0,0)
	VAR00006	Model_5	ARIMA(0,0,0)
	VAR00007	Model_6	ARIMA(0,0,0)

Model Statistics

Model	Number of Predictors	Model Fit statistics								Ljung-Box Q(18)			Number of Outliers
		Stationary R-squared	R-squared	RMSE	MAPE	MAE	MaxAPE	MaxAE	Normalized BIC	Statistics	DF	Sig.	
VAR00002-Model_1	1	.502	.502	.150	2.182	.125	4.907	.276	-3.442	.	0	.	0
VAR00003-Model_2	1	.218	.218	.122	2.822	.087	8.119	.267	-3.865	.	0	.	0
VAR00004-Model_3	1	.820	.820	.189	1.162	.134	4.018	.484	-2.984	.	0	.	0
VAR00005-Model_4	1	.003	.003	.126	2.010	.093	5.319	.241	-3.792	.	0	.	0
VAR00006-Model_5	1	.147	.147	.274	3.468	.210	7.507	.492	-2.242	.	0	.	0
VAR00007-Model_6	1	.392	.392	.174	2.149	.134	5.909	.378	-3.146	.	0	.	0

ARIMA Model Parameters

					Estimate	SE	t	Sig.
VAR00002-Model_1	VAR00002	No Transformation	Constant		-55.716	16.363	-3.405	.004
	VAR00001	No Transformation	Numerator	Lag 0	.031	.008	3.755	.002
VAR00003-Model_2	VAR00001	No Transformation	Numerator	Lag 0	.013	.007	1.973	.069
	VAR00003	No Transformation	Constant		-23.059	13.244	-1.741	.104
VAR00004-Model_3	VAR00001	No Transformation	Numerator	Lag 0	.082	.010	7.983	.000
	VAR00004	No Transformation	Constant		-152.870	20.572	-7.431	.000
VAR00005-Model_4	VAR00001	No Transformation	Numerator	Lag 0	.001	.007	.219	.830
	VAR00005	No Transformation	Constant		1.616	13.738	.118	.908
VAR00006-Model_5	VAR00001	No Transformation	Numerator	Lag 0	.023	.015	1.552	.143
	VAR00006	No Transformation	Constant		-40.242	29.809	-1.350	.198
VAR00007-Model_6	VAR00001	No Transformation	Numerator	Lag 0	.028	.009	3.005	.009
	VAR00007	No Transformation	Constant		-50.759	18.970	-2.676	.018

Residual ACF

Model		1	2	3	4	5	6	7	8	9	10	11	12	13	14	15
VAR00002-Model_1	ACF	.680	.382	.043	-.208	-.394	-.497	-.493	-.422	-.211	.007	.136	.181	.191	.084	.021
	SE	.250	.347	.372	.373	.380	.404	.441	.474	.497	.503	.503	.505	.509	.513	.514
VAR00003-Model_2	ACF	.150	-.159	-.296	-.259	-.097	-.096	.100	.226	.104	-.019	-.279	.040	.040	.055	-.009
	SE	.250	.256	.262	.282	.296	.298	.300	.302	.313	.315	.315	.330	.330	.331	.331
VAR00004-Model_3	ACF	-.036	-.293	-.481	.117	.421	-.006	-.316	-.098	.036	.228	-.004	-.040	-.026	-.014	.012
	SE	.250	.250	.271	.320	.323	.355	.355	.372	.374	.374	.383	.383	.383	.383	.383
VAR00005-Model_4	ACF	.046	-.140	.060	-.001	-.262	-.145	-.090	-.189	.030	.158	.081	-.243	.113	.079	.003
	SE	.250	.251	.255	.256	.256	.273	.277	.279	.287	.287	.293	.294	.306	.309	.310
VAR00006-Model_5	ACF	.253	.156	-.177	-.326	-.317	-.334	-.001	-.225	.117	.191	.166	.128	-.057	.023	-.096
	SE	.250	.265	.271	.278	.301	.321	.342	.342	.352	.354	.360	.365	.368	.368	.369
VAR00007-Model_6	ACF	.037	-.239	-.165	.140	.319	-.355	-.224	-.035	.120	.010	-.367	.002	.056	.109	.093
	SE	.250	.250	.264	.271	.275	.297	.323	.332	.333	.335	.335	.360	.360	.360	.362

Residual PACF

Model		1	2	3	4	5	6	7	8	9	10	11	12	13	14	15
VAR00002-Model_1	PACF	.680	-.148	-.295	-.148	-.174	-.188	-.114	-.135	.074	.017	-.155	-.135	-.041	-.255	-.055
	SE	.250	.250	.250	.250	.250	.250	.250	.250	.250	.250	.250	.250	.250	.250	.250
VAR00003-Model_2	PACF	.150	-.185	-.254	-.232	-.156	-.285	-.098	.008	-.091	-.090	-.316	.078	-.098	-.047	-.141
	SE	.250	.250	.250	.250	.250	.250	.250	.250	.250	.250	.250	.250	.250	.250	.250
VAR00004-Model_3	PACF	-.036	-.295	-.554	-.156	.162	-.232	-.311	.089	-.298	-.334	-.009	-.025	-.222	-.052	.007
	SE	.250	.250	.250	.250	.250	.250	.250	.250	.250	.250	.250	.250	.250	.250	.250
VAR00005-Model_4	PACF	.046	-.142	.075	-.030	-.248	-.135	-.164	-.227	-.009	.032	.021	-.361	-.038	-.124	.026
	SE	.250	.250	.250	.250	.250	.250	.250	.250	.250	.250	.250	.250	.250	.250	.250
VAR00006-Model_5	PACF	.253	.099	-.256	-.279	-.154	-.234	.065	-.418	-.048	.078	-.142	-.170	-.212	-.073	.035
	SE	.250	.250	.250	.250	.250	.250	.250	.250	.250	.250	.250	.250	.250	.250	.250
VAR00007-Model_6	PACF	.037	-.241	-.154	.099	.265	-.396	-.062	-.094	-.096	-.102	-.217	-.053	-.176	-.079	.125
	SE	.250	.250	.250	.250	.250	.250	.250	.250	.250	.250	.250	.250	.250	.250	.250

Model Summary

Fit Statistic	Mean	SE	Minimum	Maximum	Percentile						
					5	10	25	50	75	90	95
Stationary R-squared	.347	.291	.003	.820	.003	.003	.111	.305	.581	.820	.820
R-squared	.347	.291	.003	.820	.003	.003	.111	.305	.581	.820	.820
RMSE	.173	.056	.122	.274	.122	.122	.125	.162	.210	.274	.274
MAPE	2.299	.781	1.162	3.468	1.162	1.162	1.798	2.166	2.984	3.468	3.468
MaxAPE	5.963	1.572	4.018	8.119	4.018	4.018	4.684	5.614	7.660	8.119	8.119
MAE	.130	.044	.087	.210	.087	.087	.092	.129	.153	.210	.210
MaxAE	.356	.112	.241	.492	.241	.241	.261	.327	.486	.492	.492
Normalized BIC	-3.245	.601	-3.865	-2.242	-3.865	-3.865	-3.810	-3.294	-2.798	-2.242	-2.242

Residual ACF Summary

Lag	Mean	SE	Minimum	Maximum	Percentile						
					5	10	25	50	75	90	95
Lag 1	.188	.261	-.036	.680	-.036	-.036	.018	.098	.359	.680	.680
Lag 2	-.049	.262	-.293	.382	-.293	-.293	-.253	-.149	.213	.382	.382
Lag 3	-.169	.205	-.481	.060	-.481	-.481	-.342	-.171	.047	.060	.060
Lag 4	-.090	.201	-.326	.140	-.326	-.326	-.276	-.105	.123	.140	.140
Lag 5	-.055	.345	-.394	.421	-.394	-.394	-.336	-.180	.345	.421	.421
Lag 6	-.239	.186	-.497	-.006	-.497	-.497	-.391	-.240	-.074	-.006	-.006
Lag 7	-.171	.217	-.493	.100	-.493	-.493	-.360	-.157	.024	.100	.100
Lag 8	-.124	.216	-.422	.226	-.422	-.422	-.274	-.143	.030	.226	.226
Lag 9	.033	.126	-.211	.120	-.211	-.211	-.030	.070	.118	.120	.120
Lag 10	.096	.108	-.019	.228	-.019	-.019	.000	.084	.200	.228	.228
Lag 11	-.045	.225	-.367	.166	-.367	-.367	-.301	.038	.143	.166	.166
Lag 12	.011	.149	-.243	.181	-.243	-.243	-.091	.021	.141	.181	.181
Lag 13	.053	.091	-.057	.191	-.057	-.057	-.034	.048	.132	.191	.191
Lag 14	.056	.045	-.014	.109	-.014	-.014	.014	.067	.090	.109	.109
Lag 15	.004	.060	-.096	.093	-.096	-.096	-.031	.008	.039	.093	.093

Residual PACF Summary

Lag	Mean	SE	Minimum	Maximum	Percentile						
					5	10	25	50	75	90	95
Lag 1	.188	.261	-.036	.680	-.036	-.036	.018	.098	.359	.680	.680
Lag 2	-.152	.136	-.295	.099	-.295	-.295	-.254	-.167	-.082	.099	.099
Lag 3	-.240	.205	-.554	.075	-.554	-.554	-.360	-.255	-.097	.075	.075
Lag 4	-.124	.139	-.279	.099	-.279	-.279	-.244	-.152	.003	.099	.099
Lag 5	-.051	.210	-.248	.265	-.248	-.248	-.192	-.155	.188	.265	.265
Lag 6	-.245	.089	-.396	-.135	-.396	-.396	-.312	-.233	-.175	-.135	-.135
Lag 7	-.114	.124	-.311	.065	-.311	-.311	-.201	-.106	-.030	.065	.065
Lag 8	-.130	.179	-.418	.089	-.418	-.418	-.275	-.115	.028	.089	.089
Lag 9	-.078	.125	-.298	.074	-.298	-.298	-.146	-.069	.012	.074	.074
Lag 10	-.067	.149	-.334	.078	-.334	-.334	-.160	-.036	.043	.078	.078
Lag 11	-.136	.126	-.316	.021	-.316	-.316	-.242	-.148	-.002	.021	.021
Lag 12	-.111	.150	-.361	.078	-.361	-.361	-.218	-.094	.001	.078	.078
Lag 13	-.131	.083	-.222	-.038	-.222	-.222	-.215	-.137	-.040	-.038	-.038
Lag 14	-.105	.079	-.255	-.047	-.255	-.255	-.157	-.076	-.050	-.047	-.047
Lag 15	.000	.090	-.141	.125	-.141	-.141	-.077	.016	.057	.125	.125